

(12)

AFWAL-TR-84-2022



AD-A141 068

PROPERTIES OF AIRCRAFT FUELS AND RELATED MATERIALS

F. Neil Hodgson  
R. C. Gable  
Charlotte D. Fritsch

MONSANTO RESEARCH CORPORATION  
DAYTON LABORATORY  
DAYTON, OHIO 45407

MARCH 1984

Reproduced From  
Best Available Copy

INTERIM REPORT FOR PERIOD 15 FEBRUARY 1982 - 15 JULY 1983

20000803069

Approved for public release; distribution unlimited

DTIC FILE COPY

AERO PROPULSION LABORATORY  
AIR FORCE WRIGHT AERONAUTICAL LABORATORIES  
AIR FORCE SYSTEMS COMMAND  
WRIGHT-PATTERSON AIR FORCE BASE, OHIO 45433

MAY 15 1984

A

84 05 15 217

NOTICE

When Government drawings, specifications, or other data are used for any purpose other than in connection with a definitely related Government procurement operation, the United States Government thereby incurs no responsibility nor any obligation whatsoever; and the fact that the government may have formulated, furnished, or in any way supplied the said drawings, specifications, or other data, is not to be regarded by implication or otherwise as in any manner licensing the holder or any other person or corporation, or conveying any rights or permission to manufacture use, or sell any patented invention that may in any way be related thereto.

This report has been reviewed by the Office of Public Affairs (ASD/PA) and is releasable to the National Technical Information Service (NTIS). At NTIS, it will be available to the general public, including foreign nations.

This technical report has been reviewed and is approved for publication.

Timothy L. Dues

TIMOTHY L. DUES  
Fuels Branch

FOR THE COMMANDER

Arthur V. Churchill

ARTHUR V. CHURCHILL  
Chief, Fuels Branch  
Fuels and Lubrication Division  
Aero Propulsion Laboratory

"If your address has changed, if you wish to be removed from our mailing list, or if the addressee is no longer employed by your organization please notify AFWAL/POSF, W-PAFB, OH 45433 to help us maintain a current mailing list."

Copies of this report should not be returned unless return is required by security considerations, contractual obligations, or notice on a specific document.

UNCLASSIFIED

SECURITY CLASSIFICATION OF THIS PAGE (When Data Entered)

REPORT DOCUMENTATION PAGE		READ INSTRUCTIONS BEFORE COMPLETING FORM												
1. REPORT NUMBER AFWAL-TR-84-2022	2. GOVT ACQUISITION NO. <i>A141068</i>	3. RECIPIENT'S CATALOG NUMBER												
4. TITLE (and Subtitle) PROPERTIES OF AIRCRAFT FUELS AND RELATED MATERIALS		5. TYPE OF REPORT & PERIOD COVERED Interim Report For Period 15 Feb 82 - 15 July 83												
7. AUTHOR(s) F. N. Hodgson, R. G. Gable, and C. D. Fritsch		6. PERFORMING ORG. REPORT NUMBER F33615-81-C-2035												
9. PERFORMING ORGANIZATION NAME AND ADDRESS Monsanto Company, Dayton Laboratory Station B, Box 8 Dayton, OH 45407		10. PROGRAM ELEMENT, PROJECT, TASK AREA & WORK UNIT NUMBERS 30480515 P.E. 62203F												
11. CONTROLLING OFFICE NAME AND ADDRESS Aero Propulsion Laboratory (AFWAL/POSF) AF Wright Aeronautical Laboratories (AFSC) Wright-Patterson Air Force Base, OH 45433		12. REPORT DATE March 1984												
14. MONITORING AGENCY NAME & ADDRESS (if different from Controlling Office)		13. NUMBER OF PAGES 215												
		15. SECURITY CLASS. (of this report) UNCLASSIFIED												
		16a. DECLASSIFICATION/DOWNGRADING SCHEDULE												
16. DISTRIBUTION STATEMENT (of this Report) Approved for public release; distribution unlimited.														
17. DISTRIBUTION STATEMENT (of the abstract entered in Block 20, if different from Report)														
18. SUPPLEMENTARY NOTES														
19. KEY WORDS (Continue on reverse side if necessary and identify by block number) <table><tbody><tr><td>Jet fuels</td><td>Fuel vapors</td><td>Fuel charging tendency</td></tr><tr><td>High density fuels</td><td>Hydrocarbon type analyses</td><td>Fuel tank sealants</td></tr><tr><td>Fuel contaminants</td><td>Modified fuels</td><td>Antistatic additives</td></tr><tr><td></td><td>Fuel composition</td><td>Water separometers</td></tr></tbody></table>			Jet fuels	Fuel vapors	Fuel charging tendency	High density fuels	Hydrocarbon type analyses	Fuel tank sealants	Fuel contaminants	Modified fuels	Antistatic additives		Fuel composition	Water separometers
Jet fuels	Fuel vapors	Fuel charging tendency												
High density fuels	Hydrocarbon type analyses	Fuel tank sealants												
Fuel contaminants	Modified fuels	Antistatic additives												
	Fuel composition	Water separometers												
20. ABSTRACT (Continue on reverse side if necessary and identify by block number) Fuel tests, analyses, and analytical method development were conducted on a number of fuels of an experimental nature in conjunction with ongoing Air Force programs for studying fuel combustion behavior, turbine engine design, and other fuel related technologies. Fuels from conventional and alternate sources were studied, as were fuels of the high density missile propellant type. A wide variety of both physical and chemical properties of the fuels were measured and are tabulated. Studies conducted to aid in the solution of operational problems are also reported.														

## FOREWORD

This interim report was submitted by Monsanto Research Corporation under Contract F33615-81-C-2035. The effort was sponsored by the Aero Propulsion Laboratory, Air Force Wright Aeronautical Laboratories, Wright-Patterson Air Force Base, Ohio under project No. 30480515 with Major Donald D. Potter as Contract Monitor. Mr. F. Neil Hodgson of Monsanto Research Corporation was technically responsible for the work, which was performed during the period 15 February 1982 to 15 July 1983.

Much of the work performed during this phase of this program was planned in coordination with a number of other, related fuel technology studies being conducted at, or under the sponsorship of, the Aero Propulsion Laboratory. Such efforts include research on turbine engine combustor design, fuel combustion behavior, improved fuel characterization methodology, and alternate fossil fuel source development. The experimental results presented in this report are intended to be used in the context of those research programs, and it is expected that the significance of the data will become apparent as the technical aspects of the related programs are published. In particular, many of the fuel specimens examined during this program were experimental in nature, and the various chemical and physical properties tabulated herein should not necessarily be regarded as characteristic of particular fuel types.

The authors wish to gratefully acknowledge the excellent guidance provided by Major Donald D. Potter during this phase of the work. Special gratitude is also expressed to Mr. Tim Dues, also of the Aero Propulsion Laboratory, for the special insight he has provided in many of the tasks conducted under this program.

Appreciation and acknowledgement are also expressed to members of the Monsanto Research Corporation staff: J. V. Pustinger for his technical consultation and advice; W. H. Hedley for his close attention to management of the fiscal aspects of the program; and D. Q. Douglas, J. A. Graham, J. A. Henry, M. K. Hershey, B. M. Hughes, D. J. Lewis, S. A. Mazer, J. E. Strobel, and G. L. Thomas for their technical contributions. O. P. Tanner, Monsanto Company, St. Louis, is also recognized for the special data he has provided.

## CONTENTS

	<u>Page</u>
I. INTRODUCTION AND SUMMARY . . . . .	1
II. FUELS CHARACTERIZATION . . . . .	2
1. Complete Characterization of Fuels in Support of Various Air Force Programs. . . . .	2
2. Characterization of AEDC and NAPC Test Fuels . . .	22
3. Characterization of Test Fuels and Blends From Garrett Turbine Engine Company Tests . . . . .	23
4. Characterization of Fuels for Correlation With Engine Test Data Obtained by Another Air Force Contractor . . . . .	34
5. Hydrocarbon-Type Analysis and Density Determination on JP-4 Fuels. . . . .	48
6. Characterization of Fuels for Low Temperature Studies . . . . .	50
7. Other Characterizations Provided for Air Force Project Support . . . . .	57
III. TOTAL ANALYSIS OF FUELS AND HYDROCARBON STOCKS. . . .	60
1. Analysis of Occidental Light Shale Oil and its Vapors. . . . .	61
2. Examination of Collected Fractions of Occidental Light Shale Oil. . . . .	73
3. Analysis of Oil From Pyrolysis of Rubber Tires. .	82
IV. ANALYSIS OF FUELS RELATED DEPOSITS, CONTAMINANTS, AND IMPURITIES. . . . .	98
1. Identification of Material Found in Thermal Deposit Rinse Solvent . . . . .	98
2. Identification of Solids in Drum of Aromatic Blending Stock. . . . .	99
3. Characterization of Suspended Solids in JP-4 Fuel	111
4. Analysis of Tank Bottom Samples From Atwater Tank AW-1 . . . . .	115
5. Identification of Dark Deposit on Electrical Fuel Pump Contact Surface . . . . .	124
6. Examination of Specimens Related to Filter Plugging Problem. . . . .	130
7. Determination of Trace Metals in JP-8 Samples . .	136

## CONTENTS (continued)

	<u>Page</u>
8. Determination of Trace Metals in Fuels Used in Thermal Stability Evaluation . . . . .	136
<b>V. SPECIAL PROJECTS AND INVESTIGATIONS . . . . .</b>	<b>140</b>
1. Purification of RJ-5 and JP-10 Fuels for Use as Analytical Standards . . . . .	140
2. Comparison of Samples of Metal Deactivation Agent, N,N'Disalicylidene-1,2-Propanediamine. . .	143
3. Gel Permeation Chromatographic Analysis of Acryloid Copolymer in Oils. . . . .	154
4. Requalification of Corrosion Inhibitors According to MIL-I-25017D . . . . .	155
5. Effects of Fuel Corrosion Inhibitor Additives on the Conductivity of JP-4 with Antistatic Additives . . . . .	165
6. Analysis of Twelve Blended Hydrocarbon Mixtures .	174
7. Evaluation of the Usefulness of a Vibrating Tube Density Meter for Precision Measurements as a Function of Temperature . . . . .	184
8. Determination of the Presence of Corrosion Inhibitor in a JP-8 Involved in Fuel Pump Failure .	189
<b>REFERENCES . . . . .</b>	<b>195</b>
<b>APPENDIX A</b>	
<b>Specific Test Methods for Fuel Characterizations Described in This Report. . . . .</b>	<b>196</b>

## LIST OF FIGURES

<u>Number</u>		<u>Page</u>
1	Kinematic viscosity as a function of temperature for Sample POSF-82-C-0440. . . . .	15
2	Viscosity plot for Sample 83-POSF-1083 . . . . .	16
3	Viscosity plot for Sample 83-POSF-1004 . . . . .	17
4	Viscosity plot for Sample 83-POSF-1005 . . . . .	18
5	Chart of kinematic viscosity and extended range for 83-POSF-0758 . . . . .	19
6	Viscosity plot for Sample 83-POSF-0161 . . . . .	20
7	Viscosity plot for Sample 83-POSF-0800 . . . . .	21
8	Viscosity plot for Sample POSF-82-C-0154 . . . . .	30
9	Viscosity plot for Sample POSF-82-C-0316 . . . . .	31
10	Viscosity plot for Sample POSF-82-D-0196 . . . . .	32
11	Viscosity plot for Sample POSF-82-D-0311 . . . . .	33
12	Viscosity plot for Sample POSF-82-D-0314 . . . . .	39
13	Viscosity plot for Sample POSF-82-C-0394 . . . . .	40
14	Viscosity plot for Sample 82-POSF-0367 . . . . .	41
15	Viscosity plot for Sample 83-POSF-0744 . . . . .	45
16	Viscosity plot for Sample 83-POSF-0745 . . . . .	46
17	Viscosity plot for Sample 83-POSF-0746 . . . . .	47
18	Kinematic viscosity/temperature plot for Sample 81-POSF-0114. . . . .	54
19	Kinematic viscosity/temperature plot for Sample 81-POSF-0117. . . . .	55
20	Kinematic viscosity/temperature plot for Sample 83-POSF-0709. . . . .	56
21	Plot of simulated distillation data. . . . .	59

LIST OF FIGURES (continued)

<u>Number</u>		<u>Page</u>
22	Reconstructed total ion gas chromatogram of light shale oil Sample POSF-82-D-0321. . . . .	62
23	Reconstructed total ion chromatogram of light shale oil vapors . . . . .	62
24	Reconstructed total ion chromatograms of Sample POSF-82-D-0321, Occidental Light Shale Oil (top) and clay-separated first fraction, Sample POSF-82-D-0459 (bottom) . . . . .	76
25	Reconstructed total ion chromatograms of Sample POSF-82-D-0321, Occidental Light Shale Oil (top) and clay-separated second fraction, Sample POSF-82-D-0460 (bottom) . . . . .	77
26	Reconstructed total ion chromatograms of Sample POSF-82-D-0321, Occidental Light Shale Oil (top) and clay-separated third fraction, Sample POSF-82-D-0461 (bottom) . . . . .	78
27	Reconstructed total ion chromatogram of tire pyrolysis oil. . . . .	89
28	Chromatograms using Hall 700A detector in the Sulfur-Selective Mode. . . . .	91
29	Chromatograms using Hall 700A detector in the Halogen-Selective Mode . . . . .	93
30	Chromatogram using N/P selective detector for nitrogen compounds . . . . .	94
31	Infrared absorption spectra of needle-like material isolated from fuel. . . . .	100
32	Infrared absorption spectrum of a nylon. . . . .	101
33	Infrared absorption spectrum of solids separated from subject sample. . . . .	103
34	Infrared absorption spectrum of naphthalene reference compound . . . . .	104
35	Proton resonance spectrum of sample solids . . .	105

LIST OF FIGURES (continued)

<u>Number</u>		<u>Page</u>
36	Reference proton resonance spectrum of naphthalene. . . . .	106
37	Infrared absorption spectrum of sample filtrate after removal of solids. . . . .	107
38	Infrared absorption spectrum of original 2040-solvent . . . . .	108
39	Infrared absorption spectrum resulting from subtraction of 2040-solvent (original) spectrum from spectrum of filtrate . . . . .	109
40	Gas chromatogram of (a) 2040-solvent reference and (b) sample filtrate after removal of solids. . . . .	110
41	Infrared absorption spectrum of organic material filtered from fuel portion of tank bottom samples . . . . .	118
42	Infrared absorption spectrum of corrosion inhibitor DCI-4a . . . . .	119
43	Infrared absorption spectrum of corrosion inhibitor HITEC E515 . . . . .	120
44	Infrared reflectance spectrum of filter Sample POSF-82-S-0318. . . . .	122
45	Copper commutator surface showing dark deposit .	124
46	SEM photographs of commutator surface. . . . .	125
47	Analysis of surface of commutator by energy dispersive x-ray fluorescence. . . . .	126
48	Copper commutator on dark streak . . . . .	128
49	Copper commutator on clean region. . . . .	129
50	Infrared absorption spectrum of acetone extract of sludge solids . . . . .	132
51	Infrared absorption spectra of: a. Dried acetone extract of sludge. b. Reference carboxymethylcellulose . . . . .	133

LIST OF FIGURES (continued)

<u>Number</u>		<u>Page</u>
52	Photomicrographs of particulate material removed from medium, Sample 83-POSF-0840 (top 100x, bottom 400x) . . . . .	135
53	Gas chromatogram of distilled JP-10. . . . .	144
54	Gas chromatogram of distilled RJ-5 . . . . .	145
55	Proton Nuclear Magnetic Resonance spectrum of samples . . . . .	150
56	Integral proton NMR spectrum of Sample 83-POSF-0707 . . . . .	151
57	Integral proton NMR spectrum of Sample 83-POSF-0706 . . . . .	152
58	Integral proton NMR spectrum of Sample 83-POSF-0705 . . . . .	153
59	Gel permeation chromatogram of oil Sample A, 10 $\mu$ L injection of undiluted oil . . . . .	156
60	Gel permeation chromatogram of oil Sample A; repeat run, 10 $\mu$ L injection of undiluted oil . . . . .	157
61	Gel permeation chromatogram of oil Sample A, 30 $\mu$ L injection of oil dilute 30-fold. . . . .	158
62	Gel permeation chromatogram of oil Sample B, 10 $\mu$ L injection of undiluted oil . . . . .	159
63	Gel permeation chromatogram of oil Sample B; repeat run, 10 $\mu$ L injection of undiluted sample . . . . .	160
64	Gel permeation chromatogram of oil Sample B, 30 $\mu$ L injection of oil diluted 30-fold . . . . .	161
65	Gel permeation chromatogram of oil from 1-gallon can, 10 $\mu$ L injection of undiluted oil. . . . .	162
66	Gel permeation chromatogram of oil from 1-gallon can: repeat run, 10 $\mu$ L injection of undiluted sample . . . . .	163

LIST OF FIGURES (continued)

<u>Number</u>		<u>Page</u>
67	Gel permeation chromatogram of oil sample from 1-gallon can, 30 $\mu$ L injection oil diluted 30-fold. . . . .	164
68	Neutralization number titration curves for corrosion inhibitors as marked . . . . .	168
69	Neutralization number titration curves for corrosion inhibitors as marked . . . . .	169
70	Neutralization number titration curves for corrosion inhibitors as marked . . . . .	170
71	Neutralization number titration curves for corrosion inhibitors as marked . . . . .	171
72	Infrared absorption spectrum of method/ column blank . . . . .	191
73	Infrared absorption spectrum of hexane spike with 15 ppm DCI-4A . . . . .	192
74	Infrared spectrum of ion-exchange isolate from fuel 83-POSF-0758. . . . .	193

LIST OF TABLES

<u>Number</u>		<u>Page</u>
1	Hydrocarbon-Type Analysis. . . . .	4
2	Simulated Distillation (ASTM D 2887) . . . . .	7
3	Heat of Combustion . . . . .	11
4	Physical Properties as a Function of Temperature	13
5	Hydrocarbon-Type Analysis of AEDC and NAPC Test Fuels . . . . .	24
6	Physical Properties as a Function of Temperature for AEDC and NAPC Fuels. . . . .	25
7	Simulated Distillation Data for AEDC and NAPC Test Fuels. . . . .	27
8	Heat of Combustion Data for AEDC and NAPC Test Fuels . . . . .	29
9	Properties of Fuels and Fuel Blends from Garrett Turbine Engine Company Tests . . . . .	35
10	Simulated Distillation Data for Garrett Turbine Engine Company Test Fuels. . . . .	36
11	Hydrocarbon-Type Analysis of Garrett Turbine Engine Company Test Fuels. . . . .	37
12	Heat of Combustion of Garrett Turbine Engine Company Test Fuels . . . . .	38
13	Simulated Distillation by ASTM D 2887. . . . .	42
14	Hydrocarbon-Type Analysis. . . . .	43
15	Heat of Combustion . . . . .	44
16	Physical Properties as a Function of Temperature	44
17	Density of JP-4 Specimens. . . . .	48
18	Hydrocarbon-Type Analysis of Six JP-4 Specimens.	49
19	Low Temperature Properties of Test Fuels and Blends . . . . .	50

LIST OF TABLES (continued)

<u>Number</u>		<u>Page</u>
20	Simulated Distillation - ASTM D 2887 . . . . .	51
21	Heat of Combustion (ASTM D 240-76) . . . . .	51
22	Physical Properties as a Function of Temperature	52
23	Hydrocarbon-Type Analysis. . . . .	53
24	Density of Fuel Specimens at 15°C. . . . .	57
25	Heat of Combustion of Carbon Slurry Fuels. . . .	57
26	Simulated Distillation Data for JP-7 and JP-10 Fuels. . . . .	58
27	Components of Light Shale Oil by GC/MS . . . . .	63
28	Composition of Light Shale Oil Vapors. . . . .	66
29	Results of Trace Metal Analysis by ICP Spectrometry . . . . .	69
30	Elemental Analysis of Light Shale Oil POSF-82-D-0321 . . . . .	71
31	Integral Area of Each Type of Proton . . . . .	71
32	Proton Number of Protons by NMR. . . . .	71
33	Non-Hydrocarbon Compounds Detected in Occidental Light Shale Oil. . . . .	80
34	Permissible Workroom Airborne Concentration for Light Shale Oil Hydrocarbon Components . . . .	80
35	Toxicity Data for Light Shale Oil Components or Their Derivatives . . . . .	81
36	Elemental Analyses of Tire Pyrolysis Oil (POSF-82-B-0310) . . . . .	84
37	Hydrocarbon-Type Analysis of Tire Pyrolysis Oil (POSF-82-B-0310) . . . . .	84

**LIST OF TABLES (continued)**

<u>Number</u>		<u>Page</u>
38	Simulated Distillation and Density of Tire Pyrolysis Oil. . . . .	85
39	GC/MS Analysis of Tire Pyrolysis Oil . . . . .	86
40	Major Peak Responses for Tire Pyrolysis Oil Using GC/Nitrogen Selective Detector . . . . .	95
41	Proton NMR Analysis of Sample POSF-82-B-0310 . . . . .	95
42	Hydrocarbon-Type Analysis of Sample POSF-82-C-0301 . . . . .	113
43	Trace Metal Analysis of Fuel by ICP Spectrometry	114
44	Elements Found in the Sample Solids by Energy Dispersive X-Ray Emission. . . . .	116
45	Energy Dispersive X-Ray Emission Analysis of Filter Residue POSF-82-S-0388. . . . .	121
46	Determination of Trace Metals in JP-8 Samples by ICP Spectrometry. . . . .	137
47	Results of Trace Metal Analysis by ICP Spectrometry . . . . .	138
48	Distillation of JP-10. . . . .	141
49	Distillation of RJ-5 . . . . .	142
50	NMR Data for 83-POSF-0707. . . . .	147
51	NMR Data for 83-POSF-0705. . . . .	148
52	NMR Data for 83-POSF-0706. . . . .	149
53	Qualification Data for Corrosion Inhibitors. . . . .	166
54	Emission Spectrographic Data for Corrosion Inhibitors . . . . .	167
55	Corrosion Inhibitor Additives Used in Investigation. . . . .	173
56	Effect of Corrosion Inhibitors on Conductivity of Fuel Containing Stadis 450 Additive . . . . .	175

LIST OF TABLES (continued)

<u>Number</u>		<u>Page</u>
57	Effect of Corrosion Inhibitors on Conductivity of Fuel Containing Tolad 511 Additive. . . . .	176
58	Duplicate Measurements for Selected Corrosion Inhibitors . . . . .	177
59	Simulated Distillation Data. . . . .	179
60	Hydrocarbon-Type Analyses. . . . .	181
61	Elemental Analyses . . . . .	183
62	Mettler/Parr Digital Density Meters. . . . .	187

SECTION I  
INTRODUCTION AND SUMMARY

The Fuels and Lubrication Division of the Aero Propulsion Laboratory has the mission of insuring an adequate supply of dependable fuels for operational use. Attention must be given to every aspect of fuel technology: production, availability, properties, and quality; fuel storage, transportation, distribution, handling, and contamination; fuel additive effects and synthetic fuels for particular weapons systems; and combustion behavior, combustor design, and engine exhaust emissions. Work performed under this contract during this phase of the program has supported these efforts.

R&D support in the form of fuel chemical and physical characterization has also been provided for the Air Force Shale JP-4 production program, for studies correlating properties with engine test data, for low temperature studies and for a number of other Air Force in-house and contractual programs. Total analyses have been conducted on hydrocarbon oils from several alternate sources. Studies and analyses were conducted to determine the nature and source of fuel contaminants which cause filter plugging; to determine the interactive effects of fuel additives; to evaluate the occupational health aspects of light shale oil; and to aid in solving operational problems as they arose.

These and other studies required for research support or problem solving are described in the sections that follow.

## SECTION II

### FUELS CHARACTERIZATION

Conventional fuels in use by the Air Force include grades JP-4, JP-5, JP-7, JP-8, DF-2, and gasoline. The most commonly used fuel is JP-4, a wide-cut fuel of the gasoline type. During the course of this program, a wide variety of conventional, experimental, alternate, and synthetic fuels have been chemically and physically characterized to correlate fuel characteristics with aircraft engine performance. The analyses and measurements presented in this section were conducted either as a part of a variety of on-going Air Force research programs to aid in solving operational problems, or to define fuel composition and properties for specific engineering applications.

While not all programs for which analytical and testing effort was provided required the same measurements, data obtained on most samples included hydrocarbon-type analysis (modified ASTM D 2789 and Monsanto Method 21-PQ-38-63) simulated distillation (ASTM D 2887-73), heat of combustion (ASTM D 240-76), true vapor pressure (see Appendix 1), kinematic viscosity (ASTM D 445-79), surface tension (capillary rise method), and density (dilatometer method, see Appendix 1).

#### 1. COMPLETE CHARACTERIZATION OF FUELS IN SUPPORT OF VARIOUS AIR FORCE PROGRAMS

A variety of fuel samples were characterized in support of on-going Air Force in-house and contractual investigations. Sample numbers and types of fuels are tabulated below.

Type of Fuel	Sample number	Comments
Hydrocrackate Kerosene	POSF-82-D-0163	
JP-8	JP-8P-121481-2	
Jet A Kerosene	POSF-82-D-0165	
JP-4	82-POSF-0412	Fuel for use in Thermal Stability test method evaluation.
JP-4	82-POSF-0413	Fuel for use in Thermal Stability test method evaluation.
JP-4	82-POSF-0480	Fuel for use in Thermal Stability test method evaluation.
Experimental	82-POSF-0481	
Experimental	83-POSF-0483	
Experimental	83-POSF-1007	
Experimental	83-POSF-1008	
JP-5	POSF-82-C-0440	Used in TF-39 Combustor emissions test.
Modified JP-8	POSF-82-C-0199	
JP-4	83-POSF-1083	Analysis shows aromatic content substantially above specification.
-	83-POSF-1004	Used in F100 test and evaluation program.
-	83-POSF-1005	Used in F100 test and evaluation program.
JP-8	83-POSF-0758	Fuel pump failure investigation.
	82-POSF-0161	Derived from light pyrolysis fuel oil.
JP-8 (modified)	83-POSF-0800	Derived from light pyrolysis fuel oil.

Note: Dash indicates type of fuel is unknown.

Hydrocarbon-type analyses were conducted on many of these samples and the results are presented in Table 1, simulated distillation (ASTM D 2887) data are presented in Table 2, heat of combustion (ASTM D 240) results in Table 3, and true vapor pressure, surface tension, density, and kinematic viscosity data in Table 4. ASTM Standard Viscosity/Temperature charts are presented in Figures 1 through 7.

TABLE 1. HYDROCARBON-TYPE ANALYSIS

Compound	Weight percent					
	82-POSF-D-0163		JP-8P-121481-2		82-POSF-D-0165	
	ASTM <sup>a</sup>	Mons. <sup>b</sup>	ASTM <sup>a</sup>	Mons. <sup>b</sup>	ASTM <sup>a</sup>	Mons. <sup>b</sup>
<b>Paraffins</b>						
Cycloparaffins	32.3	33.8 <sup>c</sup>	46.8	47.0 <sup>c</sup>	41.0	39.0 <sup>c</sup>
Dicycloparaffins	21.3	- <sup>c</sup>	32.8	- <sup>c</sup>	35.9	- <sup>c</sup>
Total cycloparaffins	8.7 <sup>d</sup>	- <sup>c</sup>	1.4 <sup>d</sup>	- <sup>c</sup>	2.4 <sup>d</sup>	- <sup>c</sup>
Alkylnzenes	30.0	30.2	34.2 <sup>d</sup>	33.7	38.3 <sup>d</sup>	38.9
Indans and tetralins	16.8	19.7	14.1	16.0	16.7	18.7
Indenes and dihydronaphthalenes	19.1 <sup>c</sup>	15.5	4.1 <sup>c</sup>	3.1	2.1 <sup>c</sup>	1.9
Naphthalenes	- <sup>c</sup>	0.0	- <sup>c</sup>	0.0	- <sup>c</sup>	0.0
	1.8	0.8	0.6	0.1	1.9	1.5
 <b>82-POSF-0412</b>						
	ASTM <sup>a</sup>	Mons. <sup>b</sup>	ASTM <sup>a</sup>	Mons. <sup>b</sup>	ASTM <sup>a</sup>	Mons. <sup>b</sup>
Paraffins	48.1	48.0 <sup>c</sup>	41.1	39.1 <sup>c</sup>	48.6	48.4 <sup>c</sup>
Cycloparaffins	29.2	- <sup>c</sup>	24.7	- <sup>c</sup>	29.0	- <sup>c</sup>
Dicycloparaffins	0.0 <sup>d</sup>	- <sup>c</sup>	0.0 <sup>d</sup>	- <sup>c</sup>	0.0 <sup>d</sup>	- <sup>c</sup>
Total cycloparaffins	29.2 <sup>d</sup>	24.2	24.7 <sup>d</sup>	19.7	29.0 <sup>d</sup>	24.3
Alkylnzenes	9.8	13.5	10.9	15.4	9.7	13.3
Indans and tetralins	2.4 <sup>c</sup>	2.3	3.6 <sup>c</sup>	3.2	2.4 <sup>c</sup>	2.3
Indenes and dihydronaphthalenes	- <sup>c</sup>	0.0	- <sup>c</sup>	0.2	- <sup>c</sup>	0.0
Naphthalenes	10.5	12.0	19.7	22.4	10.3	11.7

(continued)

TABLE 1 (continued)

Compound	Weight percent				Weight percent			
	82-POSF-0481		82-POSF-0483		83-POSF-1007		83-POSF-1007	
	ASTM <sup>a</sup>	Mons. <sup>b</sup>						
Paraffins	49.7	48.1 <sup>c</sup>	79.6	67.2 <sup>c</sup>	64.4	47.8 <sup>c</sup>		
Cycloparaffins	41.3	-c	10.2	-c	14.4	-c		
Dicycloparaffins	0.2 <sup>d</sup>	-c	0.4	-c	0.5	-c		
Total cycloparaffins	41.5 <sup>d</sup>	42.1	10.6 <sup>d</sup>	13.2	14.9 <sup>d</sup>	13.6		
Alkybenzenes	5.7	6.9	9.7	19.6	20.4	38.6		
Indans and tetralins	1.6 <sup>c</sup>	1.4	0.1	0.0	0.3	0.0		
Indenes and dihydronaphthalenes	-c	0.0	-c	0.0	-c	0.0		
Naphthalenes	1.5	1.5	0.0	0.0	0.0	0.0		
83-POSF-1008								
	83-POSF-1008		POSF-82-C-0440		POSF-82-C-1083			
	ASTM <sup>a</sup>	Mons. <sup>b</sup>						
Paraffins	50.5	48.3 <sup>c</sup>	47.0	46.6 <sup>c</sup>	34.6	25.6 <sup>c</sup>		
Cycloparaffins	39.4	-c	33.3	-c	13.8	-c		
Dicycloparaffins	0.4 <sup>d</sup>	-c	1.6	-c	1.8	-c		
Total cycloparaffins	39.8 <sup>d</sup>	40.6	34.9 <sup>d</sup>	34.6	15.6 <sup>d</sup>	13.4		
Alkybenzenes	6.7	8.2	9.5	11.7	45.7	59.2		
Indans and tetralins	1.5 <sup>c</sup>	1.4	7.5 <sup>c</sup>	6.0	3.3 <sup>c</sup>	1.2		
Indenes and dihydronaphthalenes	-c	0.0	-c	0.0	-c	0.0		
Naphthalenes	1.5	1.5	1.1	1.1	0.8	0.6		

(continued)

TABLE 1 (continued)

	Weight percent					
	83-POSF-1004		83-POSF-1005		83-POSF-0758	
	ASTM <sup>a</sup>	Mons. <sup>b</sup>	ASTM <sup>a</sup>	Mons. <sup>b</sup>	ASTM <sup>a</sup>	Mons. <sup>b</sup>
Paraffins	49.2	47.0 <sup>c</sup>	49.3	47.0 <sup>c</sup>	47.0	44.5 <sup>c</sup>
Cycloparaffins	33.2	- <sup>c</sup>	33.1	- <sup>c</sup>	32.3	- <sup>c</sup>
Dicycloparaffins	0.0 <sup>d</sup>	- <sup>c</sup>	0.0 <sup>d</sup>	- <sup>c</sup>	0.3 <sup>d</sup>	- <sup>c</sup>
Total cycloparaffins	33.2	32.1	33.1 <sup>d</sup>	32.2	32.6 <sup>d</sup>	31.6
Alkylbenzenes	13.3	16.7	13.5	16.8	13.6	16.5
Indans and tetralins	2.1 <sup>c</sup>	2.0	2.0 <sup>c</sup>	1.9	2.5 <sup>c</sup>	2.3
Indenes and dihydronaphthalenes	- <sup>c</sup>	0.0	- <sup>c</sup>	0.0	- <sup>c</sup>	0.0
Naphthalenes	2.2	2.2	2.1	2.1	4.3	5.1
<hr/>						
	Weight percent					
	82-POSF-0161		83-POSF-0800		POSF -82-C-0199	
	ASTM <sup>a</sup>	Mons. <sup>b</sup>	ASTM <sup>a</sup>	Mons. <sup>b</sup>	ASTM <sup>a</sup>	Mons. <sup>b</sup>
Paraffins	0.0	0.0 <sup>c</sup>	0.5	0.0 <sup>c</sup>	40.1	42.1 <sup>c</sup>
Cycloparaffins	32.0	- <sup>c</sup>	18.8	- <sup>c</sup>	34.8	- <sup>c</sup>
Dicycloparaffins	61.7 <sup>d</sup>	- <sup>c</sup>	40.3 <sup>d</sup>	- <sup>c</sup>	7.4 <sup>d</sup>	- <sup>c</sup>
Total cycloparaffins	93.7	94.5	59.1 <sup>d</sup>	65.3	42.2 <sup>d</sup>	41.7
Alkylbenzenes	4.3	3.0	6.2	8.0	9.6	10.0
Indans and tetralins	1.7	1.7	32.2 <sup>c</sup>	24.9	5.5	4.0
Indenes and dihydronaphthalenes	- <sup>c</sup>	0.0	- <sup>c</sup>	0.0	-	0.1
Naphthalenes	0.3	0.8	2.0	1.8	2.6	2.1

<sup>a</sup>Modification of ASTM Method D 2789, values converted from volume percent using relative densities.

<sup>b</sup>Monsanto Method 21-PQ-38-63.

<sup>c</sup>Dash indicates method does not provide information on these specific compound categories.

<sup>d</sup>Sum of two preceding values.

TABLE 2. SIMULATED DISTILLATION  
(ASTM D 2887)

Percent recovered	Temperature					
	POSF-82-D-0163 °C	POSF-82-D-0163 °F	JP-8P-121481-2 °C	JP-8P-121481-2 °F	POSF-82-D-0165 °C	POSF-82-D-0165 °F
IBP, 0.5	162	324	107	225	125	257
1	164	328	118	245	130	267
5	170	338	144	292	142	288
10	175	347	156	313	150	302
20	182	360	169	336	159	319
30	188	370	179	354	167	333
40	195	384	187	369	174	345
50	202	396	196	384	180	357
60	209	408	204	399	190	373
70	220	428	213	415	200	392
80	230	446	223	433	216	422
90	247	477	235	455	236	456
95	260	501	246	475	250	482
99	283	542	269	516	267	513
FBP, 99.5	294	562	282	540	274	526

(continued)

TABLE 2 (continued)

Percent recovered	82-POSF-0413			82-POSF-0480			82-POSF-0481			82-POSF-0483			83-POSF-1007		
	°C	°F	°C	°F	°C	°F	°C	°F	°C	°F	°C	°F	°C	°F	°C
IBP, 0.5	40	103	36	97	148	299	31	88	15	59					
1	57	135	54	129	152	306	33	91	27	81					
5	89	192	84	182	178	352	57	135	28	82					
10	93	200	91	196	187	369	89	192	35	95					
20	117	243	109	228	207	404	104	219	59	138					
30	134	274	122	251	217	423	124	256	72	162					
40	161	322	143	289	234	454	131	268	90	194					
50	184	363	167	332	245	474	134	274	98	208					
60	205	401	188	370	261	501	146	296	111	232					
70	224	434	208	406	275	527	149	300	117	243					
80	232	449	228	442	282	540	151	304	138	280					
90	250	483	246	475	297	567	161	323	142	288					
95	263	506	256	494	301	575	175	347	149	300					
99	290	553	287	549	316	600	201	394	168	334					
FBP, 99.5	302	575	305	581	323	614	208	406	174	345					

(continued)

TABLE 2 (continued)

Percent recovered	Temperature			
	83-POSF-1008 °C °F	POSF-82-C-0440 °C °F	83-POSF-1083 °C °F	83-POSF-1004 °C °F
IBP, 0.5	99 210	112 233	34 92	98 208
1	113 235	124 256	35 94	103 217
5	126 259	165 328	59 138	137 279
10	134 273	181 358	74 166	149 300
20	151 304	197 387	111 232	161 322
30	160 320	206 404	143 290	170 338
40	174 345	216 422	159 319	178 352
50	182 360	222 432	157 324	189 372
60	197 387	232 449	165 330	198 388
70	205 401	239 462	174 344	211 412
80	218 424	251 483	206 402	221 430
90	232 450	263 506	237 459	235 455
95	238 460	273 523	258 496	244 471
99	256 493	298 569	293 559	259 498
FBP, 99.5	264 507	309 588	304 579	264 507

(continued)

TABLE 2 (continued)

Percent recovered	Temperature							
	83-POSF-1005 °C °F	83-POSF-0758 °C °F	82-POSF-0161 °C °F	83-POSF-0800 °C °F	83-POSF-0800 °C °F	83-POSF-0800 °C °F		
IBP, 0.5	98	208	98	209	117	243	120	247
1	104	219	102	216	138	280	144	292
5	137	279	136	278	181	357	187	360
10	149	300	150	302	186	367	193	379
20	160	320	164	328	196	385	199	391
30	169	336	175	347	200	392	207	404
40	177	351	183	361	208	406	215	419
50	188	370	196	384	214	418	223	434
60	198	388	203	398	221	430	232	449
70	210	410	216	422	232	450	241	466
80	220	428	227	441	244	471	252	485
90	235	455	239	462	259	499	265	509
95	244	471	252	485	273	524	279	534
99	260	500	270	519	307	585	311	591
FBP, 99.5	268	514	279	535	320	607	322	612

TABLE 3. HEAT OF COMBUSTION

<u>Sample</u>	<u>Gross Btu/lb</u>	<u>Net Btu/lb</u>	<u>Percent hydrogen</u>
POSF-82-D-0163	19,538 19,573 Avg. 19,555	18,369	13.00 <sup>a</sup>
JP-8P-121481-2	19,794		
JP-8 Tank WA-10	19,811		
	Avg. 19,803	18,522	14.04 <sup>a</sup>
POSF-82-D-0165	19,821 19,803 Avg. 19,812	18,549	13.84 <sup>a</sup>
82-POSF-0481	20,086 20,117 Avg. 20,102	$\Delta H_n = 20,102 - 91.23H^b$	
82-POSF-0483	20,395 20,371 Avg. 20,383	$\Delta H_n = 20,383 - 91.23H^b$	
83-POSF-1007	20,100 20,090 Avg. 20,095	$\Delta H_n = 20,095 - 91.23H^b$	
83-POSF-1008	20,078 20,113 Avg. 20,096	$\Delta H_n = 20,096 - 91.23H^b$	
POSF-82-C-0440	19,785 19,832 Avg. 19,808	18,505	13.95 <sup>a</sup>
83-POSF-1083	19,480 19,450 Avg. 19,465 Redetermination 19,443	$\Delta H_n = 19,465 - 91.23H^b$	

(continued)

TABLE 3. (continued)

Sample	Gross Btu/lb	Net Btu/lb	Percent hydrogen
83-POSF-1004	20,119 20,077 Avg. 20,098	$\Delta H_n = 20,098 - 91.23H^b$	
83-POSF-1005	19,942 19,946 Avg. 19,944	$\Delta H_n = 19,944 - 91.23H^b$	
83-POSF-0758	19,904 19,873 Avg. 19,888	$\Delta H_n = 19,888 - 91.23H^b$	
82-POSF-0161	19,618 19,640 Avg. 19,629	$\Delta H_n = 19,629 - 91.23H^b$	
83-POSF-0800	19,292 19,335 Avg. 19,314	$\Delta H_n = 19,314 - 91.23H^b$	

<sup>a</sup>Data supplied by AFWAL/POSF for calculation of net heat of combustion.

<sup>b</sup>The value for hydrogen content of the sample is not available at this time. Net heat of combustion can be calculated by this equation when percent H is obtained.

Note:  $\Delta H_n$  = net heat of combustion, Btu/lb.

H = hydrogen content of sample, %.

TABLE 4. PHYSICAL PROPERTIES AS A  
FUNCTION OF TEMPERATURE

Sample	Temperature, °F	Vapor pressure, mm/Hg	Kinematic viscosity, centistokes	Density, g/cm <sup>3</sup>	Surface tension, dyne cm <sup>-1</sup>
POSF-82-D-0163	-20.0	1.0 <sup>a</sup>	-	-	-
	32.0	4.5	-	-	-
	59.0	-	-	0.7972	-
	70.0	10.0	-	-	-
	100.0	17.0	-	-	-
JP-8P-121481-2	-20.0	<1.0 <sup>a</sup>	-	-	-
	32.0	2.5	-	-	-
	59.0	-	-	0.7951	-
	70.0	6.0	-	-	-
	100.0	10.5	-	-	-
POSF-82-D-0165	-20.0	1.0 <sup>a</sup>	-	-	-
	32.0	2.5	-	-	-
	59.0	-	-	0.8317	-
	70.0	5.0	-	-	-
	100.0	7.0	-	-	-
82-POSF-0481	59.0	-	-	0.7793	-
82-POSF-0483	59.0	-	-	0.7130	-
83-POSF-1007	59.0	-	-	0.7232	-
83-POSF-1008	59.0	-	-	0.7813	-
POSF-82-C-0440	-30.0	1.2 <sup>a</sup>	10.38	0.8436	-
	32.0	4.0	3.340	0.8188	-
	59.0	-	-	0.8081	-
	70.0	8.0	2.124	0.8033	-
	100.0	13.0	1.601	0.7917	-
	140.0	22.0	-	-	-
83-POSF-1083	-30.1	-	2.058	-	-
	-20.0	5.5 <sup>a</sup>	1.835	0.8337	28.7 <sup>b</sup>
	-4.0	-	1.548	-	-
	32.0	25.0	1.142	0.8113	26.2
	59.0	-	-	0.7996	-
	70.0	60.0	0.8730	0.79487	24.5
	100.0	114.0	0.7215	0.7819	23.0
	140.0	234.0	-	-	-

(continued)

TABLE 4. (continued)

Sample	Temperature, °F	Vapor pressure, mm/Hg	Kinematic viscosity, centistokes	Density, g/cm <sup>3</sup>	Surface tension, dyne cm <sup>-1</sup>
83-POSF-1004	-20	2.0 <sup>a</sup>	4.040	0.8244	30.4 <sup>b</sup>
	32	7.0	2.096	0.8020	27.9
	59	-	-	0.7905	-
	70	13.0	1.460	0.7857	25.9
	100	21.0	1.152	0.7728	24.4
	140	38.0	0.877	0.7557	22.5
83-POSF-1005	-20	1.2 <sup>a</sup>	3.923	0.8210	30.1 <sup>b</sup>
	32	5.0	2.046	0.8004	27.7
	59	-	-	0.7898	-
	70	10.0	1.436	0.7855	25.9
	100	17.0	1.128	0.7736	24.4
	140	33.0	0.865	0.7578	22.7
83-POSF-0758	-30	-	5.03	-	-
	-20	1.5 <sup>a</sup>	4.360	0.8242	30.6 <sup>b</sup>
	32	5.2	3.333	0.8038	28.0
	59	-	2.123	0.7925	-
	70	11.0	1.493	0.7881	26.1
	100	18.0	1.172	0.7759	24.6
82-POSF-0161	-20	4.0 <sup>a</sup>	12.458	0.9040	34.3 <sup>b</sup>
	32	8.5	4.886	0.8837	31.9
	59	-	-	0.8735	-
	70	13.0	2.980	0.8698	30.1
	100	18.0	2.161	0.8575	28.7
	140	26.0	-	-	-
83-POSF-0800	-20	3.6 <sup>a</sup>	13.316	0.9264	35.7 <sup>b</sup>
	32	7.5	4.897	0.9066	33.2
	59	-	-	0.8963	-
	70	12.0	2.927	0.8918	31.3
	100	16.0	2.121	0.8794	29.9
	140	24.0	-	-	-

<sup>a</sup>Value determined by extrapolation of Log P versus 1/T relationship.<sup>b</sup>Obtained by linear regression extrapolation of data.

Note: Dash indicates value not determined.

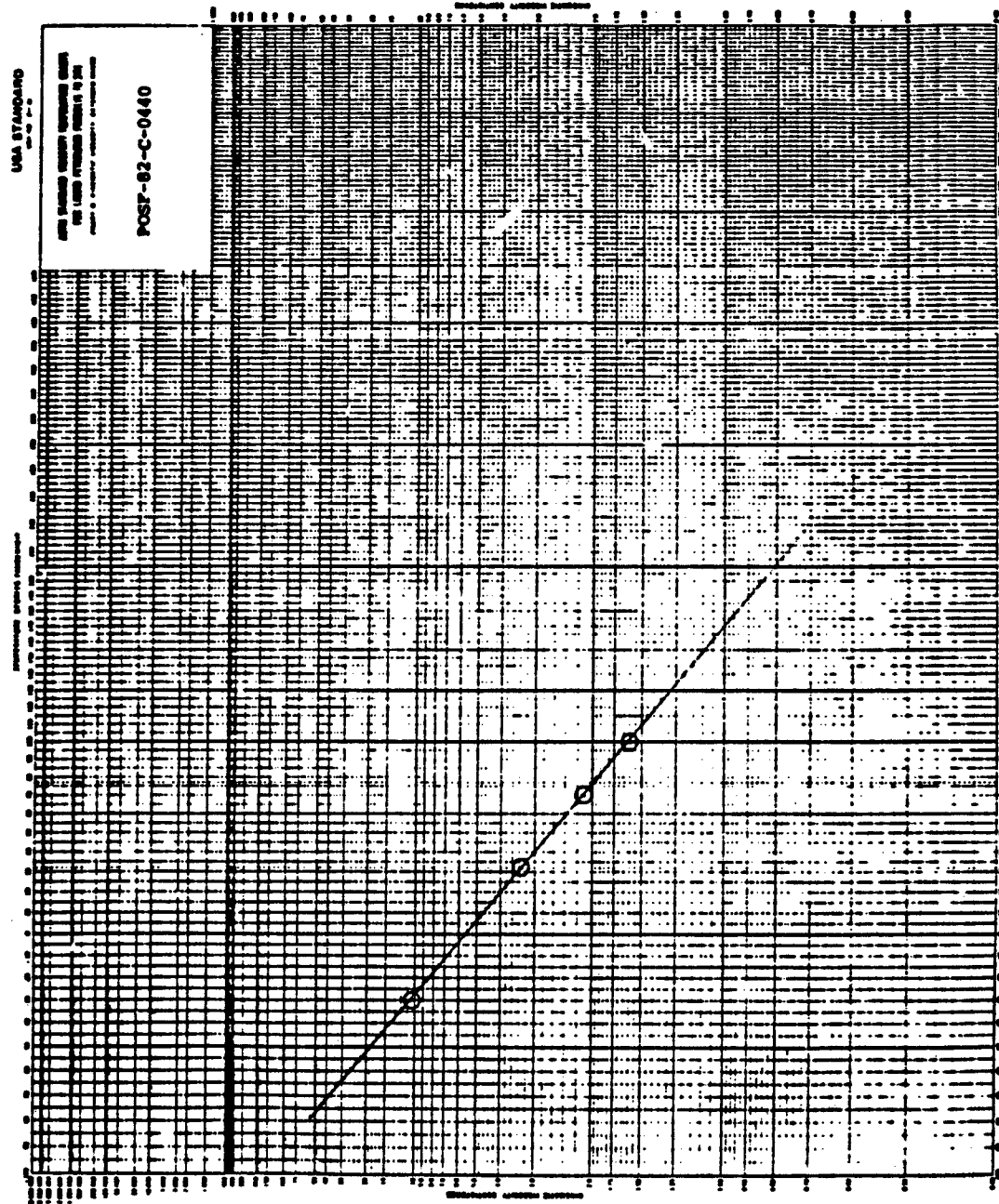


Figure 1. Kinematic viscosity as a function of temperature for sample POSF-82-C-0440.

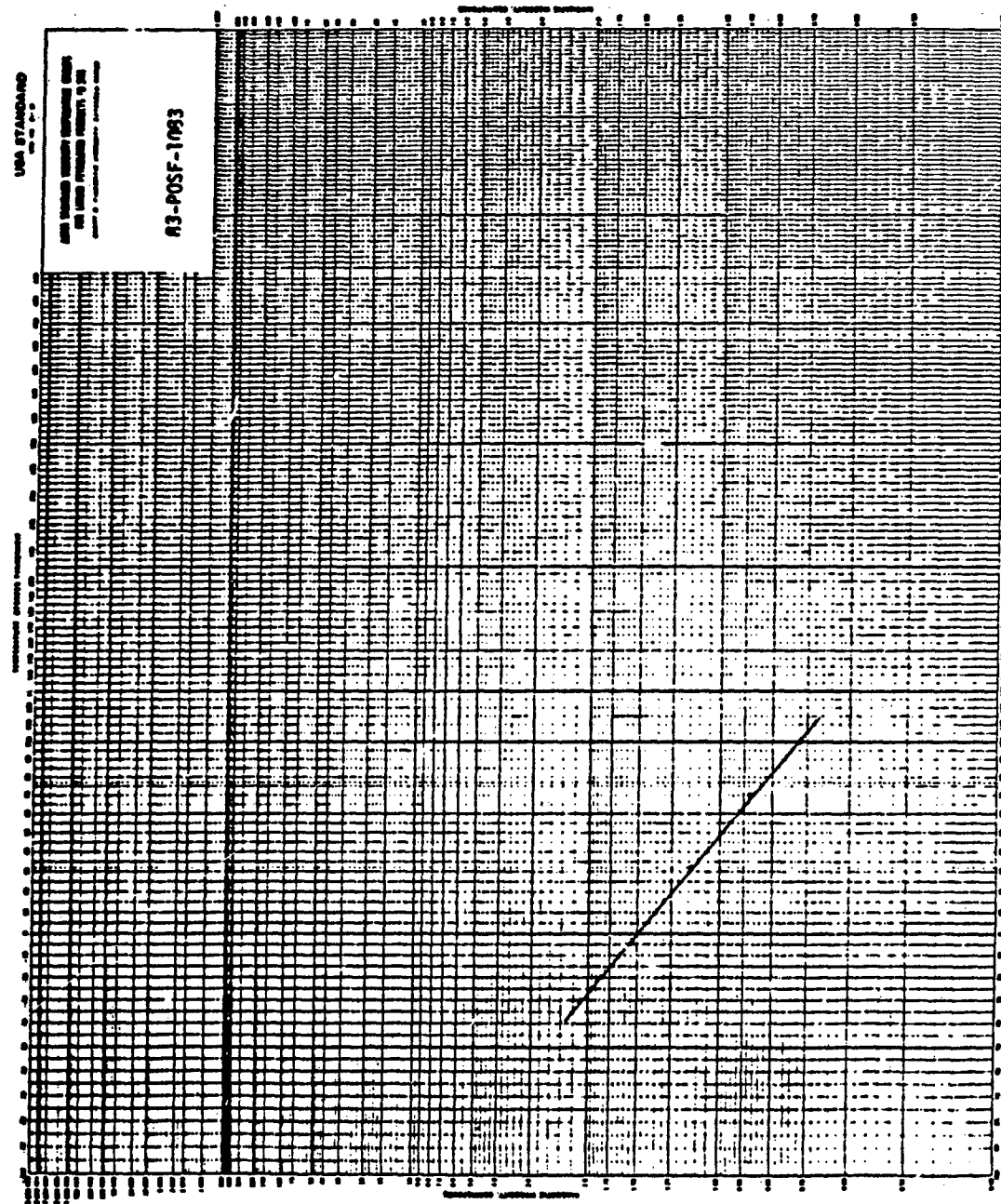


Figure 2. Viscosity plot for Sample 83-POSF-1083.

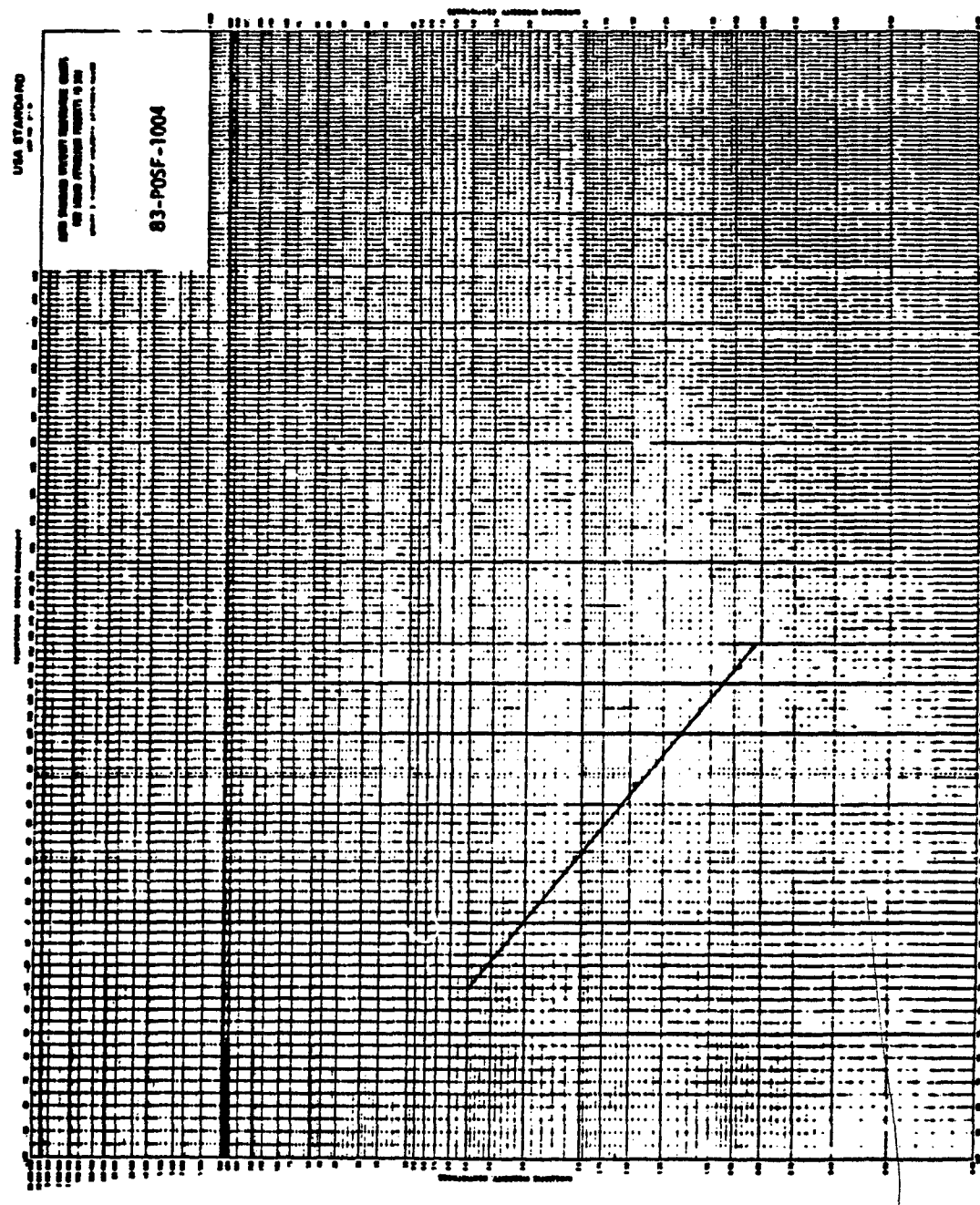


Figure 3. Viscosity plot for Sample 83-POSF-1004.

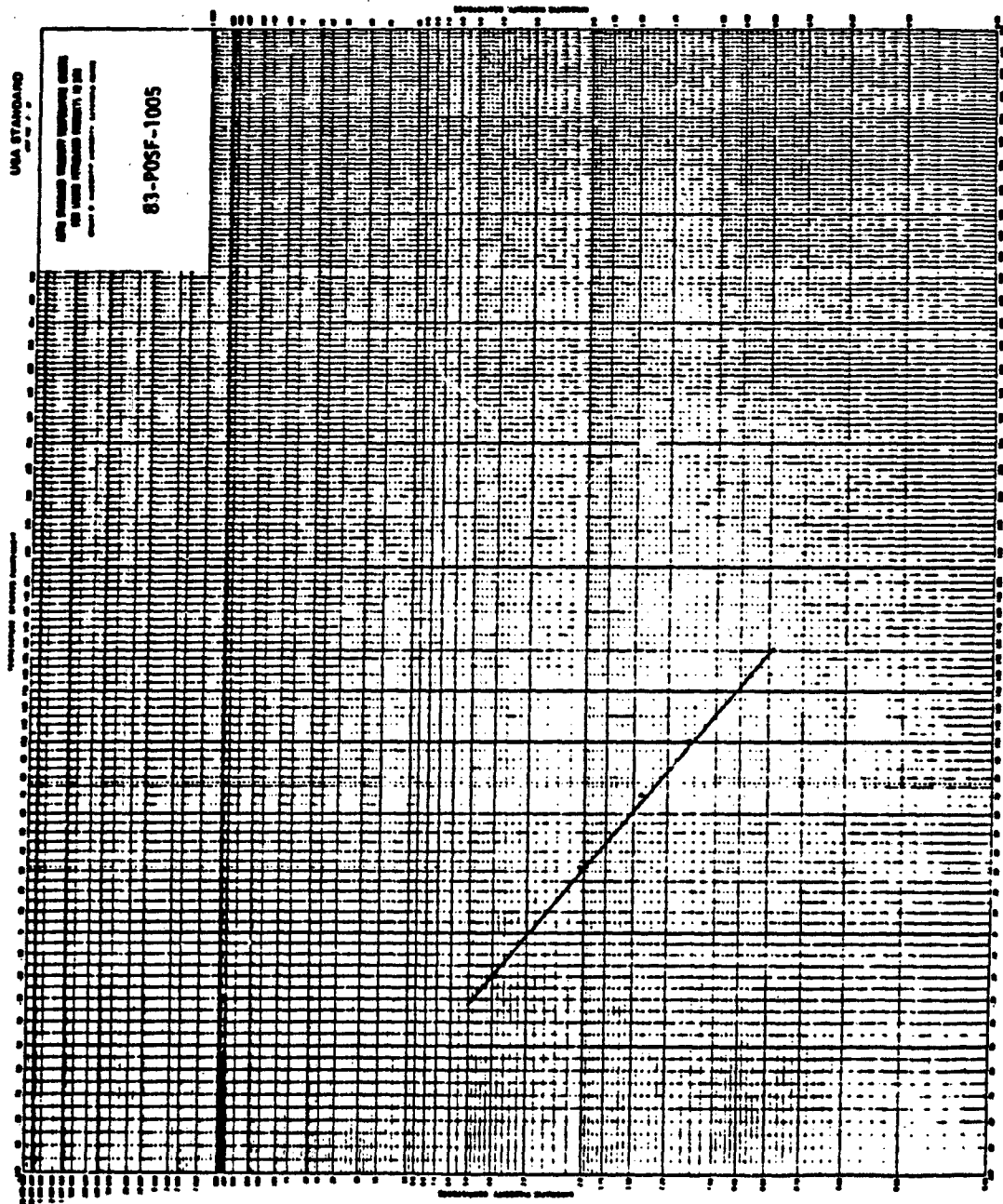


Figure 4. Viscosity plot for Sample 83-POSF-1005.

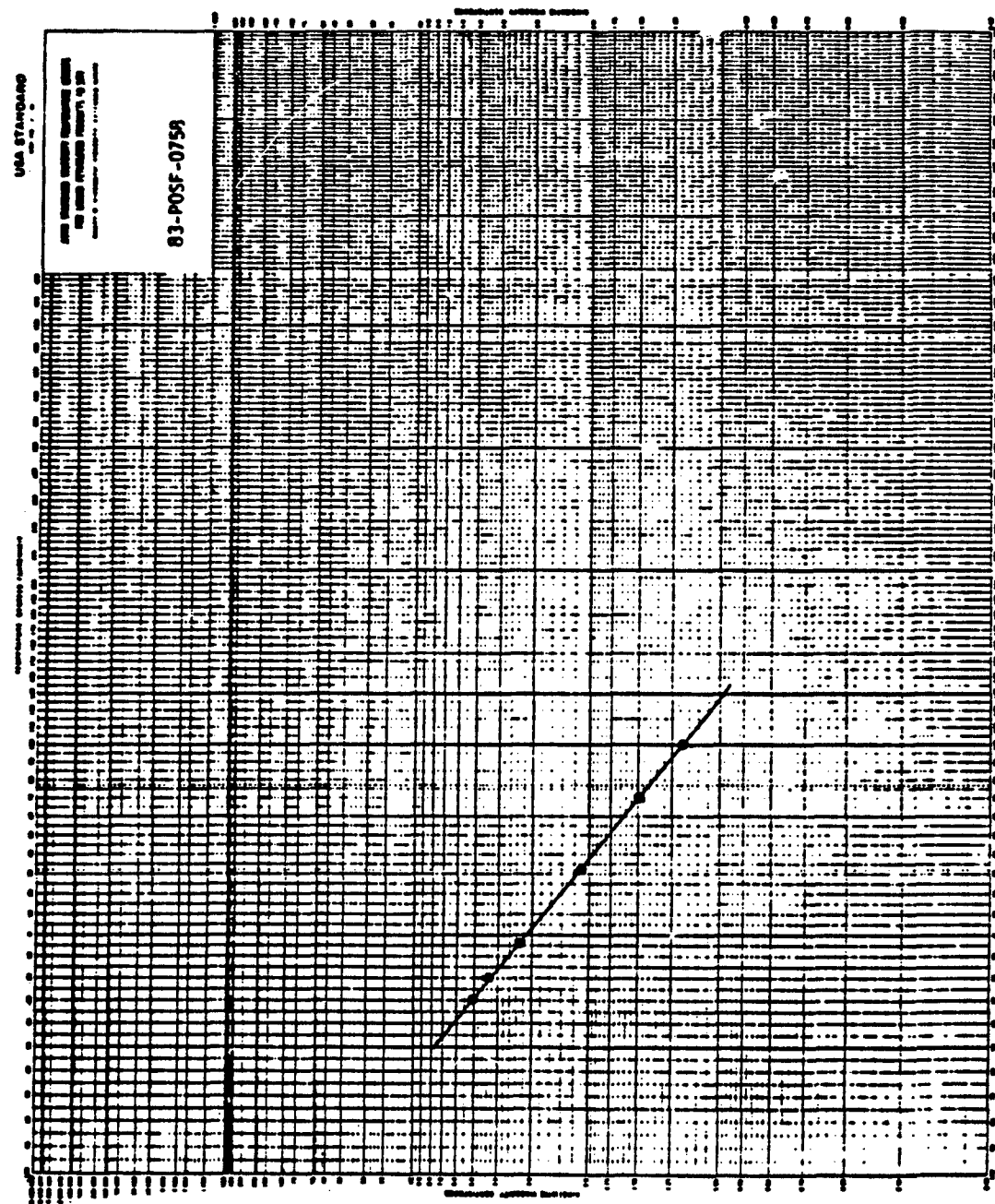


Figure 5. Viscosity plot for Sample 83-POSF-0758.

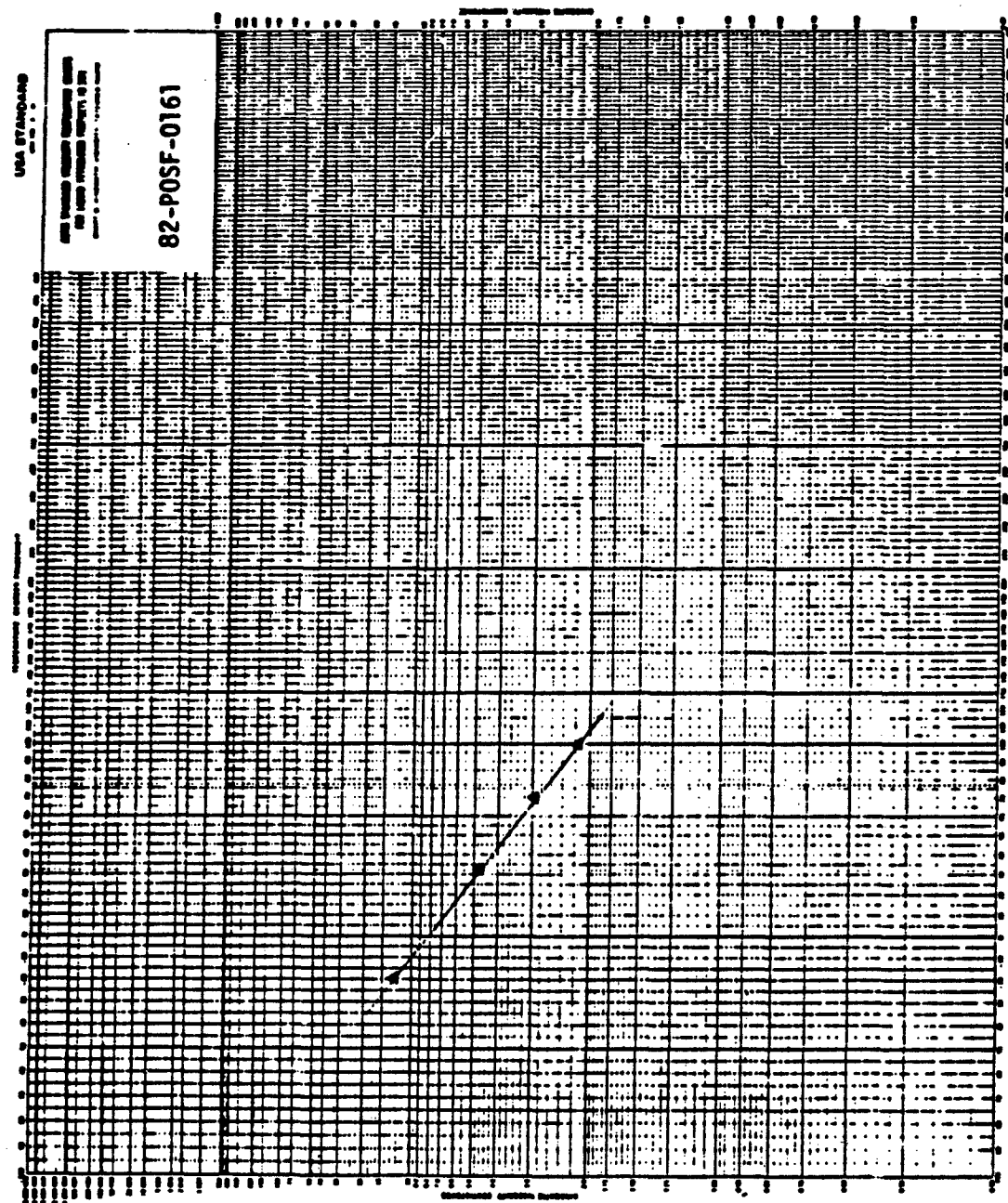


Figure 6. Viscosity plot for Sample 83-POSF-0161.

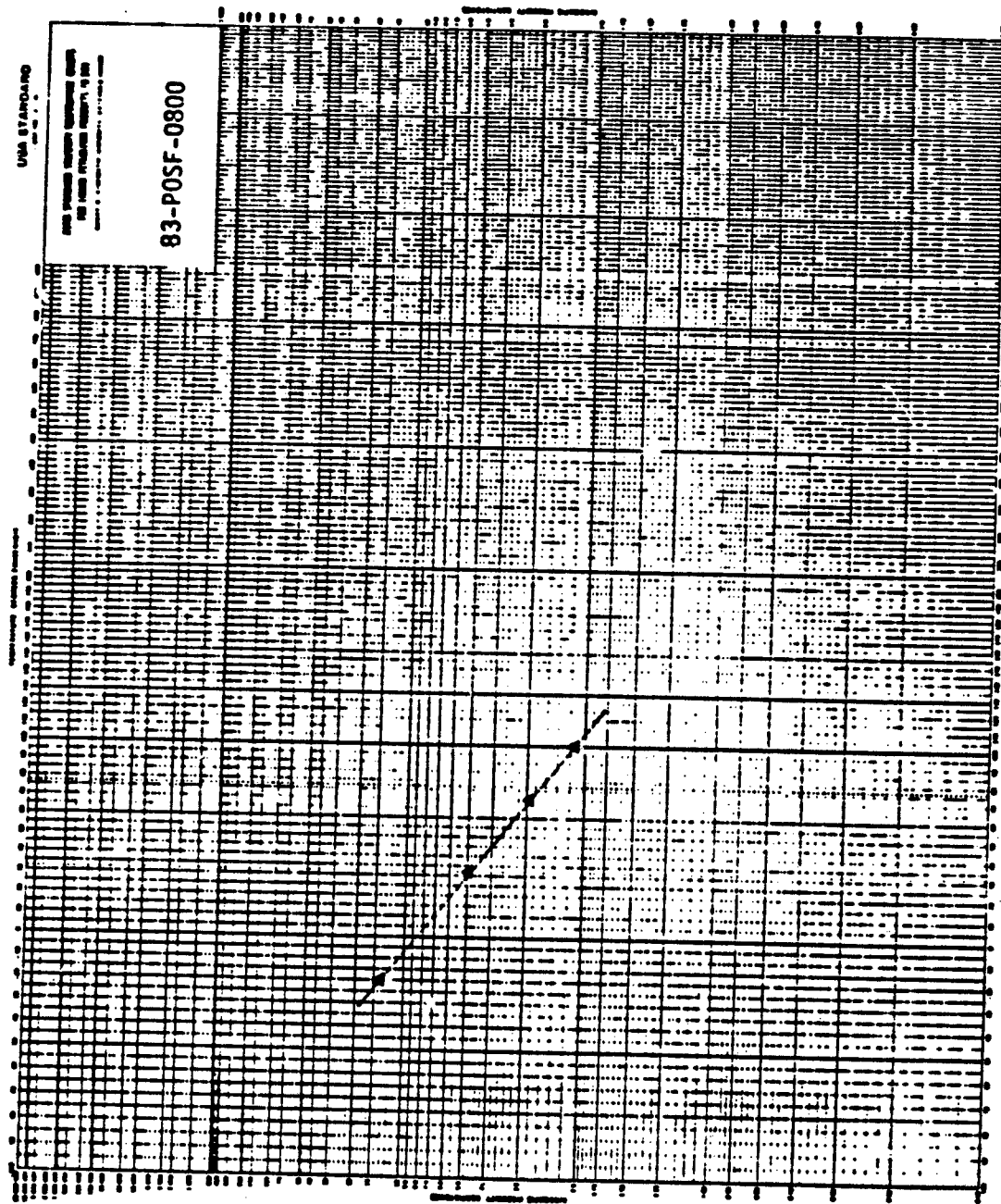


Figure 7. Chart of kinematic viscosity and extended range for 83-POSF-0800.

Trace metals and peroxide analyses were conducted on several samples (82-POSF-0412, 82-POSF-0413, and 82-POSF-0480) in this group. Trace metals analytical results are discussed and tabulated in Section IV, Subsection 8. The peroxide analyses were conducted by ASTM Method D 3703-78 which provides a minimum detectability of 0.1 ppm. No peroxides were detected in any of the three fuels tested.

Mass spectral hydrocarbon-type analyses were performed by two methods which cover different average carbon number ranges. The Monsanto method gives best results for samples having average carbon numbers in the C<sub>12</sub>-C<sub>13</sub> range. The ASTM method is preferred for samples of lower average carbon numbers. For most of the samples, results from the two methods agree fairly well. Sample 83-POSF-1007 is an exception however, having an average carbon number of 6.4 and, consequently, being best suited for analysis by the modified ASTM D 2789. Results by the Monsanto method, in this case, are considerably less accurate.

As a part of the support work conducted on the JP-8 fuels, an attempt was made to determine the presence or absence of a corrosion inhibitor in sample 83-POSF-0758. That investigation is described in Section V, Subsection 8.

## 2. CHARACTERIZATION OF AEDC AND NAPC TEST FUELS

The following fuels were characterized in support of Arnold Engineering Development Center (AEDC) and Naval Air Propulsion Test Center (NAPC) test programs.

Type of Fuel	Sample number	Comments
JP-5	POSF-82-C-0154	Used in AEDC F100 afterburner tests.
JP-4	POSF-82-C-0316	Used in AEDC F100 afterburner tests.

(continued)

Type of Fuel	Sample number	Comments
AEDC Blend 5	VN-81-116	-
AEDC Blend 6	VN-81-119	-
JP-4	POSF-82-D-0196	Used in NAPC tests of TF-30 Augmentor.
JP-5	POSF-82-D-0311	Used in NAPC tests of TF-30 Augmentor.
-	NAPC #1, 01-05-82	-
-	NAPC #4, 12-23-81	-
-	NAPC #5, 01-07-82	-
-	NAPC #6, 01-08-82	-
-	NAPC #7, 01-07-82	-
-	NAPC #8, 12-16-81	-
JP-5	VN-82-165	Navy Shale II
DFM	VN-82-166	Navy Shale II
DFM	POSF-82-5-0184	Petroleum-derived
JP-4	82-POSF-0428	
JP-4	82-POSF-0429	
JP-4	82-POSF-0619	

Note: Dash indicates type of sample unknown.

Data required for these AEDC and NAPC programs include most of the analyses and fuel properties listed in Subsection 1 of this Section. Data are presented in Tables 5 through 8. ASTM viscosity plots are shown in Figures 8 through 11.

### 3. CHARACTERIZATION OF TEST FUELS AND BLENDS FROM GARRETT TURBINE ENGINE COMPANY TESTS

Certain aircraft fuels which had been used in tests at Garrett Turbine Engine Company were characterized. Sample names and identification are listed below.

TABLE 5. HYDROCARBON-TYPE ANALYSIS OF AEDC AND NAPC TEST FUELS

Compound	Weight percent			Weight percent			Weight percent		
	POSF-82-C-0154 D 2789 <sup>a</sup>	Mons. B D 2789 <sup>a</sup>	POSF-82-C-0316 D 2789 <sup>a</sup>	Mons. B D 2789 <sup>a</sup>	POSF-82-D-0196 D 2789 <sup>a</sup>	Mons. B D 2789 <sup>a</sup>	POSF-82-D-0311 D 2789 <sup>a</sup>	Mons. B D 2789 <sup>a</sup>	
<b>Paraffins</b>									
Cycloparaffins	36.2	38.2 <sup>c</sup>	48.9	46.9 <sup>c</sup>	61.0	57.4 <sup>c</sup>	33.6	36.3 <sup>c</sup>	
Dicycloparaffins	32.7	- <sup>c</sup>	19.1	- <sup>c</sup>	17.7	- <sup>c</sup>	32.6	- <sup>c</sup>	
Total cycloparaffins	7.7	- <sup>c</sup>	7.0 <sup>c</sup>	- <sup>c</sup>	6.2 <sup>c</sup>	- <sup>c</sup>	6.3 <sup>c</sup>	- <sup>c</sup>	
Alkylbenzenes	40.4	40.3	26.1 <sup>d</sup>	24.7	23.9 <sup>d</sup>	27.9	40.9 <sup>d</sup>	39.8	
Indans and tetralins	13.2	14.1	20.2	24.5	10.2	12.1	12.8	13.5	
Indenes and dihydronaphthalenes	7.5 <sup>c</sup>	5.1	3.2 <sup>c</sup>	2.8	2.8	2.4	6.1	4.5	
Naphthalenes	2.7	2.1	1.6	1.1	2.1	0.2	0.1	0.1	
<b>VN-82-165</b>									
<b>Weight percent</b>			<b>Weight percent</b>			<b>Weight percent</b>			
D 2789 <sup>a</sup>	Mons. B D 2789 <sup>a</sup>	D 2789 <sup>a</sup>	D 2789 <sup>a</sup>	Mons. B D 2789 <sup>a</sup>	D 2789 <sup>a</sup>	D 2789 <sup>a</sup>	Mons. B D 2789 <sup>a</sup>	D 2789 <sup>a</sup>	
<b>Paraffins</b>									
Cycloparaffins	41.7	45.1 <sup>c</sup>	43.3	46.7 <sup>c</sup>	35.3	36.7 <sup>c</sup>	26.1	- <sup>c</sup>	
Dicycloparaffins	29.0	- <sup>c</sup>	26.7	- <sup>c</sup>	- <sup>c</sup>	5.3 <sup>d</sup>	- <sup>c</sup>	- <sup>c</sup>	
Total cycloparaffins	2.0 <sup>c</sup>	- <sup>c</sup>	2.9 <sup>d</sup>	- <sup>c</sup>	- <sup>c</sup>	- <sup>c</sup>	- <sup>c</sup>	- <sup>c</sup>	
Alkylbenzenes	31.0 <sup>d</sup>	31.1	29.6 <sup>d</sup>	28.6	31.4 <sup>d</sup>	29.0	- <sup>c</sup>	- <sup>c</sup>	
Indans and tetralins	12.2	14.1	8.2	9.0	9.8	10.5	- <sup>c</sup>	- <sup>c</sup>	
Indenes and dihydronaphthalenes	13.5 <sup>c</sup>	9.1	14.5 <sup>c</sup>	10.3	10.3	7.2	0.8	0.8	
Naphthalenes	1.6	0.6	4.4	3.6	13.2	15.8	- <sup>c</sup>	- <sup>c</sup>	

<sup>a</sup>Modification of ASTM Method D 2789, values converted from volume percent using relative densities.

<sup>b</sup>Monsanto Method 21-PQ-38-63.

<sup>c</sup>Dash indicates method does not provide information on these specific compound categories.  
<sup>d</sup>Sum of two preceding values.

TABLE 6. PHYSICAL PROPERTIES AS A FUNCTION OF TEMPERATURE  
FOR AEDC AND NAPC FUELS

	<u>°F</u>	<u>Vapor pressure, mm/Hg</u>	<u>Kinematic viscosity, centistokes</u>	<u>Density, g/cm<sup>3</sup></u>	<u>Surface tension, dyne cm<sup>-1</sup></u>
POSF-82-C-0154	-20	<1 <sup>a</sup>	7.657	0.8502	32.98 <sup>b</sup>
	32	3	3.182	0.8298	30.14
	70	6	2.037	0.8139	28.24
	100	9	1.543	0.8016	26.53
	140	17	- <sup>c</sup>	-	-
	180	27	-	-	-
POSF-82-D-0316	-20	8.5	2.189	0.7993	28.2 <sup>b</sup>
	32	27	1.292	0.7771	25.7
	59	-	-	0.7652	-
	70	64	0.9664	0.7608	23.8
	100	115	0.7963	0.7470	22.4
POSF-82-D-0196	-20	9.5 <sup>a</sup>	2.072	0.7882	27.6 <sup>b</sup>
	32	32	1.243	0.7653	25.0
	70	77	0.9312	0.7481	23.1
	100	144	0.7711	0.7355	21.6
POSF-82-D-0311	-20	1.4 <sup>a</sup>	8.595	0.8483	30.5 <sup>b</sup>
	32	3.6	3.438	0.8273	28.6
	59	-	-	0.8163	-
	70	7.2	2.184	0.8119	26.9
	100	11.5	1.636	0.7997	25.6
VN-82-165 Navy Shale II JP-5	59	-	-	0.8073	-
VN-82-166 Navy Shale II DFM	59	-	-	0.8346	-
POSF-82-S-1084 Petroleum de- rived DFM	59	-	-	0.8453	-
VN-81-118 (Blend #5)	-20	2 <sup>a</sup>	-	-	-
	32	5	-	-	-
	70	10	-	-	-
	100	16	-	-	-
	140	29	-	-	-
	180	48	-	-	-

(continued)

TABLE 6 (continued)

	<u>°F</u>	<u>Vapor pressure, mm/Hg</u>	<u>Kinematic viscosity, centistokes</u>	<u>Density, g/cm<sup>3</sup></u>	<u>Surface tension, dyne cm<sup>-1</sup></u>
VN-81-118 (Blend #6)	-20	2	- <sup>c</sup>	-	-
	32	6	-	-	-
	70	10	-	-	-
	100	15	-	-	-
	140	21	-	-	-
	180	32	-	-	-
NAPC #1, 01-05-82	70	-	-	0.8233	27.6
	100	-	-	0.8114	26.4
NAPC #4, 12-23-81	70	-	-	0.8127	27.3
	100	-	-	0.8015	26.1
NAPC #570 01-07-82	-	-	-	0.8109	26.9
	100	-	-	0.7995	25.7
NAPC #6, 01-08-82	70	-	-	0.8338	27.9
	100	-	-	0.8223	26.9
NAPC #7, 01-07-82	70	-	-	0.8407	27.8
	100	-	-	0.8290	26.6
NAPC #8, 12-16-81	70	-	-	0.8258	27.6
	100	-	-	0.8140	26.7
82-POSF-0428	0	8.3 <sup>a</sup>	-	-	-
	32	18	-	-	-
	59	-	-	0.8089	-
	70	41	-	-	-
	100	72	-	-	-
82-POSF-0429	0	8.9 <sup>a</sup>	-	-	-
	32	19	-	-	-
	59	-	-	0.8141	-
	70	40	-	-	-
	100	72	-	-	-
82-POSF-0618	0	8.0 <sup>a</sup>	-	-	-
	32	18	-	-	-
	59	-	-	0.8127	-
	70	40	-	-	-
	100	70	-	-	-

<sup>a</sup>Value determined by extrapolation of log P versus 1/T relationship.

<sup>b</sup>Obtained by linear regression extrapolation of data.

<sup>c</sup>Dash indicates value was not determined.

TABLE 7. SIMULATED DISTILLATION DATA FOR  
AEDC AND NAPC TEST FUELS

<u>Percent recovered</u>	Temperature					
	POSF-82-C-0154		POSF-82-C-0316		POSF-82-D-0196	
	<u>°C</u>	<u>°F</u>	<u>°C</u>	<u>°F</u>	<u>°C</u>	<u>°F</u>
IBP, 0.5	134	274	30	85	31	88
1	144	291	36	98	42	107
5	166	330	63	145	58	137
10	174	347	82	179	62	144
20	188	371	98	208	74	166
30	198	388	117	242	92	197
40	208	407	136	276	118	244
50	218	424	155	310	173	343
60	228	442	173	343	194	381
70	236	457	195	384	208	406
80	248	478	216	422	221	429
90	260	500	238	460	237	458
95	271	520	253	488	250	481
99	302	576	278	533	286	547
FBP, 99.5	317	603	288	550	300	572

(continued)

TABLE 7 (continued)

Percent recovered	Temperature					
	82-POSF-0428		82-POSF-0429		82-POSF-0618	
	°C	°F	°C	°F	°C	°F
IBP, 0.5	48	119	51	124	47	117
1	70	157	76	168	70	158
5	98	202	107	225	103	218
10	109	229	122	252	120	247
20	149	301	162	324	157	315
30	180	356	194	380	187	368
40	214	417	227	440	222	431
50	237	459	250	483	245	473
60	260	500	271	520	267	513
70	284	543	296	565	293	560
80	314	597	322	612	320	608
90	344	652	354	669	351	664
95	369	596	375	708	373	704
99	406	764	409	768	409	768
FBP, 99.5	417	783	418	784	418	784

TABLE 8. HEAT OF COMBUSTION DATA FOR AEDC AND NAPC TEST FUELS

	<u>Gross, btu/lb</u>	<u>Net, btu/lb</u>	<u>% H<sup>a</sup></u>
POSF-82-C-0154	19,780		
	19,787		
	Aver. 19,784	18,533	13.71
POSF-82-C-0316	20,006		
	19,965		
	Aver. 19,986	18,689	14.22
POSF-82-D-0196	20,141		
	20,188		
	Aver. 20,164	18,825	14.68
POSF-82-D-0311	19,760		
	19,762		
	Aver. 19,761	18,506	13.76

<sup>a</sup>Data supplied by AFWAL/POSF for calculation of net heat of combustion. Equation used for calculation:  

$$\Delta H_n = \Delta H_g - 91.23 (\%H)$$
.

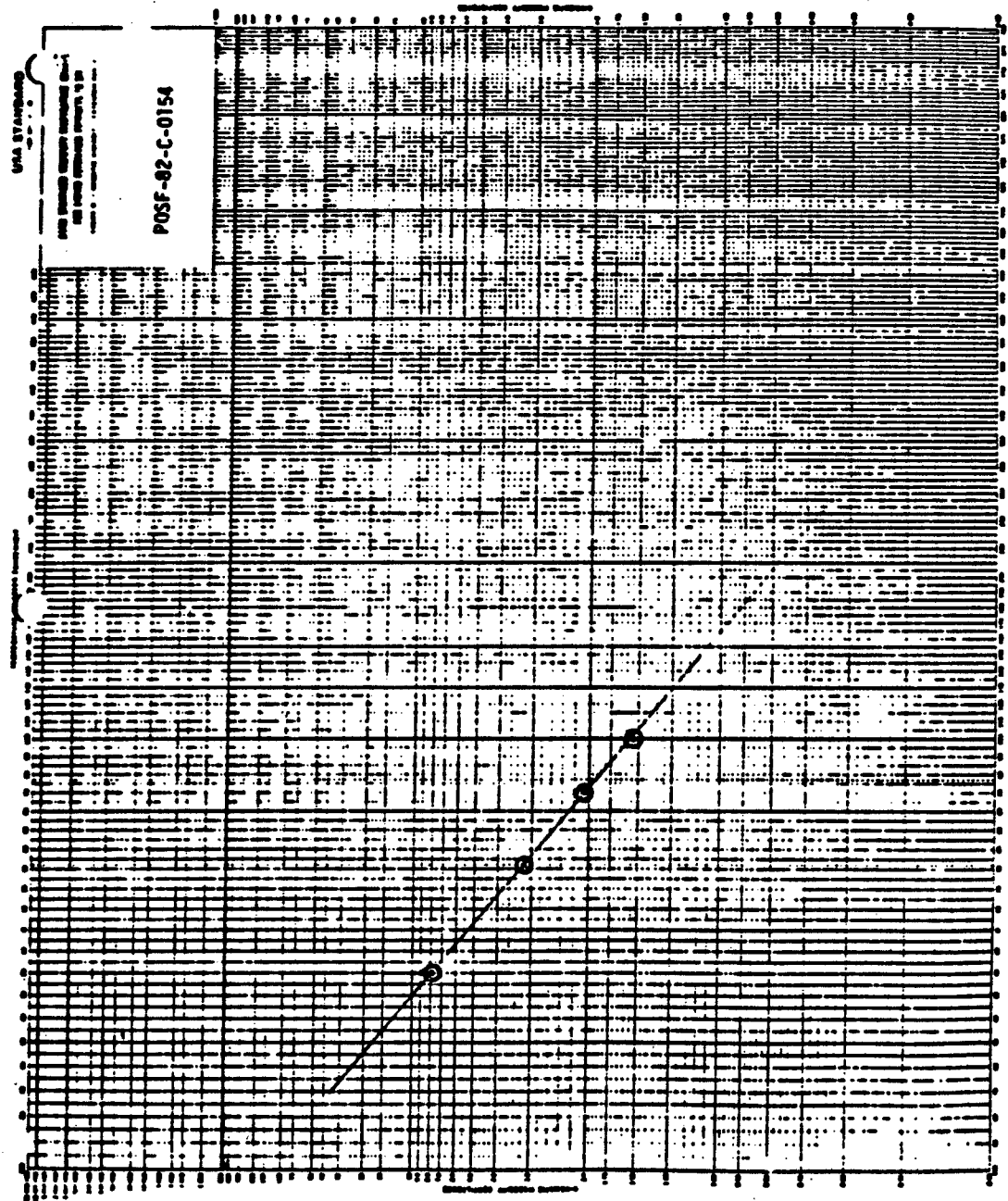


Figure 8. Viscosity plot for Sample POSF-82-C-0154.

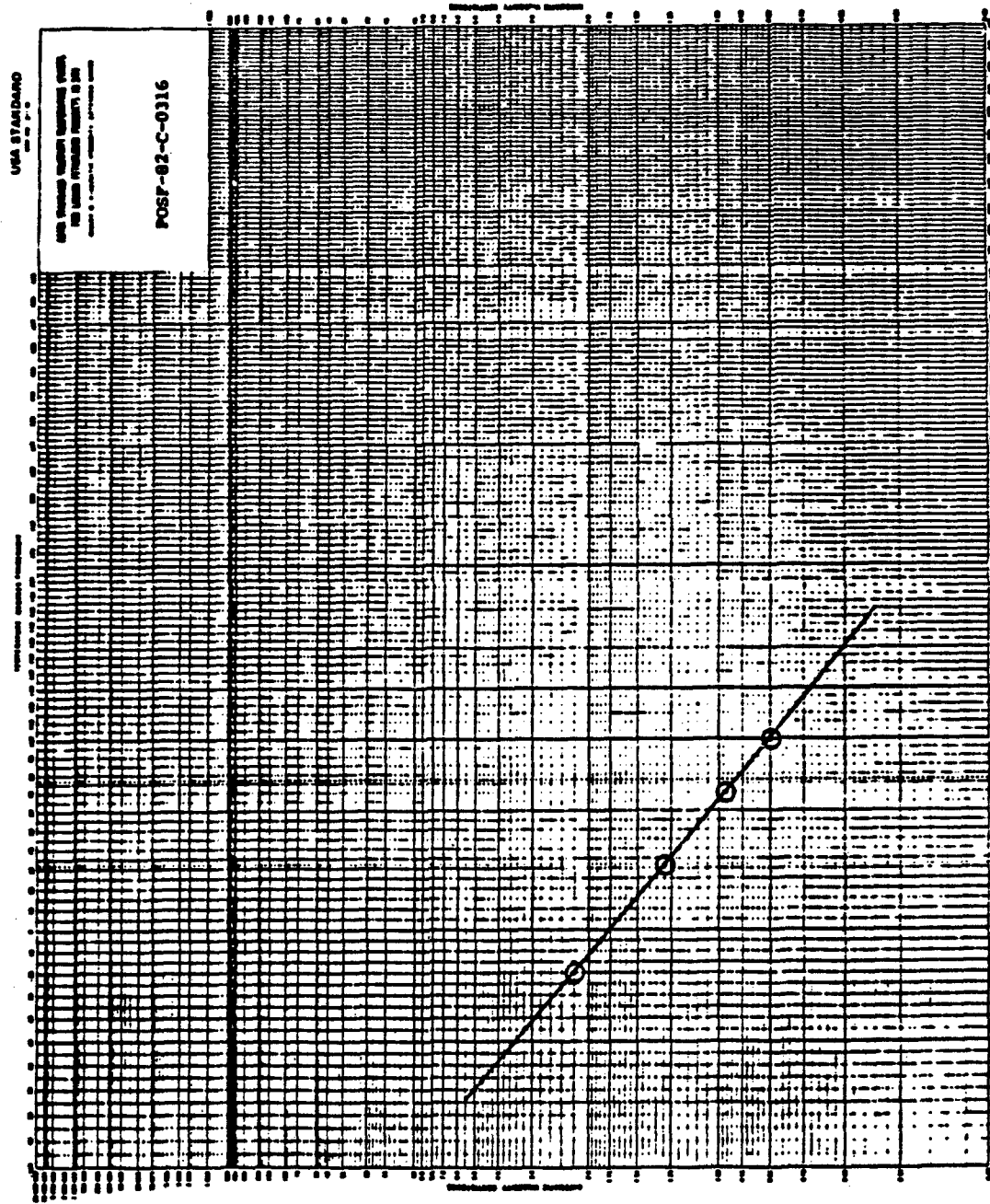


Figure 9. Viscosity plot for Sample POSF-82-C-0316.

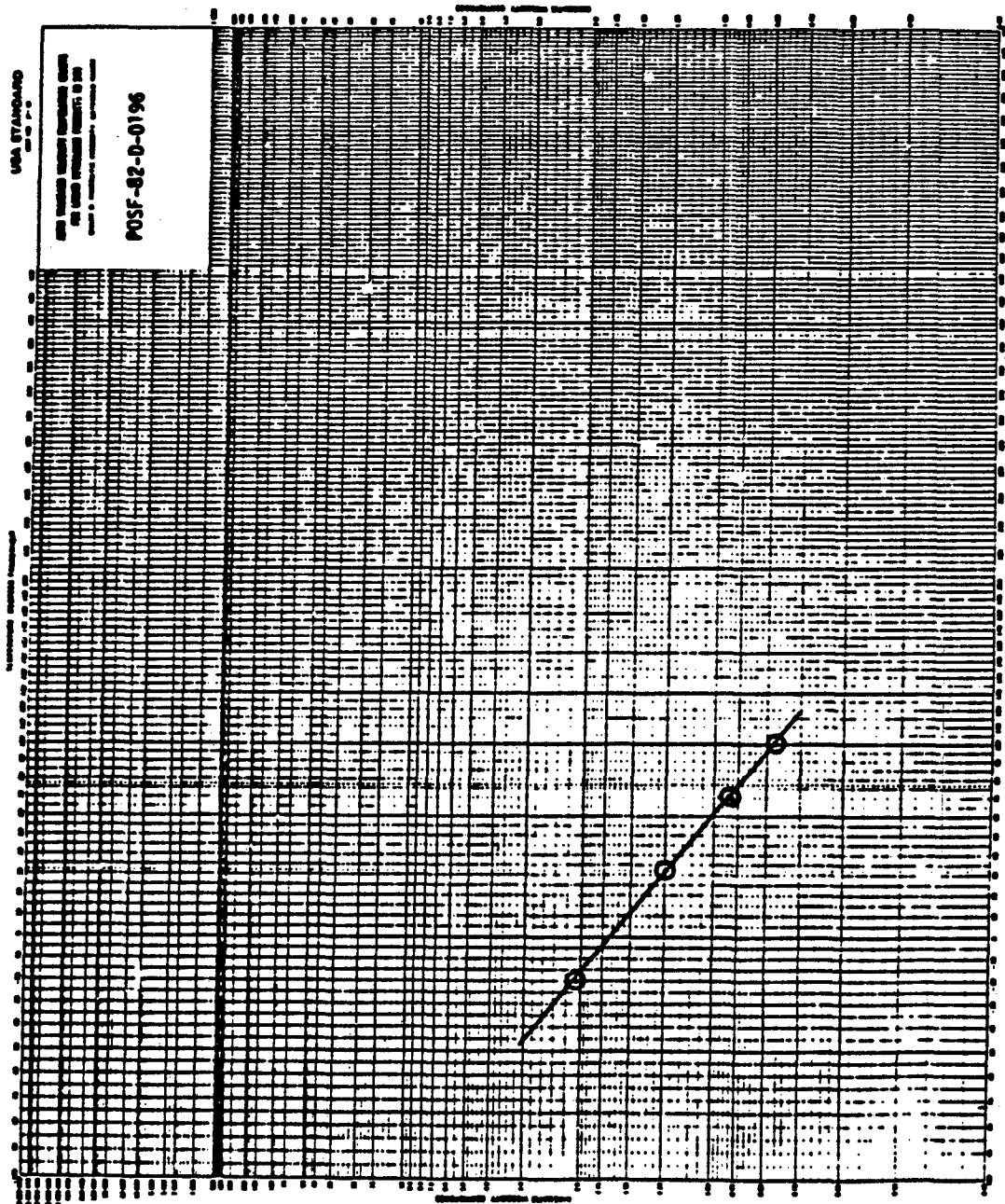


Figure 10. Viscosity plot for Sample POSF-82-D-0196.

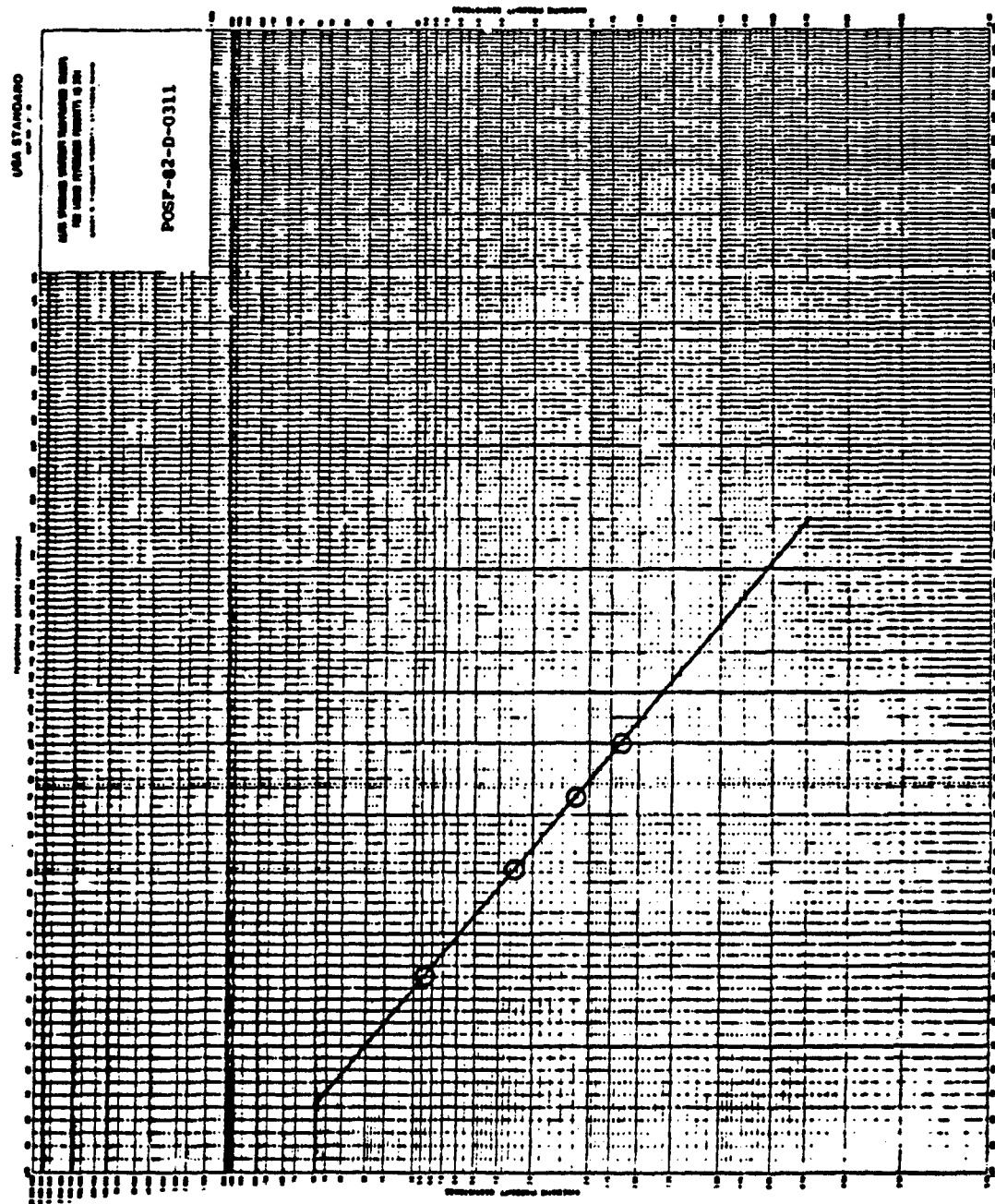


Figure 11. Viscosity plot for Sample POSF-82-D-0311.

Type of Fuel	Sample number	Comments
JP-5	POSF-82-D-0314	Used in auxillary power unit tests.
Modified Blend 3	POSF-82-C-0394	-
Blend	POSF-82-S-0357	Used in auxillary power unit tests.
JP-4	82-POSF-0367	-

Hydrocarbon-type analyses and physical property results are presented in Tables 9 through 12. Standard viscosity charts are presented in Figures 12 through 14.

#### 4. CHARACTERIZATION OF FUELS FOR CORRELATION WITH ENGINE TEST DATA OBTAINED BY ANOTHER AIR FORCE CONTRACTOR

Three fuel samples coded as follows:

83-POSF-0744 (JP-4)  
 83-POSF-0745 (JP-5)  
 83-POSF-0746 (DF-2)

were characterized for correlation with results of engine tests obtained by another Air Force contractor under contract F33615-82-C-2225. Testing and analytical results are presented in Tables 13 through 16 and in Figures 15 through 17.

Hydrocarbon-type analyses were conducted using the modified ASTM D 2789 and Monsanto 21-PQ-38-63 Methods. Additionally the DF-2 sample (83-POSF-0746) was analyzed by the ASTM D 2425 procedure. This analysis is preceded by separation of the sample into aromatic and non-aromatic fractions by elution chromatography (ASTM D 2549). The D 2425 analysis is more suitable for the DF-2 than either of the other methods.

TABLE 9. PROPERTIES OF FUELS AND FUEL BLENDS FROM  
GARRETT TURBINE ENGINE COMPANY TESTS

	<u>Density, g/cc</u>	<u>Kinematic viscosity, centistokes</u>	<u>Vapor pressure, mm/Hg</u>	<u>Surface tension, dyne cm<sup>-1</sup></u>
POSF-82-D-0314				
-20°F	0.8555	8.733	3.0 <sup>a</sup>	32.1 <sup>b</sup>
32°F	0.8345	3.474	5.8	29.7
59°F	0.8235	- <sup>c</sup>	- <sup>c</sup>	- <sup>c</sup>
70°F	0.8190	2.200	9.6	27.8
100°F	0.8070	1.648	13.5	26.5
POSF-82-C-0394				
-20°F	0.8592	- <sup>d</sup>	3.8 <sup>a</sup>	30.9 <sup>b</sup>
32°F	0.8329	2.795	14	28.6
59°F	0.8218	- <sup>c</sup>	- <sup>c</sup>	- <sup>c</sup>
70°F	0.8174	1.847	31	26.8
100°F	0.8049	1.416	52	25.4
140°F	- <sup>c</sup>	- <sup>c</sup>	98	- <sup>c</sup>
82-POSF-0367				
-20°F	0.8112	1.919	9.0 <sup>a</sup>	29.2 <sup>b</sup>
32°F	0.7893	1.155	32	26.3
59°F	0.7771	- <sup>c</sup>	- <sup>c</sup>	- <sup>c</sup>
70°F	0.7731	0.879	68	242
100°F	0.7588	0.731	115	22.5

<sup>a</sup>Value determined by extrapolation of log P versus 1/T vapor pressure relationship.

<sup>b</sup>Obtained by linear regression extrapolation of data.

<sup>c</sup>Dash indicates value not determined.

<sup>d</sup>Formation of crystal at this temperature prevented making the measurement.

TABLE 10. SIMULATED DISTILLATION DATA FOR GARRETT TURBINE  
ENGINE COMPANY TEST FUELS

Percent recovered	Temperature					
	82-D-0314		82-C-0394		82-POSF-0367	
	°C	°F	°C	°F	°C	°F
IBP, 0.5	116	242	53	127	16	61
1	131	268	58	137	18	64
5	163	325	92	198	93	199
10	179	355	119	246	103	217
20	191	376	160	321	115	239
30	197	387	176	348	123	253
40	206	402	202	396	135	275
50	215	420	219	426	143	289
60	226	439	236	456	150	302
70	237	458	254	490	163	326
80	251	484	281	538	174	345
90	263	506	319	607	190	373
95	272	522	347	657	200	392
99	291	556	390	734	224	436
FBP, 99.5	299	571	402	755	239	462

TABLE 11. HYDROCARBON-TYPE ANALYSIS OF GARRETT  
TURBINE ENGINE COMPANY TEST FUELS

Compound	Weight percent					
	POSF-82-D-0314 D 2789 <sup>a</sup>	POSF-82-S-0357 Mons. <sup>b</sup>	POSF-82-C-0394 D 2789 <sup>a</sup>	POSF-82-C-0394 Mons. <sup>b</sup>	82-POSF-0367 D 2789 <sup>a</sup>	82-POSF-0367 Mons. <sup>b</sup>
Paraffins	31.3	33.3	44.8	40.7	40.7	37.7
Cycloparaffins	29.4	-c	33.2	-c	27.6	-c
Dicycloparaffins	12.2	-c	2.9	-c	0.5	-c
Total cycloparaffins	41.6 <sup>d</sup>	40.9	36.1 <sup>d</sup>	38.1	28.1 <sup>d</sup>	26.8
Alkylbenzenes	12.2	13.0	8.0	9.7	21.4	25.7
Indans and tetralins	8.8	6.9	6.2	5.1	4.7	4.2
Indenes and dihydronaphthalenes	-c	0.5	-c	0.7	-c	0.0
Naphthalenes	6.1	5.4	4.9	5.7	5.0	5.5
					0.4	0.1

<sup>a</sup>Modification of ASTM Method D 2789, values converted from volume percent using relative densities.

<sup>b</sup>Monsanto Method 21-PQ-38-63.

<sup>c</sup>Dash indicates method does not provide information on these specific compound categories.

<sup>d</sup>Sum of two preceding values.

TABLE 12. HEAT OF COMBUSTION OF GARRETT TURBINE  
ENGINE COMPANY TEST FUELS

<u>Sample</u>	<u>Gross, Btu/lb</u>	<u>Net, Btu/lb</u>	<u>Percent hydrogen</u>
POSF-82-D-0314	19,753		
	19,774		
	Aver. 19,764	18,519	13.65 <sup>a</sup>
POSF-82-C-0394	19,616		
	19,606		
	Aver. 19,611	18,416	13.10 <sup>a</sup>
82-POSF-0367	19,831		
	19,884		
	Aver. 19,858	18,605	13.73 <sup>a</sup>

<sup>a</sup>Data supplied by AFWAL/POSF for calculation of  
net heat of combustion.

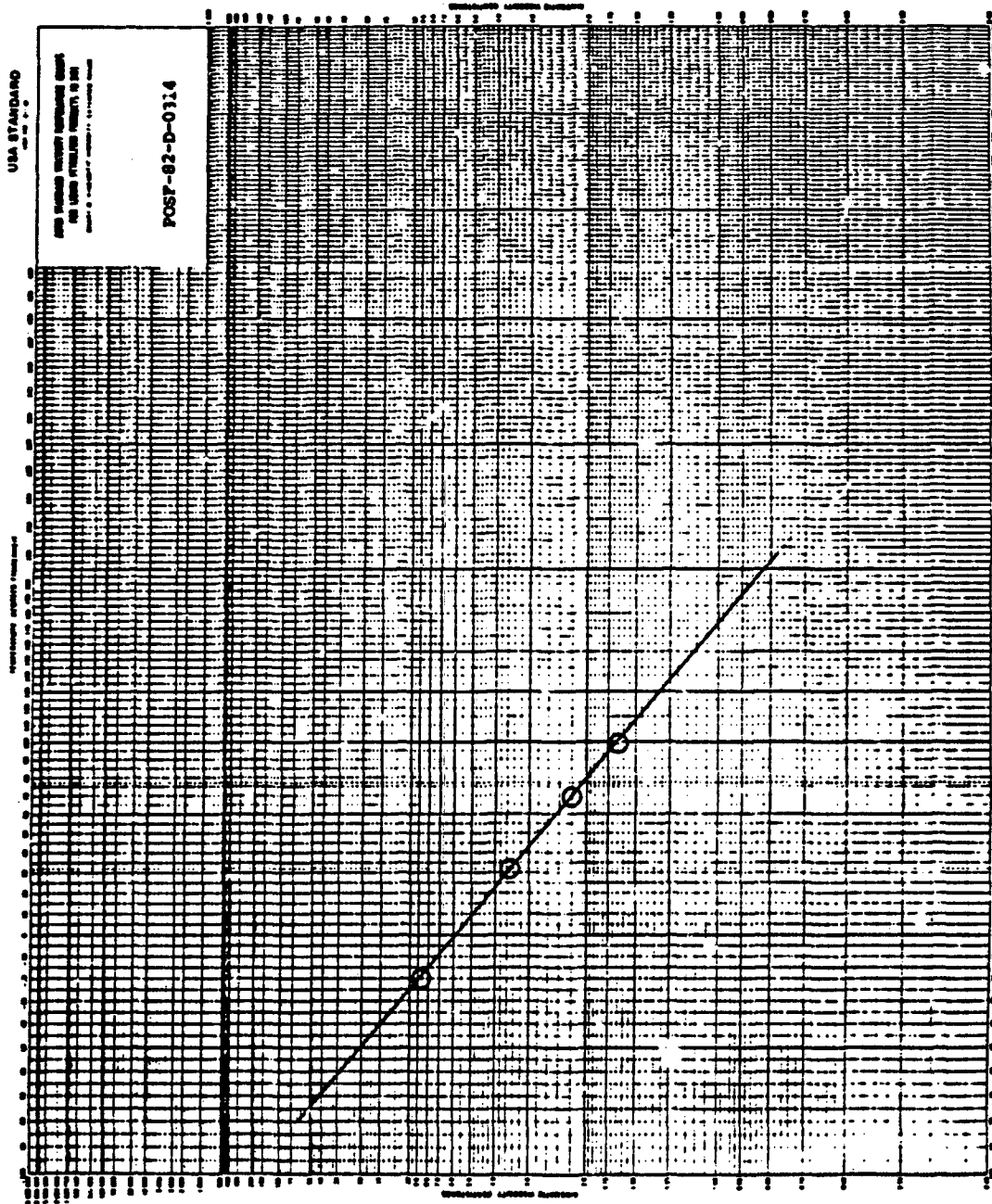


Figure 12. Viscosity plot for Sample POSS-82-D-0314.

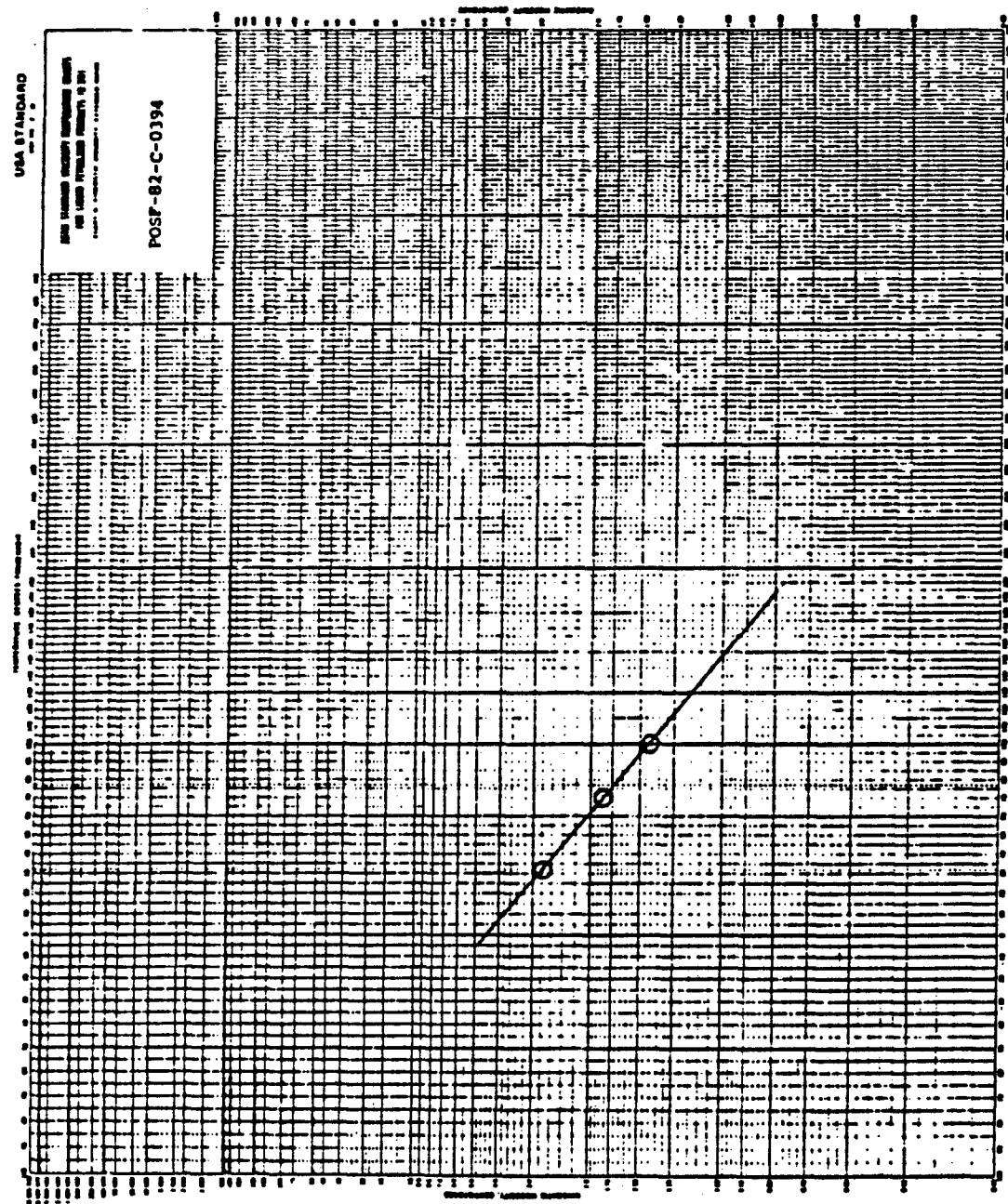


Figure 13. Viscosity plot for Sample POST-82-C-0394.

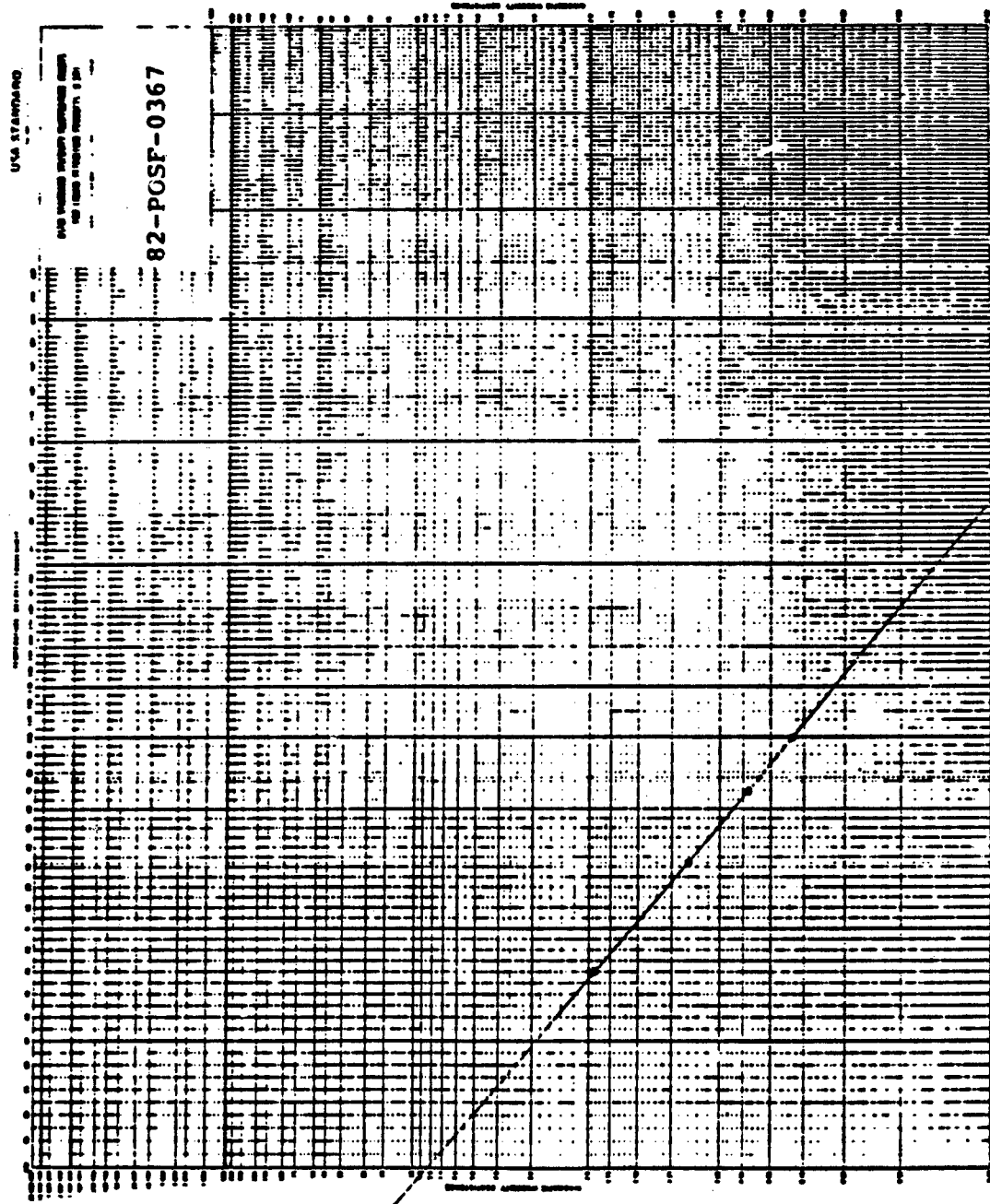


Figure 14. Viscosity plot for Sample 82-POSF-0367.

TABLE 13. SIMULATED DISTILLATION BY ASTM D 2887

<u>% Recovered</u>	Temperature					
	83-POSF-0744		83-POSF-0745		83-POSF-0746	
	<u>°C</u>	<u>°F</u>	<u>°C</u>	<u>°F</u>	<u>°C</u>	<u>°F</u>
IBP, 0.5	29	84	138	280	124	254
1	35	94	146	294	140	284
5	54	130	167	332	178	353
10	60	140	176	349	195	383
20	84	184	190	374	214	417
30	97	207	199	391	228	443
40	117	242	209	408	244	471
50	139	282	218	424	256	493
60	164	328	226	438	270	519
70	188	370	234	453	288	550
80	213	415	243	470	306	583
90	235	455	255	491	330	625
95	250	482	264	507	348	658
99	270	519	284	544	382	719
FBP, 99.5	281	538	295	563	394	742

TABLE 14. HYDROCARBON-TYPE ANALYSIS

	83-POSF-0744		Weight Percent		83-POSF-0746	
	ASTM a	Mons. b	ASTM a	Mons. b	ASTM a	Mons. b
Paraffins	56.5	48.1	38.3	38.0	42.8	42.2
Monocycloparaffins	22.0	-d	35.7	-	31.2	-
Dicycloparaffins	2.8	-	3.8	-	1.4	-
Tricycloparaffins	-	-	-	-	-	-
Total Cycloparaffins	24.8 <sup>e</sup>	25.8	39.7 <sup>e</sup>	39.2	32.7 <sup>e</sup>	30.7
Alkylbenzenes	14.5	22.7	12.5	14.9	9.1	10.8
Indans and Tetrailins	3.2	3.4	7.2	5.7	7.0	5.4
Indenes	-f	0.0	-	0.0	-	0.8
Naphthalene	-f	-f	-f	-f	-f	-f
Naphthalenes	1.0	0.0	2.5	2.2	8.5	10.1
Acenaphthenes	-	-	-	-	-	-
Acenaphthylenes	-	-	-	-	-	-
Tricylic Aromatics	-	-	-	-	-	-
Total Aromatics	18.7	26.1	22.2	22.9	24.6	27.1

<sup>a</sup>Modification of ASTM D 2789, values converted from volume percent using relative densities.

<sup>b</sup>Monsanto Method 21-PQ-38-63.

<sup>c</sup>ASTM Method D 2425 used.

<sup>d</sup>Dash indicates that method does not provide information on this compound class.

<sup>e</sup>Total of above values for cycloparaffins.

<sup>f</sup>The single compound naphthalene is not included in value for naphthalenes in this method.

TABLE 15. HEAT OF COMBUSTION

	<u>Gross Btu/lb</u>	<u>Net Btu/lb</u>	<u>% H<sup>a</sup></u>
83-POSF-0744	20,018		
	19,989		
	Aver. 20,004	18,715	14.13
83-POSF-0745	19,709		
	19,749		
	Aver. 19,729	18,485	13.64
83-POSF-0746	19,502		
	19,468		
	Aver. 19,485	18,314	12.95

<sup>a</sup>Data supplied by AFWAL/POSF for calculation of net heat of combustion. Equation used for calculation:  
 $\Delta H_n = \Delta H_g - 91.23 (\%H)$ .

TABLE 16. PHYSICAL PROPERTIES AS A FUNCTION OF TEMPERATURE

	<u>Vapor pressure mm/Hg</u>	<u>Kinematic viscosity, centistokes</u>	<u>Density, g/cm<sup>3</sup></u>	<u>Surface tension, dyne cm<sup>-1</sup></u>
83-POSF-0744				
-20°F	7.2 <sup>a</sup>	1.785	0.7931	27.3 <sup>b</sup>
32°F	34	1.124	0.7722	24.8
59°F	-	-	0.7593	-
70°F	82	0.8570	0.7549	22.9
100°F	155	0.7153	0.7414	21.4
83-POSF-0745				
-20°F	<1 <sup>a</sup>	7.104	0.8487	31.2 <sup>b</sup>
32°F	2.4	3.139	0.8288	29.0
59°F	-	-	0.8176	-
70°F	5.0	2.034	0.8133	27.4
100°F	8.5	1.527	0.8020	26.1
83-POSF-0746				
-20°F	freezes	freezes	freezes	freezes
32°F	4.0	6.246	0.8559	30.4
59°F	-	-	0.8456	-
70°F	7.0	3.534	0.8412	28.7
100°F	10.5	2.475	0.8293	27.3

<sup>a</sup>Value determined by extrapolation of Log P versus 1/T vapor pressure relationship.

<sup>b</sup>Obtained by linear regression extrapolation of data.

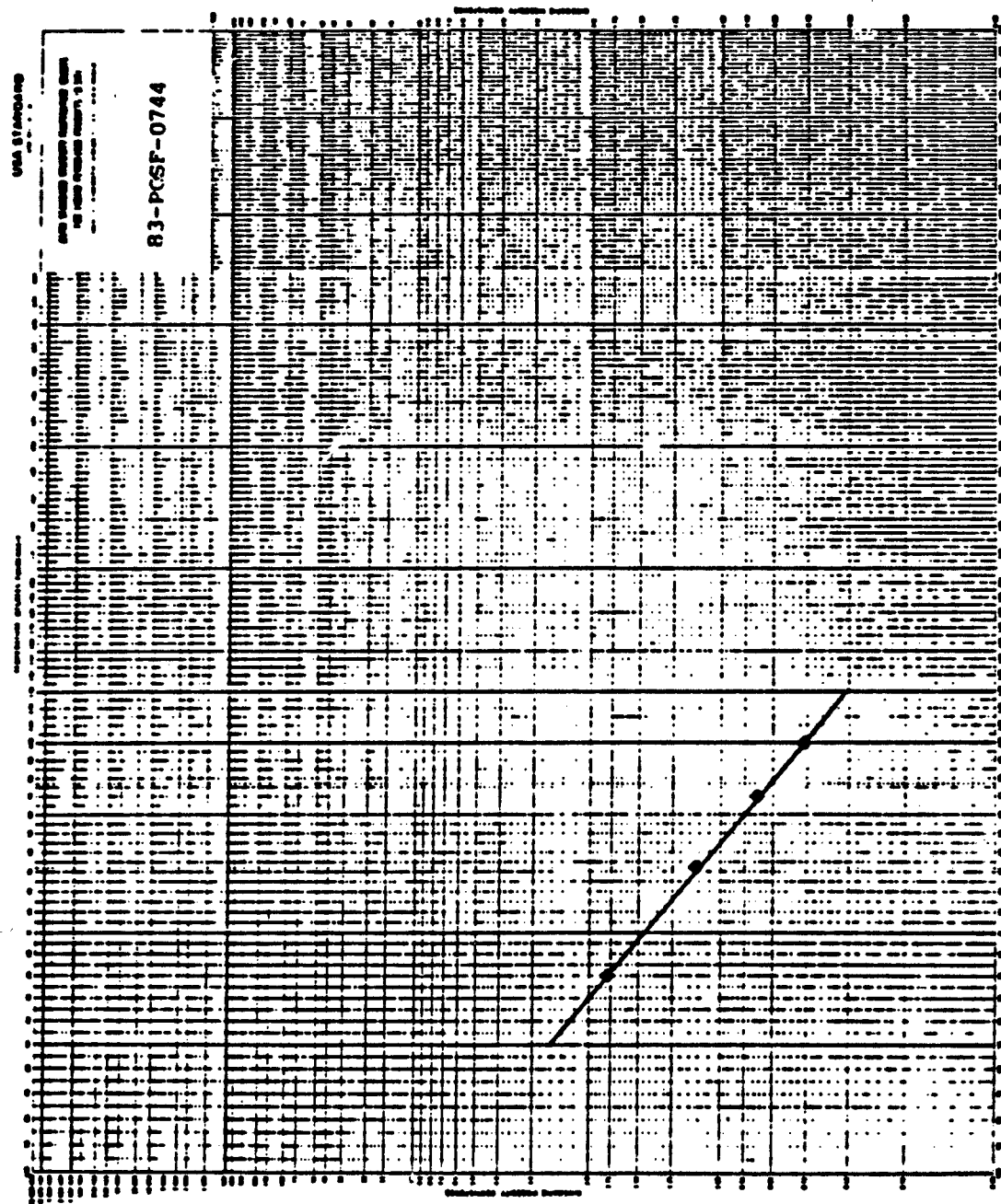


Figure 15. Viscosity plot for Sample 83-PCSF-0744.

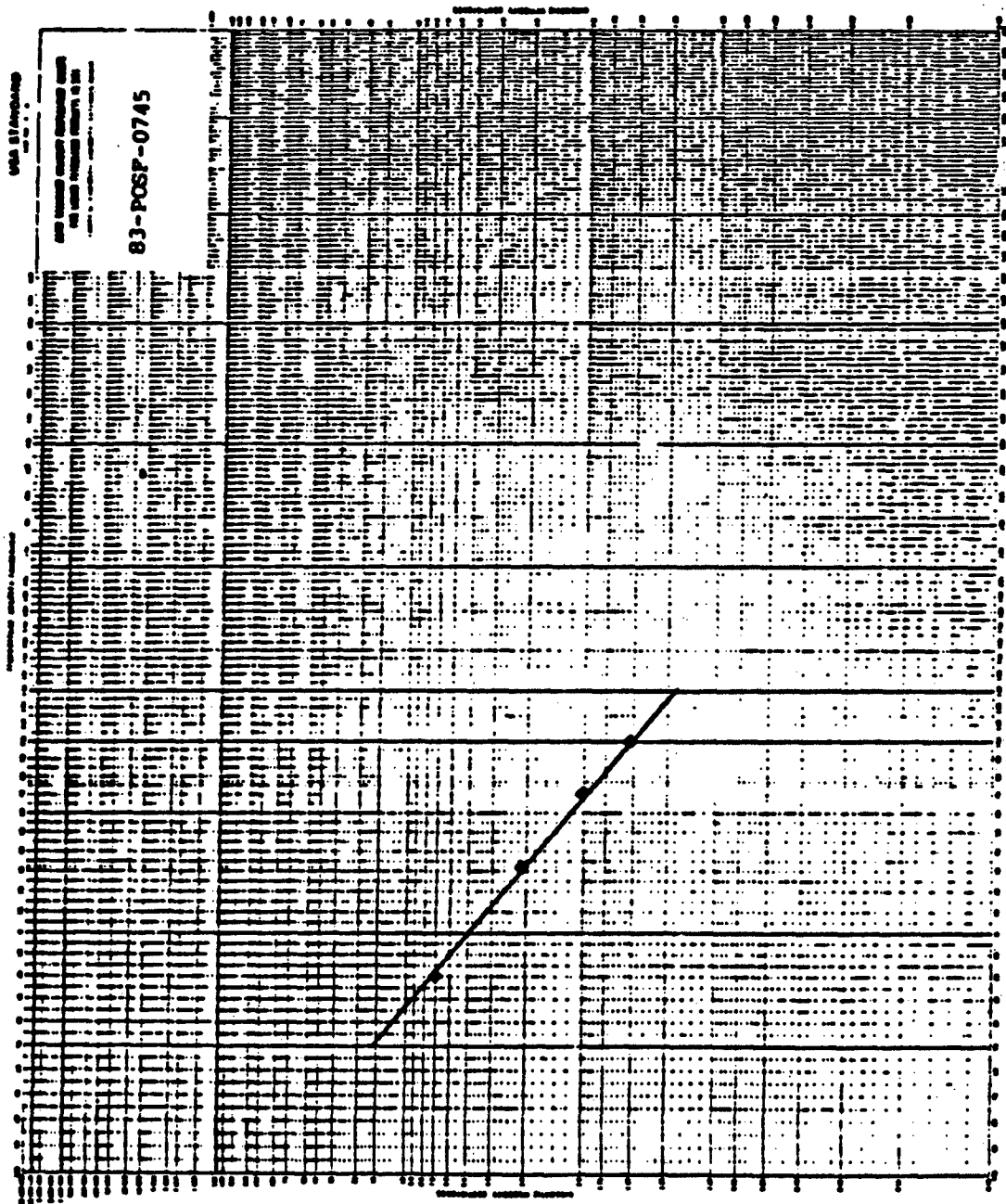


Figure 16. Viscosity plot for Sample 83-POSF-0745.

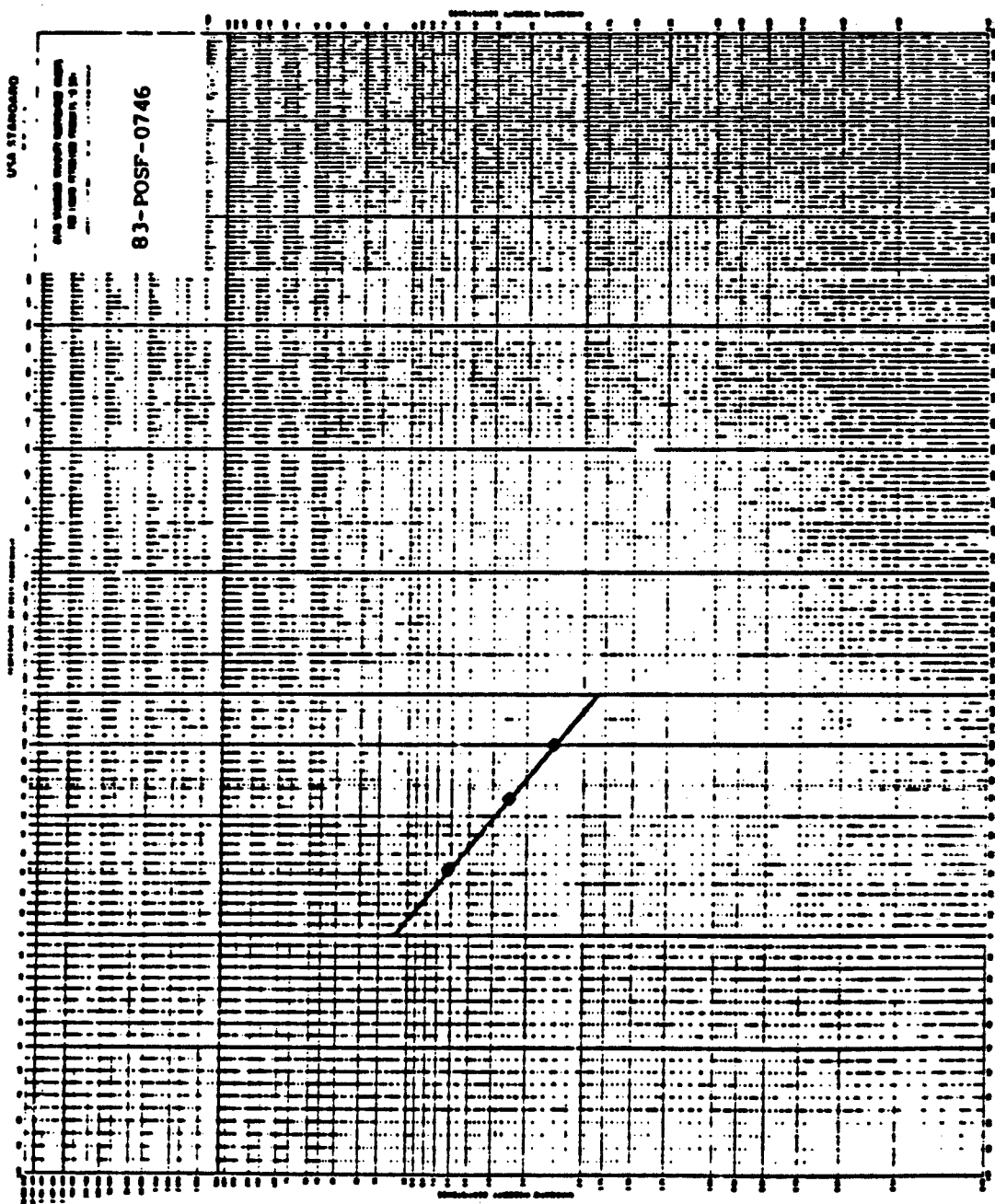


Figure 17. Viscosity plot for Sample 83-POSF-0746.

It will be noted that significant differences appear in results obtained by the two hydrocarbon type methods for the JP-4 sample 83-POSF-0744. Examination of the mass spectral data shows that this sample contains light boilers which are not accounted for by the Monsanto method. That method is intended for samples having an average carbon number of 12-13. For the JP-4 sample the modified ASTM D 2789 gives more accurate results.

##### 5. HYDROCARBON-TYPE ANALYSIS AND DENSITY DETERMINATION ON JP-4 FUELS

The composition of six JP-4 test fuels by mass spectrometric hydrocarbon-type analysis was required as a part of several on-going Air Force programs. The modified ASTM D 2789 and Monsanto Method 21-PQ-38-63 were employed for these analyses. Density at either 15 or 20°C was determined by volume dilatometry. Data are presented in Tables 17 and 18.

TABLE 17. DENSITY OF JP-4 SPECIMENS

Sample	15°C	20°C
POSF-C-81-125	0.7654	- <sup>a</sup>
POSF-C-81-126	0.7773	-
POSF-C-81-1	0.7647	-
POSF-C-81-159	0.7598	-
POSF-82-C-0364	-	0.8605
POSF-82-C-0365	-	0.7519

<sup>a</sup>Dash indicates value was not determined at indicated temperature.

TABLE 18. HYDROCARBON-TYPE ANALYSIS OF SIX JP-4 SPECIMENS

Compound	Weight percent					
	POSF-C-81-125		POSF-C-81-126		POSF-C-81-141	
	ASTM <sup>a</sup>	Mons. <sup>b</sup>	ASTM <sup>a</sup>	Mons. <sup>b</sup>	ASTM <sup>a</sup>	Mons. <sup>b</sup>
Paraffins	49.9	48.0 <sup>c</sup>	36.1	30.9	48.1	40.9
Monocycloparaffins	23.8	- <sup>c</sup>	34.4	-	28.1	-
Dicycloparaffins	6.1 <sup>d</sup>	-	5.0	-	5.3 <sup>d</sup>	-
Total cycloparaffins	29.9 <sup>d</sup>	29.8	39.4 <sup>d</sup>	43.9	33.4 <sup>d</sup>	38.2
Alkylbzenes	17.8	20.8	21.1	24.7	17.5	20.9
Indans and tetralins	1.1	0.9	1.7	0.5	0.3	0.0
Indenes and dihydronaphthalenes	-	0.0	-	0.0	-	0.0
Naphthalenes	1.3	0.5	0.7	0.0	0.7	0.0
 POSF-C-81-159						
	POSF-C-81-159		POSF-82-C-0364		POSF-82-C-0365	
	ASTM <sup>a</sup>	Mons. <sup>b</sup>	ASTM <sup>a</sup>	Mons. <sup>b</sup>	ASTM <sup>a</sup>	Mons. <sup>b</sup>
Paraffins	46.5	40.6	54.5	47.7	56.4	- <sup>e</sup>
Monocycloparaffins	25.3	-	29.3	- <sup>c</sup>	25.7	-
Dicycloparaffins	6.6 <sup>d</sup>	-	2.3 <sup>d</sup>	- <sup>c</sup>	4.1 <sup>d</sup>	-
Total cycloparaffins	31.9 <sup>d</sup>	35.2	31.6 <sup>d</sup>	33.7	29.8	-
Alkylbzenes	20.4	24.2	5.8	7.1	12.9	-
Indans and tetralins	0.3	0.0	4.9 <sup>c</sup>	4.4	0.4 <sup>c</sup>	-
Indenes and dihydronaphthalenes	-	0.0	-	1.8	-	-
Naphthalenes	0.9	0.0	3.2	5.3	0.5	-

<sup>a</sup>Modification of ASTM Method D 2789, values converted from volume percent using relative densities.

<sup>b</sup>Monsanto Method 21-PQ-38-63.

<sup>c</sup>Dash indicates method does not provide information on these specific compound categories.

<sup>d</sup>Sum of two preceding values.

<sup>e</sup>Due to the low average carbon number (7.9) of this fuel, the Monsanto method is not applicable.

## 6. CHARACTERIZATION OF FUELS FOR LOW TEMPERATURE STUDIES

Seven fuels were characterized as part of Air Force studies of fuel behavior at low temperatures. Freeze point (ASTM D 2386), pour point (ASTM D 97) and cloud point (ASTM D 2500) which were determined as required, are presented in Table 19. Three of the fuels were characterized in detail. Samples involved in these tests were:

CRM-TD-001	(Fuel 47)	Blended fuel
CRM-TD-002	(Fuel 50)	Blended fuel
CRM-TD-003	(Fuel 53)	Blended fuel
POSF-82-C-0199		JP-8/LFP-1 mixture
81-POSF-0114, Shale	JP-4,	Suntech Code: X190-223
81-POSF-0117, Shale	JP-5,	Suntech Code: X190-225
83-POSF-0709, Jet A,	AFFB-9-67	

TABLE 19. LOW TEMPERATURE PROPERTIES OF TEST FUELS AND BLENDS

Fuel code	Freeze point, °F	Pour point, °F	Cloud point, °F
CRM-TD-001 (Fuel 47)	-51	-57	- <sup>a</sup>
CRM-TD-002 (Fuel 50)	-60	-71	-
CRM-TD-003 (Fuel 53)	-63	-73	-
POSF-82-C-0199	-45	-46	-
81-POSF-0114	-89	-	-87
81-POSF-0117	-49	-	-45
83-POSF-0709	-44	-	-42

<sup>a</sup>This parameter not measured for indicated fuel.

The last three fuels were characterized in detail by the measurement of a variety of properties as presented in Tables 20 through 22. Kinematic viscosity values are plotted on ASTM charts shown in Figures 18 through 20. Hydrocarbon-type analyses were also conducted with results being given in Table 23.

TABLE 20. SIMULATED DISTILLATION

<u>% Recovered</u>	<u>Temperature</u>					
	<u>81-POSF-0114</u>		<u>81-POSF-0117</u>		<u>83-POSF-0709</u>	
	<u>°C</u>	<u>°F</u>	<u>°C</u>	<u>°F</u>	<u>°C</u>	<u>°F</u>
IBP, 0.5	15	58	134	274	124	256
1	28	82	138	281	136	276
5	67	153	150	303	162	324
10	88	191	164	327	175	348
20	98	209	182	359	194	381
30	114	238	196	385	202	396
40	122	252	210	409	212	414
50	141	286	219	426	219	426
60	160	320	228	443	228	442
70	186	367	235	456	235	456
80	212	413	244	471	244	471
90	233	451	253	488	254	489
95	243	469	261	502	261	501
99	254	489	268	515	277	530
FBP, 99.5	257	494	273	523	288	550

TABLE 21. HEAT OF COMBUSTION

	<u>Gross, Btu/lb</u>	<u>Net, Btu/lb<sup>a</sup></u>
81-POSF-0114 (Shale JP-4)	20,194 20,226	
Aver.	20,210	$\Delta H_n = 20,210 - 91.23 (\%H)$
81-POSF-0117 (Shale JF-5)	19,924 19,950	
Aver.	19,937	$\Delta H_n = 19,937 - 91.23 (\%H)$

<sup>a</sup>The value for hydrogen content of the sample (%H) is not available at this time. Net heat of combustion can be calculated by this equation when the %H is obtained.

TABLE 22. PHYSICAL PROPERTIES AS A FUNCTION OF TEMPERATURE

	<u>Kinematic viscosity, centistokes</u>	<u>Surface tension, dyne cm<sup>-1</sup></u>	<u>Density, g/cm<sup>3</sup></u>
<b>81-POSF-0114</b>			
-40°F	2.710	- <sup>a</sup>	-
-20°F	2.101	27.9 <sup>b</sup>	-
32°F	1.286	25.2	0.7710
70°F	0.9624	23.2	0.7548
100°F	0.7956	21.7	0.7416
<b>81-POSF-0117</b>			
-40°F	10.910	-	-
-20°F	7.014	31.1 <sup>b</sup>	-
32°F	3.101	28.6	0.8184
70°F	2.017	26.7	0.8040
100°F	1.516	25.2	0.7922
<b>83-POSF-0709</b>			
-40°F	11.572	-	-
-20°F	7.231	31.4 <sup>b</sup>	-
32°F	3.206	28.8	0.8218
70°F	2.083	27.0	0.8078
100°F	1.565	25.6	0.7952

<sup>a</sup>Dash indicates value was not determined at that temperature.

<sup>b</sup>Obtained by linear regression extrapolation of data.

TABLE 23. HYDROCARBON-TYPE ANALYSIS

Compound	Weight percent				83-POSF-0709	
	81-POSF-0114		81-POSF-0117		ASTM <sup>a</sup>	Mons. <sup>b</sup>
	ASTM <sup>a</sup>	Mons. <sup>b</sup>	ASTM <sup>a</sup>	Mons. <sup>b</sup>	ASTM <sup>a</sup>	Mons. <sup>b</sup>
Paraffins	51.1	45.5	40.9	40.9	38.7	38.0
Monocycloparaffins	37.9	- <sup>c</sup>	41.4	-	41.3	-
Dicycloparaffins	4.3	-	0.5	-	4.1	-
Total cycloparaffins	42.2 <sup>d</sup>	45.1	41.9 <sup>d</sup>	41.9	45.4 <sup>d</sup>	45.6
Alkylbenzenes	5.0	7.7	7.6	9.4	8.2	9.8
Indans and tetralins	1.4	1.7	8.8	7.0	5.0	4.1
Indenes and dihydronaphthalenes	-	0.0	-	0.0	-	0.0
Naphthalenes	0.3	0.0	0.8	0.8	2.7	2.5

<sup>a</sup>Modification of ASTM Method D 2789, values converted from volume percent using relative densities.

<sup>b</sup>Monsanto Method 21-PQ-38-63.

<sup>c</sup>Dash indicates method does not provide information on these specific compound categories.

<sup>d</sup>Sum of two preceding values.

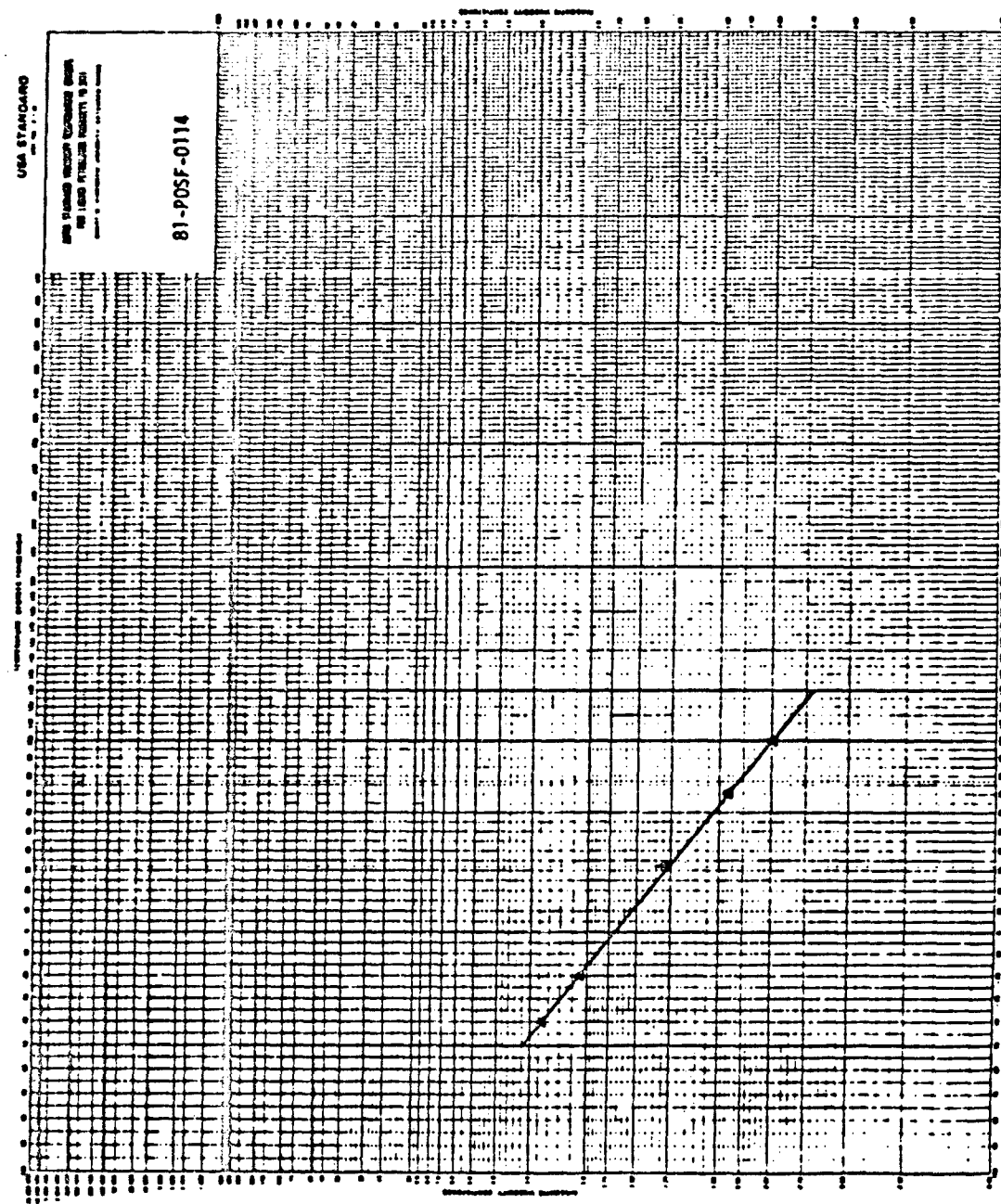


Figure 18. Kinematic viscosity/temperature plot for Sample 81-POSF-0114.

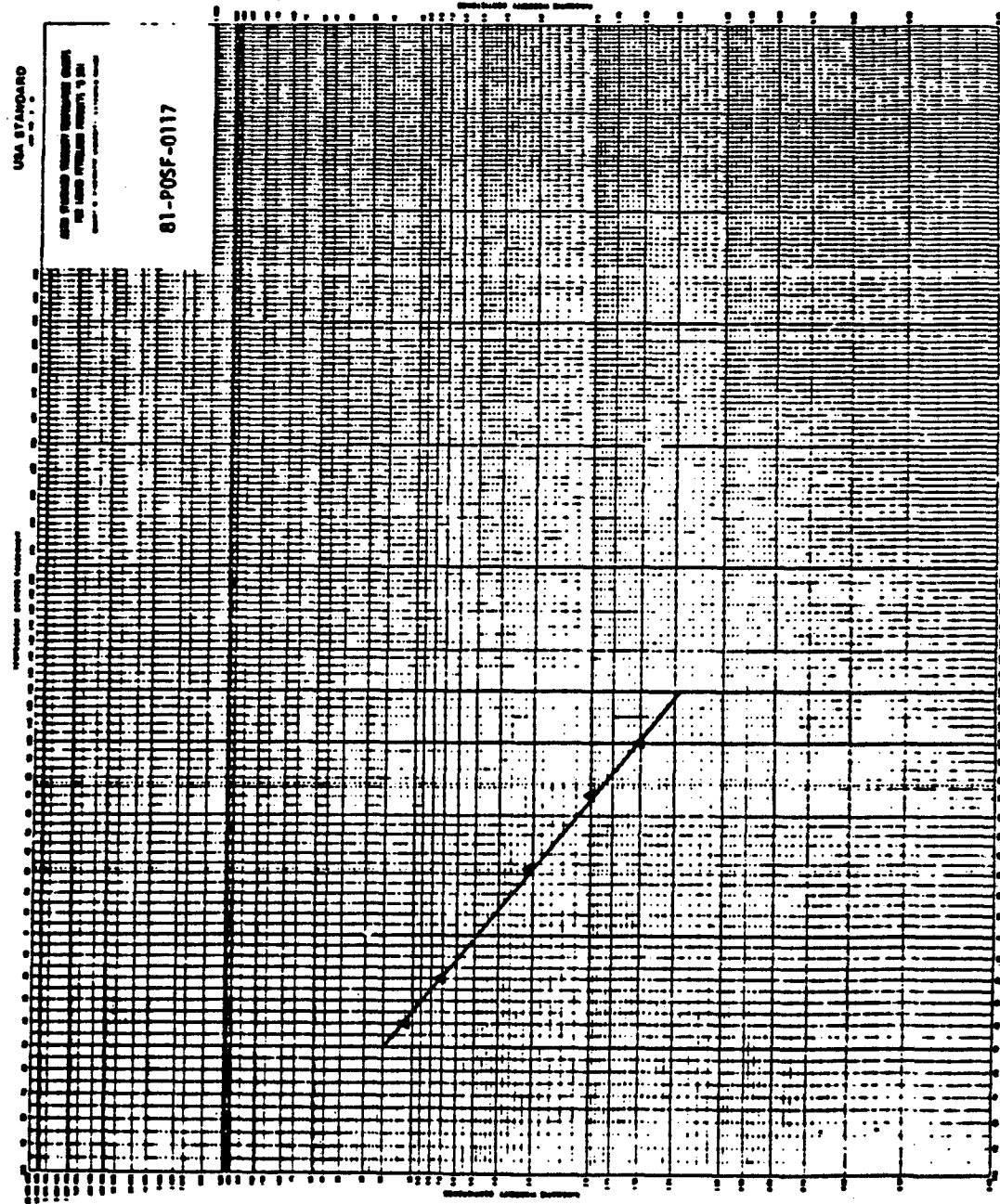


Figure 19. Kinematic viscosity/temperature plot for Sample 81-POSF-0117.

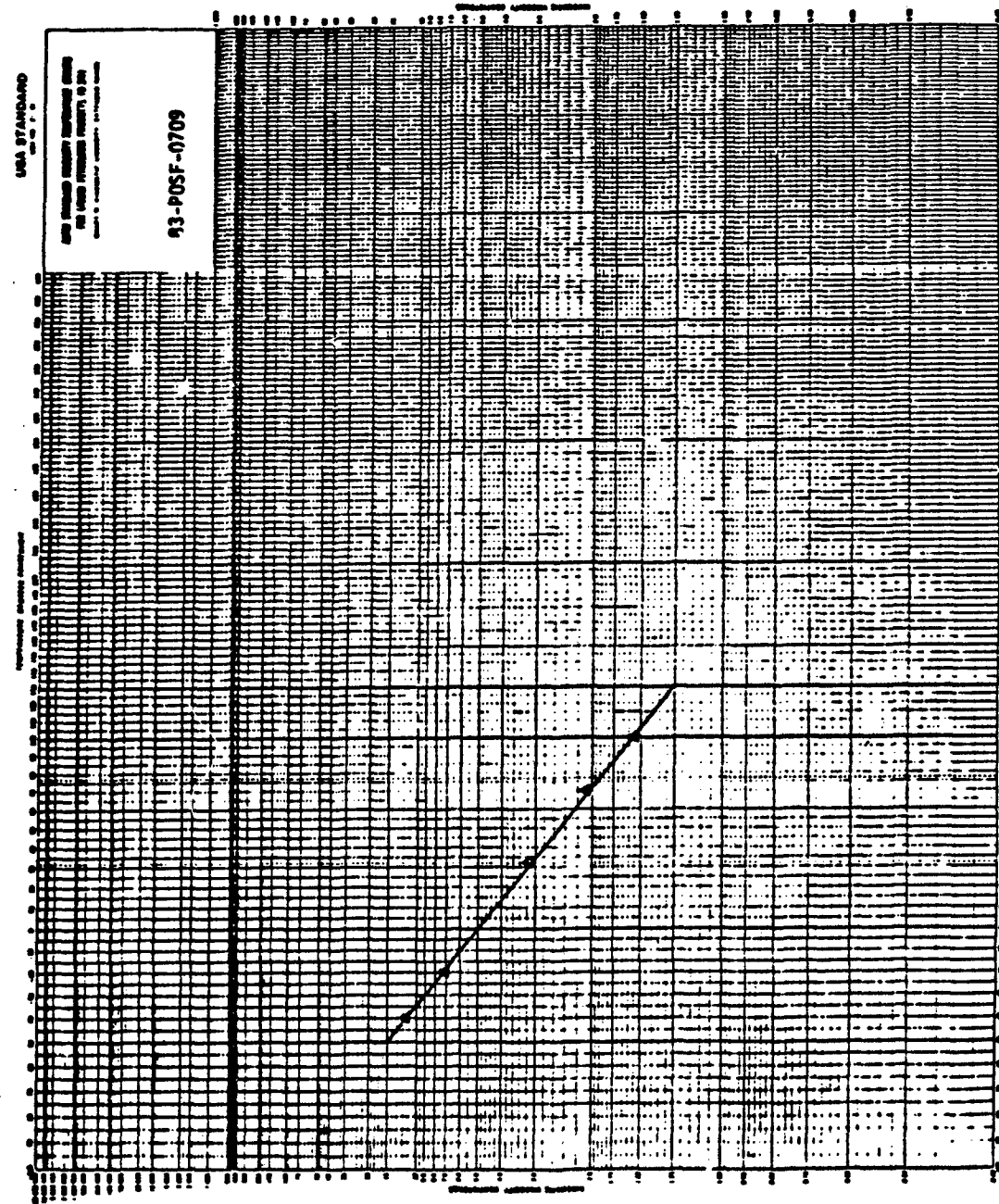


Figure 20. Kinematic viscosity/temperature plot for Sample 83-ROSF-0709.

## 7. OTHER CHARACTERIZATIONS PROVIDED FOR AIR FORCE PROJECT SUPPORT

In two unrelated project support efforts, heat of combustion and density were determined for carbon slurry fuels, and simulated distillation and density determinations were performed on a JP-7 fuel sample and on JP-10 (a single compound fuel used as a reference).

Density data are presented in Table 24, heat of combustion values are given in Table 25, and simulated distillation data appear in Table 26. Distillation plots are shown in Figure 21.

TABLE 24. DENSITY OF FUEL SPECIMENS AT 15°C

	<u>g/cc</u>
POSF-82-C-0191 (Sun. 839988) (Carbon slurry fuel)	1.2270
POSF-82-C-0192 (Sun. 840000) (Carbon slurry fuel)	1.2421
JP-7P-TK WA-10 6 Jan. 1982	0.7994
JP-10 6 Jan. 1982	0.9193

TABLE 25. HEAT OF COMBUSTION OF CARBON SLURRY FUELS

<u>Sample identification</u>	<u>Heat of combustion</u>		
	<u>Gross, Btu/lb</u>	<u>Net, Btu/lb</u>	<u>% H<sup>a</sup></u>
POSF-82-C-0191 (Sun 839988)	16,870		
	16,831		
	Aver. 16,850	16,317	5.84
POSF-82-C-0192 (Sun 840000)	16,850		
	16,884		
	Aver. 16,894	16,350	5.96

<sup>a</sup>Data supplied by AFWAL/POSF for calculation of net heat of combustion. Equation used for calculation:  $\Delta H_n = \Delta H_g - 91.23 (\%H)$ .

TABLE 26. SIMULATED DISTILLATION DATA FOR JP-7 AND JP-10 FUELS

<u>Percent recovered</u>	JP-10		JP-7P-TK WA-10	
	<u>°C</u>	<u>°F</u>	<u>°C</u>	<u>°F</u>
IBP, 0.5	53	128	146	295
1	58	137	151	304
5	115	239	172	342
10	175	347	184	364
20	184	363	198	389
30	185	366	210	410
40	186	367	218	424
50	187	369	224	435
60	188	371	231	448
70	190	373	237	459
80	191	375	245	474
90	193	380	254	489
95	212	415	260	500
99	270	518	272	522
FBP, 99.5	286	547	279	535

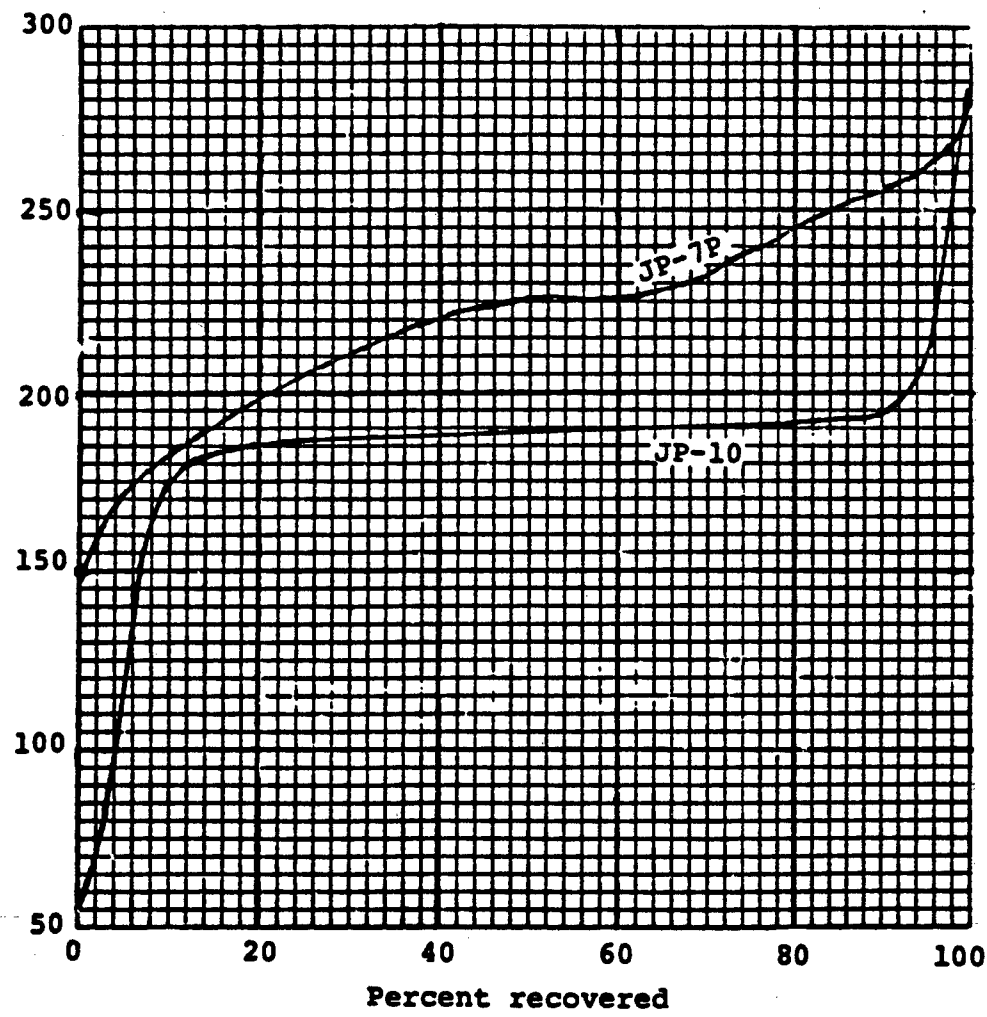


Figure 21. Plot of simulated distillation data.

### SECTION III

#### TOTAL ANALYSIS OF FUELS AND HYDROCARBON STOCKS

For most fuel related research and development programs, characterization of fuels by chemical and physical properties is adequate. In some cases however, a total and detailed analysis of a fuel's composition is required.

Gas chromatography/mass spectrometry is the technique of choice for conducting a total analysis of hydrocarbon distillate fuels, especially in cases where identification of 95% of the compounds at concentrations of 0.10 wt% or greater is desired. A 50-meter fused silica capillary column coated or bonded with a silicone liquid phase such as SP-2100 is used for the separation. The instrument employed in our laboratory is a Hewlett-Packard 5985 GC/MS system, which utilizes an HP-5840 gas chromatograph having microprocessor control and subambient temperature programming. The MS data system is based on an HP-1000 computer with 32K core memory, dual disc storage, an HP ANSWER software and a FORTRAN compiler.

Mass spectra of many hydrocarbons within a compound class, particularly paraffins and naphthenes, show very similar fragmentation and often no molecular weight peak. Since the number of possible isomeric configurations becomes very large as the carbon numbers increase, a generic identification of compounds frequently provides the best return on invested time. Thus, one compound might be identified as a  $C_{12}$  alkane or another as a  $C_{14}$  cycloparaffin. More specific information concerning compound identification has been obtained, however, by the extensive use of Kovats indices together with mass spectral data.

While GC/MS is the principal tool used for total analysis of a fuel, other data such as elemental analysis, metals content, NMR data and element-specific GC detector data are extremely useful.

### 1. ANALYSIS OF OCCIDENTAL LIGHT SHALE OIL AND ITS VAPORS

Detailed analyses were conducted on a Light Shale Oil specimen coded POSF-82-D-0321. A major purpose of the analysis was to provide data for determination of the occupational health effects of the material.

Both the shale oil liquid and its headspace vapors were analyzed by gas chromatography/mass spectrometry (GC/MS) using a Hewlett-Packard 5985 GC/MS system having a 50-meter glass capillary column coated with a silicone stationary phase. The liquid sample was diluted 100-fold with solvent prior to analysis. Deuterated anthracene was added as an internal standard. The headspace vapors were sampled by withdrawing 2 mL of vapors from the headspace of the five-gallon fuel can. A septum was placed in the lid of the can for that purpose. Chromatograms resulting from these analyses are shown in Figures 22 and 23. Instrument conditions differed for the two analyses, thus retention times are not directly comparable. Major peaks in the chromatogram have been numbered for their correlation with the analytical data presented in Tables 27 and 28. All components are listed in these tables with their retention values.

The shale oil was subjected to a trace metals analysis using inductively coupled argon plasma (ICP) spectroscopy. The fuel was filtered through a  $0.45 \mu$  Millipore HA filter to remove particulates prior to analysis. Filter contents and fuel were prepared for analysis by extracting with ULTRAR<sup>®</sup> high purity hydrochloric acid. Before conducting the acid extraction, the filter and a

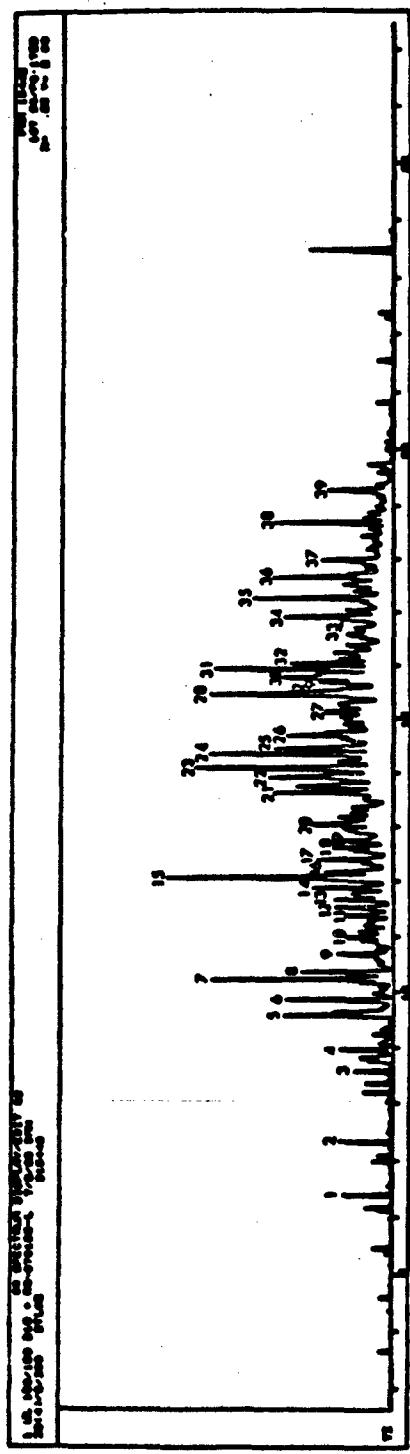


Figure 22. Reconstructed total ion gas chromatogram of light shale oil Sample POSF-82-D-0321.

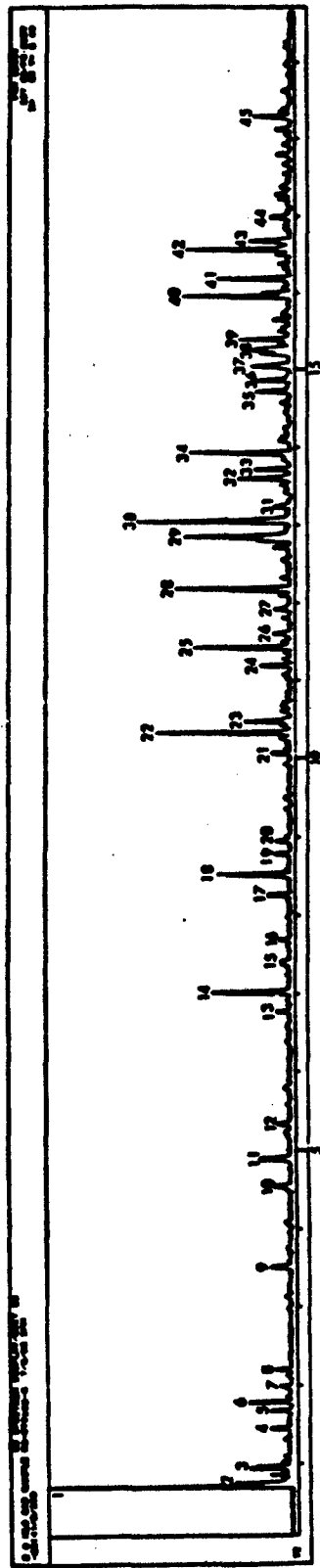


Figure 23. Reconstructed total ion chromatogram of light shale oil vapors.

TABLE 27. COMPONENTS OF LIGHT SHALE OIL BY GC/MS

Retention time, min	Compound	Chromatogram peak No.	GC/MS area, %
2.1	Benzene		1.44
2.2	Cyclohexene		0.70
3.6	Toluene		0.19
4.3	Dimethylhexane		0.10
4.5	C <sub>8</sub> paraffin, (methylheptane)		0.10
5.3	C <sub>9</sub> paraffin, isomer		0.10
5.4	Trimethylcyclohexane		0.31
6.1	Trimethylcyclohexene		0.65
6.4	Ethylbenzene	1	0.83
7.0	Dimethylbenzene		0.23
7.1	Methylethylcyclohexane		0.22
7.2	C <sub>9</sub> paraffin, isomer	2	0.86
8.2	C <sub>10</sub> paraffin, isomer		0.38
8.6	t-butylthiophene	3	0.65
9.0	C <sub>3</sub> subst. benzene	4	0.91
9.1	C <sub>10</sub> monoolefin (tetramethyl hexene)		0.12
9.2	C <sub>3</sub> subst. benzene		0.24
9.6	C <sub>10</sub> cycloparaffin, isomer	5	4.0
9.9	C <sub>10</sub> paraffin (methylnonane)	6	2.36
10.0	Diethylhexane + trimethylpyridine, approximately 50/50		0.21
10.1	Phenoxyethanol (tent.)		0.5
10.2	C <sub>3</sub> Subst. benzene	7	3.20
10.3	C <sub>4</sub> Subst. benzene	8	0.71
10.4	C <sub>11</sub> paraffin (4-methyldecane)		1.42
10.7	C <sub>11</sub> monoolefin (methyldecene)	9	0.89
11	C <sub>4</sub> alkylbenzene	10	0.60
11.1	C <sub>4</sub> subst. benzene (dimethylethylbenzene)		0.14
11.3	Trimethylpyridine		0.11
11.4	Dimethylethylpyridine	11	1.10

(continued)

TABLE 27 (continued)

Retention time, min	Compound	Chromatogram peak No.	GC/MS area, %
11.5	C <sub>4</sub> subst. benzene	12	0.07
11.7	C <sub>4</sub> subst. benzene + methylindan	13	1.23
11.9	C <sub>11</sub> paraffin, isomer	14	1.20
12.1	C <sub>5</sub> subst. benzene	15	6.10
12.2	C <sub>11</sub> cycloparaffin (cyclohexylmethylbutane)	16	1.40
12.3	C <sub>5</sub> subst. benzene + C <sub>11</sub> paraffin	17	1.44
12.4	C <sub>4</sub> subst. benzene		0.58
12.6	C <sub>12</sub> paraffin + dimethylphenol (minor)	18	2.10
12.7	C <sub>5</sub> subst. benzene (ethyltrimethylbenzene)	19	0.85
12.9	Diethylaniline		0.41
13	Methylindan	20	1.29
13.2	C <sub>11</sub> paraffin + C <sub>5</sub> subst. benzene		0.42
13.3	Acenaphthene		0.85
13.5	C <sub>5</sub> subst. benzene		0.16
13.6	Naphthalene	21	2.10
13.7	Methyltetralin + C <sub>5</sub> subst. benzene		1.90
13.8	Dimethylindan	22	3.10
13.9	Acetyltrimethylpyrrole	23	5.40
14.1	C <sub>12</sub> paraffin		0.72
14.2	C <sub>5</sub> subst. benzene	24	4.06
14.4	C <sub>13</sub> paraffin (dimethylundecane)	25	2.21
14.5	C <sub>13</sub> cycloparaffin (trimethylbutylcyclohexane)		0.34
14.6	C <sub>3</sub> substituted phenol		0.67
14.8	Trimethylindan isomer	26	1.22
14.9	Trimethylindan isomer		0.28
15.0	Ethyl tetralin		0.40
15.1	t-butyl-2-methoxyphenol	27	0.91
15.3	C <sub>13</sub> paraffin isomer	28	4.20
15.5	C <sub>3</sub> subst. indan isomer		0.62

(continued)

TABLE 27 (continued)

Retention time, min	Compound	Chromatogram peak No.	GC/MS area, %
15.7	C <sub>13</sub> paraffin isomer	29	1.39
15.8	C <sub>3</sub> subst. indan isomer	30	1.90
15.9	C <sub>13</sub> paraffin isomer	31	2.56
16.1	Methylnaphthalene isomer	32	1.19
16.2	C <sub>2</sub> substituted tetralin isomer		0.33
16.3	C <sub>13</sub> paraffin isomer		0.29
16.5	C <sub>6</sub> subst. benzene (dimethylisobutylbenzene)		0.73
16.9	C <sub>4</sub> subst. indan (tetramethylindan)	33	1.74
17.0	Diisopropenylbenzene	34	2.05
17.3	C <sub>14</sub> paraffin isomer	35	2.50
17.4	C <sub>9</sub> subst. thiophene isomer		0.40
17.5	Trimethyltetralin + phenylcyclohexylethane		0.20
17.5+	C <sub>14</sub> mono olefin (tetradecene)		0.20
17.6	C <sub>5</sub> subst. indan (pentamethyl indan)		0.31
17.7	C <sub>4</sub> subst. tetralin (butyltetralin)	36	2.23
17.8	C <sub>2</sub> subst. naphthalene (dimethyl naphthalene)		0.42
17.9	C <sub>2</sub> subst. naphthalene (ethyl naphthalene)	37	1.65
18.4	C <sub>4</sub> substituted tetralin isomer		0.82
18.7	C <sub>15</sub> paraffin isomer	38	2.14
18.8	C <sub>10</sub> subst. thiophene isomer		0.42
19.0	C <sub>15</sub> cycloparaffin isomer		0.25
19.2	C <sub>15</sub> paraffin isomer	39	1.30
19.4	C <sub>15</sub> paraffin isomer		0.19
19.6	C <sub>5</sub> subst. indan isomer		0.19
19.7	C <sub>3</sub> subst. naphthalene isomer		0.53
20.8	C <sub>16</sub> paraffin		0.25
21.6	C <sub>17</sub> paraffin		0.25
23.5	D <sub>10</sub> Anthracene-(added internal standard)		-
	TOTAL		95.73

TABLE 28. COMPOSITION OF LIGHT SHALE OIL VAPORS

Retention time, min	Compound	Chromatogram peak No.	Concentration, mg/liter
0.6	Carbon dioxide	1	4
0.7	Sulfur dioxide	2	0.7
0.8	Propane		2
0.9	1-Butene	3	1.8
0.95	Butane		1.4
1.4	2-Methylbutane	4	1.4
1.6	Dimethylcyclopropane	5	3.1
1.8	Pentane and 1-pentene	6	1.1
1.9	Cyclopentane	7	0.7
2.1	Methylethylcyclopropane		1.4
2.2	C <sub>5</sub> olefin	8	2.8
3.5	C <sub>6</sub> paraffin isomer	9	2.0
4.5	C <sub>3</sub> subst. cyclopropane (methylethyl)	10	4.4
4.8	C <sub>6</sub> paraffin (3-methylpentane)	11	1.7
5.2	Hexene	12	1.6
6.8	C <sub>6</sub> paraffin	13	7.7
7.0	Benzene	14	2.0
7.4	Cyclohexene	15	1.7
7.6	C <sub>7</sub> paraffin isomer	16	3.2
8.3	Dimethylcyclopentane	17	9.1
8.5	n-Heptane	18	2.8
8.7	C <sub>8</sub> paraffin isomer	19	2.8
8.9	C <sub>8</sub> paraffin isomer	20	2.0

(continued)

TABLE 28 (continued)

Retention time, min	Compound	Chromatogram peak No.	Concentration, mg/liter
10.1	C <sub>2</sub> subst. cyclopentene (1,5 dimethyl)	21	14.2
10.3	Toluene	22	4.3
10.4	Dimethylhexane	23	3.6
11.2	C <sub>3</sub> subst. cyclopentane (methyl, ethyl)	24	10.7
11.4	Ethyldihydrofuranone	25	3.1
11.6	C <sub>2</sub> subst. cyclohexene	26	2.8
11.9	C <sub>2</sub> subst. cyclohexene	27	18.1
12.2	C <sub>3</sub> subst. cyclohexane (trimethyl-)	28	22.2
12.8	C <sub>3</sub> subst. cyclohexene isomer	29	22.7
13.0	C <sub>2</sub> subst. benzene (dimethyl-)	30	29.4
13.2	C <sub>2</sub> subst. benzene	31	6.7
13.6	C <sub>2</sub> subst. benzene	32	5.9
13.7	C <sub>4</sub> subst. cyclopentane	33	14.7
13.9	C <sub>9</sub> paraffin isomer	34	5.0
14.7	C <sub>10</sub> paraffin (methylnonane)	35	5.6
14.9	C <sub>10</sub> paraffin isomer	36	9.5
15.0	t-Butylthiophene	37	6.7
15.2	C <sub>10</sub> cycloparaffin and olefin isomer	38	9.5
15.3	C <sub>3</sub> subst. alkylbenzene	39	7.1
15.5	C <sub>3</sub> subst. alkylbenzene		19.7
16	C <sub>10</sub> paraffin isomer and C <sub>3</sub> subst. benzene	40	9.4
16.3	C <sub>11</sub> olefin		6.5
16.6	C <sub>3</sub> subst. benzene	42	9.5
16.8	C <sub>4</sub> subst. benzene	43	3.7
17.0	C <sub>11</sub> olefin isomer	44	8.1
18.2	C <sub>11</sub> paraffin	45	

portion of the fuel were examined by the energy dispersive x-ray emission technique. The filter contents showed the presence of sulfur ( $45 \mu\text{g}/\text{cm}^2$ ) and iron ( $5 \mu\text{g}/\text{cm}^2$ ).

The filtered fuel showed a significant sulfur level but no iron was found to be present. The trace metals analyses were conducted using an ISA model JY48P ICP instrument. Results are presented in Table 29.

Elemental analysis was conducted on the sample by a commercial laboratory. These results are presented in Table 30. Oxygen was reported as being too low for combustion analysis. It could be present up to approximately the 0.5% level, however.

A proton NMR spectrum was recorded for the light shale oil to provide data on the olefin content of the sample. The spectral region from 6.0 to 4.5 ppm is characteristic of olefinic protons. Integral data were collected in this and other spectral regions using the format which has been employed for hydrocarbon type distribution. The integral area for each type of proton is presented in Table 31. The relative numbers of protons for the aromatic, olefinic and aliphatic spectral regions are summarized in Table 32. Additionally, proton aromaticity (mole ratio of aromatic protons to total protons) and mole percent olefinic protons are given.

### Discussion

In this work, GC/MS area percents are reported to quantitate the light shale oil components. While this approach does not provide the accuracy obtainable with a flame ionization detector, the values serve to provide a general overview of the material's composition.

TABLE 29. RESULTS OF TRACE METAL ANALYSIS BY ICP SPECTROMETRY

Instrument	Elements of detection	Li	Be	Ca	Cr	Fe	Al	Ca	Cu	Mo	Se
Quantification limit, Log. ppb	4,700 190	3	28	2	110	17	230	190	80	45	450
Log. off concentration, ppb	214 8.6	0.1	1.3	0.1	5	0.8	10	0.6	3.6	2	20
Acid extraction blank, ppb	x x	x	x	x	x	x	x	207	x	x	x
PGF7-92-9-0321 <sup>c</sup> (filtered liquid), ppb	x x	x	x	x	0.7	x	x	x	x	x	x
Blank filter, ppb	x x	x	x	x	3	x	x	520	x	x	x
Fuel sample on filter, ppb	x x	x	x	3	7.7	16	x	x	x	x	x
<u>Analysis of Reference Standard, ppb</u>											
True values	-	261	304	478	263	1,000	852	1,000	1,000	1,000	1,000
Observed value	-	265	312	501	298	974	854	1,110	972	1,100	994
Percent recovery	-	102	104	105	104	97	100	111	97	110	99

(continued)  
aFuel samples were effectively concentrated by a factor 22 by extraction with a small volume of aqueous acid for the analysis.

bAqueous ultrapure acid used to extract the fuel samples for analysis. An "x" shows that the element was not detected at the instrument LOQ.

cAn "x" shows that the element was not detected at the Log off concentration. The numerical values were obtained by subtracting any blank values from the observed value, then dividing by the appropriate concentration factor. These values represent the element concentration in the original sample.

dValues express concentrations related to the volume of fuel that was filtered.

TABLE 29 (continued)

Instrument	Elements of detection	V	B	CD	Fe	Mo	Si	Al	Co	Fe	Cr	Al	Si	Cr	Si
quantification limit, LOQ, ppb															
LOQ after concentration, ppb	110	105	25	23	16,300	4,700	6	6	25	24	66	6	6	24	6
acid extraction blank, ppb	5	4.0	1.1	1	656	214	0.1	0.1	1.1	1.1	1.1	1.1	1.1	1.1	1.1
ROSF-92-9-0321 <sup>c</sup> (filtered liquid), ppb	5	5	20	5	19	5	5	5	5	5	5	5	5	5	5
blank filter, ppb	5	5	5	5	5	5	5	5	5	5	5	5	5	5	5
fuel solids on filter, ppb	12	5	478	5	5	1	5	5	27	5	5	5	5	5	5
Analysis of Reference Standard, ppb															
True values	860	—	39	795	—	—	670	1,000	240	1,000	1,000	—	—	—	—
Observed value	907	—	66	863	—	—	512	1,020	326	943	1,000	—	—	—	—
Percent recovery	100	—	162	111	111	—	107	102	55	96	102	—	—	—	—

<sup>a</sup>Fuel samples were effectively concentrated by a factor 22 by extraction with a small volume of aqueous acid for the analysis.

<sup>b</sup>Agence Ultracrete acid used to extract the fuel samples for analysis. An "X" shows that the element was not detected at the instrument LOQ. An "X" shows that the element was not detected at the instrument LOQ. An "X" shows that the element was not detected at the instrument LOQ. The numerical values were obtained by subtracting any blank values from the observed value, then dividing by the appropriate concentration factor. These values represent the element concentration in the original sample.

<sup>c</sup>Values express concentration related to the volume of fuel that was filtered.

TABLE 30. ELEMENTAL ANALYSIS OF LIGHT SHALE OIL POSF-82-D-0321

<u>Element</u>	<u>Weight percent</u>
Carbon	85.16
Hydrogen	12.94
Nitrogen	0.73
Sulfur	0.70
Oxygen	- <sup>a</sup>

<sup>a</sup>Too low for combustion analysis ( $\leq 0.5\%$ ).

TABLE 31. INTEGRAL AREA OF EACH TYPE OF PROTON

<u>Spectral region, ppm</u>	<u>Integral designation</u>	<u>Integral area</u>
8.0 - 6.3	Aromatic Ring	11
6.0 - 4.5	Olefin	8
3.0 - 2.0	$\alpha$ -methyl	27
2.0 - 1.5	Methine	32
1.5 - 1.0	Methylene	104
1.0 - 0.3	Methyl	87

TABLE 32. PROTON NUMBER OF PROTONS BY NMR

<u>Relative number of protons</u>	<sup>1</sup> H aromaticity			<sup>1</sup> H olefinic content, %
	<u>Aromatic</u>	<u>Olefinic</u>	<u>Aliphatic</u>	$(f_a^H)$
1	0.73	22.7	0.04	3

The headspace vapor analysis was quantitated by use of flame ionization gas chromatography to calculate the weight of hydrocarbons present in 2cc of headspace vapor. Compound area percents from GC/MS were then used to calculate the amount of each component found in the vapor.

Compounds listed in Tables 30 and 31 are, in some cases, identified by chemical class and carbon number, or by the carbon number of substituent groups. In some cases, this generic identification is followed by specific substituent groups listed in parenthesis. These are the alkyl groups believed to be present based on mass spectral data. For example, C<sub>3</sub>-substituted cyclopentane (methyl, ethyl) indicates that the C<sub>3</sub> substitution appears to be accomplished with methyl and ethyl groups.

Cycloparaffins are, in most cases, difficult to distinguish from olefins. Subtle spectral differences frequently exist and these have been used to make the distinctions shown in the tables. The assignments must be considered tentative. Compounds designated as cycloparaffins could be the equivalent olefin in some cases.

Proton Nuclear Magnetic Resonance data indicates that a substantial amount of olefinic material is contained in the sample. To calculate the weight percent of olefinic compounds, the molecular weight and the number of double bonds per molecule (whether mono-, di- or triolefins) must be known. If, for example, it is assumed that the average olefin is a C<sub>10</sub>, and that only monoolefins are present, the average olefin would have the empirical formula, C<sub>10</sub>H<sub>20</sub>. Further, assuming that the double bond has an equal chance of being in any position (terminal or mid-chain), an average of 2.2 olefinic protons per molecule would be present or stated another way, 11% of the 20 protons are olefinic. The C<sub>10</sub>H<sub>20</sub> monoolefin would have to be present at about the 27% concentration in the sample to give the 3% olefin proton content observed. From the mass spectral data some diolefins are known to be present and some of the compounds tentatively identified as cycloolefins could, in fact, be diolefins. Additionally the distribution of olefins in the sample may favor the low molecular weight range. Some C<sub>4</sub> olefins are known to be present from the mass spectral data.

Data from Table 35 can be used directly as a comparative measure of olefin content without making any assumptions. No fuel we have examined by proton resonance NMR has shown an olefin content approaching that of the light shale oil.

## 2. EXAMINATION OF COLLECTED FRACTIONS OF OCCIDENTAL LIGHT SHALE OIL

The analysis of Occidental Light Shale Oil and its vapors was reported in Section 1. An investigation was conducted as a follow-up on that work to better define the occupational health aspects of light shale oil.

Three samples, consisting of light shale oil fractions, were submitted to this laboratory for examination and analysis. The fractions had been successively eluted from a clay column which was 5 cm in diameter and contained two liters of clay. The fractionation procedure was performed by Air Force personnel.

Sample numbers and descriptions are:

Number	Sample	Color
POSF-82-D-0321	Original light shale oil	Nearly black
POSF-82-B-0459	1st Fraction	Green
POSF-82-B-0460	2nd Fraction	Amber
POSF-82-B-0461	3rd Fraction	Brown

Before passing the material through the clay column, the sample had been allowed to stand for nearly two months with two liters of clay in approximately three gallons of POSF-82-D-0321.

Upon their arrival at MRC, the fractions were examined by a micro-filtration/optical microscopy technique and by GC/MS. Additionally, tests were conducted with a siliceous sorbent to determine compounds removed by the sorbent.

### Microscopic Examination of Fraction Particulates

In preparation for microscopic examination of particulates, sample POSF-82-D-0321 and its three fractions were filtered through a membrane filter having a pore size of 0.45  $\mu\text{m}$ . Observation of the filter deposit from untreated light shale oil showed that it consisted of black opaque (probably carbonaceous) particles in the 1-10  $\mu\text{m}$  range, with their average size being approximately 5  $\mu\text{m}$ . Additionally, clear particles in the 5-20  $\mu\text{m}$  range, probably inorganic in nature, were also present.

The filter deposit from the brown third fraction appeared to be very similar to that of the original light shale oil except that the black particles were less than 1  $\mu\text{m}$  in size and the concentration of the clear particles was significantly lower.

The amber second fraction showed a particulate composition the same as the brown third fraction except that the concentration of each type of particle was lower. The same was true of the green first fraction in which particulate concentrations were lower yet than in the amber sample.

It should not be concluded from these observations that the color of light shale oil is totally due to suspended particulates. Even after passing through a membrane filter having a pore size of 0.45  $\mu\text{m}$ , the light shale oil remained dark brown in color.

### Gas Chromatography/Mass Spectrometric Analysis

Analyses by GC/MS were conducted on all three fractions as well as on the starting light shale oil. Samples were diluted 100-fold with solvent and a deuterated anthracene internal standard was added prior to analysis. A Hewlett-Packard 5935 GC/MS system, having a 50-meter glass capillary column coated with silicon

stationary phase, was used for the analysis. Instrument conditions were the same for all four analyses so that resulting reconstructed total ion chromatograms could be compared. Each fraction is compared with the starting light shale oil in Figures 24 through 26. A peak by peak comparison of the data shows that only two components which appear in the starting shale oil are absent in the fractions. These are the compounds: trimethyl pyridine and dimethylethylpyridine.

#### Collection of Compounds on Siliceous Adsorbent

In order to determine which compounds in the light shale oil might be most affected by treatment with a siliceous adsorbent such as clay, a specimen of light shale oil was passed through a short silica gel column. After all of the shale oil had cleared the column, a pentane rinse was used to remove residual material. A more polar solvent was then used to remove any compounds which were adsorbed on the silica gel. This fraction was retained for GC/MS analysis. The following compounds were found to be present:

- dimethylpyridine
- trimethylpyridine (3 isomers)
- dimethyl ethyl pyridine
- N,N-diethyl aniline
- tetrahydroquinoline (2 isomers)
- methyl oxime benzaldehyde (2 isomers)
- dimethyl aminobenzaldehyde
- 8-hydroxyoximequinaldehyde

Some of these compounds are present in the sample at very low or trace levels, and were not detected in original analysis. It is likely that the compounds are partially, and perhaps totally, removed from the sample by clay treatment. An examination of the clay used in the treatment and generation of the sample fractions would be an excellent means of determining the components removed.

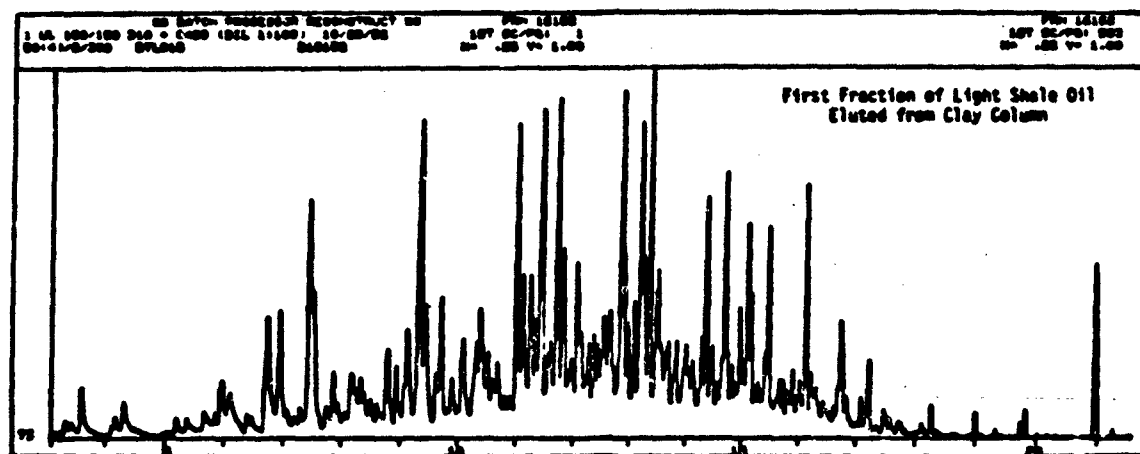
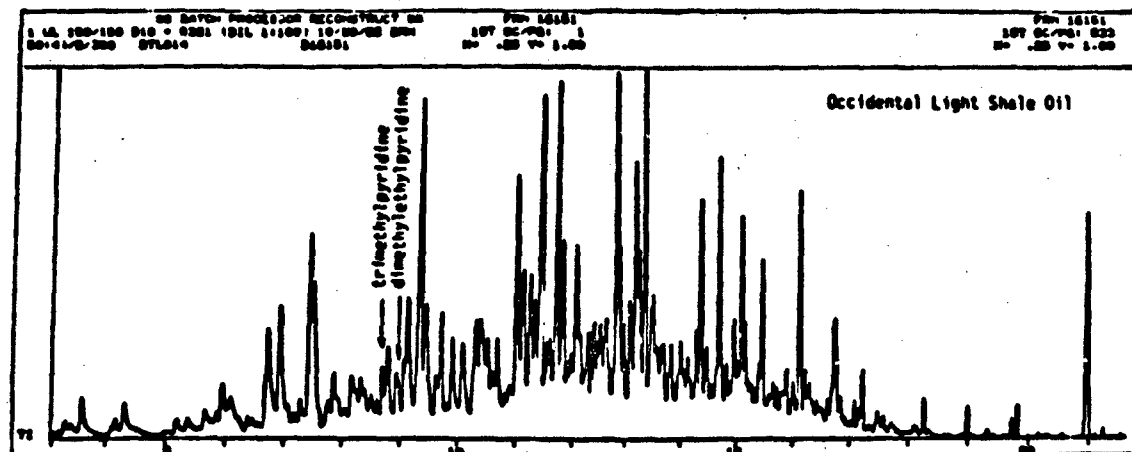
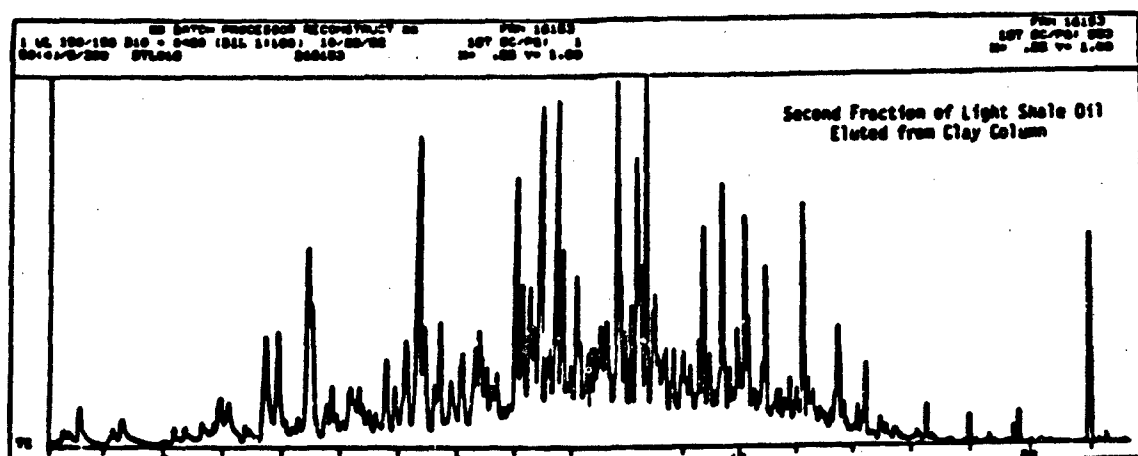
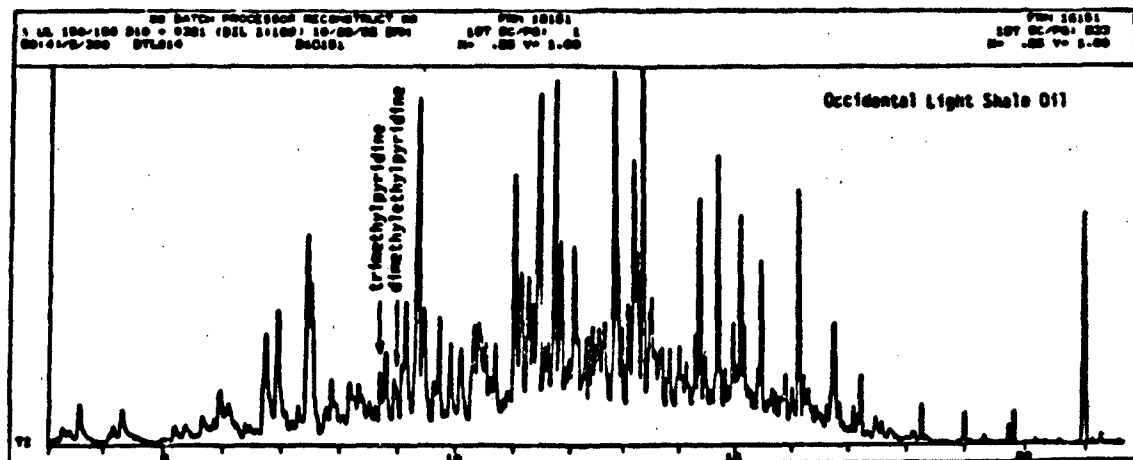
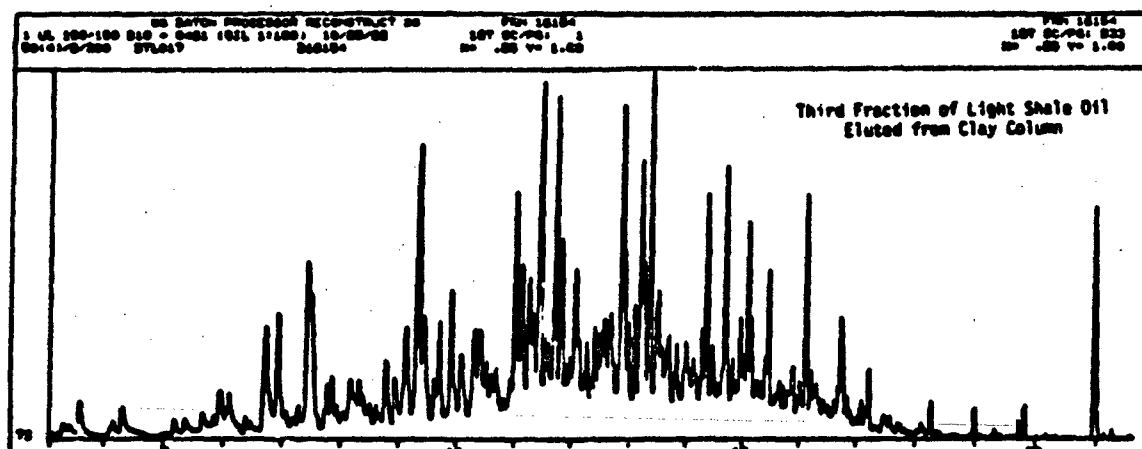
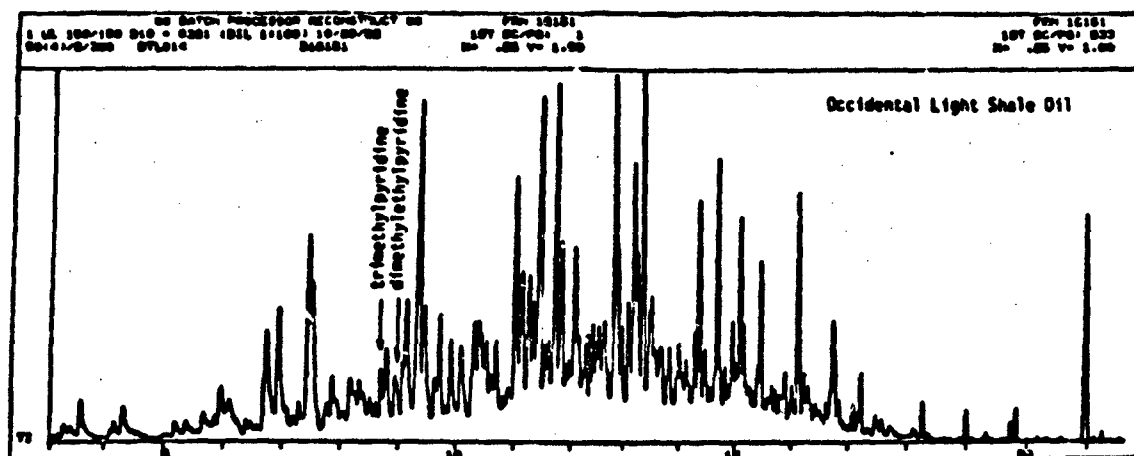


Figure 24. Reconstructed total ion chromatograms of Sample POSF-82-D-0321, Occidental Light Shale Oil (top) and clay-separated first fraction, Sample POSF-82-D-0459 (bottom).



**Figure 25.** Reconstructed total ion chromatograms of Sample POSF-82-D-0321, Occidental Light Shale Oil (top) and clay-separated second fraction, Sample POSF-82-D-0460 (bottom).



**Figure 26.** Reconstructed total ion chromatograms of Sample POSF-82-D-0321, Occidental Light Shale Oil (top) and clay-separated third fraction, Sample POSF-82-D-0461 (bottom).

### Toxicity of Light Shale Oil Components

An attempt was made to compile toxicity and occupational health information on the compounds present in light shale oil. Data on the sulfur and nitrogen compounds found to be present in the sample were particularly sought. These compounds are listed in Table 33. Table 34 presents a list of selected hydrocarbons found in the sample. Toxicity information on these common fuel components can be used as a reference in evaluating similar data for the sulfur/nitrogen compounds.

The "Registry of Toxic Effects of Chemical Substances" [Ref. 1] published annually by the U.S. Department of Health and Human Services is a compilation of all known toxicity data on chemical compounds. Information from that source was used to compile Tables 34 and 35.

Toxicity and health effect information is not available for many of the specific compounds presented in Table 33. Data for similar compounds or those differing in alkyl substitution, must be considered. While this information must be used with caution in judging the effects of the compounds in question, it can serve as a general indicator of the magnitude of toxic effects.

Inhalation data, which is the information primarily sought, is often reported in several forms such as:

TLV - threshold limit value, the airborne concentration below which nearly all workers may be exposed day after day without adverse effects.

LC-50 - the calculated concentration in air expected to cause the death of 50% of an entire experimental animal population.

TABLE 33. SULFUR AND NITROGEN COMPOUNDS DETECTED  
IN OCCIDENTAL LIGHT SHALE OIL

Compound	Toxicity number key <sup>a</sup>
2,5-Dimethylpyridine	1,2,3
2,4,6-Trimethylpyridine	1,2,3
2,3,6-Trimethylpyridine	1,2,3
2,3,5-Trimethylpyridine	1,2,3
2,4-Dimethyl-6-ethylpyridine	3
N,N-Dimethylaniline	10
5,6,7,8-Tetrahydroquinoline	11,12,13
1,2,3,4-Tetrahydroquinoline	11,12,13
4-Methyloxime benzaldehyde	14
3-Methyloxime benzaldehyde	14
4-Dimethylaminobenzaldehyde	
8-Hydroxyoximequinaldehyde	
Sulfur dioxide	6
t-Butylthiophene	4,5
Acetyltrimethylpyrrole	15
C <sub>9</sub> -thiophene	4,5
C <sub>10</sub> -thiophene	4,5

<sup>a</sup>Refers to compounds or derivatives in Table 35  
for which toxicity data are given.

TABLE 34. PERMISSIBLE WORKROOM AIRBORNE CONCENTRATION  
FOR LIGHT SHALE OIL HYDROCARBON COMPONENTS

Compound	TLV (ppm) <sup>a</sup>	TLV-TWA (ppm) <sup>b</sup>
Propane	1,000	1,000
Butane	800	-
2-Methylbutane	-	350 mg/m <sup>3</sup>
Pentane	600	1,000
Cyclopentane	600	-
Benzene	-	10 (25 ppm ceiling value)
Cyclohexene	300	300
n-Heptane	400	500
Toluene	100	200

<sup>a</sup>Threshold limit value.

<sup>b</sup>Threshold limit value - time weighted average  
for normal 8-hour work day.

TABLE 35. TOXICITY DATA FOR LIGHT SHALE OIL COMPONENTS OR THEIR DERIVATIVES

Number key	Compound	Airborne concentration, ppm <sup>a</sup>			Oral dosage, mg/kg <sup>b</sup>
		LC-50	LCLO	TLV	
1	Pyridine	4,000	-	5	891
2	4-Methylpyridine	-	1,000	-	1,290
3	5-Etheny1-2-methylpyridine	800	4,000/4 hrs	-	1,300 <sup>c</sup>
4	Thiophene	-	8,700	-	100 <sup>c</sup>
5	Methylthiophene	-	-	-	512 <sup>c,d</sup>
6	Sulfur Dioxide	-	400/1 min	2	-
7	Aniline	175/7 hrs	400/1 min	5	-
8	n-Butylaniline	-	180/8 hrs	5	440
9	2,6-Diethylaniline	-	-	-	1,620
10	N,N-Diethylaniline	-	-	-	2,690
11	Tetrahydrotetramethylquinoline	-	-	-	782 <sup>c</sup>
12	Tetrahydromethoxyquinoline	-	-	-	400 <sup>c</sup>
13	Trifluoromethylbenzaldehydoxime	-	-	-	400 <sup>c</sup>
14	-	-	-	-	128 <sup>d</sup>
15	3-Acetyl-2,4-dimethylpyrrole	-	-	-	180 <sup>e</sup>
16	4-Aminobenzaldehyde	-	-	-	71 <sup>f</sup>
					912 <sup>f</sup>

<sup>a</sup> See text for explanation of designated values.<sup>b</sup> Based on body weight.<sup>c</sup> Administered into the peritoneal cavity of mouse.<sup>d</sup> Lowest dose reported to have caused death of an animal or human.<sup>e</sup> Potential for exposure by cutaneous route; skin, mucous membranes, eyes.<sup>f</sup> Administered intravenously.

LCLo - the lowest concentration which has been reported to have caused death in humans or animals.

In many cases, toxicity data are available only for oral or intravenous dosage. Oral toxicity is usually presented in terms of an LD-50 value, the calculated dosage expected to cause the death of 50% of an entire experimental animal population. LD-50 is usually given as mg/kg of body weight. Inhalation data for compounds of low volatility are generally not available. Toxicity data for a variety of methods of administration are presented in Table 35.

Along with the light shale oil nonhydrocarbon components listed in Table 33, a toxicity number key is given which refers to compounds listed in Table 35. For example, di- and tri-methyl substituted pyridine compounds might be compared in toxicity to pyridine, methyl pyridine, or ethyl methyl pyridine. Toxicity data for the latter compounds are available and appear in Table 35.

While the data presented in this report are useful for a preliminary examination of the health effects of occidental light shale oil, a more in-depth toxicological study of the materials would be required to state specific precautions to be taken in day to day handling of the material.

### 3. ANALYSIS OF OIL FROM PYROLYSIS OF RUBBER TIRES

A sample of oil obtained from the pyrolysis of rubber tires, coded POSF-82-E-0310, was the subject of extensive characterization. This work was conducted to aid in assessing the suitability of the material for use as a possible alternate source of aviation turbine fuel.

Techniques and procedures employed in this investigation included hydrocarbon type analyses by Monsanto Method 21-PQ-38-63 and modified ASTM D 2789 Methods; boiling range by simulated distillation using ASTM D 2887; trace metals analysis using the emission spectrograph; density measurement by the dilatometer method; gas chromatography using sulfur, halogen and nitrogen selective detectors; ultimate analysis for carbon, hydrogen, nitrogen, and sulfur by microcombustion techniques; and olefin content by proton nuclear magnetic resonance.

A volume of approximately 100 mL of sample was received for the analysis. An emission spectrographic procedure was selected for trace metals analysis, rather than the acid extraction/ICP method used previously, because of the limited amount of sample available. The oil was carefully weighed into a graphite cup-electrode and volatiles were allowed to evaporate. Lithium carbonate powder was then added to duplicate the matrix of standards which were used for calibration. Results are presented in Table 36 along with ultimate analysis data.

Hydrocarbon-type analyses are presented in Table 37. Density and simulated distillation data are presented in Table 38. Comments on these analyses are contained in the discussion section.

- Gas chromatography/mass spectrometry was employed to obtain a total analysis of the sample. Component identifications based on mass spectral data were further refined to give more specific information by using chromatographic Kovats retention indices. By this approach the compound trimethylheptane, for example, could be named specifically (based on its mass spectrum and retention index) rather than listing the compound in more general terms, i.e.,  $C_{10}$  paraffin as determined by GC/MS alone. Area percents are given as an indicator of the amount of each component present. GC/MS results are presented in Table 39. The reconstructed total ion chromatogram is shown in Figure 27.

TABLE 36. ELEMENTAL ANALYSES OF TIRE PYROLYSIS OIL  
(POSF-82-B-0310)

<u>Metals analysis</u>	Concentration, ppm
Copper	100
Manganese	200
Silicon	400
Calcium	75
Iron	100
Titanium	10
Magnesium	100
Aluminum	20
Lead	1
Sodium	8
Chromium	8
Tin	2
Nickel	1

<u>Ultimate analysis</u>	Concentration, %
Carbon	87.40
Hydrogen	11.36
Nitrogen	0.17
Sulfur	0.97

TABLE 37. HYDROCARBON-TYPE ANALYSIS OF TIRE PYROLYSIS  
OIL (POSF-82-B-0310)

	Modified ASTM D 2789	Monsanto
Paraffins	10.8	8.5
Monocycloparaffins	21.6	-
Dicycloparaffins	17.7	-
Total cycloparaffins	39.3	38.3
Alkylbenzenes	24.6	27.2
Indans and tetralins	18.1	13.0
Indenes and dihydronaphthalene	- <sup>a</sup>	5.9
Naphthalenes	7.2	7.1
	100.0	100.0

<sup>a</sup> Dash indicates that Method does not provide information on these as separate compound categories.

TABLE 38. SIMULATED DISTILLATION AND DENSITY  
OF TIRE PYROLYSIS OIL

Percent <u>recovered</u>	Temperature	
	°C	°F
IBP, 0.5	52	125
1	69	156
5	112	234
10	142	287
20	207	405
30	256	494
40	293	559
50	321	610
60	348	659
70	378	712
80	410	769
90	444	832
95	467	873
99	498	928
FBP, 99.5	505	941
Density (15°C)	0.9125	gm/cc

TABLE 39. GC/MS ANALYSIS OF TIRE PYROLYSIS OIL

Retention time	Peak area	Area percent
2.13	3-Methyl 2,5 hexadiene	0.57
2.73	2-Methyl 2,4 hexadiene	1.63
2.93	Toluene	8.43
3.00	Methylthiophene	0.11
3.77	3-Ethylhexane	0.62
3.98	Dimethylcyclohexene	1.47
4.58	Dimethylcyclohexane	0.59
4.78	Ethylcyclohexane	0.81
5.05	Ethylcyclohexene	0.39
5.40	Ethylbenzene	11.56
5.62	Xylene	1.85
6.18	Styrene	0.60
6.22	Xylene	5.50
6.58	Nonane	1.22
6.78	1-Methylcyclohexene-1-carboxaldehyde	0.42
7.12	Cumene	4.09
7.67	$\beta$ -Methylstyrene	0.34
7.85	n-propylbenzene	2.65
8.07	Methylethyl benzene + ethylcyclohexane	1.65
8.48	Methylethylbenzene	0.72
8.82	Trimethylbenzene	1.00
9.12	Trimethylheptane	0.57
9.23	sec-Butylbenzene	1.32
9.48	Methylisopropylcyclohexane	1.09
9.58	Cymene	2.04
9.68	Methylisopropenylcyclohexane	0.45
9.75	Indan	0.89

(continued)

TABLE 39 (continued)

<u>Retention time</u>	<u>Peak area</u>	<u>Area percent</u>
10.20	Diethylcyclohexanes	0.79
10.30	n-Butylbenzene	1.86
10.80	C <sub>4</sub> substituted alkylbenzene	0.37
10.92	Methylindan	1.79
11.30	C <sub>5</sub> substituted alkylbenzene (phenylpentane)	0.59
11.37	2-Methyldecalin	0.78
12.03	Tetrahydroisoquinolone	1.14
12.25	Tetralin	1.48
12.47	C <sub>5</sub> substituted benzene + methyltetralin	1.91
12.87	Naphthalene	0.50
13.03	Dimethylindan isomer	1.32
13.13	Methyl tetralin	0.80
13.23	Methyl tetralin	1.04
13.38	n-Dodecane	0.44
13.73	Dimethylindan isomer	2.08
13.92	Dimethylindan isomer	0.17
14.03	Isopropylisopropenyl benzene	0.32
14.15	Dimethylindan	0.72
14.22	Trimethylindan	0.22
14.40	C <sub>3</sub> substituted indan	0.27
14.45	1-Phenylhexane	1.61
14.58	Methylnaphthyridine	0.27
14.75	Phenylhexene	1.95
14.80	Dimethyltetralin	1.81
15.00	1-Methylnaphthalene	1.55
15.10	Dimethylindol	0.43
15.23	Dimethyltetralin	1.11

(continued)

TABLE 39 (continued)

Retention time	Peak area	Area percent
15.30	2-Methylnaphthalene	0.56
15.48	Cyclohexylbenzene	0.80
15.57	C <sub>7</sub> substituted benzene	0.61
15.95	C <sub>4</sub> substituted indan	0.25
16.15	C <sub>3</sub> substituted tetralin	0.12
16.32	n-Heptylbenzene	1.23
16.52	Biphenyl	0.51
16.70	Toluene diisocyanate	0.39
16.77	Ethyl naphthalene	0.29
16.95	Dimethyl naphthalene	0.56
17.18	Ethylnaphthalene	0.38
17.50	Dimethylnaphthalene	0.31
17.77	Dimethylnaphthalene	0.35
18.05	Phenyloctane	1.40
18.30	Methylbiphenyl	1.0
18.43	Methylbiphenyl	0.26
18.62	C <sub>15</sub> Paraffin	0.60
19.00	Isopropylnaphthalene	0.42
20.07	Methylbiphenyl	0.47
20.42	Diphenylamine	0.54
20.50	p-Ditolyl	0.72
20.87	Diphenylpropane	0.54
21.63	n-Heptadecane	1.76
22.73	D <sub>10</sub> Anthracene (added as internal standard)	
22.93	C <sub>19</sub> Paraffin	0.27
24.35	Methylphenanthrene	0.74
26.83	C <sub>20</sub> Paraffin	0.27
27.98	C <sub>20</sub> Paraffin	0.33
28.12	Di-t-butylethylphenol	0.91

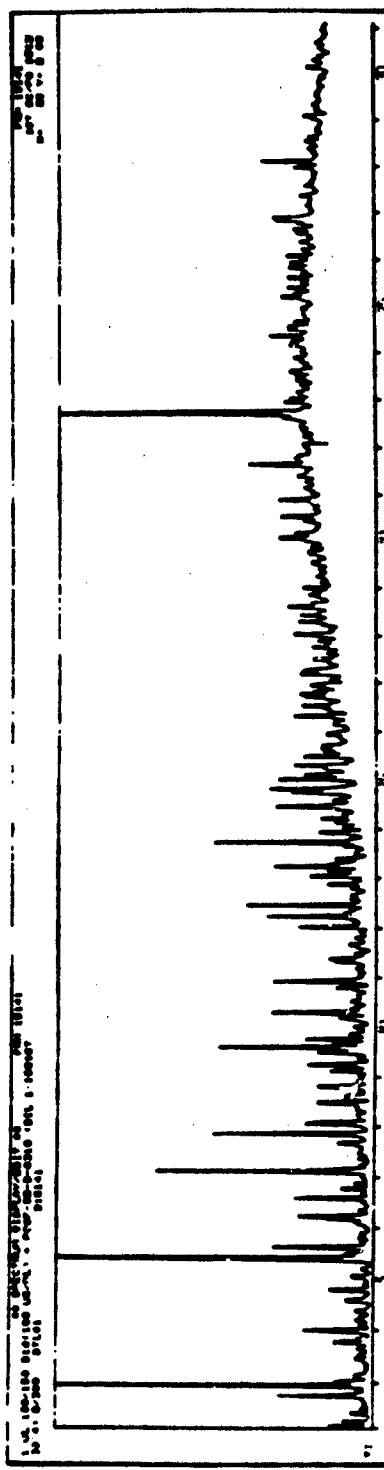
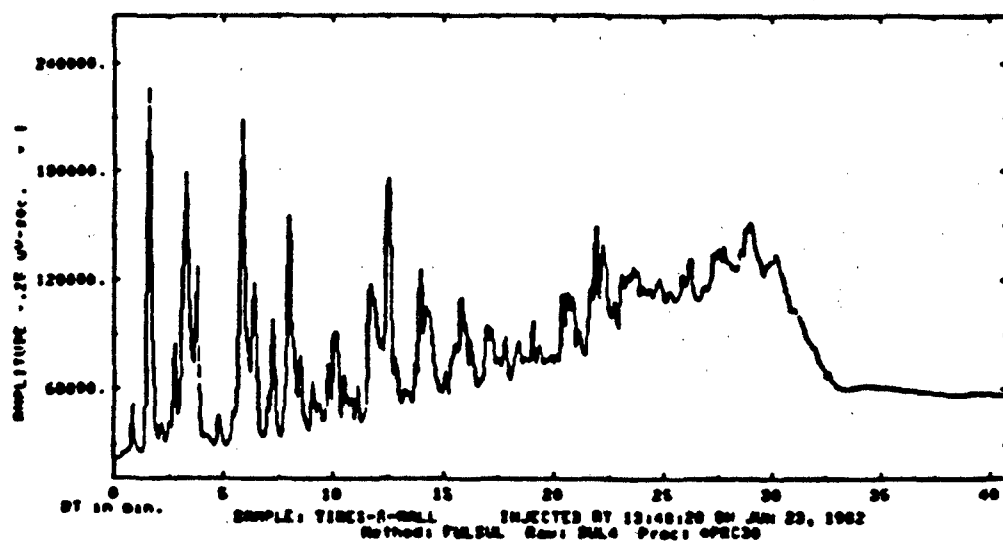


Figure 27. Reconstructed total ion chromatogram of tire pyrolysis oil.

Element-selective detectors were used to aid in characterizing this sample. A 6 ft x 1/8 in. stainless steel column packed with OV-1 stationary phase was used. This column was sufficiently flexible to allow its connection to several different chromatographs, each having slightly differing column dimension requirements. The instrumentation used included a Tracor 560 gas chromatograph having a Hall 700A electrolytic conductivity detector (ECD), configured for operation in the sulfur mode; a Hall 700A ECD configured in the halogen mode, attached to a Hewlett-Packard HP 5710 gas chromatograph; and a nitrogen/phosphorus selective detector also attached to a HP 5710 chromatograph.

It was anticipated from the value for total sulfur content (Table 36), that a number of sulfur components would likely be present in the sample. Results from an analysis using the sulfur-selective detector showed this to be the case as depicted in Figure 28. The second peak (retention time 3.30 min.) is one of the largest in the chromatogram and it corresponds to the retention time to be expected for methylthiophene. This compound has been identified by GC/MS, and quantitated at 0.11 total ion percent. Other sulfur components appear to be below the 0.1% level in the original sample and identification was not readily achieved for them by GC/MS. To compare data for the tire pyrolysis oil with that of a standard fuel, an Air Force Fuel Bank JP-4 (AFFB 14-70) was analyzed along with the sample. The chromatogram of this fuel also is shown in Figure 28. In comparing results, it should be noted that the detector response is approximately six times more sensitive for the JP-4 analysis than for the pyrolyzate analysis, indicating that the pyrolyzate has a wider variety and higher concentration of sulfur compounds than the petroleum JP-4. Examination of the integrated output (not shown) from the sample chromatogram of Figure 28 indicated that more than 50 sulfur components are present, none of which represents more than 2% of the total integrated sulfur response. No sulfur component appears to be greater than 0.1% of the total

A



B

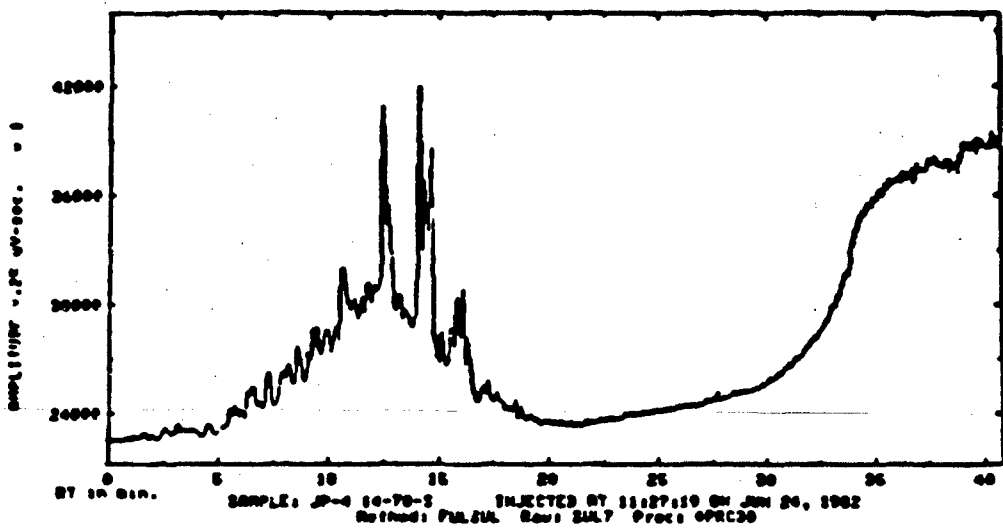


Figure 28. Chromatograms using Hall 700A detector in the Sulfur-Selective Mode.

A. Tire Pyrolysis Oil

B. JP-4 Reference Fuel (AFFB-14-70)

sample; many are in the pr. range. Special methodology would be required for the separation and identification of these compounds. This methodology can be developed if the need warrants it.

The Hall ECD, operating in the halogen mode shows no halogen compounds to be present in the sample. Chromatograms presented in Figure 29, show no responses for either the pyrolyzate or the reference JP-4, AFFB-14-70.

Chromatograms of the sample and the reference JP-4, obtained with the nitrogen selective detector, are shown in Figure 30. The reference JP-4 shows little or no nitrogen-containing material, however, the pyrolysis sample shows a moderate number of compounds as listed in Table 40. The major compounds have been identified and have been given in Table 39; however, those present at lower levels were not detected by GC/MS and are believed to have concentrations of less than 0.1 percent. These compounds could be identified by further separation and analysis if this information were desired.

Proton nuclear magnetic resonance was used to measure the olefinic content of the samples. For this purpose, the spectral region from 6.0 to 4.5 ppm, which is characteristic of olefinic protons, was integrated. The olefinic protons in the sample were found to constitute 0.4% of the total protons, as shown in Table 41. Since no well-defined peaks were observed in the 6.0-4.5 ppm spectral region, the olefinic protons should be considered to be 0.4% or less.

The average carbon number, obtained from the 50% point of the simulated distillation is 18.8. If the unlikely condition existed that all olefin compounds in the sample were monoolefins, a maximum possible value for weight percent of olefins could be determined.

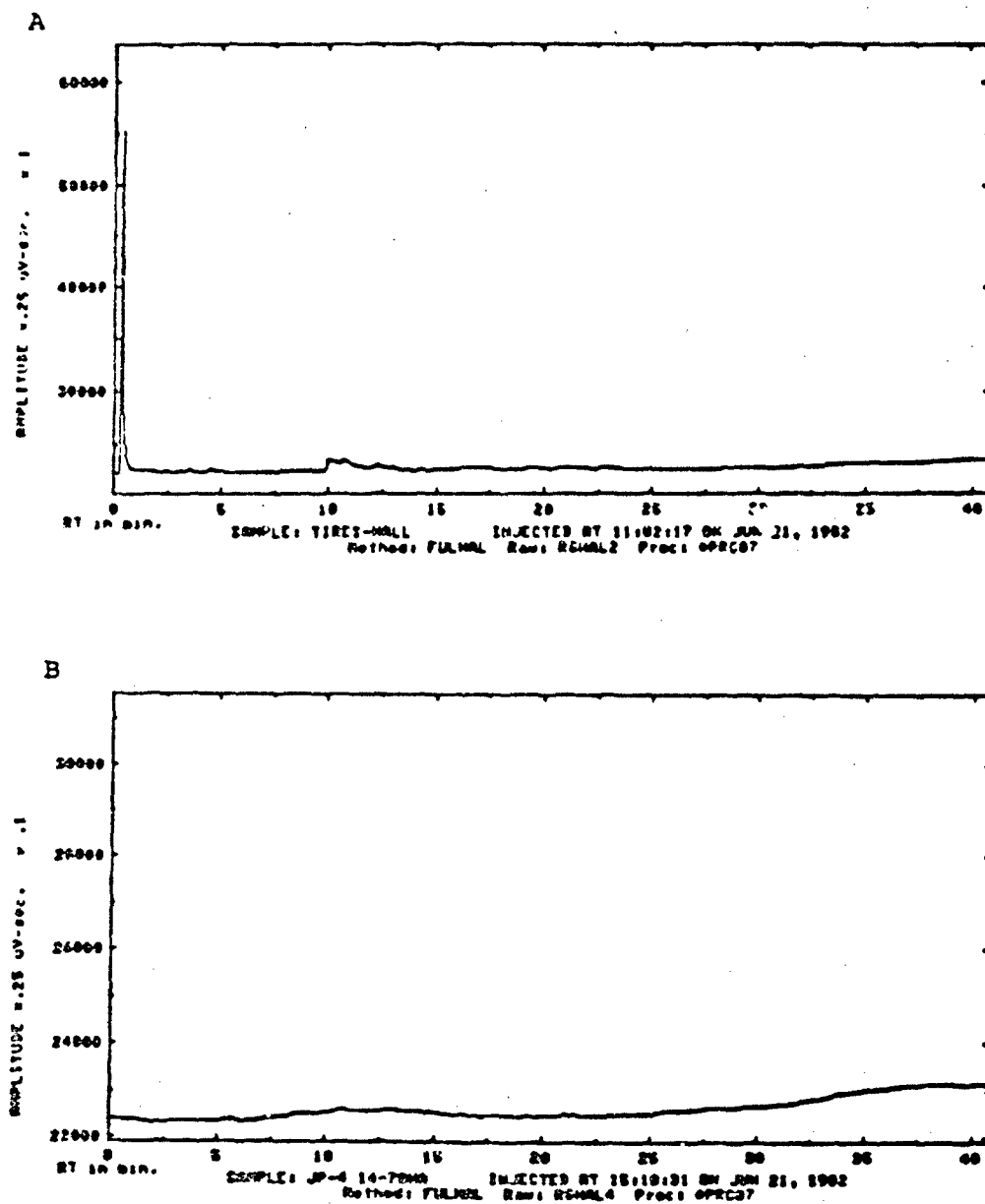


Figure 29. Chromatograms using Hall 700A detector in the Halogen-Selective Mode.

A. Tire Pyrolysis Oil  
 B. JP-4 Reference Fuel (AFFB-14-70)

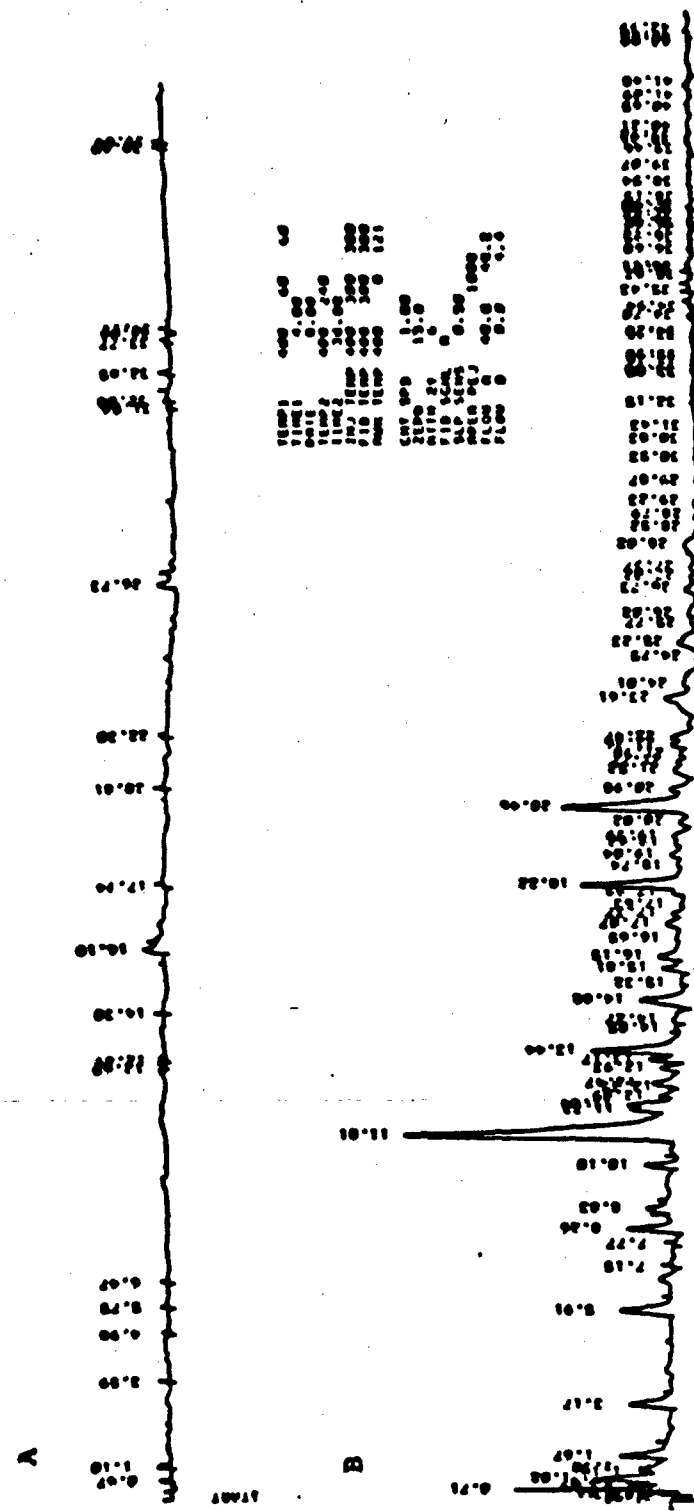


Figure 30. Chromatogram using N/P selective detector for nitrogen compounds:

- A. JP-4 Reference Fuel (AFFB-14-70)
- B. Tire Pyrolysis Oil

TABLE 40. MAJOR PEAK RESPONSES FOR TIRE PYROLYSIS OIL USING GC/NITROGEN SELECTIVE DETECTOR

Retention time, minutes	Probable compound based on GC/MS data
1.67	-
3.17	-
5.91	-
8.26	-
11.01	Tetrahydroisoquinolone
13.44	Methylnaphthyridine
14.88	Dimethylindol
18.22	Toluenediisocyanate
20.46	Diphenylamine

TABLE 41. PROTON NMR ANALYSIS OF SAMPLE POSF-82-B-0310

I. INTEGRAL AREAS OF SPECTRAL REGIONS

Spectral region, ppm	Integral designation	Integral area
8.0 - 6.3	Aromatic	22
6.0 - 6.5	Olefin	≤1 <sup>a</sup>
3.0 - 2.0	α-Methyl	28
2.0 - 1.5	Methine	43
1.5 - 1.0	Methylene	82
1.0 - 0.3	Methyl	53
TOTAL		229

II. PERCENT OF OLEFINIC PROTOMES

$$\frac{1 \times 100}{229} = 0.4\% \text{ or less}$$

<sup>a</sup>No well defined peaks observed in this spectral region.

The average monoolefin in the sample would have an empirical formula of  $C_{19}H_{38}$ . Approximately 2.2 of the 38 protons would be of an olefinic nature, or about 5.8% of the protons. Accordingly, if the entire sample consisted of such an average monoolefin, 5.8% of the protons would be olefinic protons. Since 0.4% (or less) of the protons are of an olefinic nature,

$$\frac{0.4}{5.8} \times 100 = 6.9\% \text{ or less}$$

of the sample can consist of olefins of the average carbon number. If some olefins are cycloolefins, di- or triolefins, or are attached to an aromatic molecule, this value would be reduced proportionately.

These latter types of compounds are known from GC/MS analyses to exist in the sample. Thus olefins are probably present at a weight concentration of no more than 5%.

#### Discussion

The tire pyrolysis sample which has been the subject of this work represents an unusually complex mixture because:

1. The high content of nitrogen and sulfur permits two arrays of hetero-compounds in addition to the hydrocarbons usually encountered.
2. The wide boiling range (from 52-505°C) provides ample opportunity for sample complexity in terms of numbers and kinds of components.
3. An unusually large number of compounds at very low concentrations exist in the sample and are perhaps characteristic of the manner in which the sample was produced.

This mass of low level components appears in the chromatogram shown in Figure 27 as an envelope of unresolved peaks, particularly in the latter part of the chromatogram. Though these components are below the 0.1% target level for this work, mass spectra are complicated by the appearance of extra lines due to these materials. Computer search programs are thwarted thereby, and manual searches must be conducted.

For the reasons cited above, routine analyses such as the hydrocarbon-type analysis presented in Table 37, are of questionable value for quantitative results. These analyses correctly portray the sample as being largely aromatic with a paraffin fraction that is high in naphthene content. A better hydrocarbon type analysis could be obtained by splitting the sample into two narrower cuts by distillation. The first cut then could be adequately characterized by the methods used, while the heavier cut would require a method such as ASTM D 2425.

The GC/MS analyses would also benefit from a preanalysis separation. Separation into aromatic and nonaromatic fractions would greatly aid in the analysis of samples of this complexity.

## SECTION IV

### ANALYSIS OF FUELS RELATED DEPOSITS, CONTAMINANTS, AND IMPURITIES

Despite great attention given by the Air Force and the suppliers of its fuels to ensure fuel integrity, fuels occasionally exhibit problems related to particulate or deposit formation. Any time a fuel is transferred, transported or even stored for a period of time, particulate matter may be picked up by interaction with the tank walls and/or water layer, by insoluble gum formation, or by outside contamination. Suspended material may clog filters or fuel system components having close tolerances, and thus threaten the reliability of the fuel system.

During the course of this program, several investigations have been conducted to determine the nature and possible source of fuel particulate contaminants and fuel deposits.

#### 1. IDENTIFICATION OF MATERIAL FOUND IN THERMAL DEPOSIT RINSE SOLVENT

A sample which appeared to consist of several needle-like crystals was received for identification. The sample was thought to have resulted from interaction of thermal degradation deposits, formed on stainless steel, with 300 mL of 1-methyl-2-pyrrolidone. This solvent had no apparent effect on the deposit but after removal of the stainless steel plate and decantation of the solvent, the needles were found.

Since the amount of sample was quite small, initial non-destructive tests were conducted by microscopy. Microscopic examination indicated that the rod-like material showed strong longitudinal orientation and fractured longitudinally only with difficulty. The material was not brittle but showed plastic-like properties. It was found to be birefringent with extinction at approximately 45°. On the heated microscope stage, the sample appeared to

soften at approximately 240°C with loss of orientation, while becoming shorter and wider. It was concluded from the microscopic examination that the material was of a polymeric nature.

In preparation for infrared absorption spectral analysis, the rod-like material was washed with hexane to remove any remaining 1-methyl-2-pyrrolidone. After air drying, the sample was ground and pelletized with potassium bromide. Infrared absorption spectra were recorded using the Digilab FTS-15 B/D Fourier transform spectrometer. The spectra, presented in Figure 31, show the material to be a nylon (polyamide) as indicated by the following bond assignments:

1659 $\text{cm}^{-1}$	amide I
1547 $\text{cm}^{-1}$	amide II
1450 $\text{cm}^{-1}$	$\text{CH}_2 + \text{CH}_3$
1238 $\text{cm}^{-1}$	C-N stretch and NH bend

A literature spectrum [2] of a nylon is shown in Figure 32.

### Conclusion

It seems likely that the needle-like pieces of material are bristles from a brush which inadvertently found their way into the solvent.

## 2. IDENTIFICATION OF SOLIDS IN DRUM OF AROMATIC BLENDING STOCK

An aromatic blending stock, 2040-solvent, had been stored in a 55-gallon epoxy-lined drum located at the Aero Propulsion Laboratory. Material drained from the drum was found to consist of a yellow liquid having clumps of light-colored suspended solids. The original 2040-solvent, though having a yellow hue, was completely clear, i.e., free of any turbidity or precipitate.

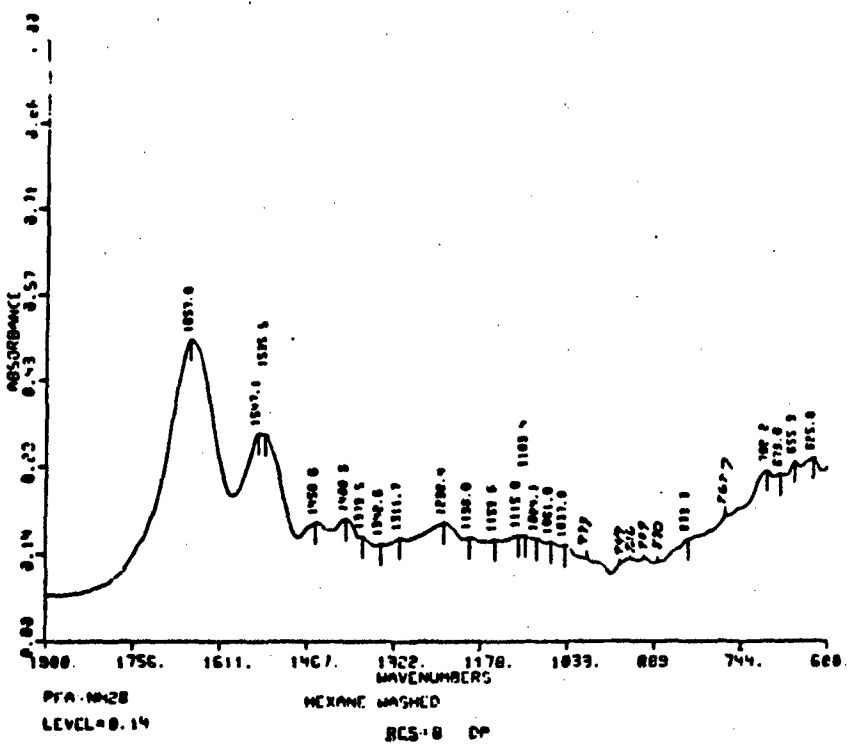
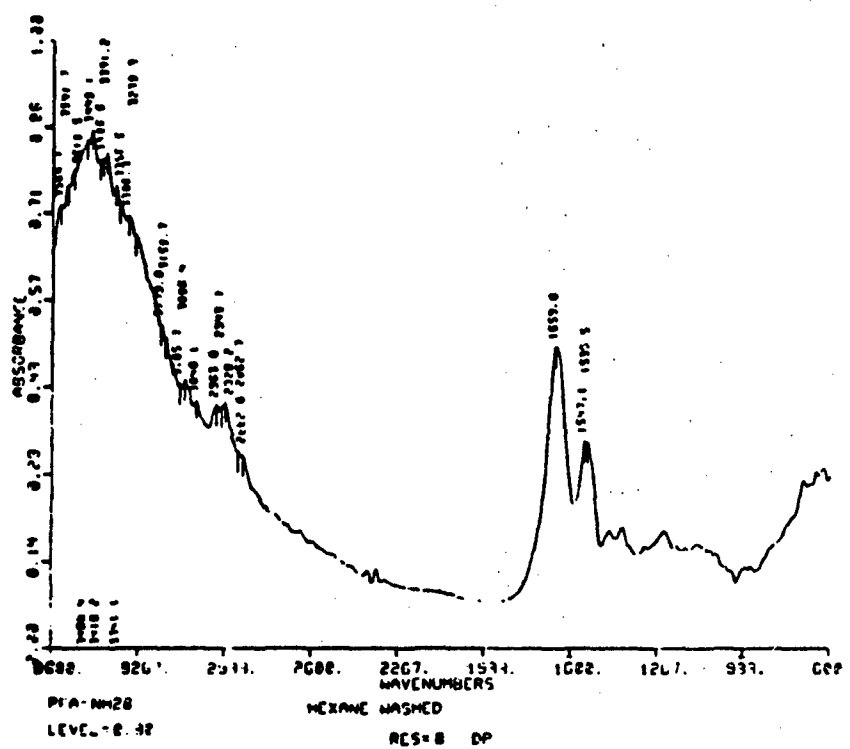


Figure 31. Infrared absorption spectra of needle-like material isolated from fuel.

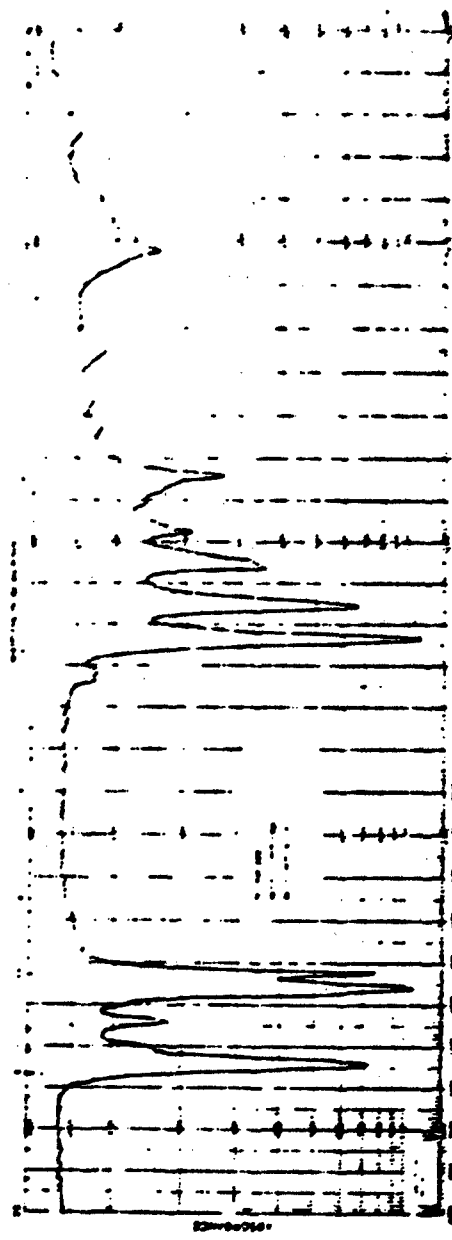


Figure 32. Infrared absorption spectrum of a nylon 121.

It was thought possible that the solvent had attacked the drum liner, though epoxy is the recommended contact material for hydrocarbon fuel storage. The specimen was analyzed to determine the identity of the solids and to establish whether the drum lining was involved in the observed changes in the subject sample.

### Experimental

The solid portion of the sample, which was readily separated from the liquid part by filtration, consisted of white crystalline material. Both infrared absorption and proton resonance spectra of the solids were recorded and are presented along with reference spectra of naphthalene [Ref. 3] in Figures 33 through 36. These data show that the solid is quite pure naphthalene. An infrared absorption spectrum of the liquid part of the sample (filtrate) was recorded (Figure 37) for comparison to a reference spectrum of 2040-solvent in its original condition (Figure 38). This original 2040-solvent will be referred to as 2040-Reference in the following discussions. A spectrum resulting from the subtraction of data shown in Figures 37 and 38 resulted in the spectrum shown in Figure 38. The latter clearly shows that the major difference between these specimens is an excess of naphthalene in the filtrate compared to 2040-Reference.

These materials were also compared by gas chromatography, with resulting chromatograms being shown in Figure 40 (a and b). The chromatogram of the 2040-Reference matches a chromatogram obtained earlier for this material, and presented in a previous report [Ref. 4]. The filtrate from the sample and 2040-Reference show essentially the same chromatographic peaks but with significantly altered intensities. The largest peak in the liquid portion of the sample was found to be due to naphthalene, which has a retention time of about 14 minutes. A Perkin-Elmer Model 3920B with 50-meter glass capillary column coated with SF-96, was used for the work. Temperature was held at 60°C for 4 minutes, then increased to 180°C at the rate of 4°C/minute.

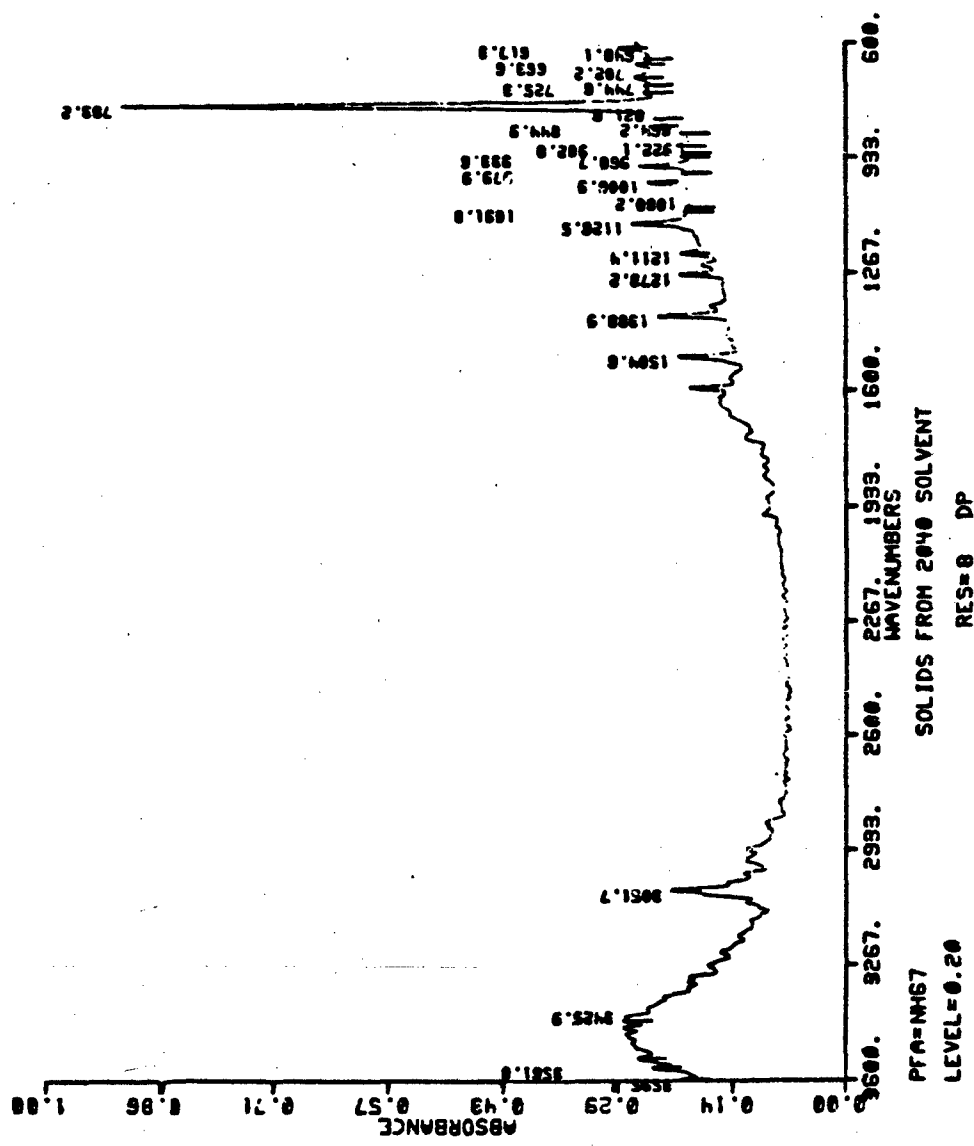


Figure 33. Infrared absorption spectrum of solids separated from subject sample.

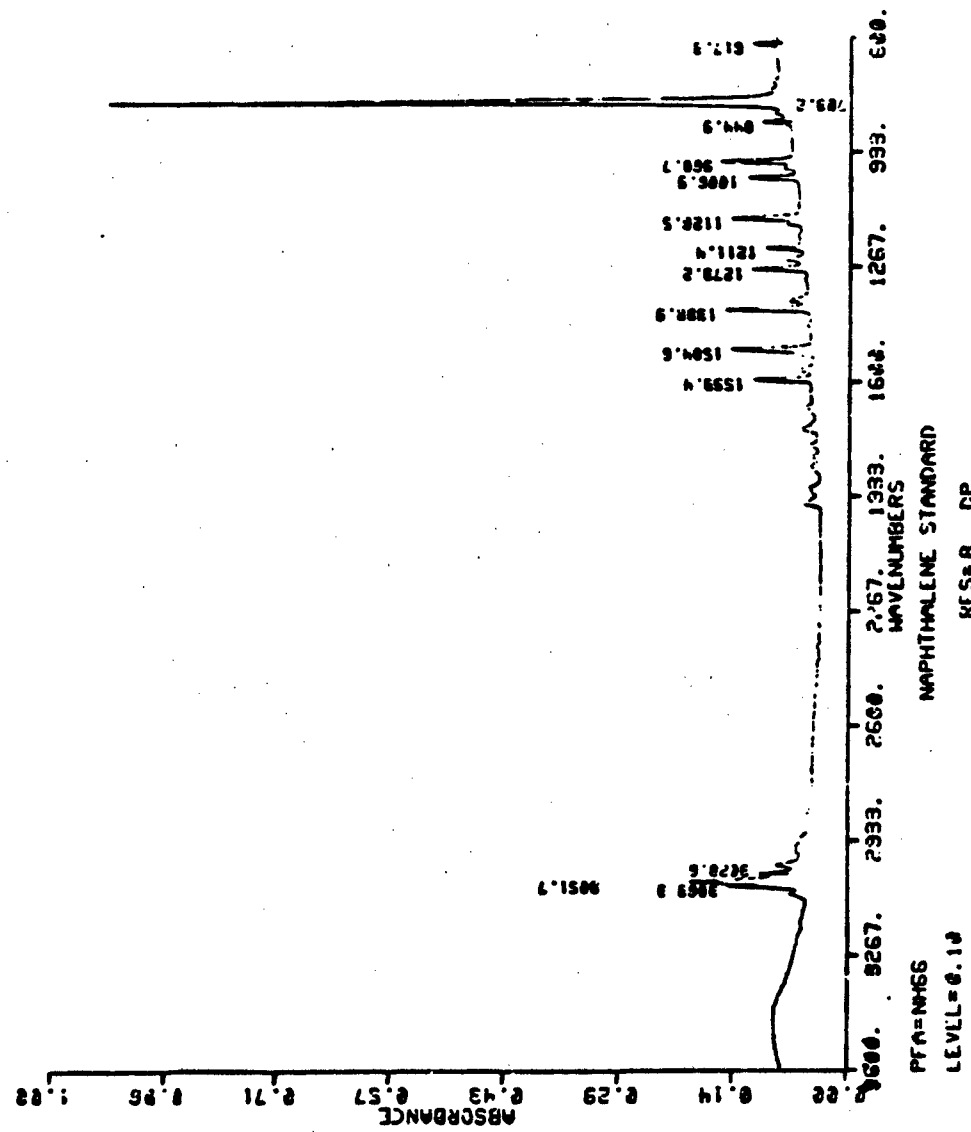


Figure 34. Infrared absorption spectrum of naphthalene reference compound.

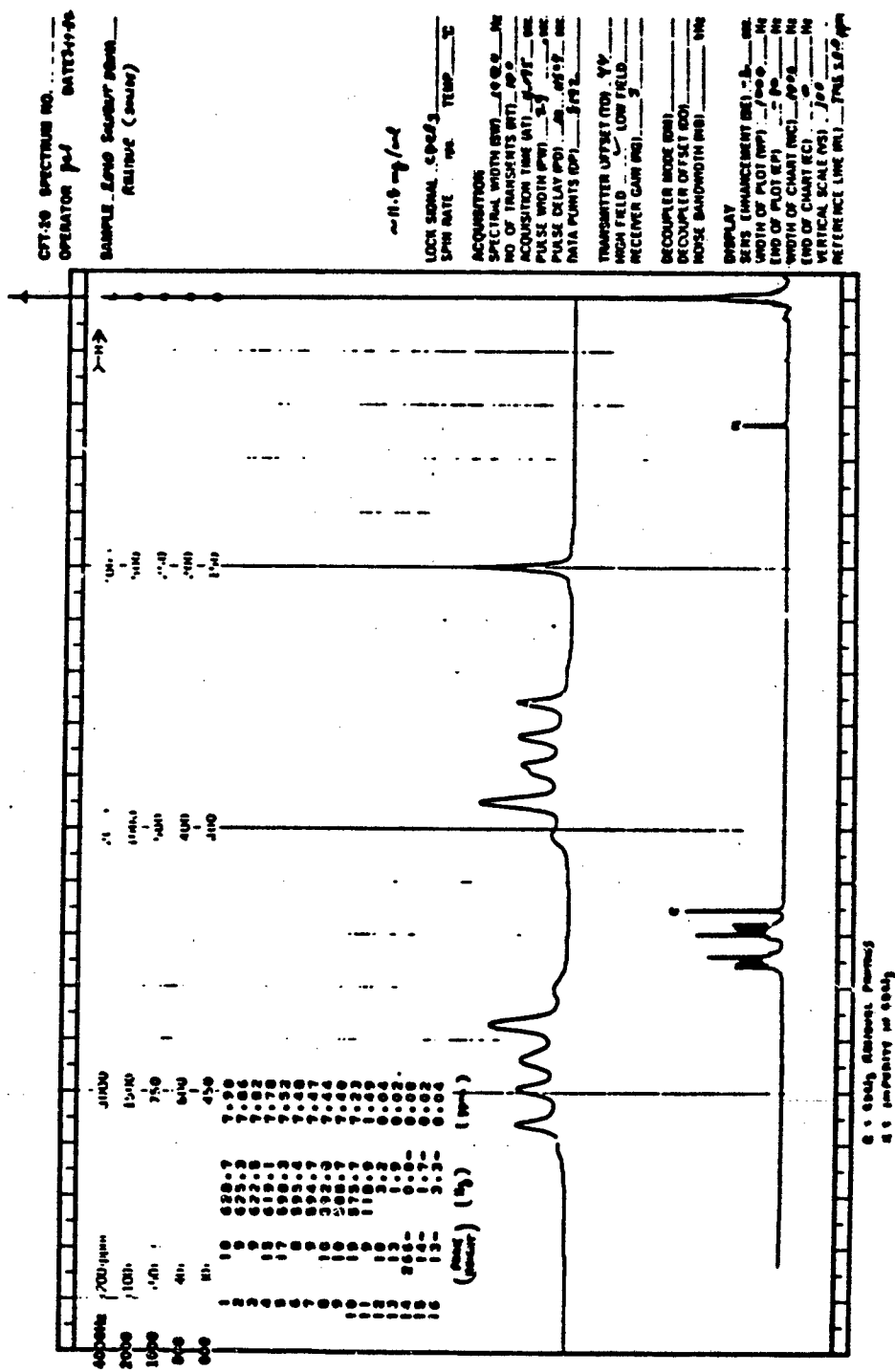


Figure 35. Proton resonance spectrum of sample solids.

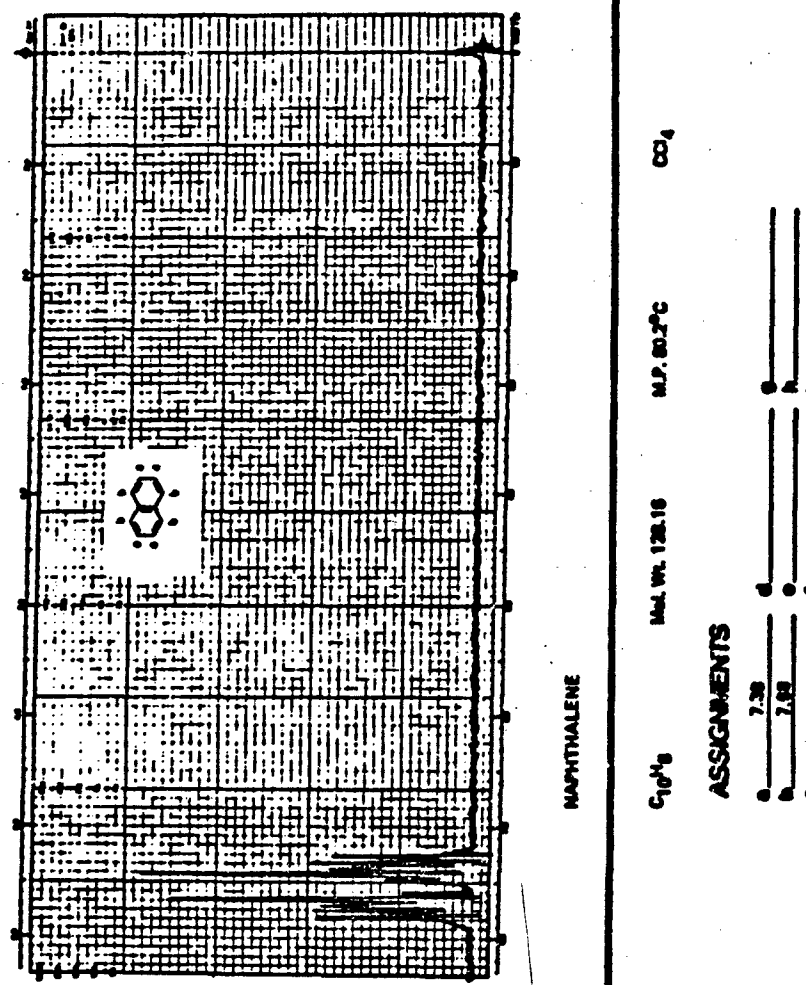


Figure 36. Reference proton resonance spectrum of naphthalene (Ref. 1).

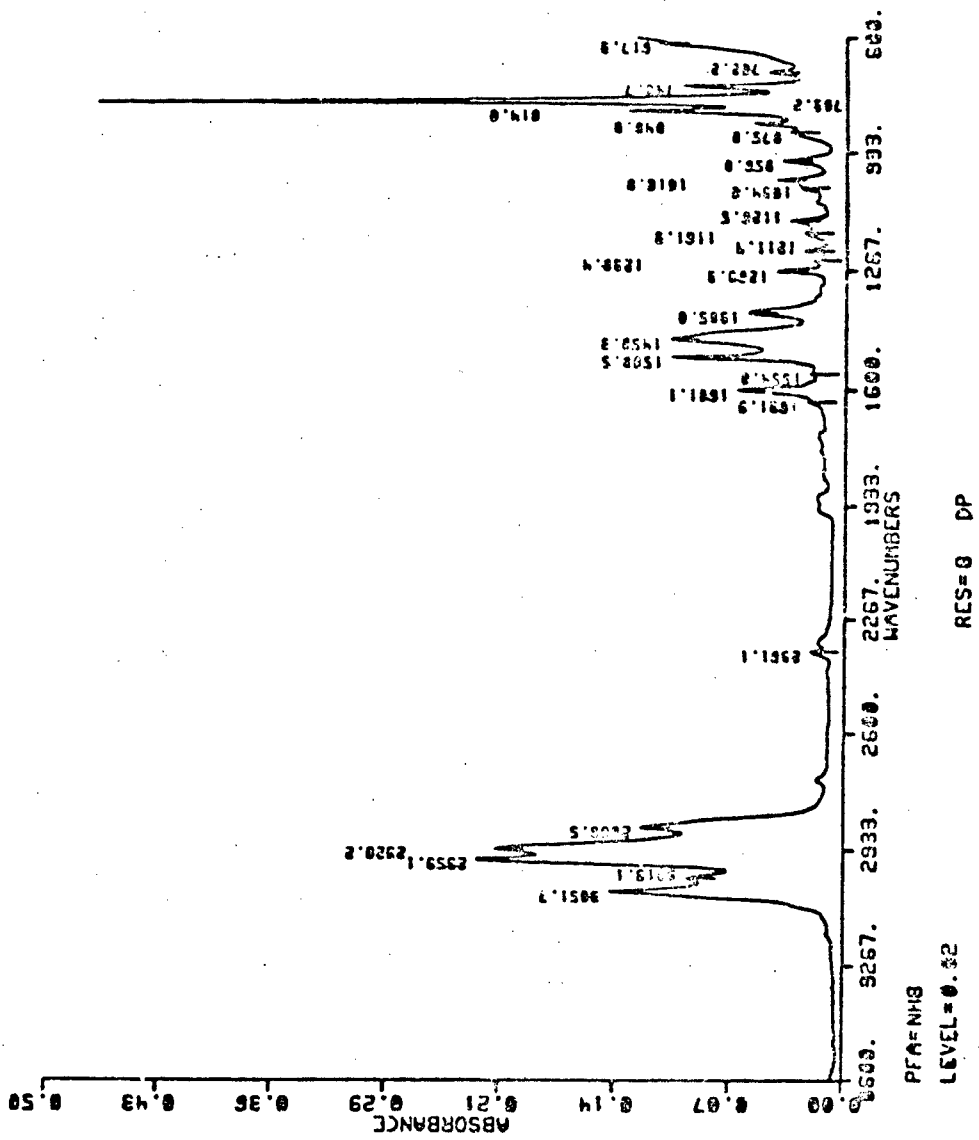


Figure 37. Infrared absorption spectrum of sample filtrate after removal of sciiids.

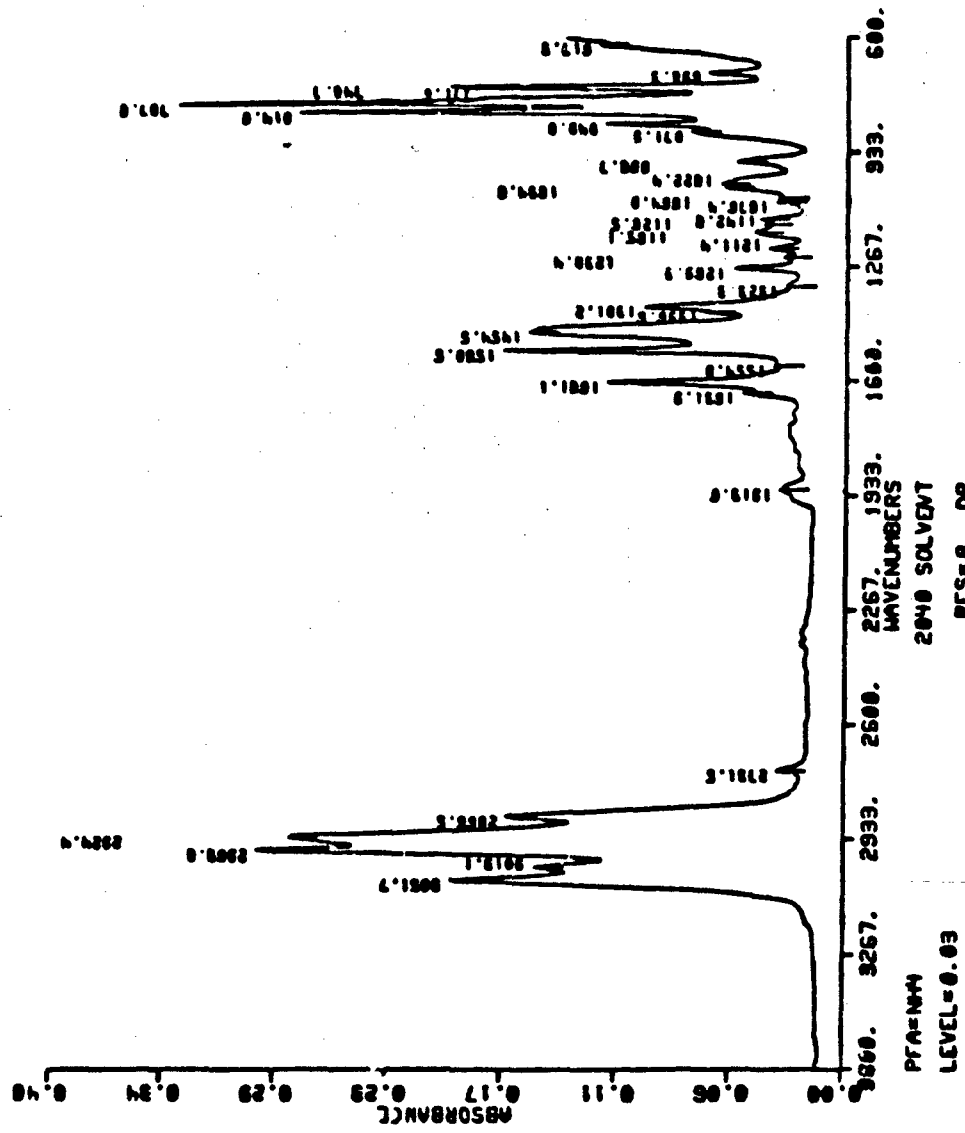


Figure 38. Infrared absorption spectrum of original 2040-solvent (2040-Reference).

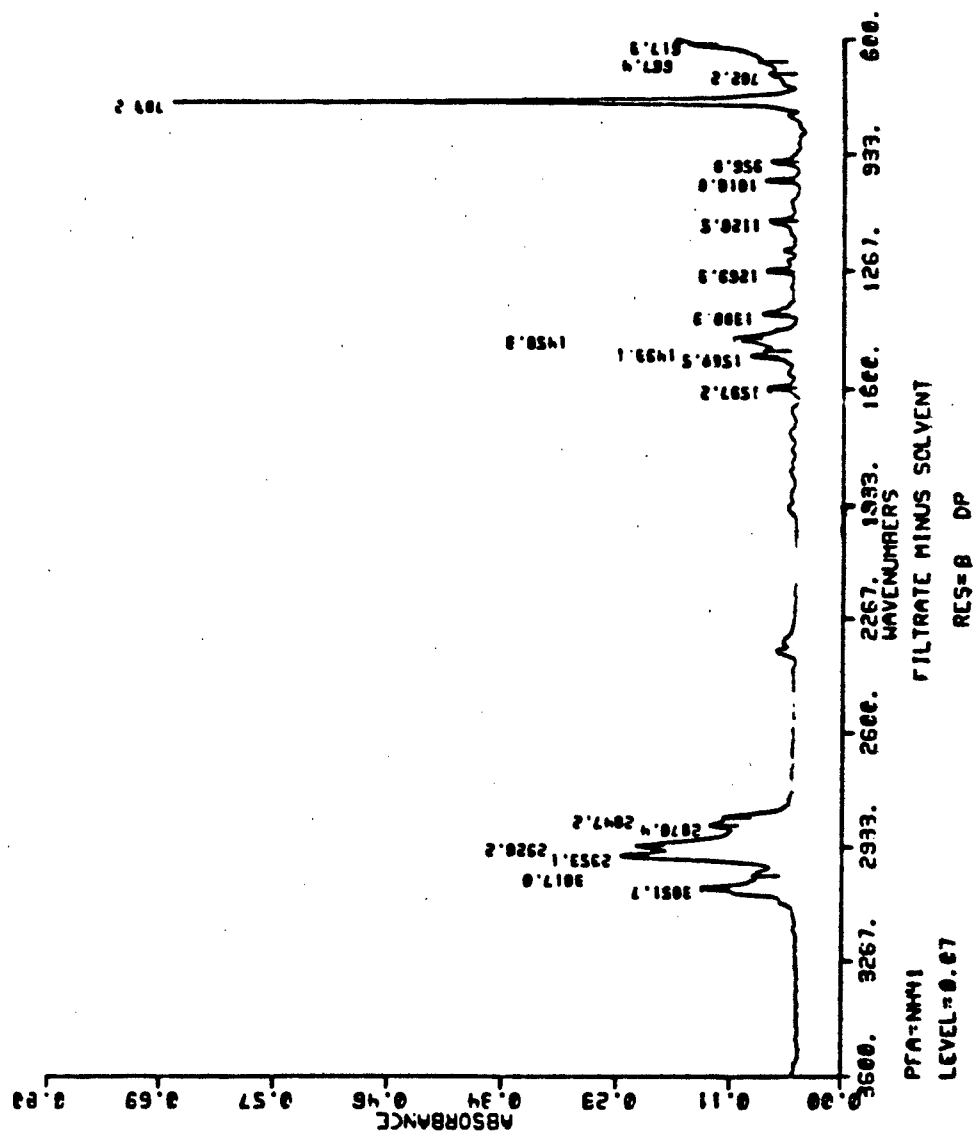


Figure 39. Infrared absorption spectrum resulting from subtraction of 2040-solvent (original) spectrum from spectrum of filtrate.

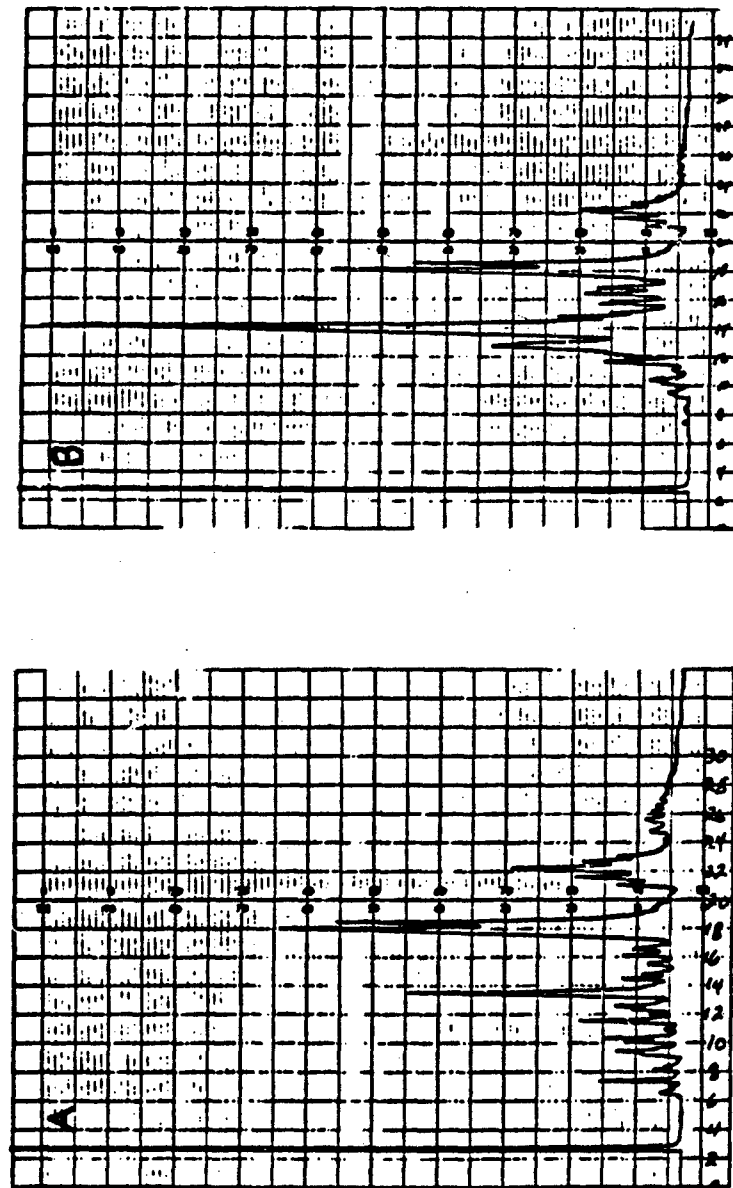


Figure 40. Gas chromatogram of (a) 2040-solvent reference and (b) sample filtrate after removal of solids.

To determine whether dissolved epoxy resin was present in the sample as received, infrared spectra of both the solid and the filtrate were examined for characteristic absorption bands as presented below [Ref. 5]:

<u>Type of epoxy</u>	<u>Expected absorption (cm<sup>-1</sup>)</u>
Based on epichlorohydrin and bisphenol-A	1515, 830, 1250 971, 917, 775
Derivatives of monovalent phenols	693
Based on bisphenol F	840, 758
Epoxy resin esters	1,739

No epoxy was found to be present and no evidence could be found for fuel/epoxy interaction. The aromatic stock, 2040-solvent is known to contain high levels of naphthalene and alkyl-substituted naphthalenes. These compounds were found to be above their normal levels in the subject sample. Polymerization or other internal reactions are extremely unlikely and would not account for the excess of naphthalene. It seems likely that nucleation and precipitation of naphthalene has occurred. Since the specimen was drawn from the bottom of the drum, a slurry of crystalline naphthalene in naphthalene-saturated solvent was obtained.

### 3. CHARACTERIZATION OF SUSPENDED SOLIDS IN JP-4 FUEL

A sample of JP-4 fuel, coded POSF-82-C-0301, which was obtained from an operational Air Force Base, showed a tendency to plug filters. A specimen of the fuel was examined to determine the identity of its particulate contaminants. Additionally, the fuel was characterized by hydrocarbon type analysis, trace metals analysis, and the determination of density at 15°C. Monsanto Method 21-PQ-38-63 and the modified ASTM D 2789 was used for hydrocarbon-type analyses. The dilatometer method was used to determine density and the value determined at 15°C was 0.7743 gm/cc.

### Experimental

After thoroughly shaking the fuel container to disperse particulates, an aliquot of the fuel was removed for filtration. The specimen was passed through a 0.45 micron millipore membrane filter. The filter which contained a heavy brown deposit was rinsed with pentane to remove residual fuel and was dried. X-ray emission spectrography was used for the nondestructive determination of the major elements present in the filter deposit.

By this technique, all elements except for the first twelve in the periodic table are detectable. Only iron was found in the filter deposit.

The color of the particulates was found to vary from light tan to a dark brown/black when examined by light microscopy. Particle size was found to range from  $0.5 \mu$  to  $35 \mu$ , with most particles being less than 4 microns in diameter. No fiberous material was found and there was no evidence of any significant amount of sand or terrestrial dust.

The filter still retained a slight odor of fuel, thus it was allowed to remain in a stream of clean air until the odor was no longer detected. Fourier transform infrared (FTIR) reflectance spectra were then recorded of the filter deposit. A spectrum of the blank filter was recorded and subtracted from the composite spectrum of filter and deposit. The spectrum showed only weak C-H bands similar to those to be expected from the fuel. Because of the weakness of the spectrum and the absence of additional definitive bands, the chief conclusion to be drawn from the data is that any organic material present in the sample constitutes only a small part of the total sample.

The composition of the fuel by hydrocarbon types, presented in Table 42, does not differ significantly from that which would be expected of a typical JP-4. The only possible exception to this generalization lies in the cycloparaffin level which is significantly greater than the level of acyclic paraffins.

TABLE 42. HYDROCARBON-TYPE ANALYSIS OF SAMPLE POSF-82-C-0301

	Weight percent	
	ASTM D 2789 <sup>a</sup>	Monsanto <sup>b</sup>
Paraffins	37.5	32.6
Monocycloparaffins	37.3	-c
Dicycloparaffins	6.6	-c
Total cycloparaffins	43.9 <sup>d</sup>	48.7
Alkylbenzenes	15.7	17.5
Indans and tetralins	1.8	1.1
Indenes and dihydronaphthalenes	-c	0
Naphthalene	1.1	0.1

<sup>a</sup>Modification of ASTM Method D 2789.

<sup>b</sup>Monsanto Method 21-PQ-38-63.

<sup>c</sup>Dash indicates method does not provide information on these specific compound categories.

<sup>d</sup>Sum of two preceding values.

The fuel was subjected to trace metals analysis using inductively coupled argon plasma (ICP) spectroscopy. The fuel was analyzed prior to filtration and then reanalyzed after removal of particulates. An ISA model JY48P inductively coupled argon plasma spectrometer was used for the analyses which were conducted on aqueous acid extracts of the fuels. The procedure provided a 20:1 concentration of the metals in the extract. Results are presented in Table 43. It will be noted that the iron level is significantly reduced in the filtered sample.

TABLE 43. TRACE METAL ANALYSIS OF FUEL BY ICP SPECTROMETRY

Elements of detection	<u>R</u>	<u>Mg</u>	<u>Be</u>	<u>Cr</u>	<u>Mn</u>	<u>Fe</u>	<u>Ti</u>	<u>Al</u>	<u>Ca</u>	<u>Cr</u>	<u>Fe</u>	<u>Si</u>	<u>Sn</u>	<u>Zn</u>	<u>Be</u>	<u>Co</u>	<u>Fe</u>	<u>Sn</u>	<u>Zn</u>	<u>Be</u>	<u>Co</u>	<u>Fe</u>	<u>Sn</u>	<u>Zn</u>	<u>Be</u>	<u>Co</u>	<u>Fe</u>	<u>Sn</u>	<u>Zn</u>	
Instrument quantification limit, LOQ, ppb	3,100	56	4	20	2	260	3	160	66	40	53	100	20	46	26	21	970	2	6	16	13	132	4							
LOQ after concentration <sup>a</sup> , ppb	155	2.8	0.2	1	0.1	13	0.15	0	3.3	2	5.7	9	1	2.3	1.3	1	36	0.1	0.3	0.8	0.35	6.6	0.2							
Acid extraction blank, ppb						0.2																								
Concentration of Elements in Fuel Samples <sup>b</sup> , ppb																														
JP-4 10SF-92-C-0301						0.2	0.9																							
JP-4 10SF-92-C-0301 after filtration						0.2	0.9																							
Analysis of Reference Standard, ppb																														
True values	-	-	261	304	470	1,000	1,000	852	1,000	376	1,000	848	-	1,000	796	-	478	1,000	348	-	165	-								
Observed value	-	-	286	293	459	874	1,030	910	925	395	1,160	966	903	-	974	829	-	459	1,000	326	-	174	-							
Percent recovery	-	-	110	96	104	87	103	107	93	106	116	97	106	-	97	104	-	104	104	94	-	105	-							

<sup>a</sup>Fuel samples were effectively concentrated by a factor 20 by extraction with a small volume of aqueous acid for the analysis.

<sup>b</sup>Aqueous ultrapure acid used to extract the fuel samples for analysis. An "x" shows that the element was not detected at the instrument LOQ.

<sup>c</sup>An "x" shows that the element was not detected at the LOQ after concentration. The numerical values were obtained by dividing the observed value by 20 to take into account the concentration effect, then subtracting any blank value obtained. These values represent the element concentration in the original fuels.

### Conclusions

No significant amount of organic solids were observed in the fuel. The amount of suspended inorganic iron particulate, likely oxides of iron, is sufficient to yield a dark filter deposit from only a few milliliters of fuel. Blockage of the fuel filter could likely occur with larger volumes of fuel.

### 4. ANALYSIS OF TANK BOTTOM SAMPLES FROM ATWATER TANK AW-1

Samples obtained from the bottom of Atwater fuel storage tank AW-1 were examined to aid in determining the cause of filter plugging by JP-4 supplied to Castle Air Force Base from that tank. Two samples coded POSF-82-B-0315 and POSF-82-B-0319 were received by this laboratory in one quart wide mouth Mason jars. The center section of the two-piece lid was reversed (installed upside down) on one of the jars. These containers were packed in vermiculite, thus great care was required to insure that the samples were not contaminated with the packing material upon opening. In addition to the two tank bottom samples, a membrane filter residue coded POSF-82-S-0318, obtained by filtering JP-4, was examined.

Two fuel additives were suggested as materials which could possibly cause filter plugging. One was polyisobutylene or a similar type of viscosity improver; the other was proposed as possible degradation products of corrosion inhibitor. Special attention was given to either confirming or denying these as causes of the filter plugging problem. Other possible causes were also suggested.

### Experimental

The two tank-bottom samples consisted of solids in contact with a liquid phase, nominally JP-4 and water. Analysis of the solids by the energy dispersive X-ray emission technique showed that iron

was by far the most abundant element detectable in the solids. All elements, except for the first 12 in the periodic table, can be detected by X-ray emission spectroscopy without special provisions or procedures. The elements found in the solids are given in Table 44. These data support a general observation that the bulk of the solids appear to consist of rust, much of which is finely divided.

TABLE 44. ELEMENTS FOUND IN THE SAMPLE SOLIDS BY ENERGY DISPERITIVE X-RAY EMISSION

Element	Estimated level
Iron	Major constituent
Calcium	Minor (<5%)
Phosphorus	Trace (<1%)
Manganese	Trace (<1%)
Zinc	Trace (<1%)
Sulfur	Trace (<1%)

The liquid portion of the sample consisted of separate aqueous and hydrocarbon phases. The aqueous portion of the sample was separated and a part of it was evaporated to dryness. The residue remaining was a white crystalline material that proved to be sodium chloride.

The sample solids were rinsed with diethyl ether and then chloroform to remove any adsorbed organic material. The volume of chloroform was then reduced by evaporation. The last portion was deposited on a rock salt plate before further evaporation to eliminate the last traces of solvent. An infrared absorption spectrum of the residue was then recorded.

The hydrocarbon portion of the sample was carefully filtered through a 0.45 micron millipore membrane filter, which retained a heavy loading of the fine particulate previously characterized as rust. In order to isolate any organic material present on the filter, the filter was thoroughly back-flushed with diethylether and then chloroform. The solvents were then combined for evaporative volume

reduction. The organic residue remaining after complete evaporation was deposited on a rock salt plate to facilitate recording of an infrared absorption spectrum.

The spectrum obtained for this specimen, and the one recorded for the previous rinse of the sample solids, were nearly identical. A representative spectrum is shown in Figure 41. The spectrum is characteristic of the predominant paraffin hydrocarbons found in JP-4. The material appears to be a fuel residue. Spectra recorded for reference specimens of DCI-4a and Hitec E-515 corrosion inhibitors are shown in Figures 42 and 43. A major feature common to spectra of these corrosion inhibitors is the carbonyl (C=O stretch) band at 5.7 - 5.8 microns. The carbonyl functionality would be likely to remain a part of the structure of that additive's major degradation products as well. A carbonyl band is not present in any of the sample spectra. Consequently it seems unlikely that corrosion inhibitor degradation products are present as particulate matter in the fuel. Polyisobutylenes, too, have distinctive spectral features which include a prominent band at 8.1 microns and a doublet at 7.2 and 7.3 microns. A doublet at 10.5 and 10.8 is also usually present. These are clearly not present in the spectrum shown in Figure 41.

The oxides of iron have no significant absorption bands in the spectral region being used for these measurements.

The filter residue differs from one examined previously and described in Technical Operating Report 2035-012 in that, in this case, the number and relative concentration of metals present in the residue is much greater. The filter deposit analysis is presented in Table 45.

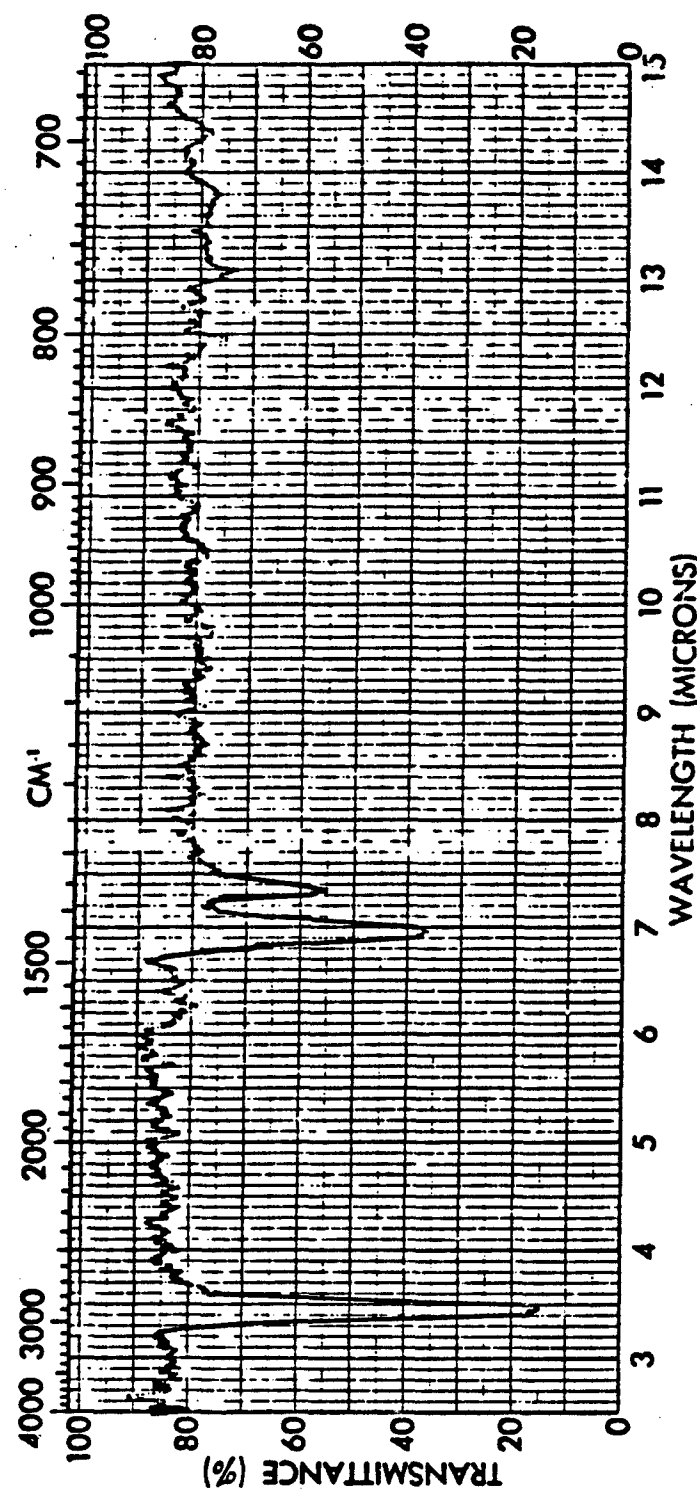


Figure 41. Infrared absorption spectrum of organic material filtered from fuel portion of tank bottom samples.

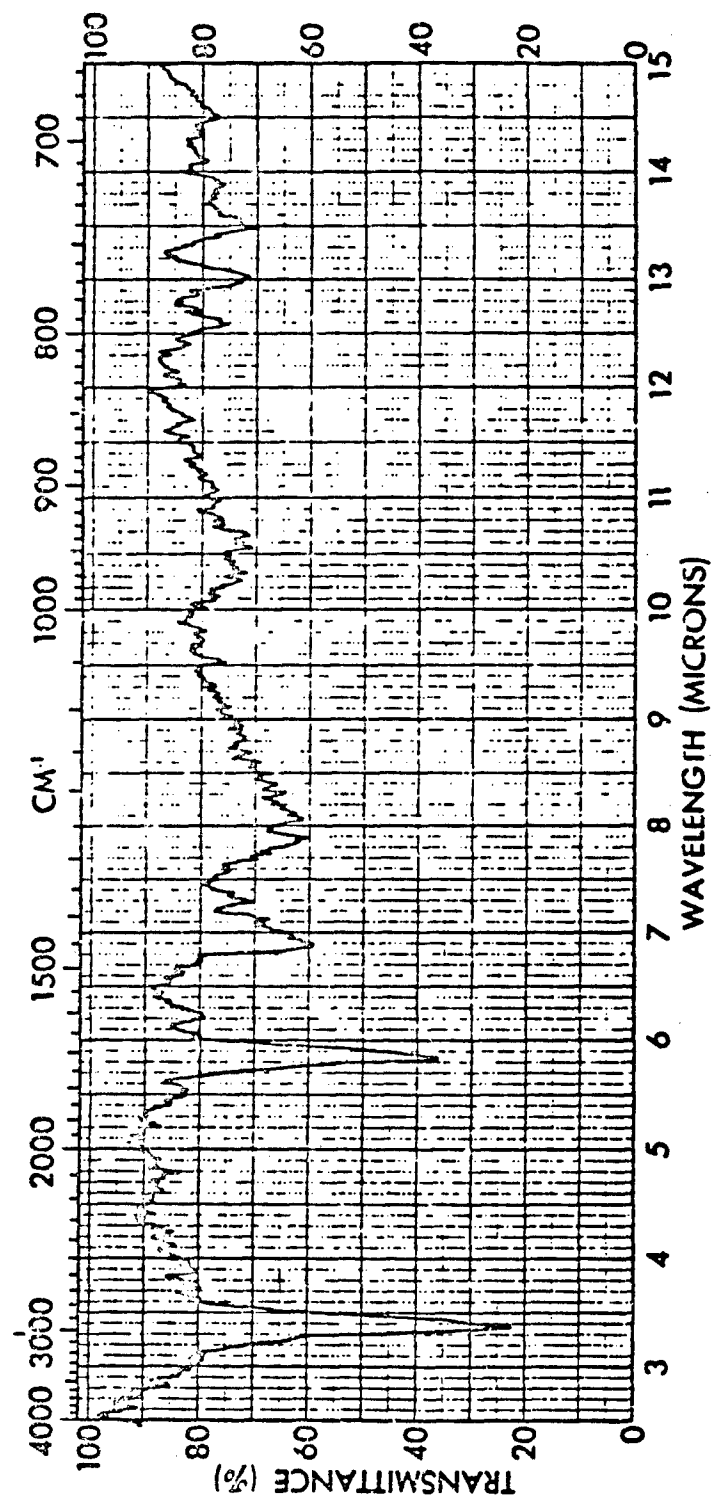


Figure 42. Infrared absorption spectrum of corrosion inhibitor DC1-4a.

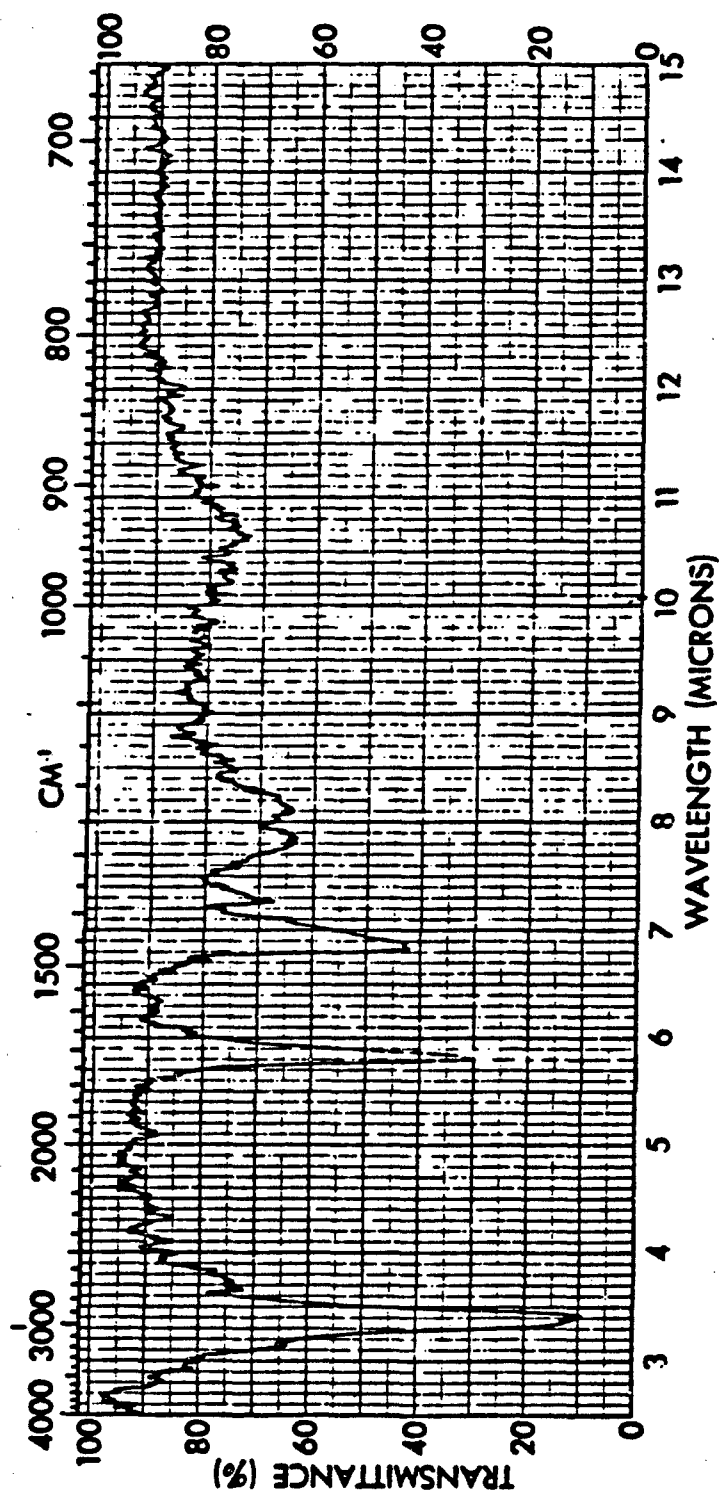


Figure 43. Infrared absorption spectrum of corrosion inhibitor HITEC E515.

TABLE 45. ENERGY DISPERITIVE X-RAY EMISSION ANALYSIS  
OF FILTER RESIDUE POSF-82-S-0318

Element	Appropriate level
Iron	Major component
Zinc	Major component
Calcium	Minor component
Manganese	Minor component
Chromium	Minor component
Silicon	Minor component
Sulfur	Minor component
Phosphorus	Minor component
Titanium	Minor component
Potassium	Minor component
Aluminum	Trace component
Sodium	Trace component
Magnesium	Trace component

Microscopic examination of the filter specimen showed the material to be largely of a dark brown color. Some tan or amber colored particles were present which appeared to be the same, or similar to those filtered from the JP-4 discussed in Technical Operating Report 2035-012. The temperature of the material was gradually increased on the heated stage of the microscope. The tan particles appeared to degrade at about 225-250°C suggesting that they were a gum or resin. The number of such particles was relatively small compared to the overall filter residue.

Some of the particles were quite reflective and had an almost metallic appearance when viewed with a hand lens. Microscopic examination, however, showed them to be slightly transparent and not of a metallic nature.

The filter residue, sample POSF-82-S-0318, was subjected to Fourier Transform Infrared reflectance (FTIR) measurement with spectra being recorded for both sample and blank filter. A spectrum resulting from spectral subtraction of data for blank and sample is shown in Figure 44. A prominent feature of the spectrum is the presence of

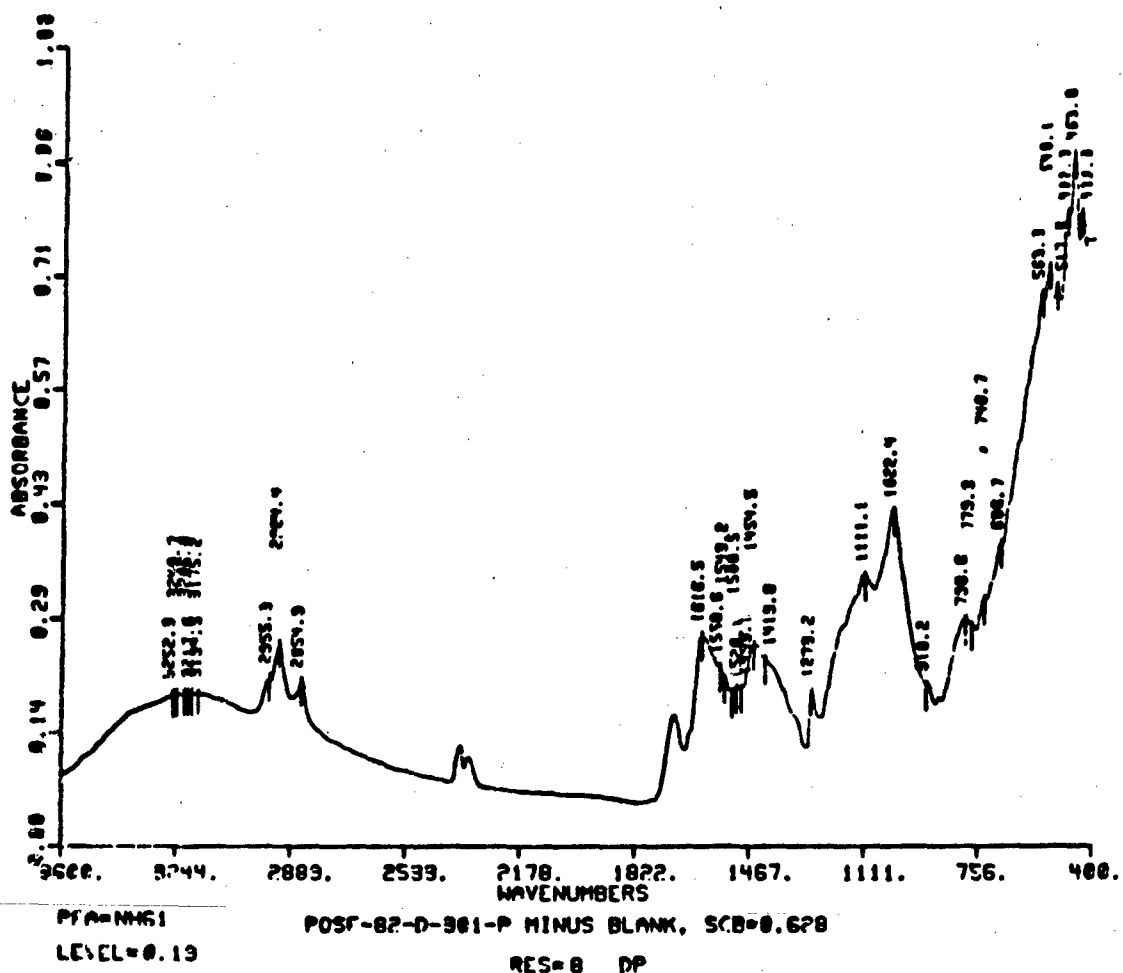


Figure 44. Infrared reflectance spectrum of filter Sample POSF-82-S-0318.

strong aliphatic C-H band. The absence of carbonate, nitrate, nitrite and cyanide bands is noteworthy. The spectrum however has no distinctive features which would distinguish it from that of a fuel residue. The organic portion of the residue is, in fact, probably due to residual fuel.

#### Discussion of Results

Regardless of the precautions taken to control the introduction of particulate matter during fuel storage or transport, some dispersed particles will be found in nearly all fuels in the form of gums, resins, metal particles, oxides, sand, etc. Only occasionally, however, are amounts sufficient to cause filter plugging encountered.

Water is a common component of fuel storage tanks, collecting as a result of condensation, rain, groundwater, or as a result of transporting the fuel. Water itself presents no immediate problem in restricting fuel-flow through a filter, however it can give rise to other species that can impede fuel flow. Corrosion rates, for example, are greatly increased by the presence of water, especially if a significant concentration of salt is also present, as was the case in the current tank bottom specimens.

#### Conclusions

- Several conclusions can be stated as a result of this investigation:

- 1) A large amount of iron oxide of small particle size is dispersed in the fuel tank bottom samples and in fuels contained in it (see previous section).
- 2) A small amount of gum or resin particles are present in the fuel part of the tank bottom. These do not appear to be present at a sufficiently high level to cause flow restrictions in the filter.

- 3) No significant amount of organic matter is recovered from the fuel.
- 4) Final definition of the cause of filter plugging could best be achieved by examination of a filter that has been plugged. One could probably then conclusively state the nature of the obstructing contaminant.

#### 5. IDENTIFICATION OF DARK DEPOSIT ON ELECTRICAL FUEL PUMP CONTACT SURFACE

The copper commutator surface on an electrical fuel pump armature was examined to determine the identity of a dark deposit which developed after the pump was allowed to stand in JP-10. The pump reportedly had not been run, however, the deposit appeared where the brushes contacted the copper surface. The disassembled fuel pump, displaying the dark deposit, is shown in Figure 45. The commutator deposit is shown in Figure 46 as it appears by Scanning Electron Microscopy (SEM) at magnifications of 100 and 1,000 times. Accompanying the fuel pump was a brush which had been removed from the pump. The pump and brush were received under sample code number 83-POSF-0839.

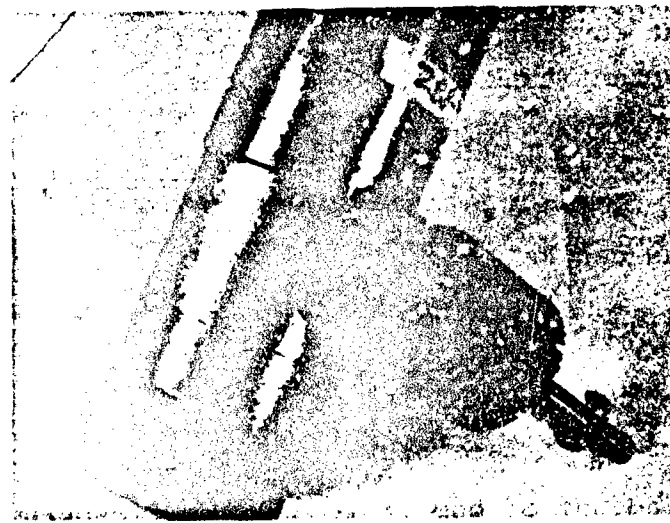
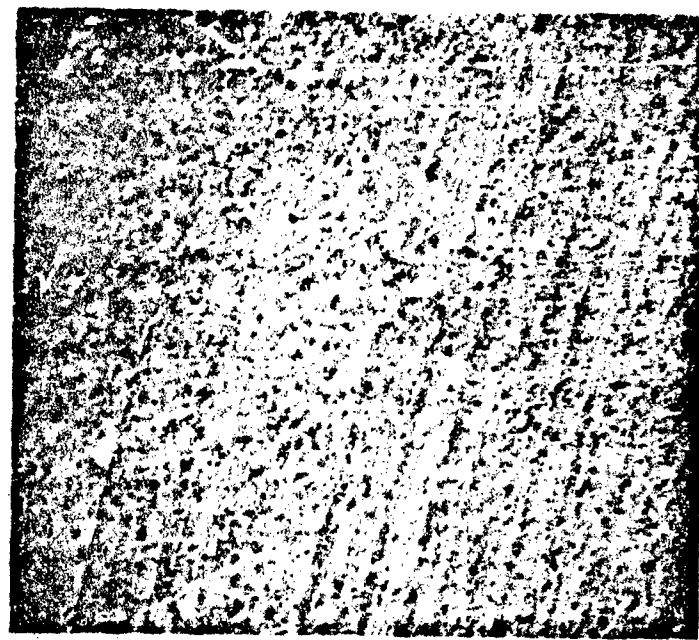
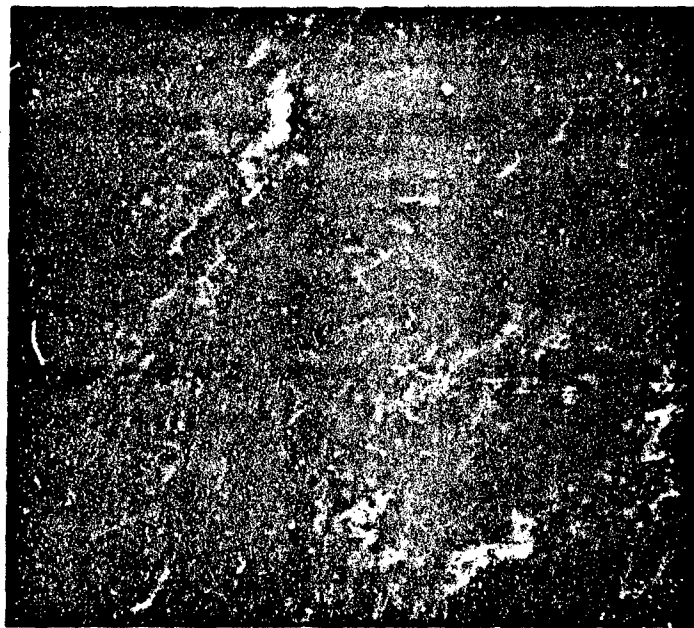


Figure 45. Copper commutator surface showing dark deposit.



100X



1000X

**Figure 46.** SEM photographs of commutator surface.

X-ray diffraction (XRD) analysis of the brush indicated that it consisted essentially of pure graphite. Attempts to record an X-ray diffraction pattern of the black deposit, however, were unsuccessful. The pattern obtained was that of only the copper substrate.

Similar results were obtained in examining the sample by X-ray fluorescence. No elements other than copper were detected (Figure 47). The technique cannot be used for detection of elements having atomic numbers less than that of sodium. However, elements often associated with corrosion, such as sulfur, the halogens, phosphorus, etc., were established as being absent.

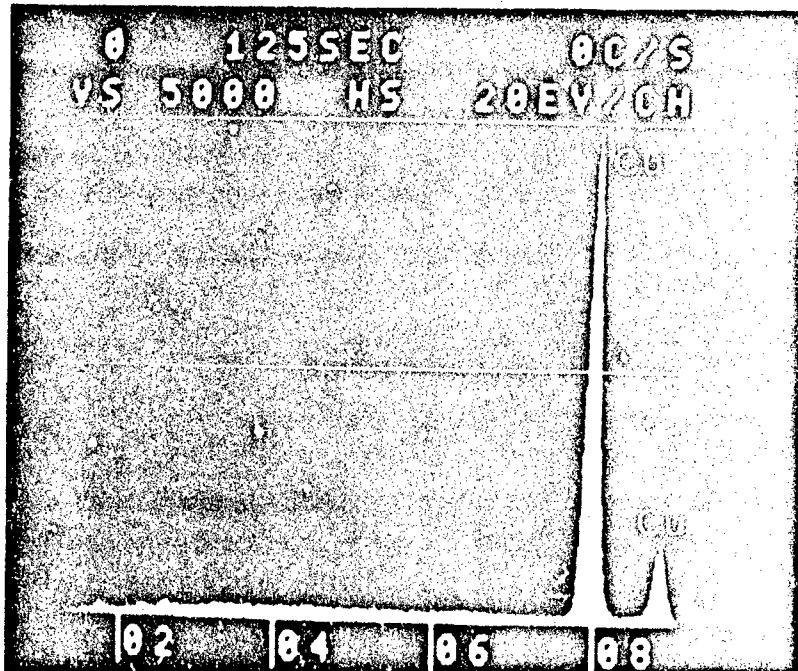


Figure 47. Analysis of surface of commutator by energy dispersive x-ray fluorescence.

Because of the involvement of JP-10, it was suspected that the material might be organic in nature. An infrared reflectance spectrum was recorded using Fourier Transform Infrared (FTIR) instrumentation. No evidence of organic material was obtained by this technique.

None of the analytical techniques discussed in the foregoing paragraphs is effective in detecting the presence of a carbon film with the possible exception of x-ray diffraction. Carbon is best detected by a surface analysis technique such as electron spectroscopy. The specimen was taken to an off-site laboratory\* for examination by Auger Electron Spectroscopy (AES). Figures 48 and 49 show spectra of the deposit, and of the clean copper, respectively. Both surfaces were sputtered prior to recording spectra to remove adsorbed contaminants.

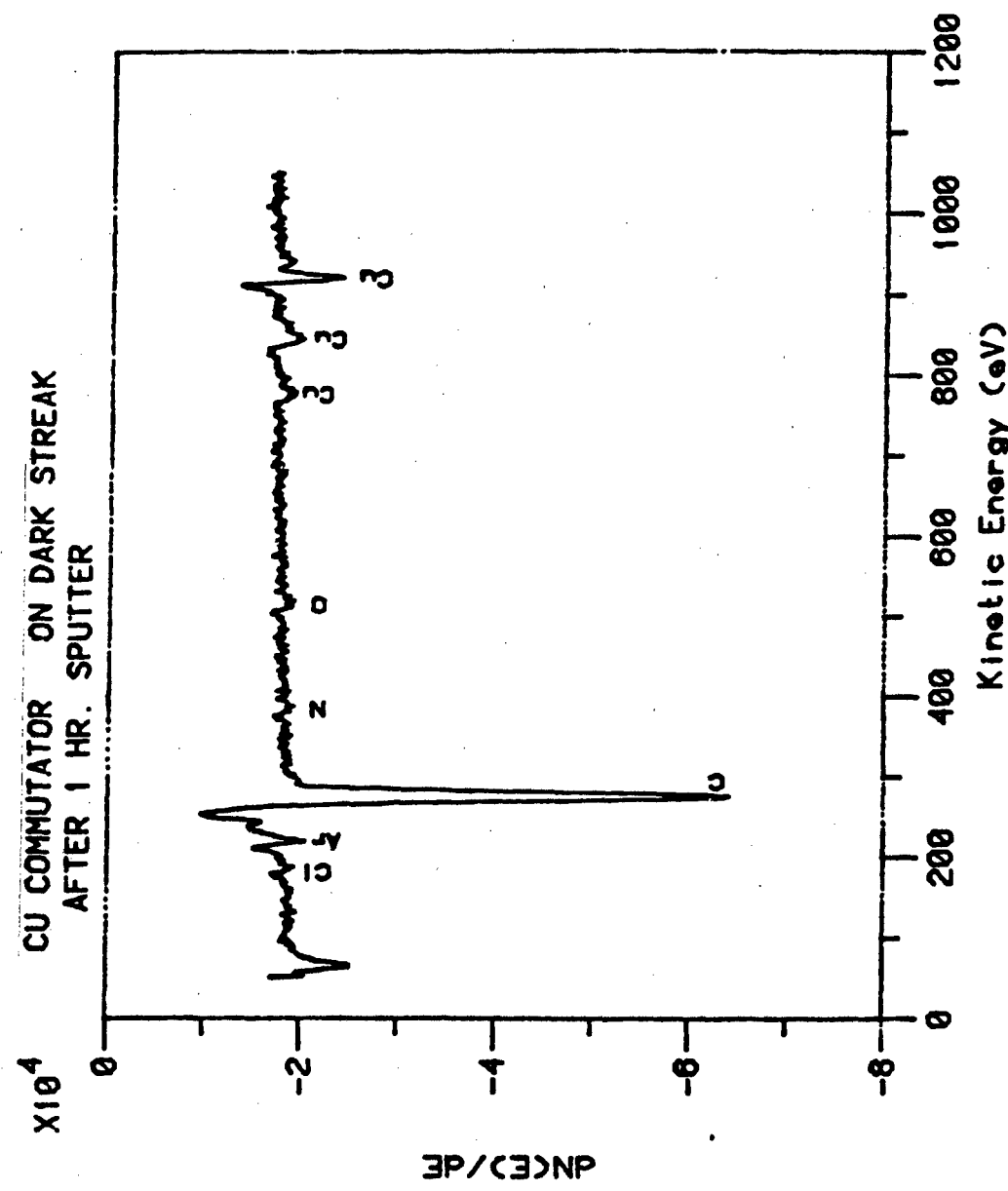
Carbon is the only element detected in the deposit. The low levels of copper, oxygen and other elements preclude the possibility of the deposit being a copper oxide or another copper compound.

#### Results and Discussion

The deposit was found to be essentially carbon. No x-ray diffraction pattern was obtained, possibly indicating that the material is non-crystalline. The small amount of material present and other physical constraints, however, could have produced the same result.

---

\*Auger Spectra and SEM photographs were recorded at the Metals and Ceramics Laboratory, University of Dayton Research Institute.



Run Date: 31-MAR-68  
File: 63109.02

Figure 48. Copper commutator on dark streak.

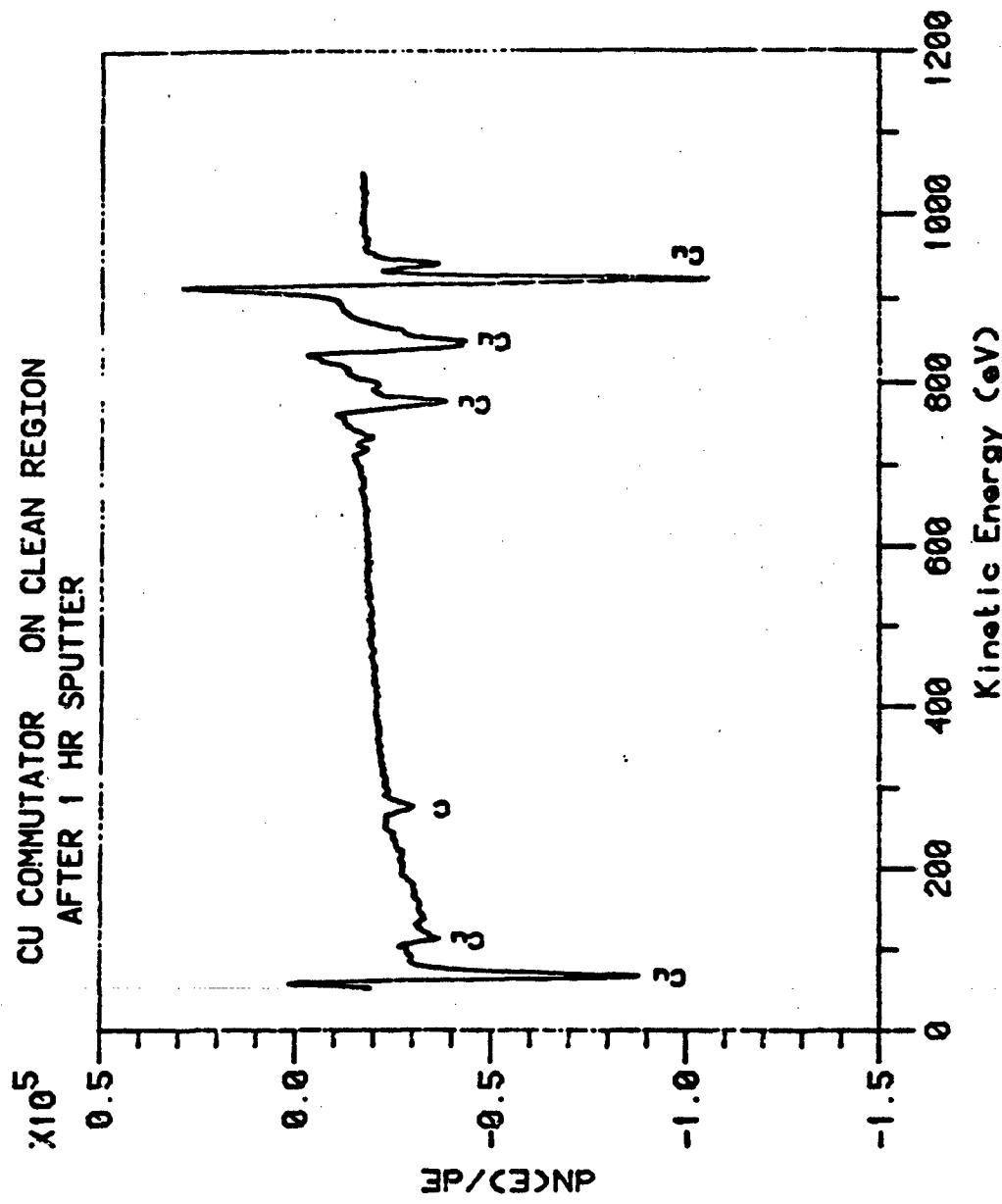


Figure 49. Copper commutator on clean region.

Run Date: 31-May-05

The effect of the deposit on pump performance is, of course, of primary interest. Good electrical conductivity across the graphite brush/copper interface is important to good pump operation. Moreover, complete electrical insulation of one copper plate from adjoining plates is also essential. While the electrical conductivity of the deposit has not been measured quantitatively, differences in electrical conductivity could be detected by moving a pair of ohmmeter probes across the surface of the deposit and copper plate. No electrical leakage from one plate to an adjoining plate could be detected with an ohmmeter (resistance  $> 1 \times 10^6$ ).

It can be concluded that such a deposit could adversely affect pump performance particularly if allowed to accumulate over a period of time.

#### 6. EXAMINATION OF SPECIMENS RELATED TO FILTER PLUGGING PROBLEM

Two samples, related to problems of slow filtration and filter plugging by a fuel, were submitted to this laboratory for analysis. One sample was a sludge taken from a JP-4 storage tank, while the other sample consisted of a residue contained on a filter. The samples were coded as shown below.

<u>Sample</u>	<u>Sample number</u>
JP-4 Storage tank sludge	83-POSF-0756
Filter residue	83-POSF-0840

##### Storage Tank Sludge (83-POSF-0756)

The JP-4 storage tank sludge, submitted in a one-gallon can, consisted of a fuel and water mixture which contained material resembling a brown mud. Centrifugation of a homogenized specimen of the material produced separate layers of clear fuel and water with the suspended solids largely being accumulated at the top of

the water layer. In contrast to the fuel, which was slightly yellow but clear, the water layer maintained its deep brown color even after centrifugation.

A portion of the solids which were isolated by centrifuging were drained of liquid and extracted with a small volume of acetone. Most of the acetone was decanted from the solids and then evaporated to dryness. The thick residue was again taken up with acetone, which was then added drop-wise to a rock salt plate; solvent was simultaneously evaporated. The plate was placed in a desiccator for several hours to remove moisture. An infrared absorption spectrum of the residue was then obtained using a Perkin Elmer Model 137 sodium chloride spectrophotometer. Important features of the resulting spectrum, as shown in Figure 50, include an OH band at approximately 3 microns, a C-H band at 3.5 microns and an ionized carboxyl band at 6 microns. In order to determine whether the OH band was due to water or to an integral part of an organic compound, the specimen was desiccated for an additional 18 hours. The spectrum of the thoroughly dried sample, shown in Figure 51a, is compared to the spectrum of carboxymethylcellulose (Figure 51b). Though the presence of this material in fuel cannot be readily explained, the acetone extracted portion of the sludge appears to be carboxymethylcellulose or a similar compound. Analysis of the solids directly by infrared spectrophotometry was unfruitful because of the opaqueness of the sample.

The sludge was filtered under vacuum to obtain a layer of solids. After air-drying, a portion of the solid was analyzed by x-ray emission and diffraction. Iron was found to be a major constituent, with small amounts of calcium, silicon, and a trace of sulfur also being present. X-ray diffraction showed that the major crystalline material was  $Fe_3O_4$ , with  $SiO_2$  ( $\alpha$  - quartz) being a minor component.

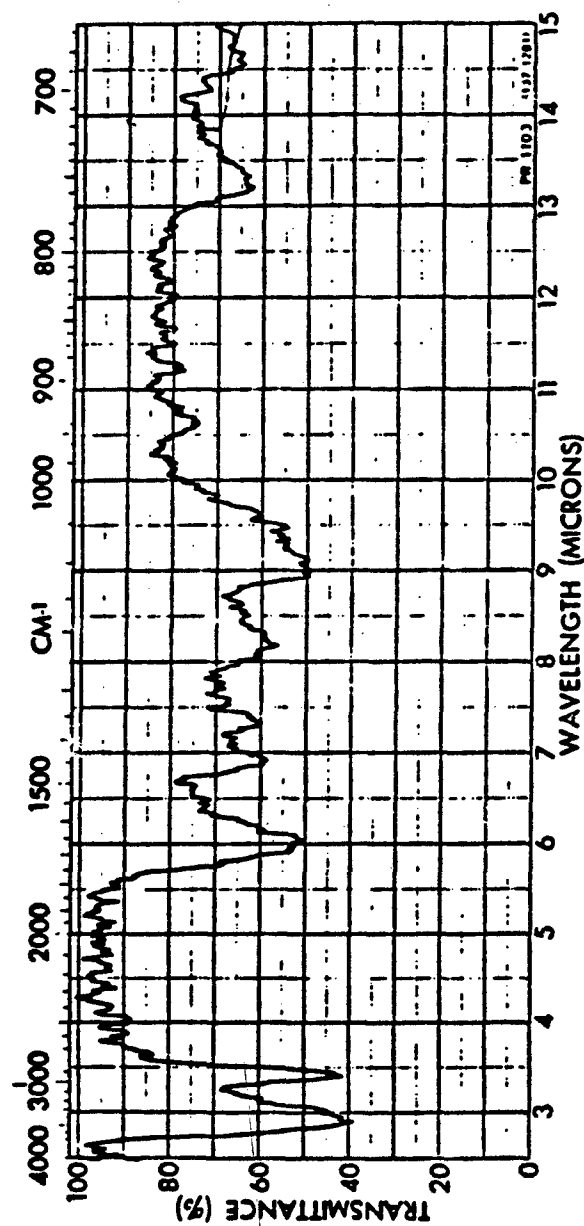


Figure 50. Infrared absorption spectrum of acetone extract of sludge solids.

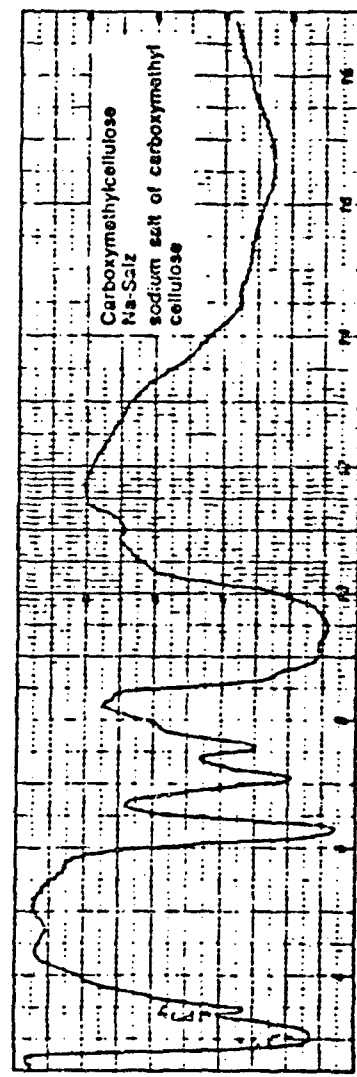
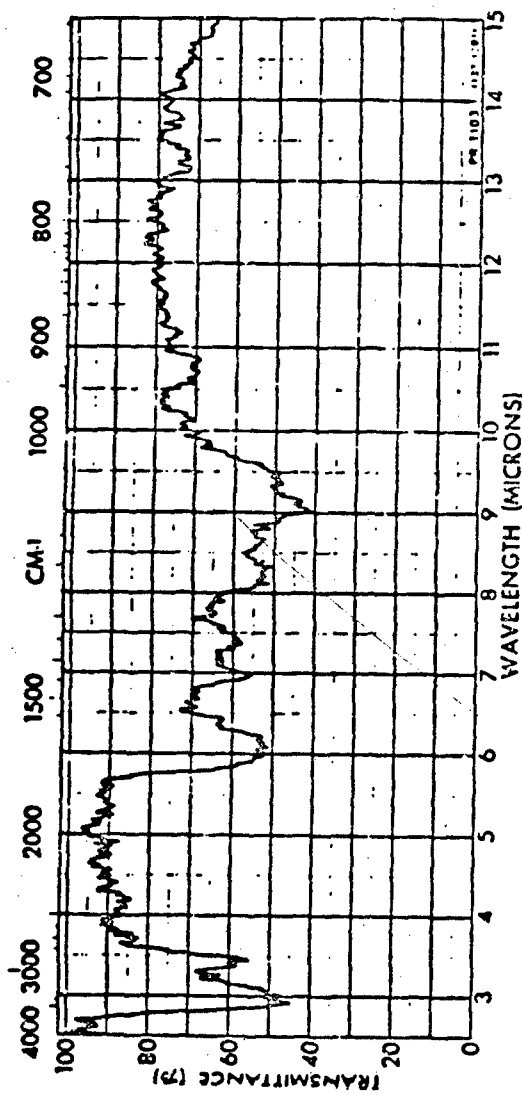


Figure 51. Infrared absorption spectra of:  
 a. Dried acetone extract of sludge.  
 b. Reference carboxymethylcellulose [6].

A second portion of the air-dried solids was ashed and ignited. The ash, which amounted to 52% by weight, consisted essentially of  $\text{Fe}_2\text{O}_3$  and  $\text{Fe}_3\text{O}_4$ .

Filter Residue - 83-POSF-0840

The large filter, which contained a black residue, was examined by x-ray emission, x-ray diffraction, and light microscopy. X-ray emission showed that iron was a major element, and silicon and potassium were minor constituents. The x-ray technique detects all elements having atomic numbers greater than that of sodium. X-ray diffraction showed that  $\alpha$ -quartz ( $\text{SiO}_2$ ) was present. The x-ray scattering showed the presence of amorphous material but the scattering pattern was not consistent with that of pure carbon.

Particles were dislodged from the filter by a fine stream of solvent (acetone) through the back side of the filter. The solvent was then evaporated and the material was examined by light microscopy. The particles appeared to be only very slightly affected (dissolved) by the solvent (Figure 52).

Infrared transmission spectrophotometry yielded no data on the isolated particles. Reflectance spectrophotometry of the filter surface yielded only spectral data for the filter medium. No blank filter was available for use in spectral subtraction, however, visual observation of the data showed only absorptions which were expected of the filter itself. The particulate material appeared to be a carbonaceous resin mixed with, or containing, occluded iron oxide.

Results and Discussion

The presence of water and some rust at the bottom of a fuel storage tank is not unusual. Carboxymethylcellulose, or a similar



Figure 52. Photomicrographs of particulate material removed from medium, Sample 83-POSF-0840 (top 100x, bottom 400x).

compound, is believed to be the key component in the sludge formation. The sludge was found to consist of that compound along with iron oxides (rust)  $\text{SiO}_2$  (sand), and carbonaceous resin or varnish particles. Carboxymethylcellulose, which is used commercially as a thickening agent, provides a medium for aggregating the particles and keeping them in suspension.

The carbonaceous resin has not been fully characterized at this time. It appears to provide, at best, only a weak infrared absorption spectrum. Further characterization of the resinous material would require separation of the individual residue components.

#### 7. DETERMINATION OF TRACE METALS IN JP-8 SAMPLES

Samples of JP-8 Tank F3, before and after tests on HBA at 330°C, were analyzed for trace metals content using an ISA Model JY48P inductively coupled plasma (ICP) spectrometer. The ICP analyses were conducted on aqueous acid (ultrapure HCl) extracts of the fuels which provided a concentration factor of 10 for the metals. The test results for an acid extraction blank, the fuel samples, and a reference standard are shown in Table 46.

The elements Al, Fe, Cu, and metals present in stainless steel were particularly sought, though none were detected.

#### 8. DETERMINATION OF TRACE METALS IN FUELS USED IN THERMAL STABILITY EVALUATION

Three fuels, which were used by the Air Force (AFWAL/POSF) to evaluate methods for determining fuel thermal stability, have been analyzed for trace-metals content using the ISA Model JY48P ICP spectrometer as discussed in the previous subsection (7). Data are presented in Table 47. The three JP-4 fuels were numbered 82-POSF-0412, 82-POSF-0413, and 82-POSF-0480. Results of a complete characterization of these three fuels are presented in Section II, subsection 1, of the report.

TABLE 46. DETERMINATION OF TRACE METALS IN JP-8 SAMPLES BY ICP SPECTROMETRY

Elements of detection	<u>Li</u>	<u>Mg</u>	<u>Ca</u>	<u>Na</u>	<u>Al</u>	<u>Si</u>	<u>Cr</u>	<u>Fe</u>	<u>Co</u>	<u>Ni</u>	<u>Mo</u>	<u>W</u>	<u>V</u>	<u>Sn</u>	<u>Pb</u>	<u>Bi</u>	<u>Ge</u>	<u>As</u>	<u>Se</u>	<u>Te</u>	<u>U</u>
Instrument																					
Quantification limit, ppb	4,900	150	2	72	2	650	13	300	630	73	65	800	15	20	17	230	1,300	10	20	35	100
Log after concentration, ppb	600	15	0.2	7	0.2	65	1.3	30	63	7.3	0.6	80	1.5	3	1	1.7	20	130	1	2	3.6
Gold extraction blank, ppb	2	2	2	2	2	2	2	2	2	2	2	2	2	2	2	2	2	2	2	2	2
Concentration of Elements in Fuel Samples <sup>a</sup>																					
JP-8 Fuel P3- from drum	2	2	2	2	2	2	2	2	2	2	2	2	2	2	2	2	2	2	2	2	2
JP-8 Fuel P3- after test on Hg at 330°C	2	2	2	2	2	2	2	2	2	2	2	2	2	2	2	2	2	2	2	2	2
Analyses of Reference Standard <sup>b</sup>																					
True value	-	207	322	502	359	1,070	800	940	1,120	1,050	1,020	879	-	64	1,000	-	923	1,110	1,110	-	177
Observed value	-	261	366	476	363	1,060	832	1,000	1,000	1,000	1,000	848	-	59	1,000	-	1,000	1,000	1,000	-	165
Percent recovery	-	-	110	105	103	94	107	99	96	112	105	102	104	-	109	106	-	93	111	111	-

<sup>a</sup>Fuel samples were effectively concentrated by a factor of 10 by extraction with a small volume of aqueous acid for the analysis.

<sup>b</sup>Supernatant aqueous acid used to extract the fuel samples for analysis. An "x" shows that the element was not detected at the instrument log.

<sup>c</sup>The "x" shows that the element was not detected at the log after concentration. The numerical values were obtained by dividing the observed value by 10 to take into account the concentration effect, then subtracting any blank value obtained. These values represent the element concentration in the original fuel.

TABLE 47. RESULTS OF TRACE METAL ANALYSIS BY ICP SPECTROMETRY

<u>Elements of detection</u>	<u>Be</u>	<u>Cr</u>	<u>Mn</u>	<u>Pb</u>	<u>Ti</u>	<u>Al</u>	<u>Ca</u>	<u>Cu</u>	<u>Ho</u>	<u>V</u>	<u>B</u>
Instrument quantification limit, LOQ, ppb	2	50	4	230	25	150	150	30	45	60	15
LOQ after concentration, ppb	0.1	2.2	0.2	10	1.1	6.7	6.7	1.3	2.0	2.7	0.7
Acid extraction blank, ppb	x	x	x	x	x	x	171	x	67	x	x
82-POSF-0412 <sup>c</sup> , ppb	x	x	x	x	x	x	12	x	4	x	2
82-POSF-0415 <sup>c</sup> , ppb	x	x	x	x	x	x	12	x	2	x	x
82-POSF-0480 <sup>c</sup> , ppb	x	x	x	x	x	x	12	x	3	x	x
<u>Analysis of reference standard, ppb</u>											
True values	200	500	520	1,000	200	620	1,000	400	120	1,000	-
Observed value	211	540	568	1,100	208	587	1,140	420	124	997	-
Percent recovery	106	108	109	110	104	95	114	105	103	100	-

(continued)

TABLE 47 (continued)

<u>Elements of detection</u>	<u>Cd</u>	<u>Fe</u>	<u>Na</u>	<u>Sn</u>	<u>Zn</u>	<u>Ba</u>	<u>Co</u>	<u>Mg</u>	<u>Ni</u>
Instrument quantification limit, LoQ, ppb	15	30	5,000	770	29	50	40	10	80
LoQ after concentration, ppb	0.7	1.3	220	34	1.3	2.2	1.8	0.4	3.6
Acid extraction blank, ppb	x	x	x	x	29	x	x	1.3	x
82-POSF-0412 <sup>c</sup> , ppb	x	7	x	x	0.9	x	x	2	9
82-POSF-0413 <sup>c</sup> , ppb	x	4	x	x	0.4	x	x	1	x
82-POSF-0480 <sup>c</sup> , ppb	x	4	x	x	2.1	x	x	2	8
<u>Analysis of reference standard, ppb</u>									
True values	180	680	-	-	690	880	510	1,000	260
Observed value	199	650	-	-	706	846	523	1,030	274
Percent recovery	111	96	-	-	102	96	103	103	105

<sup>a</sup>Fuel samples were effectively concentrated by a factor of 22.5 by extraction with a small volume of aqueous acid for the analysis.

<sup>b</sup>Aqueous ultrapure acid used to extract the fuel samples for analysis. An "x" shows that the element was not detected at the instrument LoQ.

<sup>c</sup>An "x" shows that the element was not detected at the LoQ after concentration. The numerical values were obtained by subtracting any blank values from the observed value, then dividing by the appropriate concentration factor. These values represent the element concentration in the original sample.

SECTION V  
SPECIAL PROJECTS AND INVESTIGATIONS

A number of special projects and investigations were conducted to aid in the solution of operational problems, to improve existing test methodology, to respond to particular unanticipated needs as they arose, or to make measurements of a non-routine nature.

1. PURIFICATION OF RJ-5 AND JP-10 FUELS  
FOR USE AS ANALYTICAL STANDARDS

The analysis of JP-10 and RJ-5, according to procedures given in MIL-P-87107B, requires specimens of these fuels which are free of contaminants and impurities. In order to provide pure samples of these fuels, JP-10 from drum 31 and RJ-5 from Batch #3 were vacuum distilled on a Todd Vigreux fractionating column. The vacuum was controlled by a pressure stabilizing device which allowed any selected vacuum to be maintained. Gas chromatographic analyses were conducted on each distilled fuel to determine purity. The fuels were then sealed in 2 mL septum-top vials, and ten vials of each fuel were transported to the Aero Propulsion Laboratory for distribution.

Distillation of JP-10

Approximately 100 mL of JP-10 was distilled at a 5:1 reflux ratio at a pressure of 50 mm of mercury. The fractions obtained, and their refractive indices, are given in Table 48. The distillation temperature did not exceed 99°C. Successive 1-milliliter fractions were collected until the refractive indices of at least three adjacent cuts agreed within  $\pm 0.0002$ , and then a 50-milliliter fraction was collected and retained.

TABLE 48. DISTILLATION OF JP-10

<u>Fraction number</u>	<u>Fraction size, mL</u>	<u>Refractive Index, <math>N_D^{25}</math></u>	<u>Sample disposition</u>
1	1	1.4841	Cloudy-discarded
2	1	1.4845	Cloudy-discarded
3	1	1.4846	Cloudy-discarded
4	1	1.4852	Cloudy-discarded
5	1	1.4856	Discarded
6	1	1.4855	Discarded
7	1	1.4858	Discarded
8	1	1.4861	Discarded
9	1	1.4862	Discarded
10	1	1.4863	Discarded
11	1	1.4866	Discarded
12	1	1.4868	Discarded
13	1	1.4867	Discarded
14	1	1.4868	Discarded
15	50	1.4871	Retained
16	1	1.4871	Retained

Distillation of RJ-5

Approximately 100 mL of RJ-5 Batch #3 was distilled at an 8:1 reflux ratio at a pressure of 50 mm of mercury. Collection was started with the distillation pot at 175.5°C; the lower column, at 162°C; the mid-column at 157.5°C, and the column top at 169°C. The fractions obtained during distillation, and their refractive indices, are given in Table 49. After the first three fractions, 5 milliliter fractions were collected throughout the entire experiment in order to retain existing isomer ratios. The collected fractions were composited and thoroughly mixed prior to sealing in septum vials. The final refractive index of the composite fuel was 1.5414 compared to 1.5413 for the starting fuel,

TABLE 49. DISTILLATION OF RJ-5

<u>Fraction number</u>	<u>Fraction size, mL</u>	<u>Boiling range at 50 mm/Hg, °C</u>	<u>Refractive Index, N<sub>D</sub><sup>25</sup></u>	<u>Sample disposition</u>
1	2.5	156-168	1.5238	Hazy-discarded
2	2.5	168-169	1.5361	Lt. yellow-discarded
3	2.5	169	1.5382	Clear-discarded
4	5	169-169.5	1.5391	Retained
5	5	169.5	1.5393	Retained
6	5	169.5	1.5396	Retained
7	5	169.5	1.5396	Retained
8	5	169.5-170	1.5401	Retained
9	5	170	1.5404	Retained
10	5	170-170.5	1.5408	Retained
11	5	170.5-171	1.5413	Retained
12	5	171	1.5419	Retained
13	5	171	1.5424	Retained
14	5	171-171.5	1.5427	Retained
15	5	171.5	1.5430	Retained
16	5	171.5	1.5434	Retained
17	5	171.5-172	1.5438	Retained
18	5	172	1.5439	Retained
Residuum,	7.03	>172		Yellow viscous-discarded

thus showing that except for purification, the overall composition of the fuel was not significantly altered.

#### GC Analyses of Distilled Fuels

Gas chromatographic analyses were performed on the purified fuels using a Perkin-Elmer Model 3920B chromatograph equipped with a 50-meter glass capillary column having a 0.01-inch ID and coated with SF-96 stationary phase. Instrument parameters included:

Type detector: Flame ionization  
Carrier gas: 1 mL/min nitrogen  
Column temperature: Program 50-200°C at 8°C/min  
Injection port: 200°C  
Detector temperature: 200°C  
Recorder: 1 mv  
Electrometer range: 10

The calculated percent purity values for the distilled fuels are:

JP-10 (C-10) - 99.79  
RJ-5 (C-14) - 99.66

These values are based on peak area percents as computed by a Hewlett-Packard 3354 Laboratory Data System. Peaks which are a part of the normal fuel composition (isomers) were summed to obtain the total percent composition.

The gas chromatogram for distilled JP-10 is presented in Figure 53 and that of RJ-5 is shown in Figure 54.

Fractions were sealed in 2 mL septum-capped vials. Each cap, which was crimped over the glass vial, contained a Teflon-lined silicone septum. RJ-5 vials were labeled "C-14" and JP-10 vials, "C-10".

2. COMPARISON OF SAMPLES OF METAL DEACTIVATOR AGENT,  
N,N'DISALICYLIDENE-1,2-PROPANEDIAMINE

Three samples coded:

83-POSF-0705 DuPont Metal Deactivator, Lot #L-41  
83-POSF-0706 DuPont Metal Deactivator #2, Lot #L561  
83-POSF-0707 Solid Labeled N,N-Disalicylidene-1,2-Propanediamine

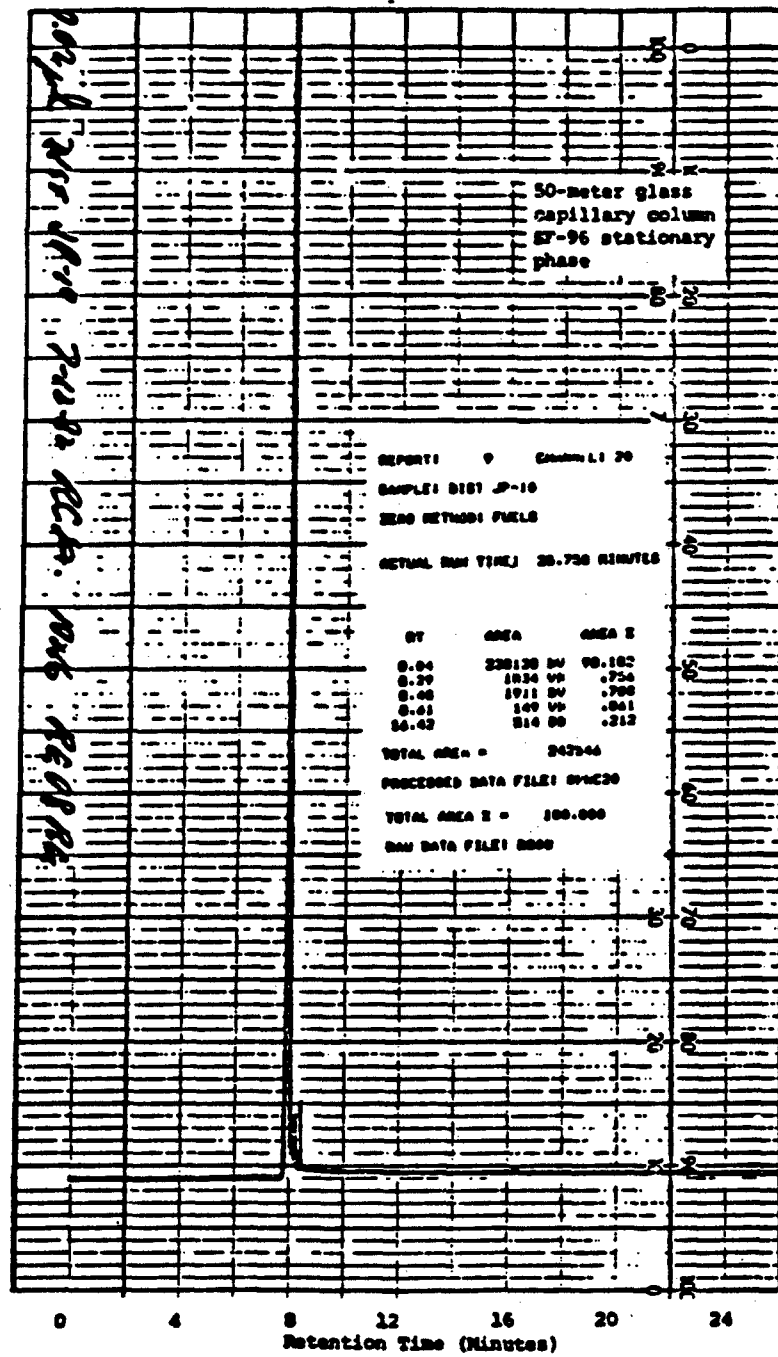


Figure 53. Gas chromatogram of distilled JP-10.

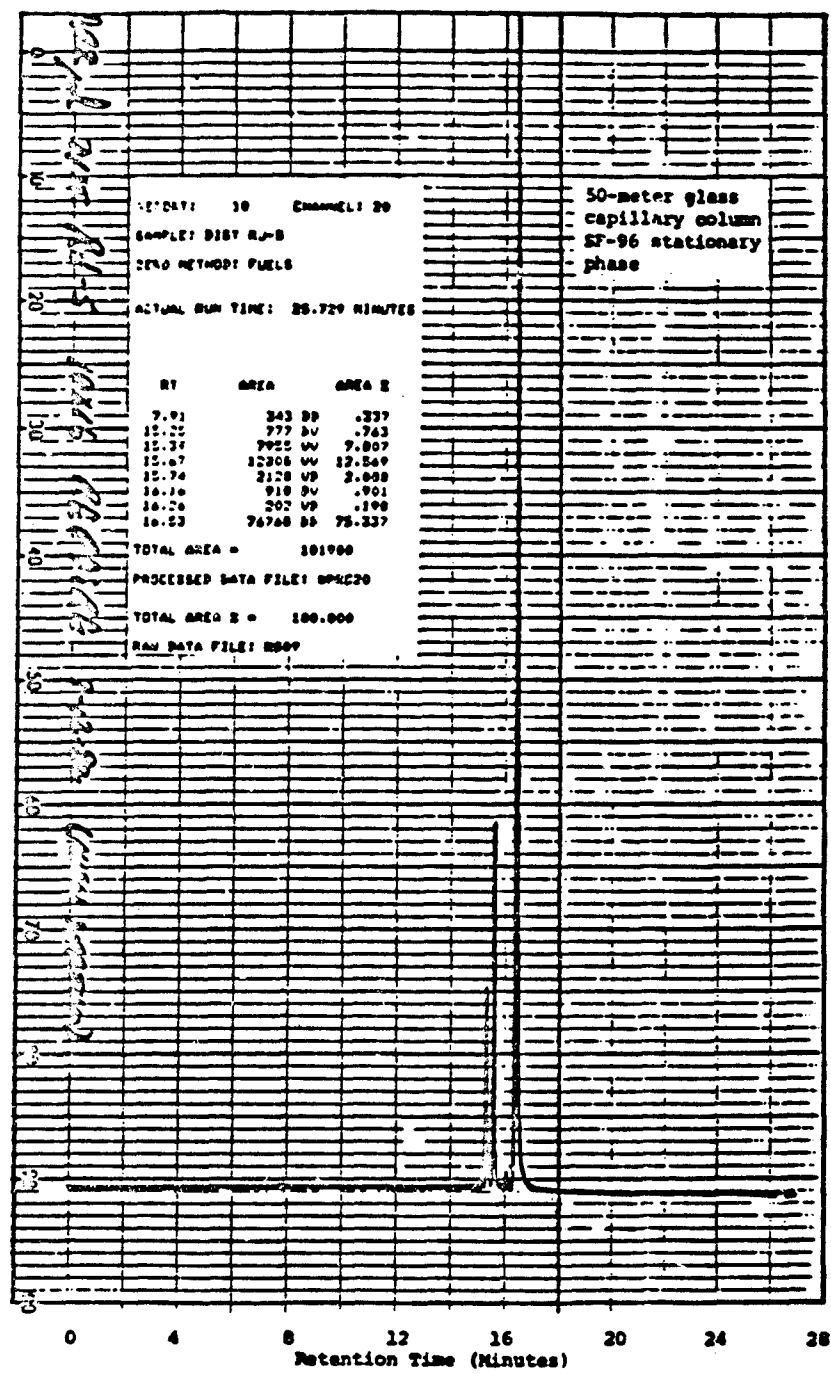


Figure 54. Gas chromatogram of distilled RJ-5.

were compared to determine if they contained a common major component, N,N' disalicylidene-1,2-propanediamine. Samples -0705 and -0706 are known to be DuPont Metal deactivator, consisting of xylene solutions of N,N' disalicylidene-1,2-propanediamine. Sample -0707 is a yellow solid material. Analyses were required to confirm or deny that this material is the solute in the other two samples.

#### Procedure and Results

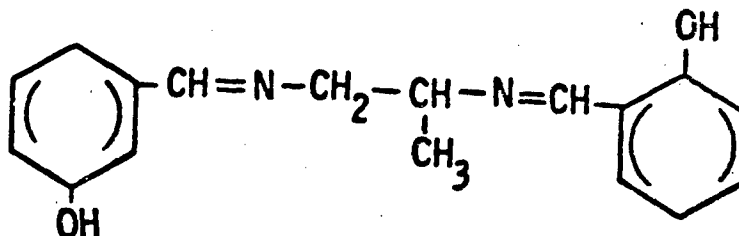
Proton nuclear magnetic resonance was selected as the method of analysis. All samples were analyzed under identical conditions and in the absolute intensity mode for direct comparison of integral values. A Varian CFT-20 Fourier Transform instrument was used for the analysis. The solvent used was DMSO-d<sub>6</sub>. Tetramethyl silane (TMS = 0.0 ppm) was used as a reference compound.

Proton NMR data are presented in Tables 50 through 52 and Figures 55 through 58. These data indicate that the solid, sample 83-POSF-0707, is the major component in the liquid samples, being present in -0705 at 76% (wt.) and in -0706 at the 39% level. The liquid samples, in addition to xylene, contain a minor component having an ethyl group which may be a small amount of ethyl benzene in the xylene.

#### Discussion of Data

The level of the major component was calculated on the basis of the integral value corresponding to the N=CH band at 8.57 ppm. This band has no apparent interference in any of the samples.

TABLE 50. NMR DATA FOR 83-POSF-0707



Expected Structure

<u>Chemical shift</u>	<u>Relative peak area</u>	<u>Assignment</u>
10.4 (singlet)	1.5 <sup>a</sup>	phenolic OH
8.57 (split peak)	2.1	Ar - <u>CH</u> = N
7.4-6.7 (multiplets)	8.3	aromatic protons
3.8 (multiplets)	3.2	N-CH <sub>2</sub> - <u>CH</u> - N
3.29 (singlets)	1.0 <sup>a</sup>	labile type proton (includes labile impurity present in DMSO-d <sub>6</sub> )
2.5 (multiplet)	-	residual <sup>1</sup> H in DMSO-d <sub>6</sub>
1.3 (multiplet)	3.0	C - <u>CH<sub>3</sub></u>

<sup>a</sup>Partial labile exchange has already taken place; upon adding D<sub>2</sub>O these peaks coalesce to approximately 3.8 ppm.

TABLE 51. NMR DATA FOR 83-POSF-0705

<u>Chemical shift</u>	<u>Relative peak area</u>	<u>Assignment</u>
10.4 (singlet)	1.5 <sup>a</sup>	phenolic OH
8.57 (split peak)	2.0	Ar - <u>CH</u> = N
7.5-6.7 (multiplets)	9.7	aromatic protons
		CH <sub>3</sub>
3.8 (multiplets)	3.1	N - CH <sub>2</sub> - <u>CH</u> - N
3.29 (singlets)	2.4 <sup>a</sup>	labile type proton (includes labile impurity present in DMSO-d <sub>6</sub> )
2.5 (multiplet)	-	residual <sup>1</sup> H in DMSO-d <sub>6</sub>
2.3-2.1 (more than one environment)	2.1	in region for Ar - CH <sub>3</sub> (eg. xylene)
		H
1.3 (multiplet)	3.0	C - <u>CH<sub>3</sub></u>

<sup>a</sup>See note, Table 50.

TABLE 52. NMR DATA FOR 83-POSF-0706

<u>Chemical shift</u>	<u>Relative peak area</u>	<u>Assignment</u>
10.4 (broad)	1.0 <sup>a</sup>	phenolic OH
8.57 (split peak)	2.0	Ar - <u>CH</u> = N
7.5-6.7 (multiplets)	18.5	aromatic protons
		CH <sub>3</sub>
3.8 (multiplet)	3.6	N - <u>CH<sub>2</sub></u> - <u>CH</u> - N
-3.3 (broad)	1.6 <sup>a</sup>	labile type proton (includes labile impurity present in DMSO-d <sub>6</sub> )
2.6 (quartet)	1.1	
2.5 (quartet)	-	residual <sup>1</sup> H in DMSO-d <sub>6</sub>
2.3-2.1 (more than one environment)	13.7	in region for Ar - CH <sub>3</sub> (eg. xylene)
		H
1.3 (multiplet)	4.6	C - <u>CH<sub>3</sub></u>
1.7		CH <sub>2</sub> - <u>CH<sub>3</sub></u> (possibly ethyl benzene)

<sup>a</sup>See note, Table 50.

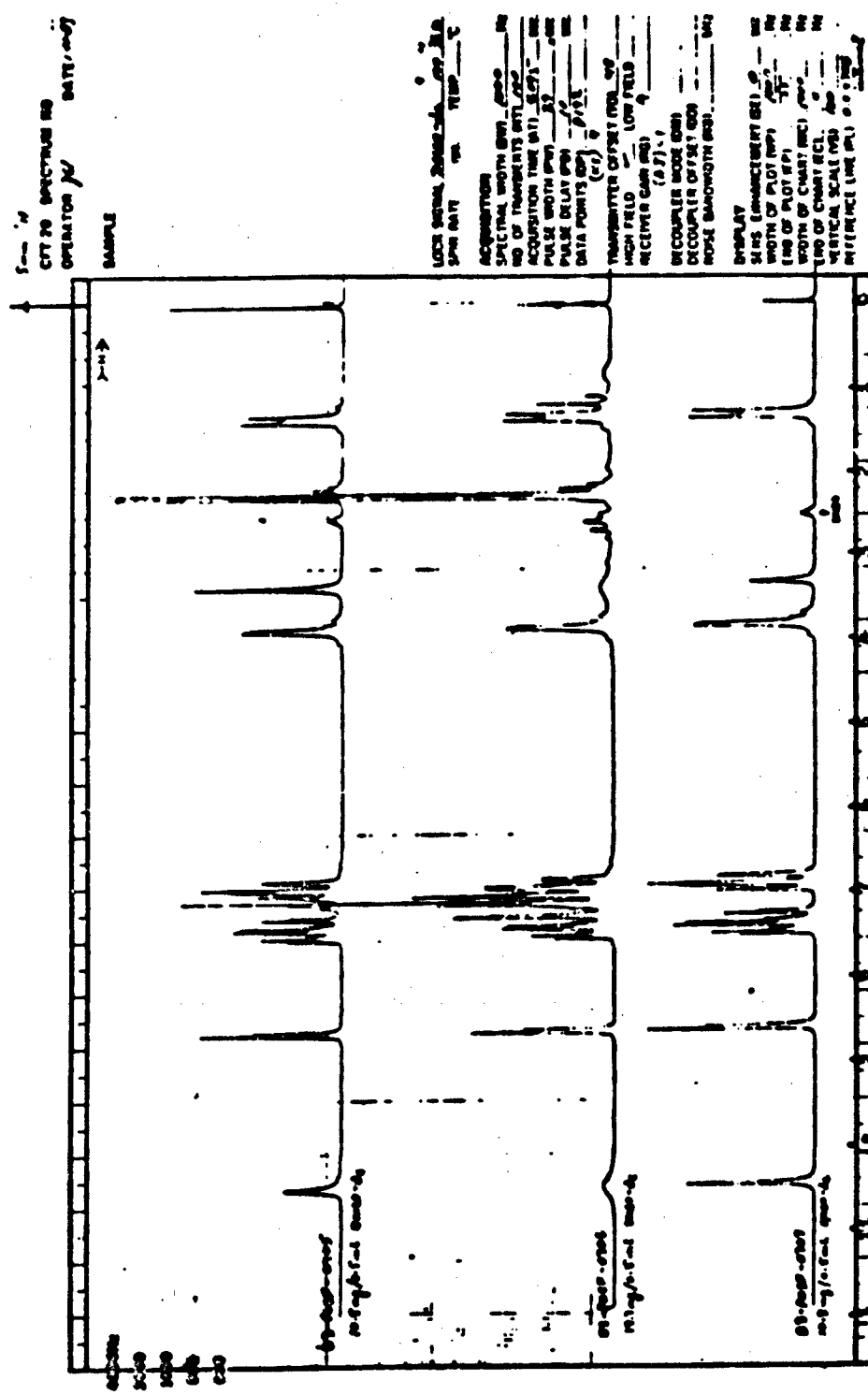


Figure 55. Proton Nuclear Magnetic Resonance spectra of samples.

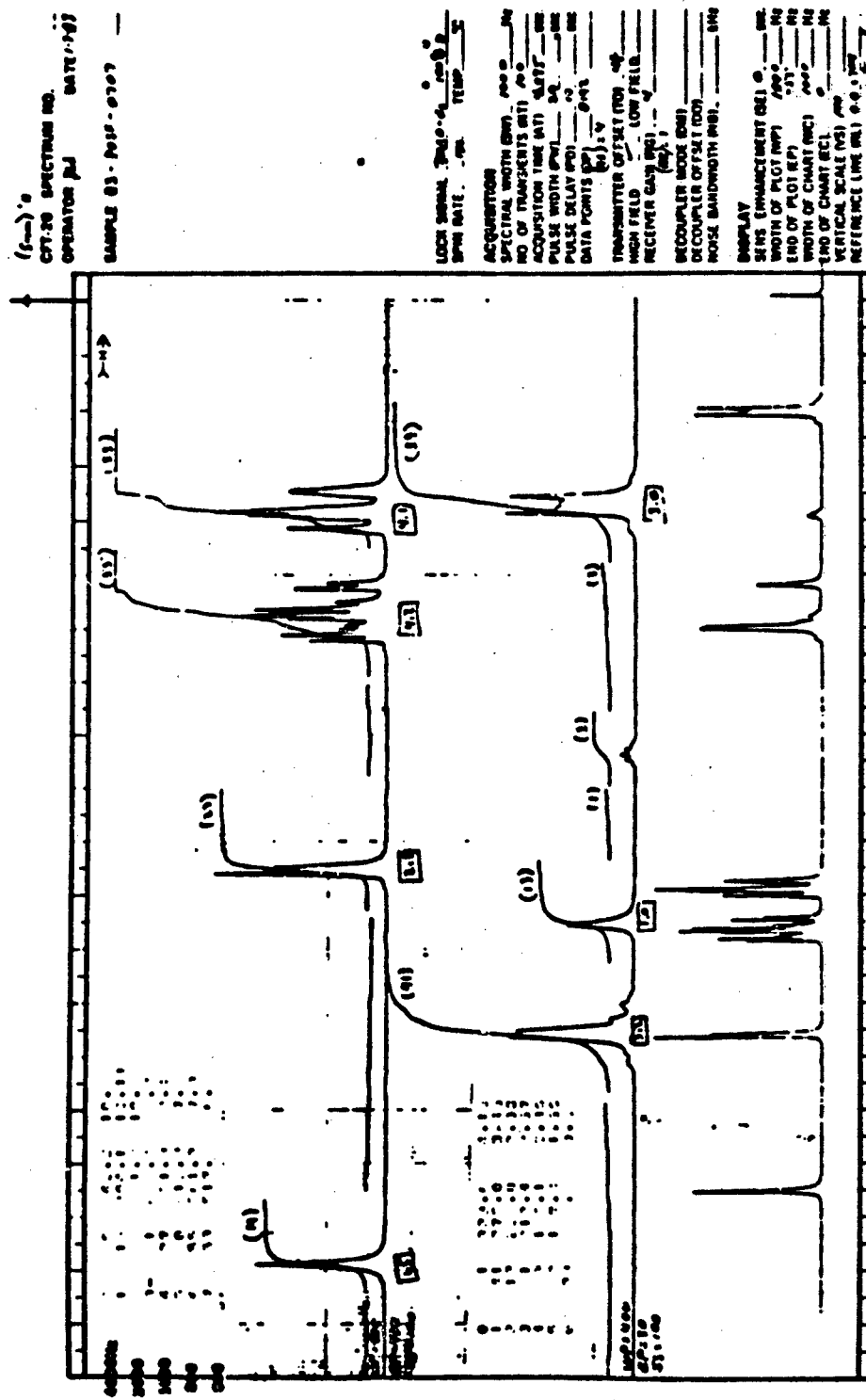


Figure 56. Integral proton NMR spectra of Sample 83-POSF-0707.

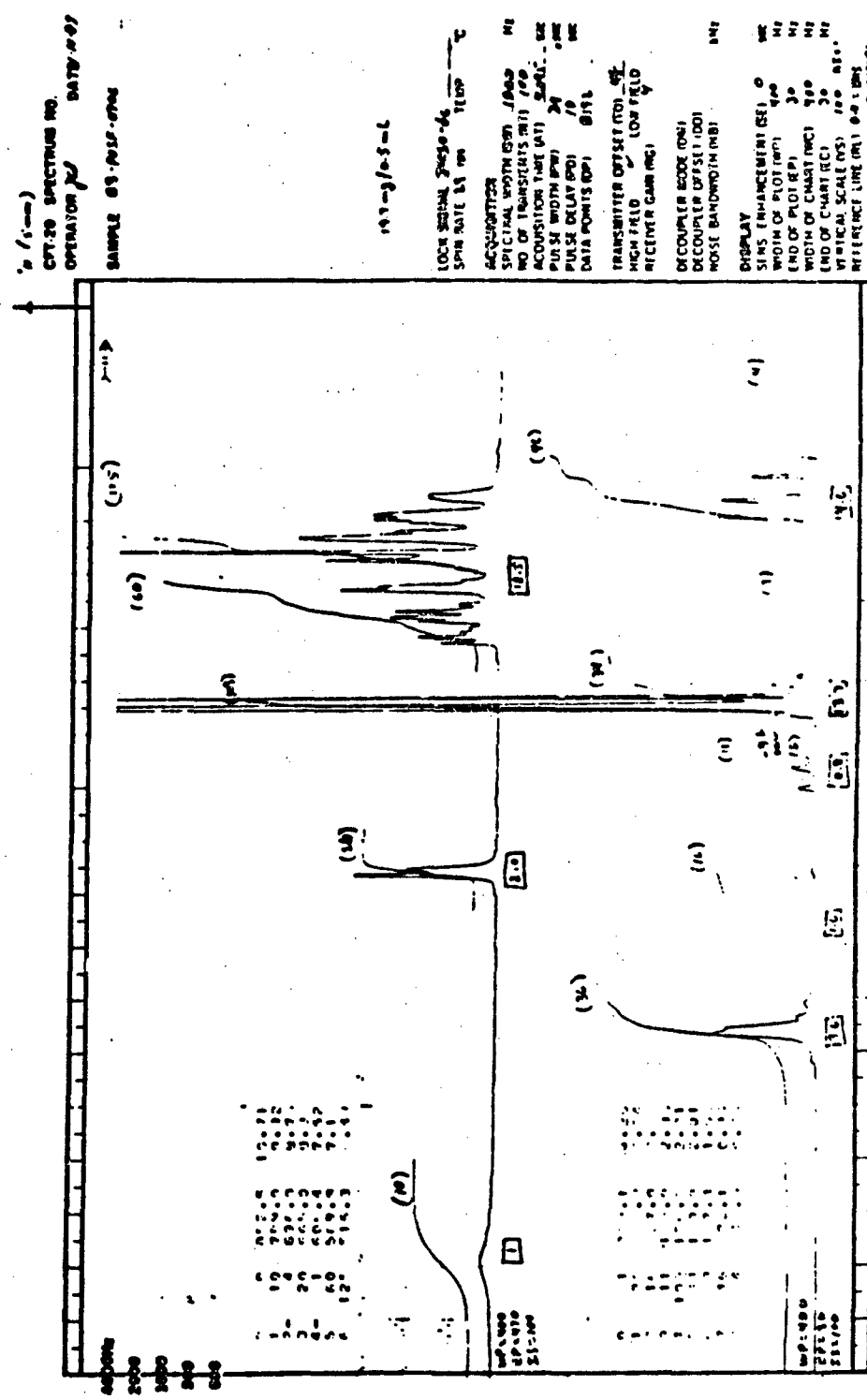


Figure 57. Integral proton NMR spectra of Sample 83-POSE-0706.

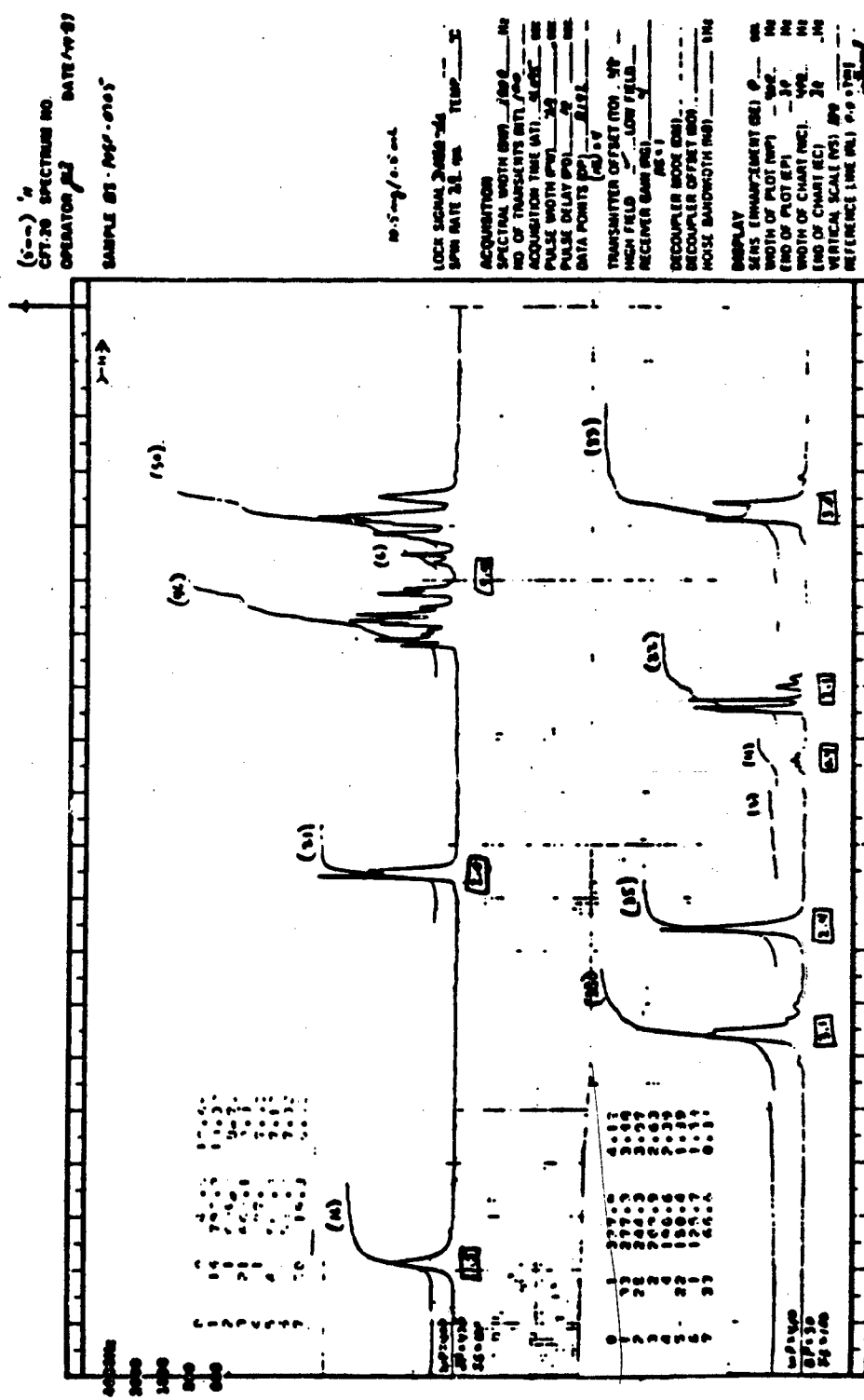


Figure 58. Integral proton NMR spectra of Sample 83-POSF-0705.

Sample -0707 was used as a reference material and was assigned a value of 100%. Calculations were performed as shown below.

$$\text{Wt. \% of 0707 in liquids} = \frac{\text{Wt. of sample in (mg)} \times \text{area of N = CH in mix} \times 100\%}{\text{Wt. of liquid (nmr sp.)} \times \text{area of N = CH in reference in (mg)} \times \text{area of N = CH in reference in (nmr sample)}}$$

$$\text{Wt \% of -0707 in 0705} = \frac{10.3 \text{ mg} \times 21 \times 100\%}{10.5 \text{ mg} \times 27} = 76\%$$

$$\text{Wt \% of -0707 in 0708} = \frac{10.3 \text{ mg} \times 20 \times 100\%}{19.7 \text{ mg} \times 27} = 39\%$$

The NMR patterns of the major component are in agreement with the structure of N,N' disalicylidene-1,2-propanediamine. Major bands for the samples are listed in Table 53 through 55.

### 3. GEL PERMEATION CHROMATOGRAPHIC ANALYSIS OF ACRYLOID COPOLYMER IN OILS

Three oil specimens were analyzed by gel permeation chromatography to determine the relative content of acryloid copolymer. Acryloid copolymers are used to modify the viscosity index and lower the pour point. In this work, integrated chromatograms of the three oils, which include tabulated area counts for each peak, were provided. Sample designations are:

- 0-78-8 Gallon can
- 0-78-8 Lot 12 A can
- 0-78-8 Lot 12 B can

The instrumentation used consisted of a Waters Associates, Inc. Model M6000A pump, a Rheodyne Model 7125 loop injector, and a Micromeritics Model 785 variable wavelength detector. Data were recorded by means of a Spectro-Physics 4100 recorder/integrator. Waters Associates, Inc., Microstyragel 100 $\text{\AA}$  and 500 $\text{\AA}$  columns were used. The solvent used was Burdick and Jackson HPLC-grade tetrahydrofuran. Detection was at the wavelength of 254 nm.

Neat as well as diluted samples were chromatographed. For the duplicate neat runs at 2.0 absorbance units full scale (AUFS), 10  $\mu$ L injections of each sample were used. Chromatograms are presented in Figures 59 through 67. Area counts, area percent and retention times are given on each chromatogram. It will be noted that peaks for undiluted samples have saturated the detector, thus diluted samples should be employed for calculations involving these peaks.

#### 4. REQUALIFICATION OF CORROSION INHIBITORS ACCORDING TO MIL-I-25017D

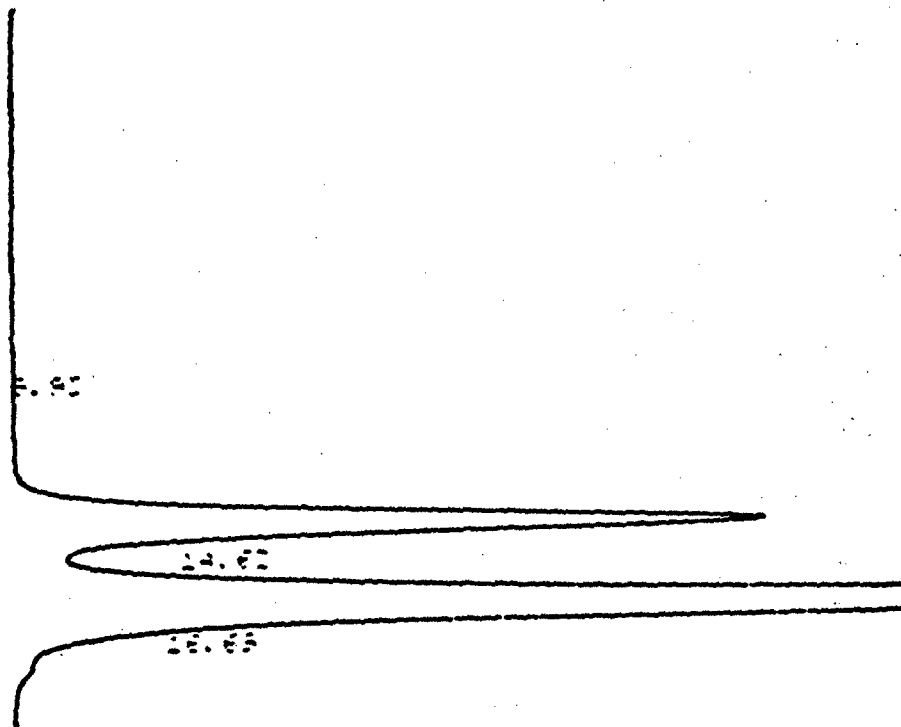
Fifteen corrosion inhibitors have been tested (results are contained in Table 53) to determine their qualification according to MIL-I-25017D. The following tests were conducted:

- a. Ash Content, ASTM D 482
- b. Pour Point, ASTM D 97
- c. Density at 15°C, ASTM D 1298
- d. Viscosity at 37.8°C, ASTM D 445
- e. Flash Point, ASTM D 56
- f. Neutralization Number, ASTM D 664
- g. pH According to Para. 4.6.13 MIL-I-25017C
- h. Emission Spectrographic Analysis

Of the eight properties listed above, only ash content and pour point are limited by MIL-I-25017D. The others are only to be determined and reported.

It should be noted that for some samples, the amount of material available was not sufficient for all tests. Only in the case of flash point, however, did this deficiency prevent the completion of all measurements. The flash point of four samples could not be determined because of insufficient sample. Additionally, in some cases sufficient sample was not available to fill the pour point test jar fully to the mark. All samples in this category

INJECT TIME 01:25:23



01:25:23

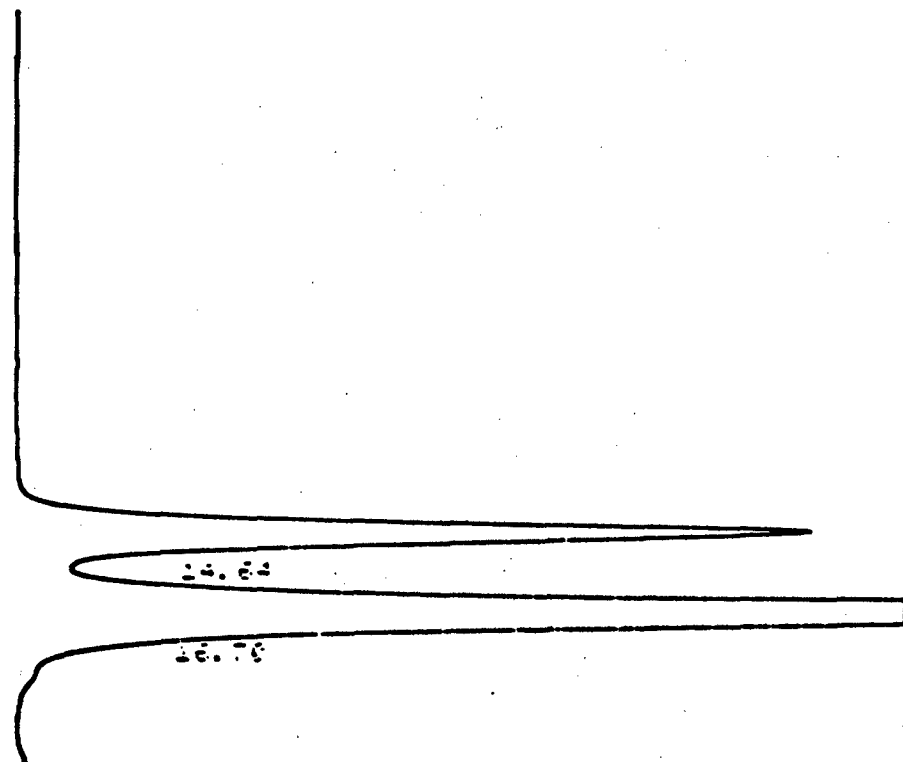
FILE 1	METHOD 0.	RUN 3	INDEX 3
AREA#	AREA%	RT	AREA SC
1	0.017	9.53	398 01
2	14.524	14.63	817034 02
3	65.459	16.69	1549108 23
TOTAL	100.		2366540

Figure 59. Gel permeation chromatogram of oil Sample A,  
10  $\mu$ L injection of undiluted oil.

TOTAL 100.

2921634

INJECT TIME 02:12:02

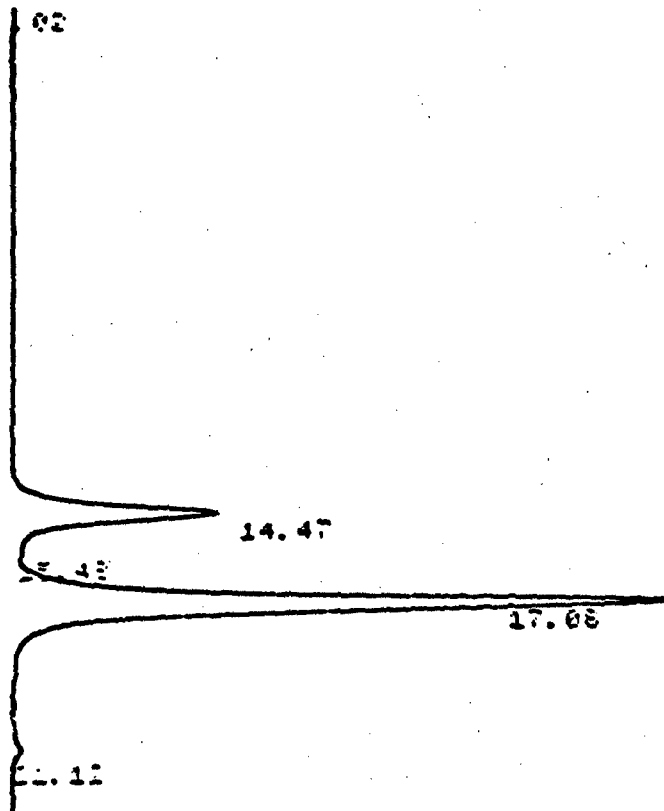


02:12:02

FILE 1	METHOD E.	RUN 5	INDEX 5
PEAK #	AREA%	RT	AREA BC
1	24.711	14.64	228266 82
2	65.299	16.7	1557979 23
TOTAL	100.		2286267

Figure 60. Gel permeation chromatogram of oil Sample A; repeat run, 10  $\mu$ L injection of undiluted oil.

STATION TIME 22:37:12



22:37:12

FILE 1 METHOD 6. FUN 12 INDEX 12

PEAK #	AREA%	RT	AREA BC
1	0.016	0.02	112 01
2	25.981	14.47	171992 02
3	0.408	15.48	2927 02
4	74.739	17.08	526297 03
5	0.807	21.12	5786 01
TOTAL	100.		717214

Figure 61. Gel permeation chromatogram of oil Sample A, 30  $\mu$ L injection of oil diluted 30-fold.

INJECT TIME 04:25:06

02

14.71

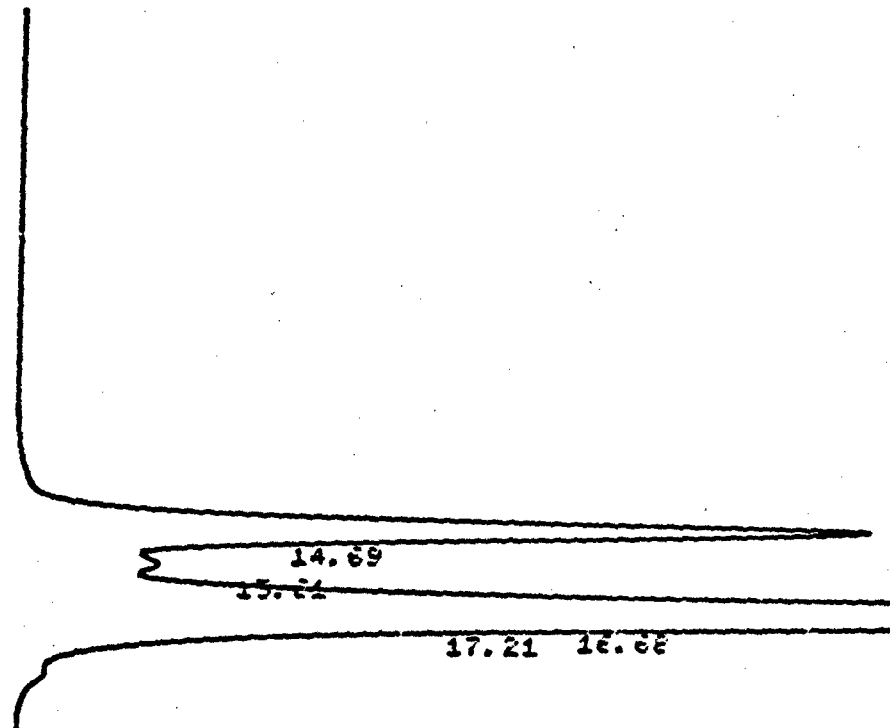
16.63

04:25:06

FILE	METHOD	RUN	INDEX	8
PEAK #	AREA%	RT	AREA BC	
1	0.002	8.03	80	81
2	15.049	14.71	931881	82
3	64.946	16.63	1726811	23
TOTAL	100.		2658772	

Figure 62. Gel permeation chromatogram of oil Sample B,  
10  $\mu$ L injection of undiluted oil.

INJECT TIME 03:01:52

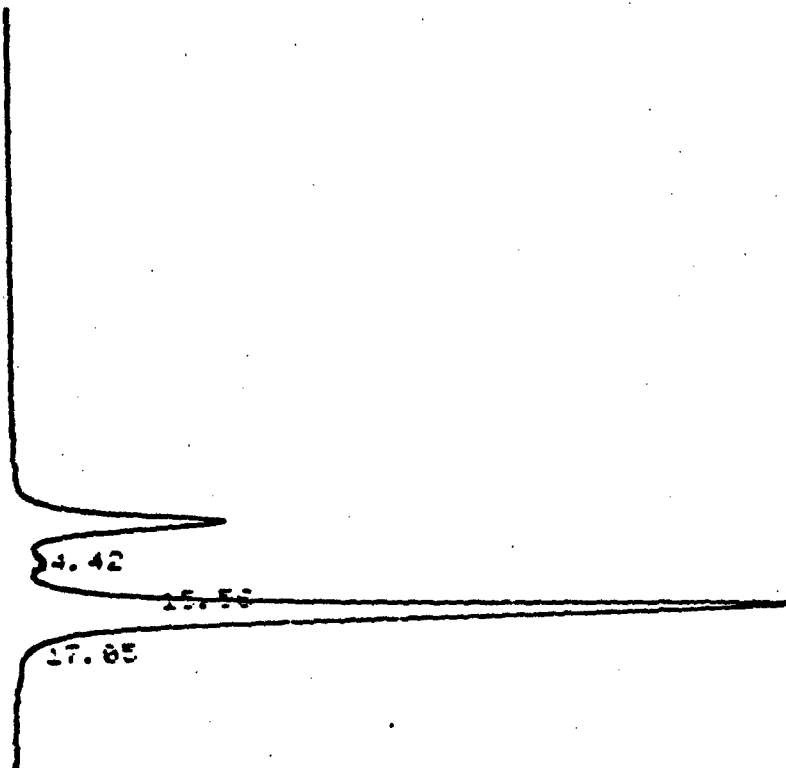


03:01:52

FILE 1	METHOD 2.	RUN 7	INDEX 7
PEAK #	APEAK	RT	ARER BC
1	32.925	14.69	858458 02
2	3.452	15.61	89171 02
3	41.179	16.68	1063645 02
4	22.443	17.21	579688 23
TOTAL	100.		2582954

Figure 63. Gel permeation chromatogram of oil Sample B; repeat repeat run, 10  $\mu$ L injection of undiluted sample.

INJECT TIME 00:28:18

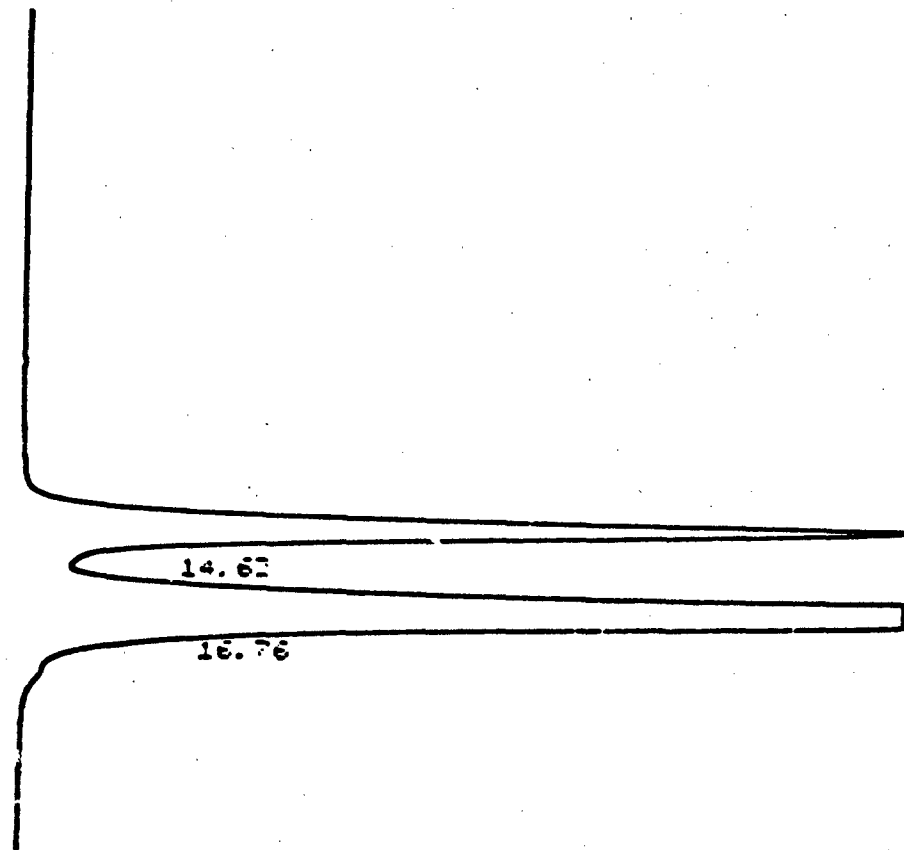


00:28:18

FILE 1	METHOD 0.	RUN 14	INDEX 14
PEAK#	AREA%	RT	AREA BC
1	21.647	14.42	186111 02
2	2.171	15.56	18667 02
3	75.182	17.05	654988 02
TOTAL	100.		859766

Figure 64. Gel permeation chromatogram of oil Sample B,  
30  $\mu$ L injection of oil diluted 30-fold.

INJECT TIME 05:33:40



05:33:40

FILE 1      METHOD 0.      RUN 10      INDEX 10

PEAK#	AREA%	RT	AREA BC
1	25.688	14.63	846905 02
2	64.312	16.76	1526326 03
TOTAL	100.		2373311

Figure 65. Gel permeation chromatogram of oil from 1-gallon can, 10  $\mu$ L injection of undiluted oil.

INJECT TIME 04:57:21

9.94

14.71

16.70

21.18

04:57:21

FILE	METHOD	RUN	INDEX
1	8.	9	9
PEAK#	AREA%	RT	AREAC
1	0.014	9.94	349 01
2	32.962	14.71	839383 02
3	62.94	16.7	1579372 02
4	2.063	21.18	58967 03
TOTAL	100.		2470071

Figure 66. Gel permeation chromatogram of oil from 1-gallon can, repeat run, 10  $\mu$ L injection of undiluted sample.

INJECT TIME 00:51:14

.01

14.50

17.10

00:51:14

FILE	METHOD	0.	RUN	15	INDEX	15
PERIOD	AREAZ		RT		AREA	BC
1	0.017	0.03	120	01		
2	24.404	14.5	176327	92		
3	73.38	17.1	546095	03		
TOTAL	100.		722542			

Figure 67. Gel permeation chromatogram of oil sample from 1-gallon can, 30  $\mu$ L injection oil diluted 30-fold.

except for one (Apollo PR1-19) exhibited pour points well below the specification maximum, therefore the amount of sample is not believed to represent a major problem with this measurement.

The ash content measurement procedure, ASTM D 482, suggests the use of up to 100 grams of sample to give up to 20 mg of ash. Sample quantity limitations prevented the use of samples of this size. Sample weights are reported with the ash content values.

### Results

Data from all tests are reported in Tables 53 and 54. Titrimetric data from which neutralization numbers have been calculated are presented in Figures 68 through 71. Each plot in these figures includes a titration curve for a reagent blank.

The data indicate that all corrosion inhibitors are within specification for tests in which limits are given. The requirement that ash content must not exceed 0.10% is clearly met by all materials. Similarly, the requirement that the maximum allowable pour point be -18°C is also met by all of the samples.

### 5. EFFECTS OF FUEL CORROSION INHIBITOR ADDITIVES ON THE CONDUCTIVITY OF JP-4 WITH ANTISTATIC ADDITIVES

A study was conducted to determine the effects of corrosion inhibitors on the electrical conductivity of two samples of the same fuel, each containing a different static dissipator additive. The objective of this work was to find the maximum allowable concentration of each inhibitor which when added to the fuel caused a change in conductivity of less than 140%.

Samples provided for the study consisted of two 55 gallon drums of JP-4, one (sample 83-POSF-0753) containing Stadis 450 additive and the other (sample 83-POSF-0754) containing Tolad 511. The

TABLE 53. QUALIFICATION DATA FOR CORROSION INHIBITORS

Inhibitor identification	Ash content Weight. q	Ash content q	Density at 15°C. g/cc	Viscosity at 37.8°C. cs	Flash point. °C	Total acid number, mg KOH/q	pH	Pour point, °C
1 Apollo PRI-19	14.8975	0.012	0.9250	225.4	-b	131	6.4	-18 <sup>c</sup>
2 ARCO 4410	15.6335	0.019	0.9559	352.6	86	158	6.6	-20
3 ARCO 4445	17.2530	0.001	0.9201	19.76	63	79	7.2	-59
4 DCI-4A	7.5622	0.025	0.9475	58.36	37	121	7.0	-40
5 DCI-6A	12.2009	0.023	0.9515	58.41	34	147	6.4	-40
6 HITEC E-515	13.0045	0.020	0.8778	50.56	-b	97	5.8	-45 <sup>c</sup>
7 HITEC E-580	9.8358	0.019	0.9198	138.2	84	71	7.2	-20
8 LUBRIZOL-541	36.8329	0.003	0.9609	30.33	27	136	6.3	-46
9 MOBILAD F-800	29.4360	0.008	0.8590	28.21	42	79	7.1	-56.5
10 NALCO 5403	16.3569	0.017	0.9253	28.01	-b	87	7.2	-56 <sup>c</sup>
11 NALCO 5405	9.2144	0.004	0.9314	72.55	66	129	6.4	-40
12 P3305 (Emery 9855)	11.7782	0.010	0.8947	102.0	60	113	7.2	-42
13 TOLAD 245	10.5213	0.000	0.9479	10.26	-b	58	6.6	-56 <sup>c</sup>
14 TOLAD 249	18.3475	0.000	0.9100	12.21	j9	92	6.4	-56.5
15 UNICOR J	13.2614	0.006	0.9342	76.57	67	113	7.2	-54 <sup>c</sup>

<sup>a</sup>Insufficient material to give up to 20 mg ash as stated in ASTM D 482.<sup>b</sup>Insufficient material to perform test.<sup>c</sup>Insufficient material to fill cold test jar to specified mark.

TABLE 54. EMISSION SPECTROGRAPHIC DATA FOR CORROSION INHIBITORS

Inhibitor	Al	Cu	Cr	Fe	Pb	Element, <sup>a</sup> ppm						Ti	
						Mn	Mg	Ni	P	Si	Na	Sn	
Apollo PRI-19	0.2	x	x	4.1	x	0.6	1.8	x	x	2.9	4.7	x	x
ARCO 4410	x	x	1.3	5.0	x	0.4	x	0.5	x	x	x	x	x
ARCO 4445	x	x	x	2.8	x	x	<0.6	x	x	x	x	x	x
DCI-4A	2.9	x	x	21	x	0.5	1.4	x	x	x	x	x	0.7
DCI-6A	3.2	x	x	5.3	x	0.4	1.1	0.3	x	x	x	x	1.1
HITEC E-515	0.3	0.2	x	0.7	x	x	1.3	x	<200 <sup>b</sup>	x	4.0	x	x
HITEC E-580	x	x	x	x	33	x	0.7	x	x	x	x	x	1.3
LUBRIZOL-541	x	x	x	3.2	0.3	0.1	0.5	x	x	x	4.2	1.1	x
MOBILAD F-800	x	x	x	x	x	x	<0.3	x	x	x	x	x	x
MALCO 5403	1.9	0.5	x	3.8	1.3	0.2	1.9	0.6	x	13	1.9	x	x
MALCO 5405	0.3	0.2	x	8.3	x	0.5	x	x	x	x	x	x	x
P3305	x	x	x	0.1	x	x	0.3	x	x	x	x	x	x
TOLAD 245	x	x	x	3.3	x	x	0.3	x	x	x	x	x	x
TOLAD 249	x	x	x	0.3	x	x	0.6	x	x	x	x	x	x
UNICOR J	x	x	x	0.5	x	x	0.2	x	x	x	x	x	x

<sup>a</sup>x indicates element was not detected.

<sup>b</sup>Upper limit of quantification of this method.

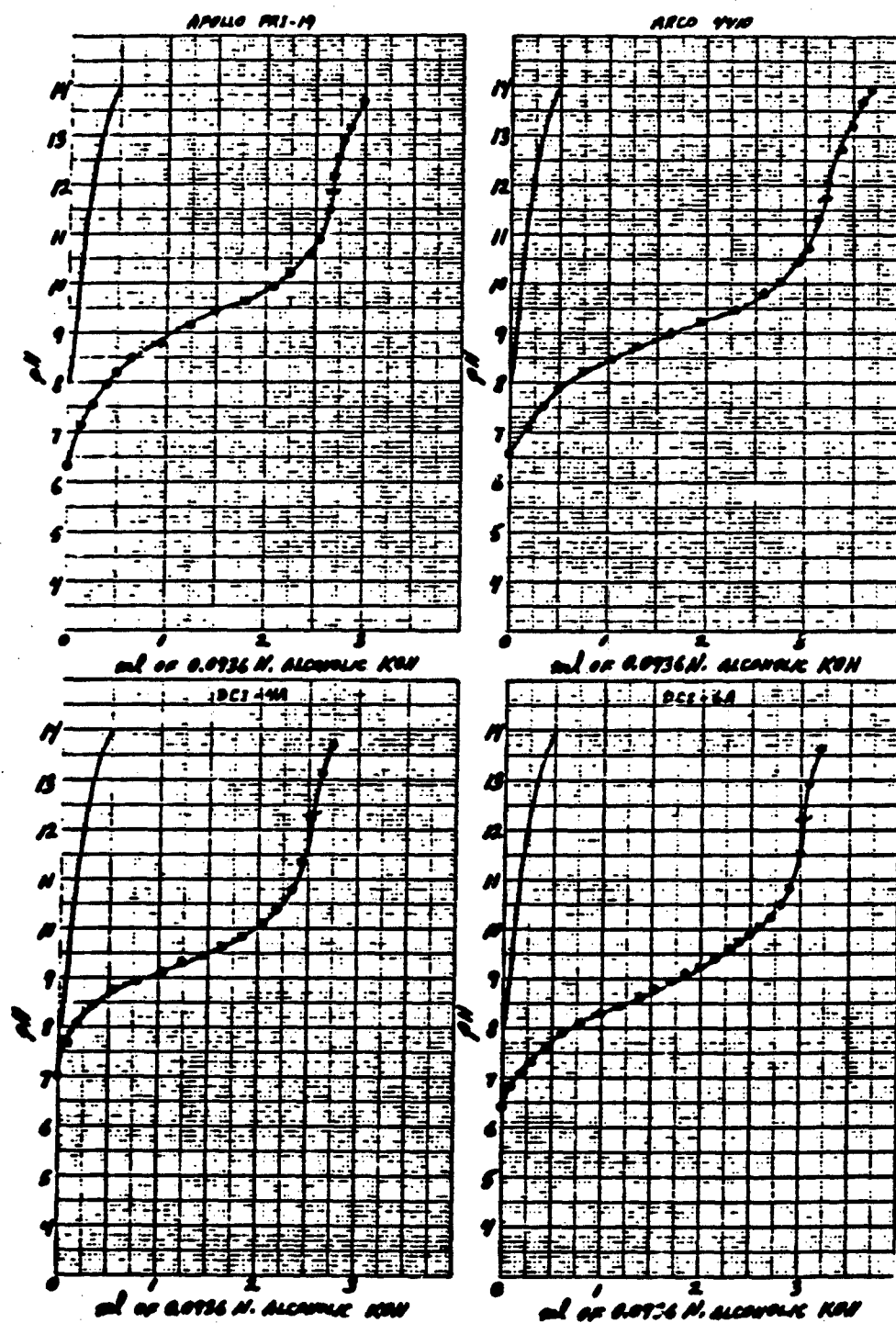


Figure 68. Neutralization number titration curves for corrosion inhibitors as marked.

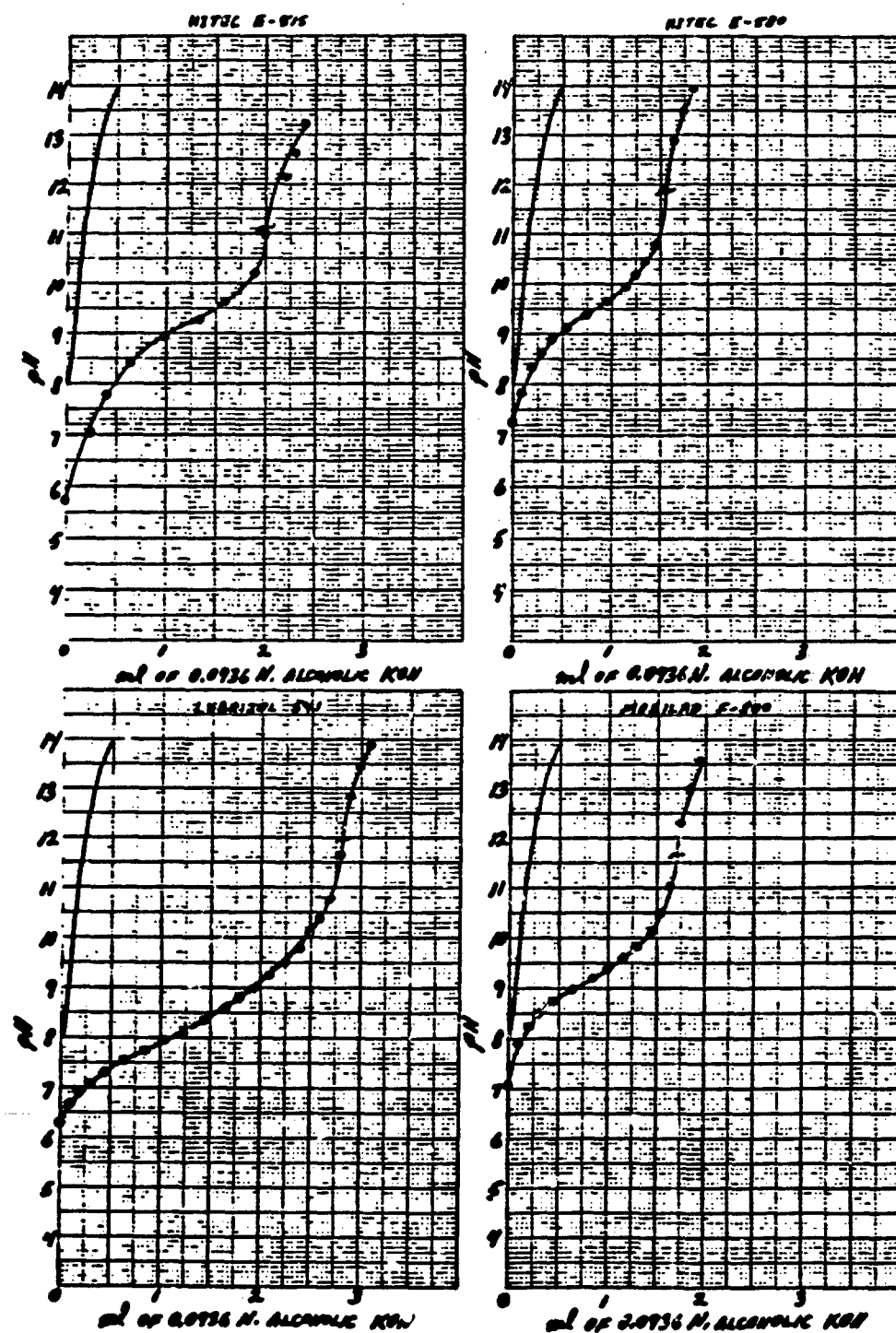


Figure 69. Neutralization number titration curves for corrosion inhibitors as marked.

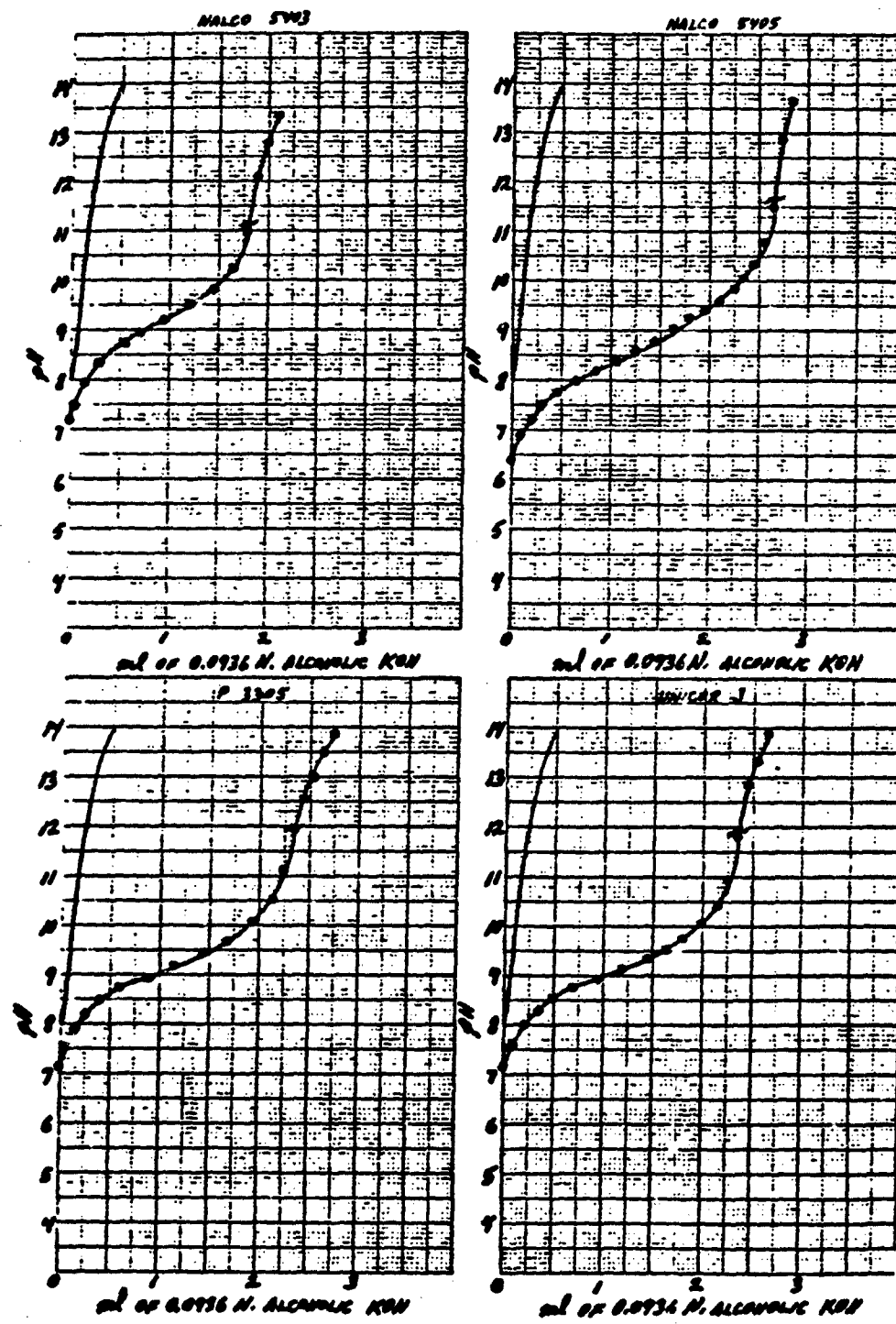


Figure 70. Neutralization number titration curves for corrosion inhibitors as marked.

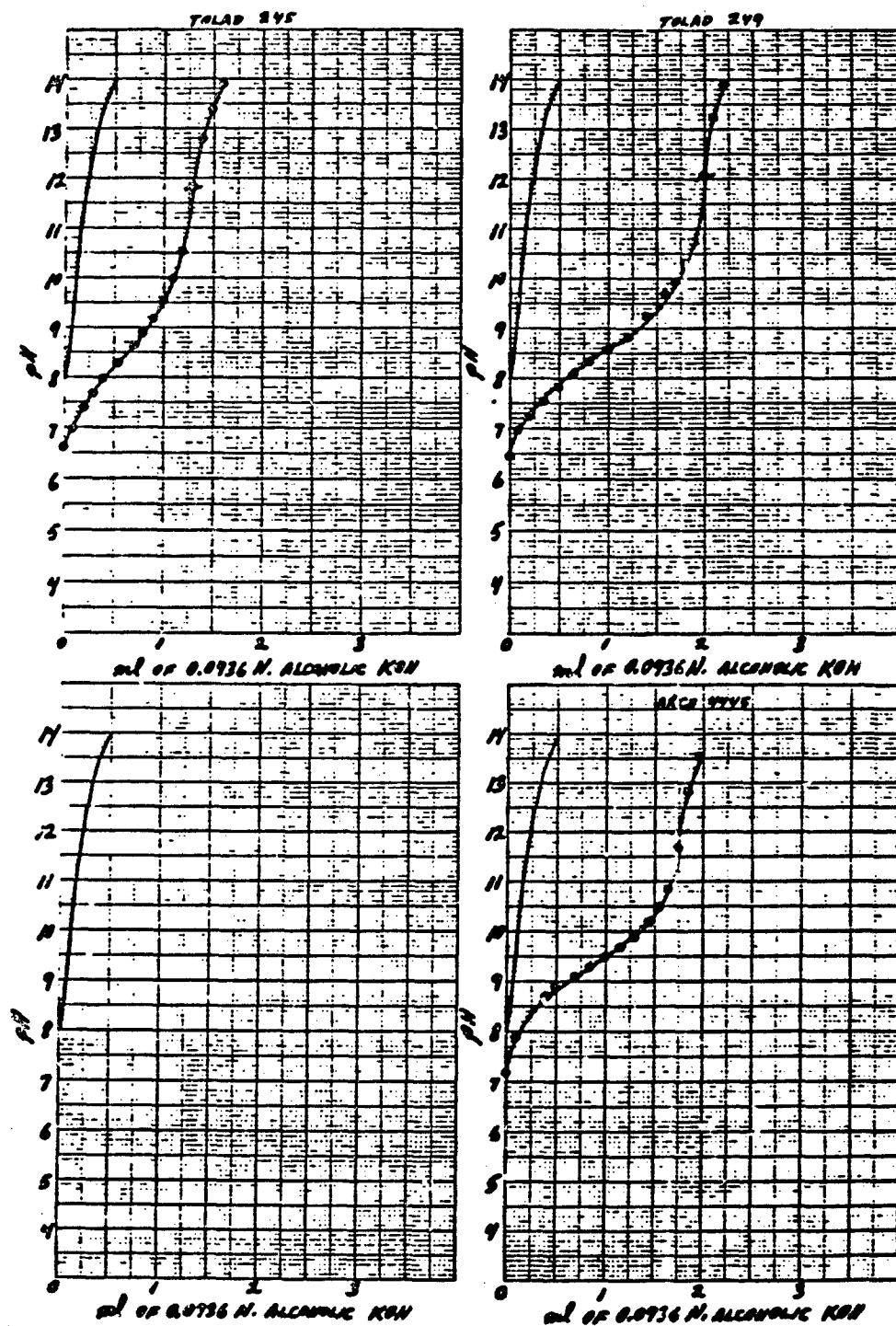


Figure 71. Neutralization number titration curves for corrosion inhibitors as marked.

conductivity of each fuel was  $400 \pm 100$  pS/m. Additionally, fourteen corrosion inhibitors were provided; these are listed in Table 58 along with their sample numbers and maximum allowable and minimum effective concentrations. Thirty-six 1-gallon epoxy-lined metal cans were supplied by AFWAL/POSF Fuels Branch for use in the study. Sixteen of the cans were deactivated for use with TOLAD-511 and the other sixteen, for use with Stadis 450. Deactivation of the cans was required to prevent changes in additive concentration by loss to the container walls.

#### Procedure

Specimens of each of the two base fuels were prepared to contain one of the 14 corrosion inhibitors at its maximum concentration, as shown in Table 55. One-half gallon of fuel was used for each of the 28 specimens. Control solutions containing no inhibitor were also taken. All solutions were prepared on a weight/volume basis with one lb/1000 bbl being equivalent to 2.85 mg/liter.

Each specimen was mixed for at least one hour on a shaker and then allowed to equilibrate for 24 hours.

Electrical conductivity measurements were performed according to ASTM method D 1314. A measurement was taken of the base fuel before addition of inhibitor, as well as of the equilibrated specimen containing inhibitor. If the two measurements differed by more than  $\pm 40\%$ , the concentration of the inhibitor was incrementally reduced by dilution with the appropriate base fuel. The highest concentration of inhibitor which would affect the conductivity by no more than  $\pm 40\%$  was sought. The lowest concentration tested was the minimum effective concentration given in Table 55. All measurements were taken at  $23.5^{\circ}\text{C} \pm 0.5^{\circ}\text{C}$ . The test cell and glassware were rinsed with test fuel before use. After use, and before the next measurement, glassware and cells were rinsed with iso-octane, then air dried.

TABLE 55. CORROSION INHIBITOR ADDITIVES USED IN INVESTIGATION

<u>Corrosion inhibitors</u>	<u>Sample code</u>	<u>Concentration, 1b/1,000 bbl</u>	
		<u>Minimum effective</u>	<u>Maximum allowable</u>
APOLLO PRI-19	82-POSF-0492	3	8
ARCO 4410	82-POSF-0490	3	8
DCI-4A	82-POSF-0498	3	8
DCI-6A	82-POSF-0499	3	8
HITEC E-515	82-POSF-0495	7.5	16
HITEC E-580	82-POSF-0702	3	8
LUBRIZOL 541	83-POSF-0703	3	6
MOBILAD F-800	82-POSF-0491	3	8
NALCO 5403	83-POSF-0704	3	8
NALCO 5405	82-POSF-0493	3	8
P3305	82-POSF-0497	4.5	12
TOLAD 245	82-POSF-0489	7.5	12
TOLAD 249	82-POSF-0494	3	8
UNICOR J	82-POSF-0496	3	8

### Results and Conclusions

The results are presented in Tables 56 and 57. In the base fuel containing Stadis-450, all corrosion inhibitors lowered the conductivity to some extent. Only Apollo PRI-19 and Hitec E-515 produced changes greater than 40% at the maximum permissible concentration. Even at their minimum effective concentrations, these two inhibitors produced a change in conductivity of greater than 40%. In the base fuel containing TOLAD-511, none of the corrosion inhibitors changed the conductivity by more than 40%.

Results were verified by repeating tests involving selected corrosion inhibitors. Data from these duplicate tests are presented in Table 58. All repeated conductivity values were obtained immediately after the 24-hour equilibration period of the new solutions. In making the initial measurements, values for the final concentrations were recorded up to five days after the initial higher concentration solutions were prepared. Nevertheless, observations agree well with respect to the inhibitor concentration giving less than  $\pm$  40% change in conductivity.

### 6. ANALYSIS OF TWELVE BLENDED HYDROCARBON MIXTURES

Analyses were conducted to determine blend compositions by methods which have been used for analysis of turbine engine fuels. Actual sample compositions were known only to personnel of the Aero Propulsion Laboratory's Fuel Branch (AFWAL/POSF); however, analytical data obtained showed that some blends contained as few as five compounds; most contained no more than several dozen. Two samples, that were exceptions appeared to be distillate fuels. Also, some of the blends consisted of low boiling compounds belonging to one class of compounds, and high boiling compounds of another class.

TABLE 56. EFFECT OF CORROSION INHIBITORS ON CONDUCTIVITY OF FUEL CONTAINING STADIS 450 ADDITIVE

Conductivity of base fuel, ps/m			Inhibitor	Inhibitor concentration lb/1,000 bbl	Conductivity with inhibitor, ps/m	Change, %
Initial	Final	Average				
474	479	476	APOLLO PRI-19	8.06	23.0	-67
474	479	476	APOLLO PRI-19	7.05	20.1	-65
474	462	468	APOLLO PRI-19	6.03	17.2	-65
474	462	468	APOLLO PRI-19	5.05	14.4	-58
474	462	468	APOLLO PRI-19	4.00	11.5	-53
474	493	484	APOLLO PRI-19	3.02	8.6	-50
474	493	484	ARCO 4410	8.00	22.8	-21
474	493	484	DCI-4A	7.96	22.7	-08
474	493	484	DCI-6A	8.00	22.8	-21
474	493	484	HITEC E-515	16.00	45.6	-85
474	493	484	HITEC E-515	14.00	39.9	-84
474	493	484	HITEC E-515	12.00	34.2	-84
474	493	484	HITEC E-515	10.00	28.5	-83
474	493	484	HITEC E-515	8.00	22.8	-81
474	490	482	HITEC E-515	7.50	21.4	-82
474	467	470	HITEC E-580	8.03	22.9	-10
474	467	470	LUBRIZOL 541	6.00	17.1	-36
474	467	470	MOBILAD F-800	8.03	22.9	-11
474	470	472	NALCO 5403	8.00	22.8	-09
474	470	472	NALCO 5405	8.00	22.8	-31
474	470	472	P3305	12.00	34.2	-09
474	470	472	TOLAD 245	12.00	34.2	-30
474	470	472	TCLAD 249	8.03	22.9	-29
474	470	472	UNICOR J	8.03	22.9	-07

TABLE 57. EFFECT OF CORROSION INHIBITORS ON CONDUCTIVITY  
OF FUEL CONTAINING TOLAD 511 ADDITIVE

Conductivity of base fuel, ps/m	Inhibitor			Conductivity with inhibitor, ps/m	Change, %	
	Initial	Final	Average	Inhibitor concentration lb/1,000 bbl	Inhibitor concentration mg/L	
376	372	374	374	APOLLO PRI-19	7.96	22.7
376	372	374	374	ARCO 4410	7.92	22.6
376	372	374	374	DCI-4A	8.00	22.8
376	372	374	374	DCI-6A	7.96	22.7
376	372	374	374	HITEC E-515	16.13	46.0
376	340	358	358	HITEC E-580	8.00	22.8
376	340	358	358	LUBRIZOL 541	6.00	17.1
376	340	358	358	MOBILAD F-800	7.96	22.7
376	343	360	360	NALCO 5403	8.03	22.9
376	343	360	360	NALCO 5405	7.92	22.6
376	343	360	360	P3305	12.00	34.2
376	343	360	360	TOLAD 245	11.96	34.1
376	343	360	360	TOLAD 249	8.30	22.8
376	343	360	360	UNICOR J	8.00	22.8

TABLE 58. DUPLICATE MEASUREMENTS FOR SELECTED CORROSION INHIBITORS

Conductivity of base fuel, ps/m			Conductivity with inhibitor, ps/m			Change, %
Initial	Final	Average	Inhibitor	Inhibitor concentration lb/1,000 bbl	mg/L	
<u>Base fuel with Stadis 450</u>						
474	486	480	APOLLO PRI-19	3.02	8.6	262
474	486	480	HITEC E-515	7.50	21.4	-74
474	486	480	LUBRIZOL 541	6.00	17.1	-360
474	486	480	NALCO 5405	8.00	22.8	366
474	486	480	TOLAD 245	12.00	34.2	-24
						-22
<u>Base fuel with TOLAD 511</u>						
376	343	360	APOLLO PRI-19	8.00	22.8	239
376	343	360	P3305	12.00	34.2	329
376	356	366	P3305 (repeat)	12.00	34.2	333
						-09

Mass spectral hydrocarbon-type analyses have several universal characteristics which may impact analytical results for samples of this kind. In MS type analyses, the pattern coefficient matrix is selected on the basis of the average carbon number of the sample. Thus when the boiling range (carbon number range) is severely biased with respect to compound type, the criteria for matrix selection are less valid and the methods lose accuracy.

Mass spectral-type methods are primarily intended for the analysis of distillate fuels, or for blends of distillate fuels. Contrary to what might be expected, these analyses applied to mixtures having a small number of components may produce results lacking in accuracy. This is true because the methods are based on statistical considerations which are not operative for blends of a limited number of compounds.

In this investigation, twelve blended hydrocarbon mixtures were characterized by means of simulated distillation (ASTM D 2887); hydrocarbon-type analysis by both the modified ASTM D 2789 method and Monsanto method 21-PQ-38-63; and elemental analyses by a commercial microanalytical laboratory. Data are presented in Tables 59 through 61.

The Monsanto method for hydrocarbon-type analysis is intended for use on samples having average carbon numbers in the  $C_{12-13}$  range. The modified ASTM D 2789 method is best suited for samples of lower carbon number. Samples in the intermediate range of approximately  $C_{10}$  usually give good results by either method, as indicated by the agreement of the two results for Samples VN-81-211; -212; -217, and -220.

#### Comparison of Results With Blend Compositions

After completion of the analyses and release of a report presenting the results (Technical Operating Report 2035-036, 30 November 1982),

TABLE 59. SIMULATED DISTILLATION DATA

Percent recovered	VN-82-210		VN-82-211		VN-82-212		VN-82-213		VN-82-214	
	°C	°F								
IBP, 0.5	27	81	177	81	177	80	177	82	180	92
1	82	179	81	178	81	178	82	180	93	200
5	83	182	100	212	83	181	112	233	94	202
10	88	191	137	279	100	212	139	283	95	204
20	102	216	164	328	151	304	169	336	98	208
30	125	257	182	361	182	361	184	362	103	218
40	140	284	193	379	186	366	200	391	112	234
50	153	307	210	410	199	391	216	420	114	238
60	184	363	220	428	217	422	219	427	140	284
70	190	374	234	453	224	436	231	448	171	340
80	218	424	237	459	236	456	238	460	176	349
90	246	476	253	487	250	483	254	490	218	424
95	268	514	262	504	261	501	269	516	219	426
99	287	549	281	538	286	546	287	548	220	428
FBP, 99.5	288	551	287	549	287	548	289	552	220	429

(continued)

TABLE 59 (continued)

Percent recovered	VN-82-216		VN-82-217		VN-82-218		VN-82-219		VN-82-220		VN-82-221	
	°C	°F										
0.5	82	179	145	293	92	128	80	177	145	293	82	180
1	82	180	151	303	93	200	81	177	151	303	82	180
5	83	182	167	333	99	211	83	181	167	333	83	182
10	90	194	181	358	103	217	93	200	181	358	84	184
20	102	216	197	387	139	282	112	233	197	387	87	189
30	114	236	209	408	168	335	175	248	209	408	102	216
40	140	283	217	423	171	339	177	350	217	423	104	220
50	149	299	223	434	175	346	217	422	223	434	218	424
60	172	342	231	447	178	352	219	426	231	447	234	454
70	186	366	237	458	227	441	228	443	237	458	237	458
80	218	424	245	473	236	456	287	548	245	473	287	549
90	242	467	254	488	262	504	289	552	254	488	290	553
95	256	492	260	500	285	546	290	554	260	500	291	555
99	269	516	273	524	288	551	291	555	274	525	292	558
FBP, 99.5	284	544	283	542	289	552	292	557	285	545	293	559

TABLE 60. HYDROCARBON-TYPE ANALYSES

		Weight Percent				
		VN-82-210	VN-82-211	VN-82-212	VN-82-213	VN-82-214
Paraffins	ASTM <sup>a</sup>	40.3	31.6	38.1	50.4	52.9
	Monsanto <sup>b</sup>	34.4	30.6	39.1	48.4	32.1
	Blend value <sup>c</sup>	38.2	30.3	35.9	48.6	53.3
Monocyclo- paraffins	ASTM	18.9	31.9	40.5	29.1	18.2
	Monsanto	-	-	-	-	8.5
Dicyclo- paraffins	ASTM	4.6	2.0	7.0	2.7	0.0
	Monsanto	-	-	-	-	0.0
Total cyclo- paraffins	ASTM	23.5 <sup>e</sup>	33.9	47.5	31.8	18.2
	Monsanto	21.0	31.1	45.0	30.7	17.0
	Blend value <sup>c</sup>	29.4	36.4	51.9	33.1	14.4
Alkylbenzenes	ASTM	21.3	25.2	11.0	13.4	28.9
	Monsanto	27.8	29.9	11.9	16.2	50.1
	Blend value <sup>c</sup>	21.1	31.1	10.8	16.5	32.2
Indans and tetralins	ASTM	0.0	9.3	3.1	4.4	0.0
	Monsanto	0.0	7.5	3.0	3.8	0.0
	Blend value <sup>c</sup>	0.0	1.8	0.9	1.3	0.0
Indenes and dihydro- naphthalenes	ASTM	- <sup>c</sup>	-	-	-	3.2
	Monsanto	0.0	0.0	0.0	0.0	0.0
	Blend value <sup>c</sup>	0.0	0.0	0.0	0.0	0.0
Naphthalenes	ASTM	14.9	0.0	0.3	0.0	0.0
	Monsanto	16.7	0.8	1.0	0.9	0.0
	Blend value <sup>c</sup>	11.2	0.4	0.4	0.4	0.0

(continued)

TABLE 60 (continued)

		VN-82-216	VN-82-217	VN-82-218	VN-82-219	VN-82-220	VN-82-221
Paraffins	ASTM <sup>a</sup>	23.7	46.3	15.5	73.8	47.2	25.7
	Monsanto <sup>b</sup>	12.1	46.5	8.7	77.2	46.3	42.4
	Blend value <sup>c</sup>	22.5		15.8	78.3		36.2
Monocyclo- paraffins	ASTM	15.2	42.7	9.9	11.8	42.9	56.3
Dicyclo- paraffins	ASTM	4.2	4.5	0.0	0.0	4.0	0.0
	Monsanto	- <sup>d</sup>	-	-	-	-	-
Total cyclo- paraffins	ASTM	19.4 <sup>e</sup>	47.2	9.9	11.8	46.9	56.3
	Monsanto	16.9	46.3	6.0	3.0	47.0	33.0
	Blend value <sup>c</sup>	24.5		5.5	7.0		48.9
Alkylbenzenes	ASTM	37.1	5.1	56.9	4.4	5.0	2.4
	Monsanto	49.7	5.2	67.9	7.1	4.9	3.9
	Blend value <sup>c</sup>	43.6		69.5	5.8		14.9
Indans and tetralins	ASTM	6.9	0.6	6.4	0.0	0.3	15.6
	Monsanto	6.6	0.7	5.7	0.0	0.6	14.8
	Blend value <sup>c</sup>	1.7		0.0	0.0		0.0
Indenes and dihydro- naphthalenes	ASTM	- <sup>d</sup>	-	-	-	-	-
	Monsanto	0.0	0.0	0.0	0.0	0.0	0.0
	Blend value <sup>c</sup>						
Naphthalenes	ASTM	12.9	0.8	11.3	10.0	0.6	0.0
	Monsanto	14.7	1.2	11.7	12.8	1.2	1.0
	Blend value <sup>c</sup>	9.4		9.2	8.9	0.0	0.0

<sup>a</sup>Modification of ASTM Method D 2789, values converted from volume percent using relative densities.

<sup>b</sup>Monsanto Method 21-PQ-38-63.

<sup>c</sup>Concentration in hydrocarbon blend prepared at AFWAL/POSF.

<sup>d</sup>Dash indicates method does not provide information on these specific compound categories.

<sup>e</sup>Sum of two preceding values.

TABLE 61. ELEMENTAL ANALYSES

Sample	Carbon weight percent	Hydrogen weight percent	Nitrogen ppm
VN-82-210	87.22	12.54	12
VN-82-211	86.47	12.98	9
VN-82-212	85.56	13.80	<11
VN-82-213	86.05	13.80	20
VN-82-214	86.70	13.46	16
VN-82-215	86.47	12.54	18
VN-82-216	88.37	11.46	22
VN-82-217	85.30	14.34	11
VN-82-218	88.51	10.70	17
VN-82-219	85.63	14.06	10
VN-82-220	85.21	14.26	27
VN-82-221	85.69	13.92	<13

blending compositions were made available for comparison and are given in Table 60. It will be noted that results for Sample VN-82-214 by the two methods do not agree well, however, the data by the ASTM agrees fairly well with the blending value. The average carbon number of this blend is quite low indicating that the ASTM method is the more appropriate one. The blend only contains six components and, as such, would ordinarily be unsuitable for a hydrocarbon-type analysis.

Samples VN-82-217 and VN-82-220 are identical samples of a JP-7 which was used to prepare sample blends -211, -212, and -213. The blend values were thus computed from the analysis of the JP-7 and the amounts of pure hydrocarbon which were added. One compound used for blending was cyclohexylbenzene. This compound was considered as an alkylbenzene in computing the blend composition. Structurally it is similar to an indan or tetralin and its contribution to the composite mass spectra is more like that of those compounds. The analysis of these three samples thus show values

for indans/tetralins which are higher than those listed for the blend composition value. This same compound was used in other blends and in each case appears as an indan/tetralin. In the case of Sample VN-82-221, only five compounds were used in the blend, with cyclohexylbenzene being the only aromatic constituent.

#### 7. EVALUATION OF THE USEFULNESS OF A VIBRATING TUBE DENSITY METER FOR PRECISION MEASUREMENTS AS A FUNCTION OF TEMPERATURE

Interest in revising fuel volume reduction tables stimulated an interest in methods for the accurate determination of density as a function of temperature. An investigation was conducted to determine the potential usefulness of a vibrating tube type density meter for precision measurements of fuel density.

Density measurements on fluids are usually conducted by one of several classical approaches:

- (a) Determination of the weight of a known volume of fluid (pycnometry).
- (b) Determination of the volume of a known weight of fluid (dilatometry).
- (c) By the measurement of volume displacement (hydrometry or hydrostatic weighing).

Of these, only dilatometry is very well suited for use over a wide range of temperatures. With the development of the vibrating tube density meter, however, another approach to density measurement as a function of temperature has become available. Moreover, it promises greater precision than is available by any other technique except for carefully controlled hydrostatic weighing. Work sponsored in part by the American Petroleum Institute has been conducted at the NBS Laboratories utilizing a vibrating tube meter to obtain data for the calculation of volumetric factors for petroleum [Ref. 7]. An evaluation of the feasibility and cost of

using such a meter for precise density measurements on aircraft fuels was conducted using the referenced report along with literature on commercially available density metering systems.

The principal upon which the device is based is uncomplicated and may be stated simply; the resonant frequency of a body having a fixed geometry changes with changes in its mass. In the device, a U-shaped tube is filled completely with sample by means of a syringe, a pump, or vacuum. The sample tube is then electromagnetically excited at its resonant frequency. The density of the sample can be determined precisely by measuring the oscillation period of the sample tube. Accuracy is reported to be unaffected by the fluid's viscosity, surface tension, or volatility. Several different models of a commercial density meter having varying precisions are available through Mettler Instrument Corporation.

#### Comparison of Density Meters to Classical Methods for Density Measurement

The dilatometer method is fairly representative of the classical density techniques. A single measurement by this technique usually requires about 45 minutes for operations, including cleaning the dilatometer, loading, taring, and weighing, temperature equilibration and cathetometer measurement of sample volume, usually three independent readings and then one about five minutes later to verify equilibration. The dilatometer constant is reestablished with each group of samples. When only one or two samples are available, calibration becomes an important time factor. The method as outlined above is conservative and has several steps which are included solely to improve quality assurance. The technique has a precision of  $\pm 1$  or  $2 \times 10^{-4}$  g/cm<sup>3</sup>.

Mettler Corporation's ADS45 density measuring system has a similar precision ( $1 \times 10^{-4}$  g/cm<sup>3</sup>). The system includes a DMA40D density meter, and a thermostated cooling unit for the sample cell giving

temperatures from  $-10^{\circ}\text{C}$  to  $25^{\circ}\text{C}$ . Density can be measured up to  $60^{\circ}\text{C}$  using an external constant temperature bath. The price of the system is \$14,750.

The ADS55 density measuring system offers higher precision ( $\pm 1 \times 10^{-5} \text{ g/cm}^3$ ) and the capability to conduct measurements at temperatures from approximately  $-10^{\circ}\text{C}$  to  $60^{\circ}\text{C}$  with temperature control of  $\pm 0.005^{\circ}\text{C}$ . The price of this system is \$21,265. Both of these systems include autosamplers which can accommodate up to 20 samples. The time typically required for a test is cited as 5 minutes or less for the 4-place system and 6 minutes or less for the 5-place system. The temperature range of the 5-place system can be expanded by purchase of a remote sample cell at a cost of about \$6,500.

A third system, offering six-place precision ( $1.5 \times 10^{-6} \text{ g/cm}^3$ ) employs two remote cells in the differential mode. The effects of small variations in temperature are thereby minimized. An autosampler cannot be used on this system. The system includes: DMA 60 precision digital density meter, remote cells, a cooling unit for operation down to  $-20^{\circ}\text{C}$  and a heating unit for temperature up to  $150^{\circ}\text{C}$ , a digital calculator and a remote cell that can be used at temperatures from  $-150^{\circ}\text{C}$  to  $+150^{\circ}\text{C}$ . The cost of this system is \$27,685 and the test time is cited at 8 minutes or less.

Since all of these systems are componentized, many options are available, at varying costs, for covering the temperature ranges of interest. All systems require about  $0.7 \text{ cm}^3$  of sample and cover a density range of 0 to  $3 \text{ gm/cm}^3$ . Each is equipped with a microcomputer to convert period values directly to density. The three systems are summarized in Table 65.

TABLE 62. METTLER/PARR DIGITAL DENSITY METERS

1. 4-Place Precision System Includes

- DMA 45 calculating meter
- SP-2 autosampler
- HP 975 programmable calculator with DMA interface, cable, and program
- Neslab thermostat
- Endocal 150 cooling unit

Price: \$14,965<sup>a</sup>

2. 5-Place Precision System Includes

- DMA 55D calculating meter
- SP-2 autosampler
- HP 97S programmable calculator with DMA interface, cable, and program
- Exacal 100 UHP constant temperature bath  $\pm 0.005^{\circ}\text{C}$
- Endocal 350 cooling unit

Price: \$21,345

3. 6-Place Precision System Includes

- DMA 60 precision digital density meter
- DMA 602 remote cells (2)
- Exacal 150 UHP constant temperature bath
- Endocal 350 cooling unit
- HP 97S programmable calculator with DMA interface, cable, and program
- DMA 602 HT cell for measurement at  $-150^{\circ}\text{C}$  to  $150^{\circ}\text{C}$

Price: \$27,685

<sup>a</sup>Pricing and technical changes may be made without notice.

Practical Operation of the Vibrating Tube System

Operation time is reduced with these systems since no weighing or volume measurement is required. The sample tube, however, must be completely and reproducibly filled, e.g., air bubbles, etc., are a source of error.

Though individual measurements can be made rapidly, a proper sequence of samples, rinses, calibration standards, etc., should be established to produce a test method that can be validated. Whetstone, et al. [Ref. 7] use water, air and xylene<sup>a</sup> for calibration, running a daily sequence as:

air, water, air, xylene, air, petroleum  
sample, air; etc., values

Air readings provide a check of the cleanliness of the cell, especially after its occasional cleaning with toluene and alcohol, as required. The system used in the NBS study provided 6-place precision. A typical day's operation for the NBS Lab would include 6 to 20 petroleum samples as well as calibration and verification runs. Their time per sample varied from 24 to 80 minutes each or an average of 52 minutes per sample. Factors which must be considered in evaluating the time involved are:

- (1) Obtaining data with 6-place precision requires more time than if only 4- or 5-place precision is obtained by the same method.
- (2) The NBS goal was not rapid sample throughput. It seems reasonable that with a goal of throughput in mind, a procedure could be developed to allow at least three density determinations at the same temperature, per hour. This number, or more is assured for the 4-place and 5-place systems with four or five samples per hour being quite likely.

---

<sup>a</sup>Xylene with its possible isomer problem is unusual for a standard, however, it is referred to numerous times in Ref. 6. The compound actually used may have been toluene since in one case it is parenthetically called methyl benzene.

At the rate of 3 samples per hour, the cost is estimated at \$12-\$14 per density measurement (or at 4-5 samples per hour, \$8 per measurement). This cost could be reduced even more with systems having autosamplers, since a number of measurements may be possible with little dedicated operator time.

In summary, estimates of true analytical costs are tenuous for methods which have not yet been developed and validated. It is clear, however, that great precision and, with proper calibration, accuracy is available using the vibrating tube instrumentation. Analyst time, and thus cost, will assuredly be less, because required operations are reduced.

#### 8. DETERMINATION OF THE FRESENCE OF CORROSION INHIBITOR IN A JP-8 INVOLVED IN FUEL PUMP FAILURE

The question of whether an operational fuel contains corrosion inhibitor frequently arises whenever fuel pump failure occurs. The presence of corrosion inhibitor contributes to fuel lubricity and its absence can be a causative factor in pump failure. A JP-8, Sample 83-POSF-0758 was examined in an effort to determine whether it contained corrosion inhibitor. Fourteen corrosion inhibitors of various types and compositions have been approved for use in aviation turbine fuels. A single analytical procedure which could provide unambiguous results for any corrosion inhibitor that might be present was not available. Examination of infrared absorption spectra, which were recorded for each of the fourteen approved corrosion inhibitors, however, showed that all had common features including a carbonyl (-C=O) band at approximately 5.8  $\mu$ m.

The JP-8 fuel was processed through an ion exchange column containing a nonaqueous anion exchange resin. The procedure used, in general, followed DuPont Petroleum Laboratory's Method M-14 for DCI-4A in jet fuel. Infrared spectroscopy is the analytical

technique employed in that procedure. The method specifies the use of Amberlyst A-29 anion exchange resin. A column/method blank was obtained by conducting the analysis using a pure solvent rather than fuel. An infrared absorption spectrum of the blank is shown in Figure 72. As will be noted from the spectrum, a small amount of organic material is obtained from the resin. A reference solution consisting of hexane spiked at the 15 ppm level with DCI-4A was prepared. The infrared spectrum from the analysis of this material is shown in Figure 73. A spectrum from the fuel Sample 83-POSF-0758 is presented in Figure 74. These data strongly suggest that a corrosion inhibitor is present in the fuel, though the specific one cannot be identified due to the similarity of their spectra. A comment must be made on this DuPont method. Though intended for the determination of DCI-4A in fuel, our previous evaluation of the analytical method [Ref. 8] has shown that several problems with the procedure render it ineffective for quantitative analysis. The most notable weaknesses are: a) the inability of the recommended resin column to completely remove DCI-4A from the fuel, and b) the high blank obtained from the resin. In the present tests, modifications which we have recommended for the procedure were employed. Results, however, are presented as being only qualitative.

Other tests conducted on this fuel are presented in Section 1, subsection 1. All physical properties, simulated distillation and hydrocarbon-type analyses fall within the range normally observed for a JP-8 sample.

Visual examination of the fuel specimen revealed a beaded film on the interior surface of the glass bottle above the fuel level. The appearance of the film suggested it was a fuel-immiscible phase, probably water. After carefully withdrawing the fuel from the bottle, the film was removed by rinsing the film with 5 mL of methanol. Analysis of the methanol rinse and a methanol blank, using the Karl Fischer Method for water, showed that about 30 mg

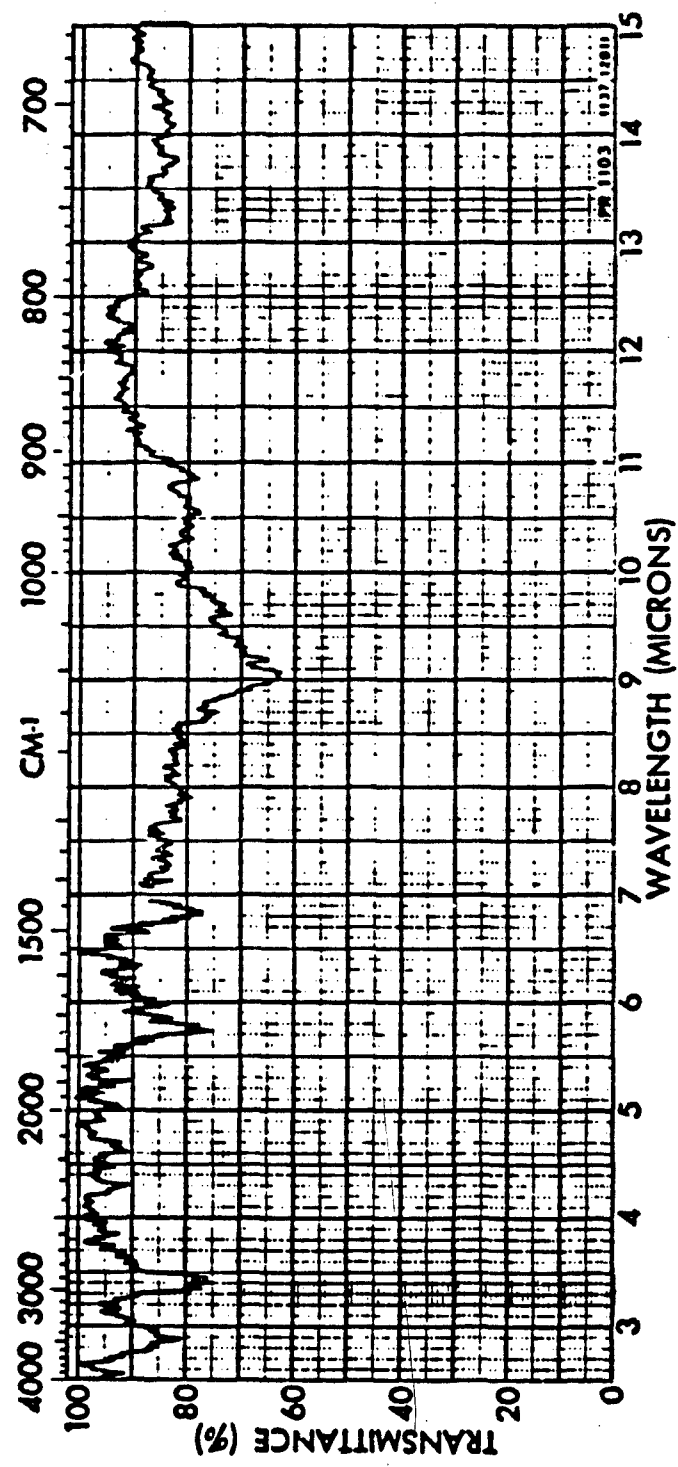


Figure 72. Infrared absorption spectrum of method/column blank.

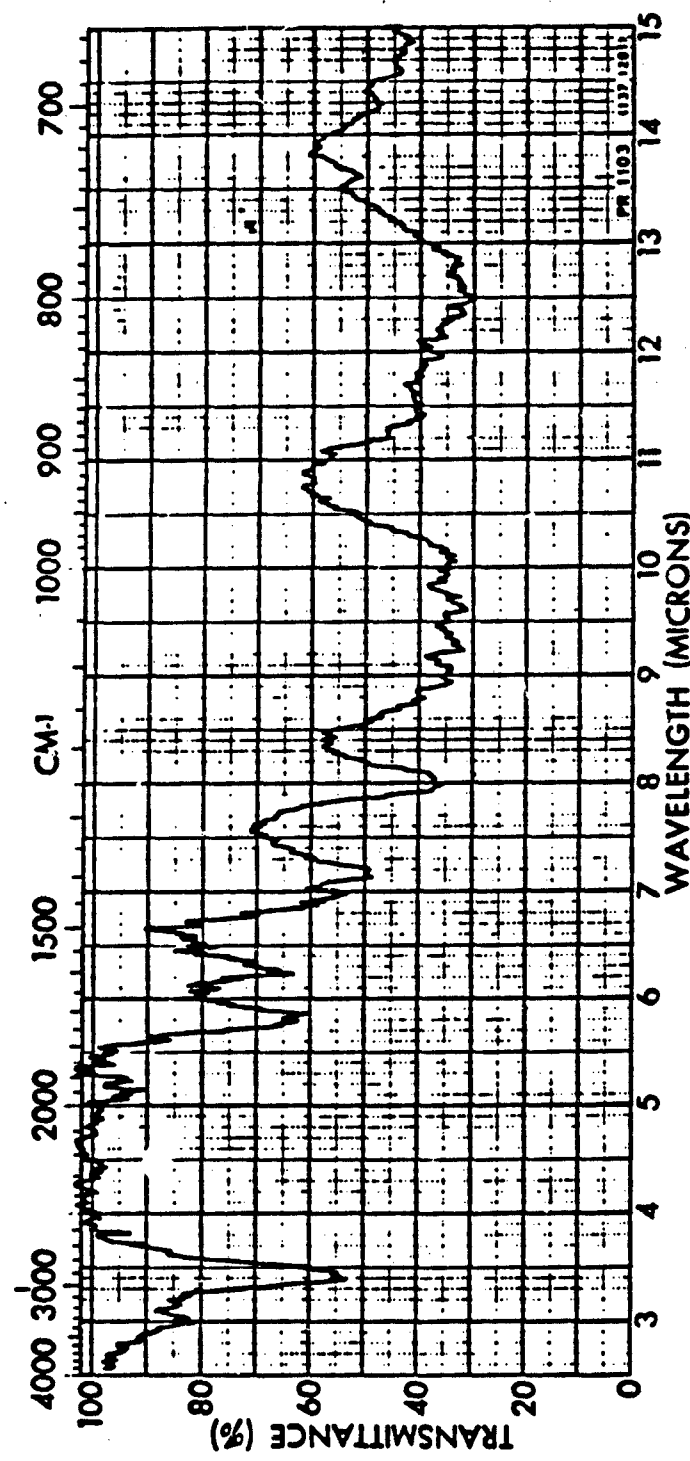


Figure 73. Infrared absorption spectrum of hexane spike with 15 ppm DCI-4A.

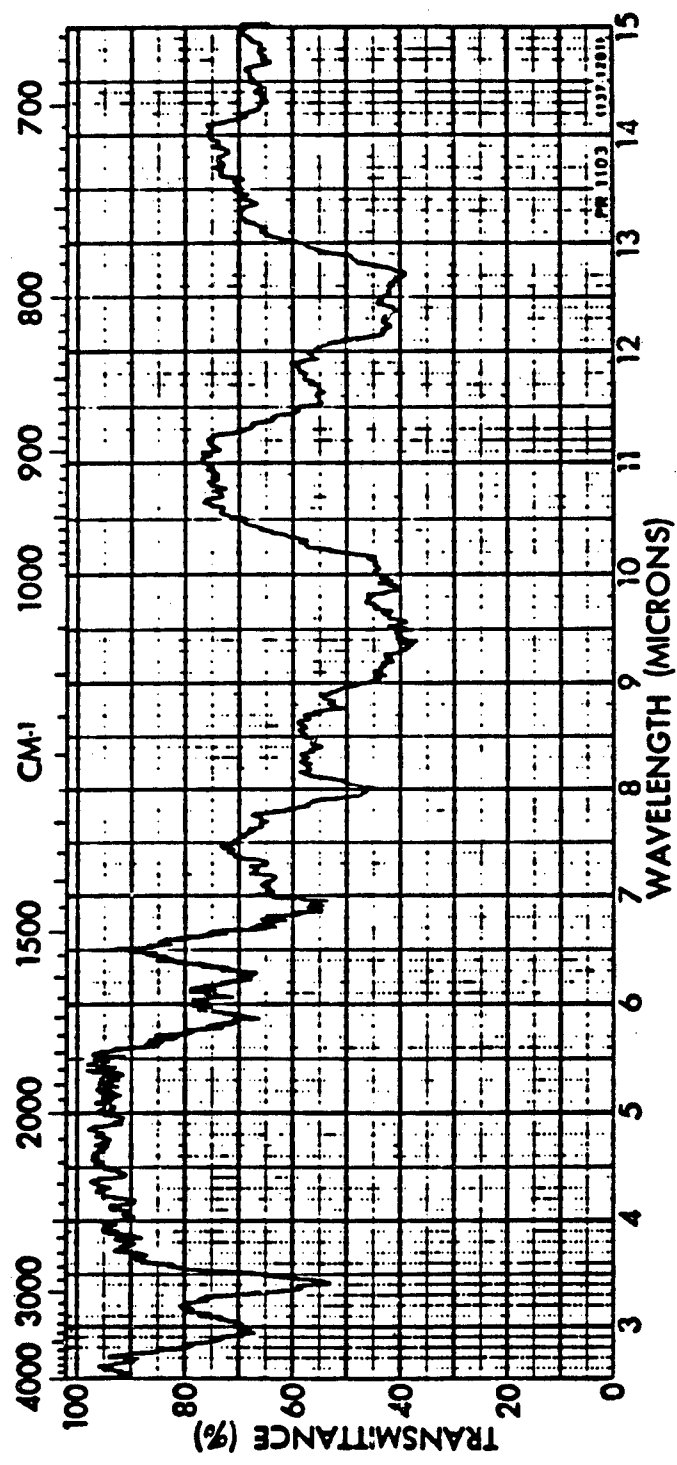


Figure 74. Infrared spectrum of ion-exchange isolate from fuel 83-POSF-0758.

of water had been present on the inner surface of the bottle. Either the fuel contained suspended water which later coalesced on the bottle wall, or the water-saturated fuel experienced temperature changes which caused water to leave solution.

#### Conclusions

To summarize findings, no deficiencies which might cause fuel pump failure nor abnormalities were observed in the fuel. The only unusual characteristic noted is the presence of water in the sample as discussed in the foregoing paragraphs.

## REFERENCES

1. "Registry of Toxic Effects of Chemical Substances," U.S. Department of Health and Human Services, Public Health Service, NIOSH, 1980 Edition, Vols. 1 and 2.
2. "An Infrared Spectroscopy Atlas for the Coatings Industry," published by Federation of Societies for Coatings Technology, (1980).
3. "Sadler Guide to NMR Spectra," W. W. Simons and M. Zanger. Sadler Research Laboratories, Inc., p. 401, 1972.
4. "Analysis of Aircraft Fuels and Related Materials," AFAPL-TR-79-2016, F. N. Hodgson and J. D. Tobias, p. 148, March 1979.
5. "Infrared Analysis of Polymers, Resins, and Additives, An Atlas, Vol. 1," D. O. Hummel. Wiley-Interscience, pp. 173-175, 1971.
6. IBID, Spectra Number 256.
7. "Density and Thermal Expansion Coefficients of Petroleum," J. R. Whetstone, J. M. Cameron, C. L. Carroll, W. L. Gallagher. National Engineering Laboratories, NBS. Sept. 1978.
8. Hodgson, F. N., Evaluation of DuPont Laboratory Method M-14 for the Determination of DCI-4A, Report No. 74-1, Contract No. F33615-74-C-2002, 12 January 1974.

## APPENDIX A

### SPECIFIC TEST METHODS FOR FUEL CHARACTERIZATIONS DESCRIBED IN THIS REPORT

Several physical and chemical property tests were repeatedly conducted for a number of the projects described in this report. For the sake of conciseness and to avoid repetition, the test methods are described in this Appendix only.

#### DENSITY AND SPECIFIC GRAVITY

This method covers the laboratory determination, using a pyrex dilatometer, of the density of fuels normally handled as liquids. The dilatometer method is most suitable for determining the density of mobile transparent liquids ranging from 100°F to -65°F. In this procedure, the liquid is introduced into a clean, weighed dilatometer which is then reweighed. The sample is brought to the prescribed temperature by immersing the dilatometer in a vertical position into a constant temperature bath. After temperature equilibrium has been reached, the dilatometer scale is read by means of a cathetometer.

Density is defined as the mass of liquid per unit volume at prescribed temperature. In this method, the unit of mass is the gram and the unit of volume, the milliliter.

The dilatometer should be thoroughly cleaned with chromic acid cleaning solution or laboratory detergent, then rinsed well with distilled water and dried at 105 to 110°C, or rinsed with pure, dry acetone and dried by applying an aspirator to the open end of the dilatometer. Cleaning should be performed in this manner in order to have a sharply defined miniscus during calibration of the dilatometer. Ordinarily, the dilatometer may be cleaned between test determinations by washing with a suitable solvent,

such as toluene, and rinsing with pure, dry acetone. Periodic cleaning with glassware detergent solution is recommended.

The volume of the dilatometer, when equilibrated at various test temperatures must be determined by means of a cathetometer. This is called the K value for that temperature. Freshly-boiled and cooled distilled water can be used for calibrating at 70°F and 100°F and good reagent grade solvents can be used for determining the K values at lower temperatures. Densities of the solvents at low temperature can be determined by using the International Critical Tables and the density of water at various temperatures can be found in the Handbook of Chemistry and Physics. When using the cathetometer, measure the span between two graduation marks on the dilatometer. This will be approximately 0.190 cm for a graduation interval of 0.05 ml. This should be measured at several places to assure consistency. Having determined the span of a 0.05 ml interval, the volume of the liquid can then be interpolated. It is more precise to determine the volume by the cathetometer than to estimate it by visual observation.

Procedure - Adjust a constant temperature bath to maintain the prescribed temperature. Weigh the clean, dry dilatometer and stopper to the nearest 0.1 mg and record the weight.

Fill the dilatometer to approximately the 1.5 ml graduation mark on the dilatometer by means of a hypodermic syringe. Remove any bubbles that might have been formed while transferring the sample.

Weigh the stoppered dilatometer and sample to the nearest 0.1 mg. Record the weight. Place the dilatometer in a suitable holder in the constant temperature bath adjusted to the test temperature within  $\pm 0.05^{\circ}\text{F}$ . When the sample has reached equilibrium (about 15 minutes) take readings of the miniscus by means of a cathetometer. Read the cathetometer to the nearest 0.005 cm. Take several readings of the miniscus until reproducible readings

are obtained. After consistent readings have been made, remove the dilatometer from the bath and clean with a suitable solvent, rinse with pure dry acetone and proceed to the next test.

### Calculations

$$\text{density, g/cc} = \frac{m}{K-R}$$

where  $m$  = mass of sample in grams

$K$  = dilatometer constant at given temperature,  
volume of dilatometer to full mark

$R$  = dilatometer reading at given temperature,  
ml below full mark

### TRUE VAPOR PRESSURE

True vapor pressure is the maximum vapor pressure that a volatile mixture such as an aircraft fuel can exert at a given temperature. In theory, this property should be measured in the absence of sample vapor because vaporization of a portion of the sample changes the composition of the mixture and thus changes the vapor pressure. In practice, true vapor pressure must be measured at such a small vapor-to-liquid ratio that any change in the composition of the fluid produces a negligible change in vapor pressure, i.e., within the experimental error of the method.

For true vapor pressure measurements as a function of temperature, a micro vapor pressure apparatus as described in ASTM D 2551-80 was used. The micro vapor pressure apparatus incorporates a mercury-sealed orifice for sample introduction, and the entire unit is surrounded by a glass outer jacket through which fluid from a constant temperature bath is circulated. Using this device, a known volume of sample is introduced into an evacuated, temperature-controlled chamber of known volume. The rise in pressure in the bulb is due to the vapor pressure of the sample and

the partial pressure of any dissolved air. In order to obtain a vapor pressure measurement without a contribution due to air, the air was first removed from the sample before the measurement was conducted. A cryogenic degassing procedure is used for this purpose.

Classically the vapor pressure temperature relationship is expressed by:

$$\log P = A - B/T$$

where A and B are constants, P = absolute pressure and T = absolute temperature. The line resulting from a plot of this equation on semilog paper is useful over a limited range for estimating vapor pressure at temperatures intermediate to those at which measurements were taken.

#### HYDROCARBON TYPES BY MASS SPECTROMETRY

Hydrocarbon-type analyses were conducted by three separate mass spectral methods, depending on the fuel. A modification of ASTM Method D 2789 was used for JP-4 and gasoline-type fuels. ASTM Method D 2425, which first requires an ASTM D 2549 separation of the fuel into aromatic and paraffinic fractions, was utilized mainly for diesel fuels. Monsanto Method 21-PQ-38-63, developed for hydrocarbon feed stocks with an average carbon number in the range of 12 to 13, was used for JP-8 type fuels. Nonstandard fuels were usually analyzed by more than one mass spectral method. All of these analyses are based on the summation of characteristic mass spectral lines for each compound type. A matrix of n equations, relating each of n hydrocarbon types to the summed peak values, is constructed. A computer solution of these simultaneous equations provides a quantitative measure of each compound type present.

As noted above, ASTM D 2425 analysis must be preceded by a separation of fuel aromatics from nonaromatics using a procedure such as that described in ASTM D 2429. The D 2549 method, as currently presented in Part 24 of the 1980 Annual Book of Standards, required a small procedural modification in order to be used for JP-8. This modification did not change the essential features of the separation, but only involved the method for removing the chromatographic solvent. The modified methodology was developed in MRC laboratories and has been employed for a number of years. An official modification of ASTM D 2549 to achieve the same effect is under study by ASTM Committee D-2 on Petroleum Products and Lubricants. By the ASTM D 2549 procedure, a steam bath is employed to evaporate solvent from the fractions obtained by elution chromatography. In the MRC modification, no heat is applied. Instead, a stream of dry nitrogen is used for desolvation. Evaporation of solvent, in fact, reduces the temperature to below ambient. After the major part of the solvent has evaporated, the weight of the fraction is carefully monitored as the final traces of solvent are removed. Complete removal of solvent is signalled by a marked decrease in the slope of the time/weight loss curve, or in some cases, by the attainment of a constant weight. MRC analysts are experienced in this procedure, which requires a short period of dedicated attention for the processing of each fraction by the analyst.